SOLUTE BUDGET OF THE RIO GRANDE ABOVE EL PASO, TEXAS

By

Elizabeth Marie Bastien

Submitted in Partial Fulfillment of the Requirements for the Degree of

Master of Science in Hydrology

New Mexico Institute of Mining and Technology

Socorro, New Mexico

May 2009

ABSTRACT

The Rio Grande basin experiences a dramatic increase in total dissolved solids (TDS) with distance downstream from the headwater streams in Colorado (~40mg/L) to the southern edge of the Upper Basin in El Paso (over 1000 mg/L). High TDS concentrations can lead to human health issues; endangered aquatic life; and economic losses. Previous research from the past century primarily focused on electrical conductivity, total dissolved solids and chloride, yet the causes remained poorly understood. In order to gain a deeper understanding of solute behavior within the Rio Grande, major ion data was compiled for eleven Rio Grande locations including data from 1905-1907, 1931-1936, and where available between 1930-2005. Chemical trends showed an overall solute load decrease with time, primarily due to flood protection structures such as reservoirs and diversion dams, the irrigation network and a pulse of high saline water from accumulated salts flushing from previously undrained agricultural land. The Rio Grande evolves from a calcium-bicarbonate water near the headwaters into a sodium-chloride-sulfate water near El Paso. The chemical variation can in part be attributed to deep brine seepage and the presence of Elephant Butte Reservoir, where calcium, magnesium and bicarbonate loads decreased substantially below Elephant Butte Dam. This suggests carbonate mineral precipitation within the lake. In addition, the river chemistry is altered by interaction with soil minerals as it percolates beneath agricultural fields. A mass balance model generated for water and each major ion during the decades

between 1930 and 2005 computed the total discharge and load passing each reach by a summation of all known aqueous sources of solutes and of water. The water and chloride mass balance models yielded results that closely matched the measured quantities at each river cross-section with percent differences varying between 0.08-36% for water and a negligible difference for chloride. Reactive solute models for calcium, sodium, magnesium, sulfate, bicarbonate and potassium could not be closed with the known source quantities indicating that an additional process affected the behavior of these solutes. These residual solute quantities were attributed to mineral interactions, presumably occurring in river and irrigation channels and/or agricultural and riparian lands. A geochemical mass balance-modeling program (NETPATH) computed mineral interactions responsible for the residual solute quantities. Mineral interactions were dominated by mineral availability along the flow path, with silicate weathering processes in northern reaches transitioning into cation exchange, sedimentary dissolution and dedolomitization processes in southern reaches. Modeling demonstrated that mineral interactions, tributary inflows, wastewater treatment plant effluents and geologically controlled brine seepage contribute significant quantities of salt to the Rio Grande. The finding that mineral interactions significantly affect solute behavior in the river has serious implications for water quality management strategies. Unlike brine inflow or the other sources, mineral interactions cannot be controlled and might adversely interfere with proposed migration techniques.

ACKNOWLEDGEMENTS

I wish to acknowledge Sustainability of semi-Arid Hydrology and Riparian Areas (SAHRA), a National Science Foundation Technology Center and the Salinity Management Coalition for funding this research. Many thanks are given to the state, federal and local professionals who provided access to data and information for this research. I send special thanks to my advisor Dr. Fred Phillips for invaluable assistance throughout the research process and the advisory committee: Dr. Enrique Vivoni and Dr. Robert Bowman. Further thanks go to Heather Lacey, Gretchen Olsener, Shasta Marrero, Marty Frisbee, and Carlos Aragon for assistance, advice and friendship. Finally, I wish to thank my family and friends, especially my parents Denise and Michael Bastien for continual guidance and support.

TABLE OF CONTENTS

LIST OF FIGURES

LIST OF TABLES

CHAPTER 1
INTRODUCTION

1.1 River Salinization

Understanding the causes and mechanisms for salinization in river basins is crucial to supporting human societies. Over forty percent of worldwide food production is grown from irrigated agricultural acreages in arid regions [*Johnson, 2002*]. Arid and semiarid environments are particularly difficult areas to meet water quality and quantity demands. In arid regions, surface waters tend to decrease in quality in the lower reaches of river basins, mainly from an increase in dissolved solids or salinity [*Lippincott, 1939*]. Poor quality water can lead to human health issues; endangered aquatic life; and economic losses, resulting from corrosion of municipal and commercial pipes, unusable water and crop yield reduction [*Postel, 1999*]. The salinity increase is often attributed to irrigated agriculture [*Lippincott, 1939*]. Sustaining an ample supply of good quality water to human populations remains a vital concern.

The Rio Grande is one of the longest rivers flowing through the semiarid southwestern United States. With its headwaters in southern Colorado and traveling 1,900 miles south through New Mexico, it forms a large part of the international boundary between the United States in Texas and Mexico. The salinity of the river increases by approximately two orders of magnitude as it flows from Colorado into Texas. Approximately 89% of the available water in the river [*Moore and Anderholm*,

2002] is used to irrigate 914,000 acres of agricultural land [*Ellis, 1993*] in the Upper Rio Grande (indicating the region from the headwater streams in Colorado to El Paso, Texas). Irrigation waters in the Rio Grande basin are diverted from the river at various locations into riverside canals, which transport water to interior canals for use on croplands. As river salinity rises, the irrigation water salinity also rises creating concern for many farmers, particularly near the New Mexico-Texas border where irrigation water quality is lower than in the northern basin.

1.2 Major Ion Behavior in Typical River Systems

The amount of dissolved solutes in a river system is derived from the concentration of existing solutes, riverbed seepage into or out from the shallow ground water aquifer, deeper aquifer seepage and point source inflows. Identifiable sources of salt include tributaries, shallow ground water, deep saline ground water, geothermal, industrial, municipal (i.e wastewater treatment plants) and atmospheric deposition. Each solute is controlled by a distinct set of variables and therefore each behaves uniquely within the same river system. The major ions can be divided into two major categories: conservative and reactive. Conservative solutes do not interact with the soil material or undergo biologic decay, whereas the reactive solutes may interact with soil minerals. Of the major ions considered in this report, chloride is the only conservative solute. The remaining solutes (calcium, sodium, magnesium, potassium, bicarbonate and sulfate) likely interact through mineral weathering reactions, ion exchange, biological uptake, and mineral precipitation and dissolution reactions. Major-ion behavior in river systems has been studied extensively and widely reported. Two such

works are: The Geochemistry of Natural Waters 3rd Edition [*Drever*, 2002] and Treatise on Geochemistry (Volumes 5 and 9) [*Holland and Turekian*, 2007].

Evaporation is one factor that affects both conservative and reactive solutes equivalently. Evaporation processes, including open-water evaporation, vadose-zone evaporation and plant transpiration, deplete water quantity and contribute to solute increases through the concentration of salt. Concentration due to evaporation may lead to ion over-saturation and mineral precipitation. Manipulation of the river enhances evaporation through reservoirs, irrigation networks and main channel alterations.

1.3 Purpose and Scope of Thesis

Irrigated agriculture has previously been named the principal cause of increasing salinity in the Rio Grande [*NRC*, *1938*; *Lippincott*, *1939*; *Trock et al, 1978*]; however, recent studies have identified deep brine as a significant additional salinity source [*Mills*, 2003]. *Mills* [2003] focused on high-resolution sampling data from August 2001 and January 2002 to identify and characterize brine seepage chemistry and location. *Lacey* [2006] expanded upon *Mills* [2003] by investigating chloride trends and brine seepage through time, modeling Rio Grande monthly chloride and bromide chemistry from 1975-2005. This thesis will further define the understanding of brine seepage by calculating inflow on a decadal basis over the available period of record from 1930-2005 at strategic locations along the Rio Grande. In addition, major-ion chemistry will be utilized to develop a detailed understanding of the salt budget. Previous researchers [*Wilcox*, 1957; *Williams*, 2001] presented major-ion chemistry of the Rio Grande to evaluate the various segments of the salt balance, however, few

interpretations of the observed patterns were provided. Serving to extend these chemical results both spatially and temporally, this work presents historic river chemistry data for major cations and anions (chloride, sodium, calcium, magnesium, potassium, sulfate and bicarbonate) as decadal averages from 1934-2005, as well as a brief period from 1905-1907. General chemistry compositions, concentrations and solute burdens are given for 11 stations along the Upper Rio Grande (headwaters in Colorado to El Paso, Texas). A solute mass balance model was generated to identify mechanisms and model chemical transitions between sampling locations along the river. The solute budget model quantified these mass transfers and suggested that mass-transfer residuals were due to mineral/ion interactions. In order to understand these reaction mechanisms, a geochemical mass balance program, NETPATH [*Plummer*, 1991], was utilized to model the chemical reactions both at the microscale (site study in Lemitar, New Mexico) and the macroscale (Rio Grande). Rio Grande geologic, hydrology, irrigation framework, and anthropogenic alterations are included in this presentation.

1.4 Note on Units

Various types of data are presented throughout this thesis, an attempt will be made to present all data in SI units. However, certain types of data will be presented in English units to conform with the historical irrigation precedent, which is most familiar to hydrologists, farmers and engineers working in the Rio Grande basin. Quantities related to irrigation diversion and reservoir storage capacity are commonly presented using the English units of acre-feet/year and acre-feet. When English units are reported,

the equivalent SI units will also be given wherever possible. Solute load quantities will be presented in kg/month and discharges will be presented in L/month. Common unit conversions that may be of use include in the following: 1 acre-ft = 1.2×10^3 m^3, 1 acre-ft = 1.2×10^6 L, 1 acre-ft/yr = 1.02×10^5 L/month, 1 ft^3/s = 723.97 acre-ft/yr, 1 ft^3 = 28.32 L and 1 ft^3/s = 7.34×10^7 L/month.

CHAPTER 2
HYDROGEOLOGIC SETTING AND ANTHROPOGENIC FEATURES

2.1 General Basin Characteristics

From its headwaters in the San Juan Mountains in Colorado, the Rio Grande traverses 1,900 miles (3,034 km) before discharging into the Gulf of Mexico. This project concentrates on the upper 1200 km of the Rio Grande from the San Juan Mountains in Colorado to El Paso, Texas. Within this study area, the Rio Grande drains 118,880 km^2 of basin surface area. The average rainfall varies from 120 cm in the headwaters to less than 20 cm on the semiarid valley floor at the southern end of the basin [*Levings et al.*, 1998]. Southern Rocky Mountain snowmelt and summer monsoon storms contribute the majority of Rio Grande flow; the system is climatically controlled and highly sensitive to prolonged periods of drought. Downstream from the headwaters, the following tributaries contribute significant discharge to the Rio Grande: Goose Creek, the South Fork of the Rio Grande, Pinos Creek, Conejos River, Costilla Creek, the Red River, the Rio Pueblo de Taos, the Rio Hondo, Embudo Creek, the Rio Chama, the Santa Cruz River, the Santa Fe river, Galisteo Creek, the Jemez River, the Rio Puerco and the Rio Salado. South of the Rio Salado, no natural tributaries flow consistently enough to be included in this study. Figure 2.1 displays a map illustrating select cities, mountain ranges and tributaries in the Upper Rio Grande Basin.

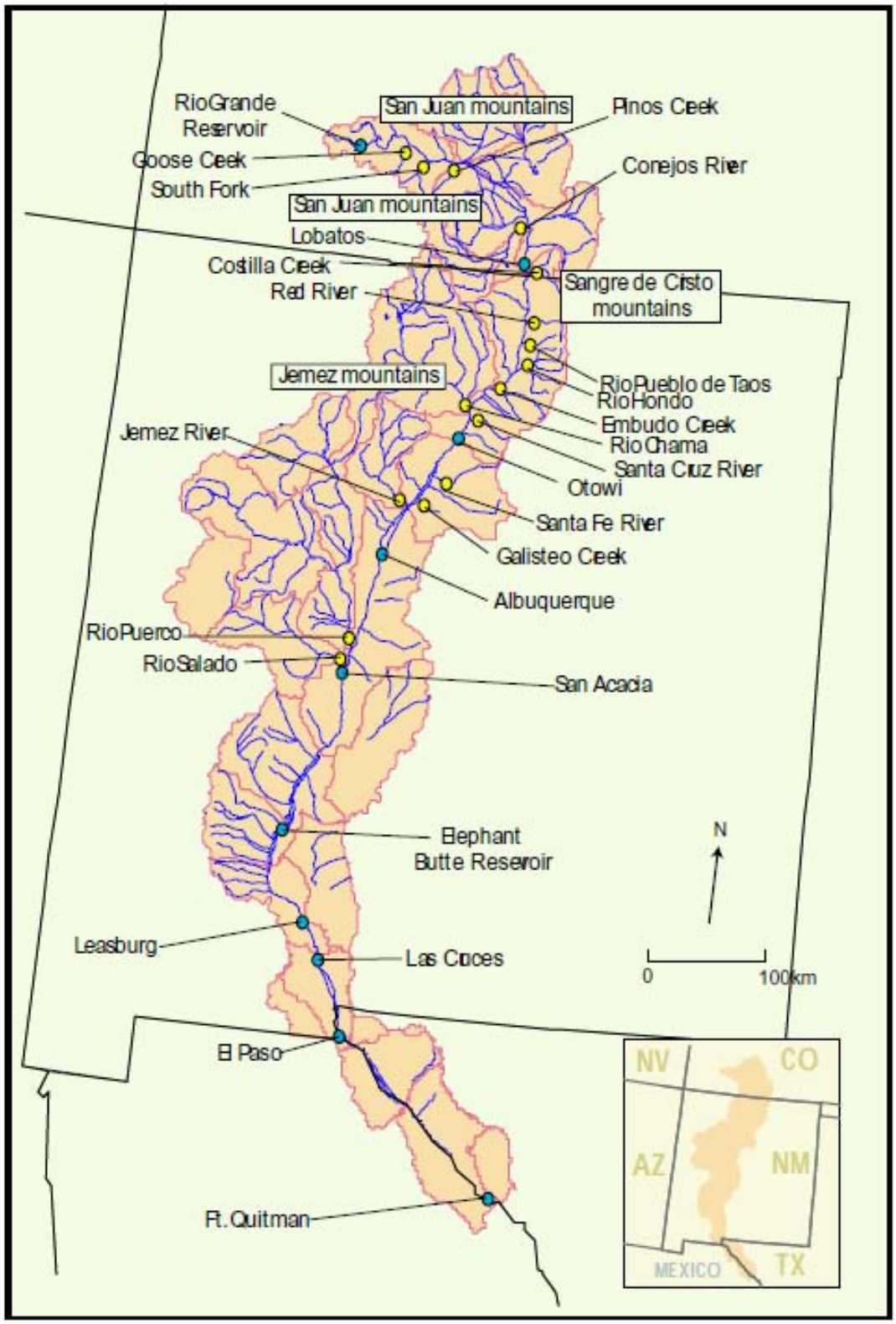

Figure 2.1. Upper Rio Grande Basin, with major snowmelt generating mountains, tributaries (yellow circles) and cities (blue circles) labeled for reference. [*Mills, 2003*]

The Rio Grande supports a wide variety of land uses including municipal, agricultural, industrial and riparian corridors along both the tributaries and the main channel of the Rio Grande. Agriculture is the largest water user, diverting approximately 89% of the river's flow (data taken from 1990) [*Moore and Anderholm, 2002*]. As illustrated in Figure 2.2, crop consumptive use accounts for 37% of total yearly Rio Grande depletions, roughly 226,810 acre-feet (2.79×10^8 m^3) of water per year between Cochiti and Elephant Butte Reservoir (based on information collected for the year 2000) [*Papadopulos and Associates, 2000*]. Riparian evapotranspiration and reservoir evaporation account for the majority of the remaining depletions with 37% and 21%, respectively. Evapotranspiration (ET) significantly controls water quantities in the Rio Grande basin. In northern sections of the basin the annual potential evaporation is approximately 70% of annual precipitation. This strongly contrasts southern area potential evaporation, which can reach over 1000% of annual precipitation [*Levings, 1998*]. Evapotranspiration is highly variable ranging from 0.24 to 1.53 m^3/s over a 32-mile section from Bernalillo to Isleta in the summer (data from 1985) compared to 0.057 to 0.11 m^3/s in the winter months (data from 1996-2000) [*Veenhuis*, 2002]. The ET seasonal difference is largely created by flood irrigation, crop transpiration, and climate.

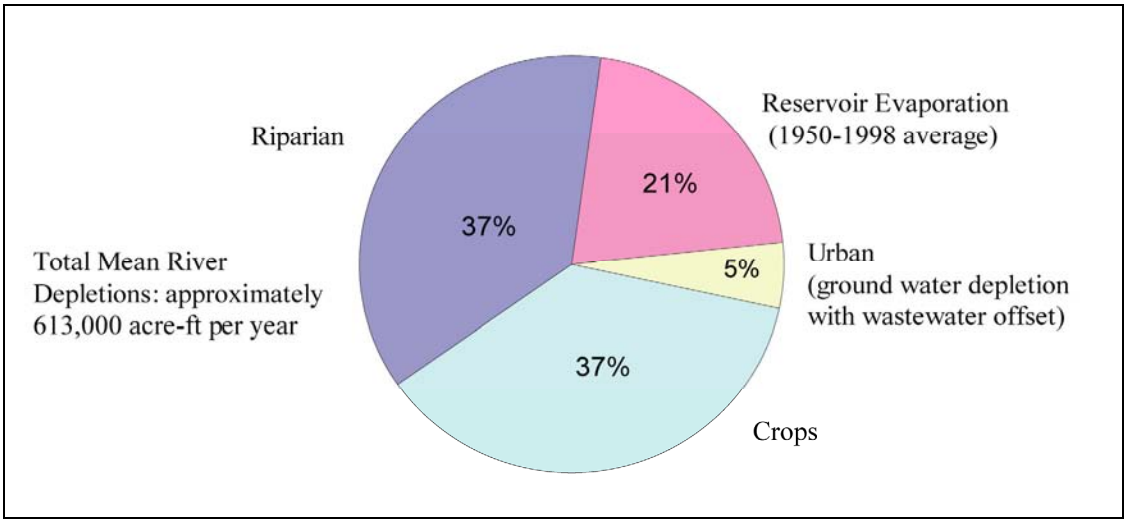

Figure 2.2. Total river depletions from the Middle Rio Grande in 2000. [*Papadopulos and Associates*, 2000]

2.2 Geologic Setting

The Rio Grande is entrenched into the Rio Grande rift, a geologic structure bounded with faults on the east and west, with alluvial-filled grabens (or sedimentary basins) in the center (Figure 2.3) [*Wilkins, 1998*]. The rift consists of longitudinally arranged linked alluvial basins, with less permeable volcanic and sedimentary rocks encircling the Rio Grande floodplain and valley floor (Figure 2.4, general geologic map of New Mexico). Alluvial basins range in thickness from 1 to 6 kilometers [*Wilkins, 1998*]. A regional map is shown in Figure 2.5, illustrating the Rio Grande watershed and aquifer basins: San Luis, Espanola, Albuquerque, Socorro, Palomas and the Mesilla basin. The northern part of the San Luis basin is closed with respect to both surface and ground water indicating there is no natural connection to the Rio Grande system. The remaining basins affect the chemistry of the Rio Grande through the release of saline brine as discussed in Chapter 3.

2.3 Hydrologic Setting

For most areas of the river, the Rio Grande is hydraulically connected to the shallow floodplain aquifer as well as the deeper basin-fill aquifer formed by the Santa Fe group. Surface/ground water interactions vary by location and season; certain river sections gain water from the aquifer while others discharge into the shallow aquifer. Diverted irrigation water can alter the interaction between the river and shallow ground water. During the irrigation season, the canal network may reverse natural river hydraulic gradients as flow from irrigation canals is sent toward the nearest drainage channel rather than to the Rio Grande. Gaining reaches are documented in the northern part of the Rio Grande near Lobatos and the southern part below Caballo Dam. *Winograd* [*1959*] reported a gain of 2.7 m^3/s from groundwater seepage between Lobatos and the Red River. The section between Caballo Dam and Hatch gained 0.62 m^3/s [*Wilson et al., 1981*]. In contrast, several sections of the river lose water to the aquifer, notably the stretch between Bernalillo and San Marcial as well as in the Mesilla Valley [*Mills*, 2003]. Water lost from the river to the shallow aquifer is likely returned to the river or might enter the deep aquifer and become completely lost from the surface system. *Veenhuis* [2002] identified an average loss of 6 m^3/s during the winter between Bernalillo and the Rio Bravo Bridge in Albuquerque, and also noted that 2.5 m^3/s entered the deeper Santa Fe aquifer. Summarizing previous studies, *Veenhuis* [2002] reported flow losses to the deep aquifer in the range of 1.9-7% in the winter and 5.9-6.4% in the summer. *Papadopulos and Associates* [2002a] measured summer seepage between San Acacia and San Marcial in the range of 7-10 m^3/s and noted that no

relationship between discharge quantity and seepage rate could be found. Finally in the southern end of the study area, *Wilson* [1981] reported winter losses of 0.9 m^3/s between Las Cruces and the Mesilla diversion dam.

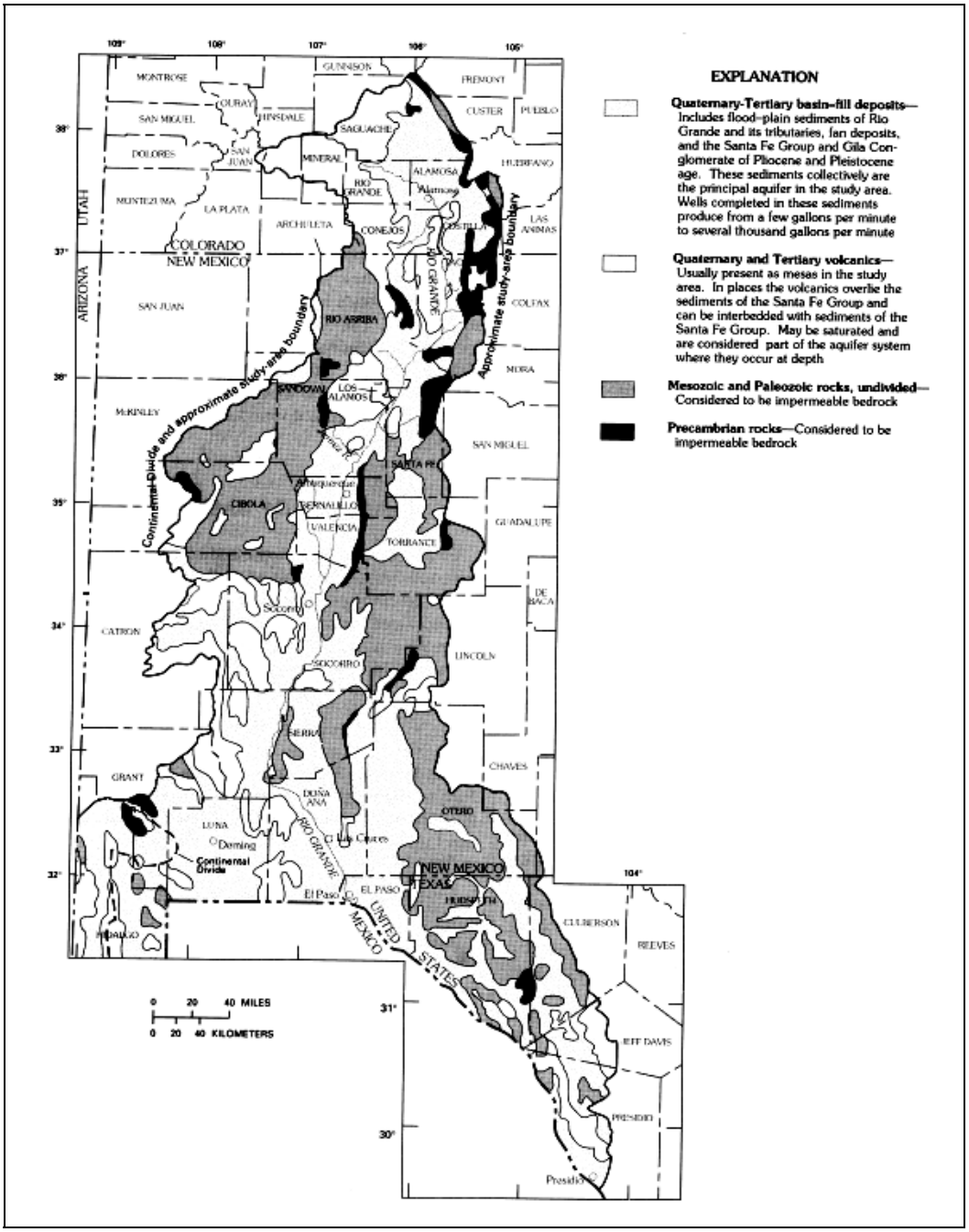

Figure 2.3. General geology of the Rio Grande Basin. [*Wilkins, 1998*]

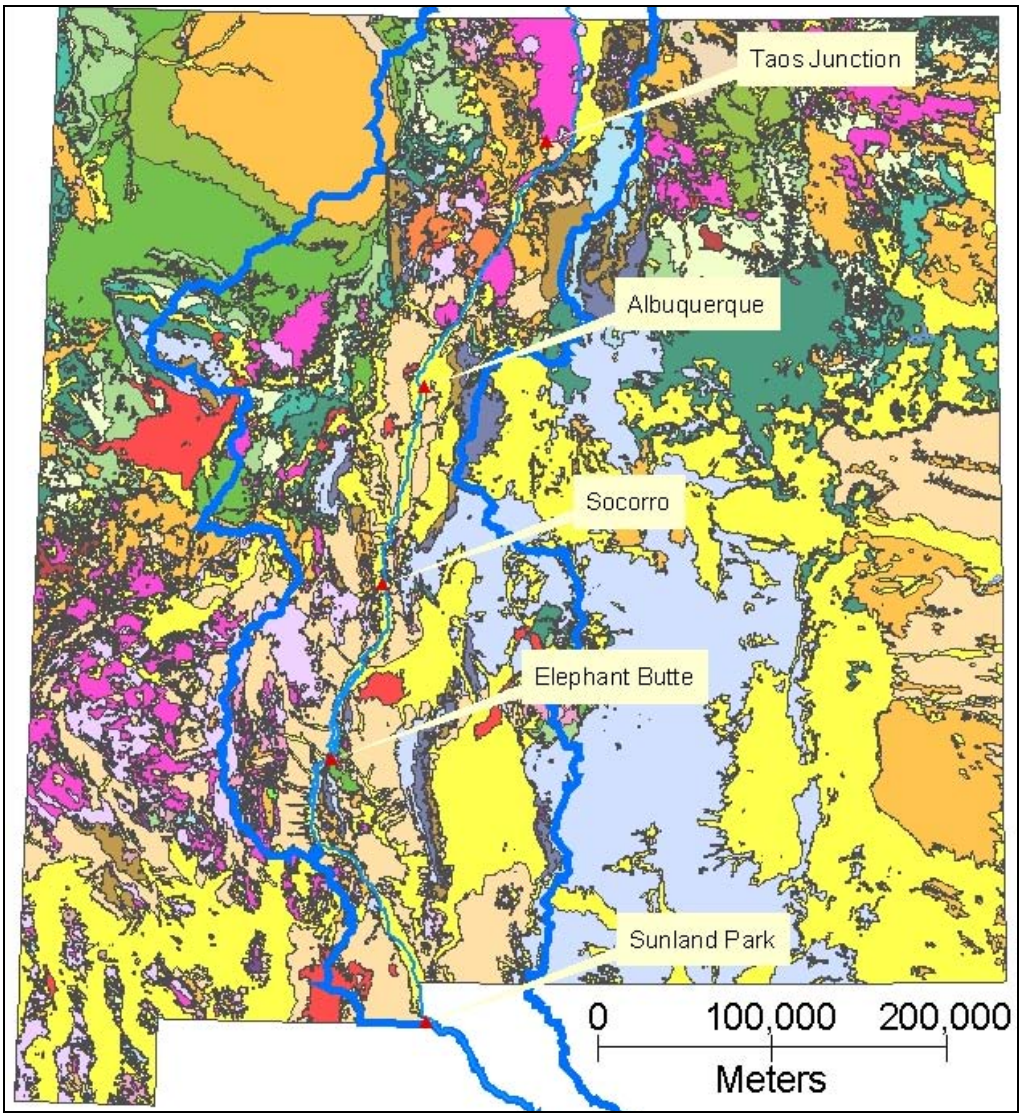

Legend

- water
- playa
- Q - Quaternary sediments
- Qb - Quaternary basaltic volcanic rocks
- Qs - Quaternary silicic volcanic rocks
- QT - Quaternary-Tertiary sediments
- QTv - Quaternary-Tertiary volcanic rocks
- T - Tertiary sedimentary rocks
- Tv - Tertiary volcanic rocks undifferentiated
- Tb - Tertiary basaltic volcanic rocks
- Ts - Tertiary silicic volcanic rocks
- Ti - Tertiary intrusive rocks
- TK - Cretaceous-Tertiary rocks
- TKv - Cretaceous-Tertiary volcanic rocks
- K - Cretaceous rocks undivided
- Ku - Cretaceous sedimentary rocks above Kmv
- Kmv - Cretaceous Mesaverde group (incl gallup ss and Crevasse can. fm.)
- Km - Cretaceous Mancos shale
- Kl - Cretaceous sedimentary rocks below Km
- Kv - Cretaceous volcanic rocks
- Ki - Cretaceous intrusive rocks
- J - Jurrassic sedimentary rocks
- @ - Triassic sedimentary rocks
- Pz - Paleozoic rocks undivided
- P - Permian sedimentary rocks
- P& - Pennsylvanian-Permian sedimetary rocks
- & - Pennsylvanian sedimentary rocks
- M_ - Mississippian to Cambrian rocks
- p_ - Precambrian rocks undifferentiated

Figure 2.4. Geologic map of New Mexico. Datum = NAD 27, UTM 13N [New Mexico Bureau of Geology, 2008, acquired from Lewis Gillard, GIS specialist].

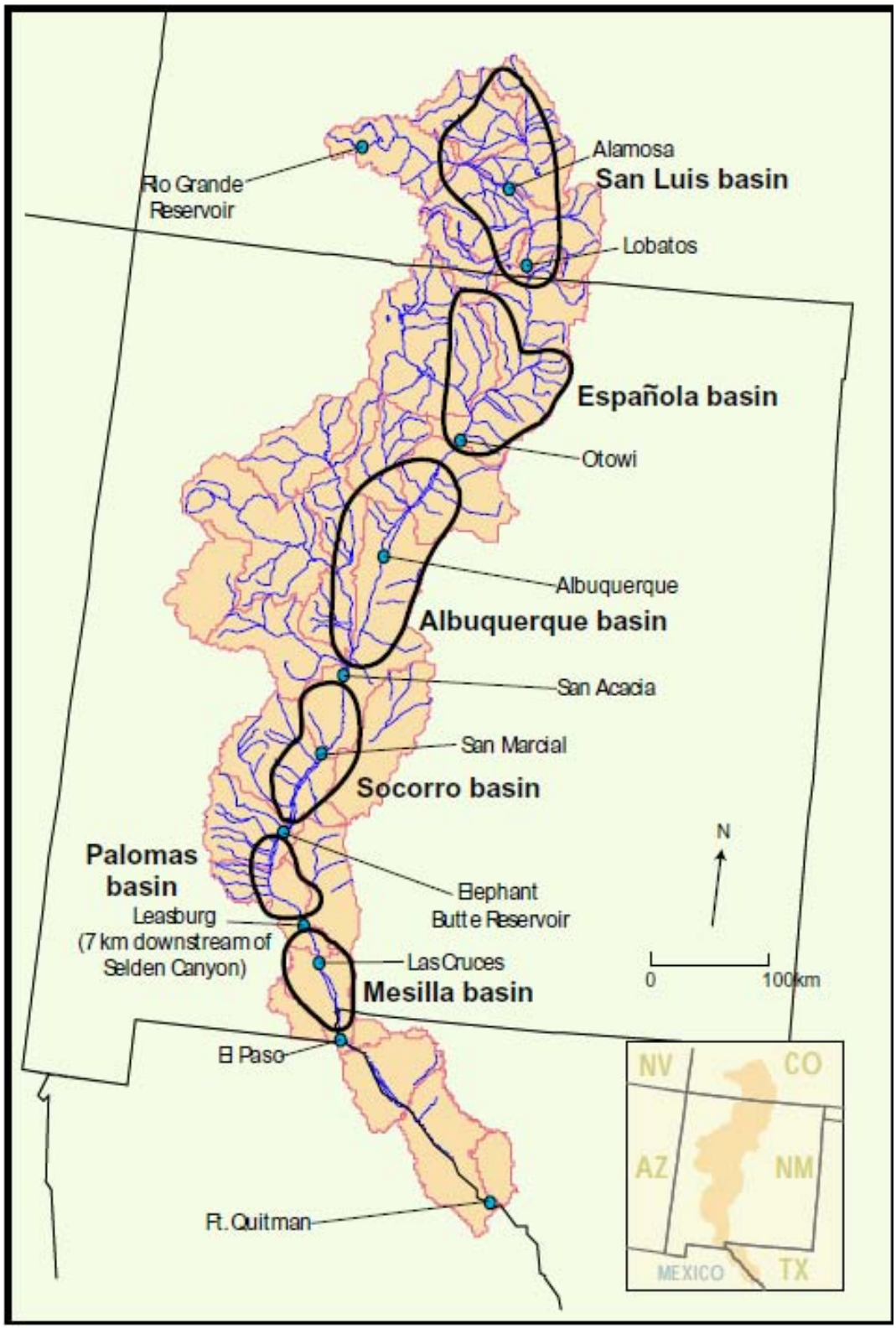

Figure 2.5. Map of the Rio Grande Basin with sedimentary basins outlined. [*Mills, 2003*]

2.4 Anthropogenic Features of the Rio Grande

Many man-made alterations affect the natural flow of the Rio Grande. Reservoirs impede flow and store quantities of water to negate the effects of drought, sustain agriculture, and produce energy. A complex network of drains and canals also affects river flow through diversion of water away from the main channel, onto agricultural fields and returns to the river as runoff or groundwater. As referred to in this thesis, the irrigation network consists of canals and drains that distribute and return water to the Rio Grande. A canal is that part of the network that diverts water from the Rio Grande for distribution to agricultural fields. A drain is classified as the part of the irrigation network that collects agricultural runoff and ground water than transports the water back to the Rio Grande. The following section will discuss the history and purpose of these anthropogenic alterations as well as present a brief summary of water rights.

2.4.1 Water Distribution

According to New Mexico Statutory Chapters: Chapter 27 Water Law, Rio Grande water belongs to the public at large, although it may be diverted for beneficial uses such as irrigation, commercial or municipal. Individual water users are supplied with Rio Grande water in ranked order based on the date their water claim was established. However, each state has an obligation by law to send a particular quantity of water by way of the Rio Grande to the down-stream bordering state (or nation as in the case of Texas to Mexico) [*Rio Grande Compact Commision*, 1999]. The Rio Grande Compact, an agreement between Colorado, New Mexico and Texas, mandates

delivery quantities on the Rio Grande. The Compact was established in 1938 with the goal of equitably distributing Rio Grande water to the three states and Mexico. The quantities of water delivered to each state as well as the quantity delivered to Mexico are regulated under the Compact agreement. Required quantities, which vary depending on water supply, are established based on measured discharge at specific gaging stations [*Johnson and Shoemaker*, 2002; *Rio Grande Compact Commission*, 1999]. Key locations on the Rio Grande continue to be extensively monitored to determine the quantity of water that must be delivered to the downstream entity. Over the past century chemical data has been collected periodically to monitor the quality of Rio Grande water. The Compact only vaguely mentions that the downstream delivered water must be of "good" quality.

2.4.2 Irrigation and Drainage Network History

As early as the sixteen hundreds, New Mexican lands were irrigated with water diverted from the Rio Grande. Pueblo Indians were the first regional farmers supplying water through primitive, single community canals. Spanish influence in the 17th century expanded these solitary canals into a large-scale canal network which provided water and replenished topsoil on agricultural lands [*Scurlock*, 1998]. *Scurlock* [1998] estimated roughly 26,000 acres were irrigated from 22 ditches in the Middle Rio Grande (from Cochiti Dam to the area that became Elephant Butte Reservoir) in the early 1600s (Table 2.1). The irrigation network grew until 1880, when previously irrigated lands began to become unusable due to a rise in the local ground-water table and salt accumulation in shallow soils [*Scurlock*, 1998]. In 1880, almost 44,000 acres

were receiving water from Rio Grande diversions. By 1896, the irrigated acreage had fallen to 32,000 then fluctuated well below 50,000 acres until the 1940's [*Wozniak*, 1987]. According to an Office of the State Engineer report, approximately 60,000 acres (or 30%) of agricultural lands between Cochiti and San Marcial were no longer fertile in 1918 [*Scurlock*, 1998]. Reported causes for such a decline in irrigated acreage were three-fold: a rising water table (measuring 6 inches below ground surface in many parts of the Middle Rio Grande in 1912), salt accumulation, and increased water diversion in the San Luis Valley [*Scurlock*, 1998]. Lands that were irrigated but poorly drained accumulated solutes in the soil through evaporation. When irrigation water evaporates, salts remain in the soil or infiltrate into the ground water causing many soils to become saline. A complete drainage system to mitigate these agricultural dilemmas was not established until the 1930's.

Table 2.1. Irrigated agriculture in the Middle Rio Grande Valley. [*Scurlock*, 1998; *Wozniak*, 1987]

Year	No. of Ditches	Irrigated Acreage
1600	22	25,555
1880	82	44,000
1896	71	32,000
1910	79	45,220
1918	55	47,000
1925	60	40,000
1942	8*	60,000

* = Number of Main Canals

2.4.3 Anthropogenic Structures arranged by Geography

To minimize the effect of drought, dams and reservoirs were constructed throughout the basin. Beginning with the construction of Elephant Butte Dam in 1916,

the Rio Grande basin was able to support expanded agricultural activities as well as a growing population. Additional dams and irrigation diversions were added along the entire Upper Rio Grande throughout the twentieth century. The current system within the study area consists of three major dams (Cochiti, Elephant Butte, and Caballo) and six diversion dams (Angostura, Isleta, San Acacia, Percha, Leasburg and Mesilla) operated by federal government agencies and local irrigation districts. These structures store and release water for irrigation and protect against flooding. The quantity of diverted water is monitored and controlled through gaging stations, however, irrigation return flow is largely ungaged due to the nature of water rights appropriations [*Mills*, 2003].

2.4.3.1 Rio Grande Headwaters to Cochiti Lake

The oldest dam on the Rio Grande sits high in the headwaters above all of the irrigation and major settlements (Figure 2.6). The Rio Grande Reservoir dam was constructed in 1911 for the storage of irrigation water. Controlled by the San Luis Valley Irrigation District (established 1905), the reservoir can hold up to 52,000 acre-feet (6.4×10^7 m^3) (Table 2.2) and store snowmelt runoff during the non-irrigation season (November – March). Reservoir releases supply agricultural land and the Alamosa National Wildlife Refuge [*USBR*, 2008].

Southern Colorado farmers utilized individual diversion canals from smaller tributaries prior to 1870, which were vastly expanded during the 1880's with an extensive network of canals that routed water from the main channel of the Rio Grande [*NRC*, 1938]. Acreages in this region were abandoned in the early twentieth century due to a rise in the local ground water table. Vacated acreages were reclaimed once a

large-scale drainage project was completed in 1921 [*NRC*, 1938]. By the early 1930s over 400,000 acres in the San Luis Valley were irrigated with Rio Grande water [*NRC*, 1938]. Modern usage requires almost one million acre-feet to irrigate 645,000 acres of cropland (data from 1990, still a reasonable estimate) [*Ellis*, 1993]. The Colorado Division of Water Resources has closely monitored the flow of Rio Grande water into irrigation ditches since 1950, but many agricultural-drain return flows remain ungaged.

The only federal water project in the Colorado portion of the Rio Grande is the San Luis Valley Project. Large quantities of Rio Grande water were diverted for irrigation in the San Luis Valley making it difficult for Colorado to meet its Compact obligation. The San Luis Valley Project was established in 1940, such that Colorado could continue to use Rio Grande water for irrigation as well as meet Compact obligations. By way of the Franklin Eddy Canal (or sometimes referred to as the Closed Basin Canal), closed-basin ground water is routed into the Rio Grande [*CDWR*, 2000]. Since the Closed Basin water is derived from ground water wells in a hydrologically closed system, the water carries a greater amount of total dissolved solids than that carried in the river channel, thus creating water quality concerns for downstream entities. The Closed Basin Canal is gaged and water quality parameters (particularly TDS) are monitored by the U.S. Bureau of Reclamation (USBR).

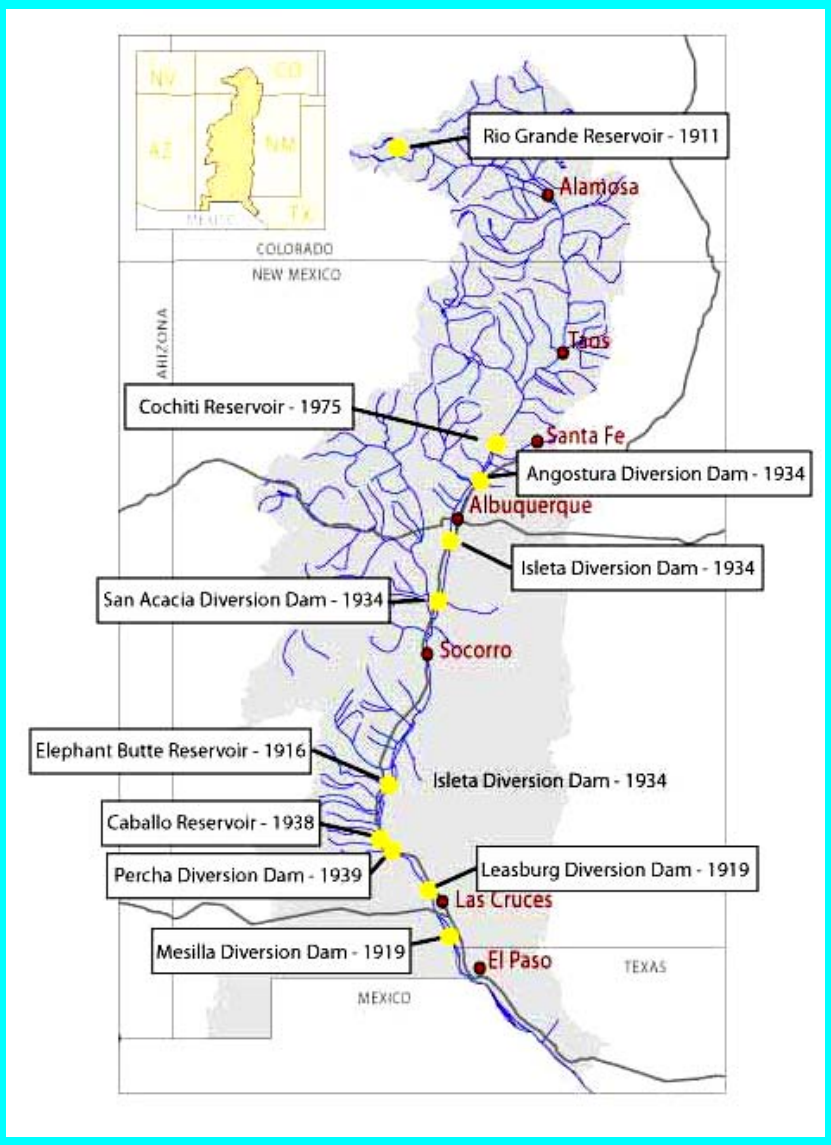

Figure 2.6. Reservoir and diversion installation dates along the upper Rio Grande. [*USBR*, 2008]

Table 2.2. Reservoir and diversion: capacity, managing authority, and length of reservoirs and diversion dams on the Rio Grande. [*USBR*, 2008].

Reservoir	Capacity (m^3)	Managing Authority	Length (m)
Rio Grande	6.4×10^7	San Luis Valley Irrigation District	ND
Cochiti	7.2×10^8	US Army Corps of Engineers	32,180
Elephant Butte	2.7×10^9	US Bureau of Reclamation	64,000
Caballo	4.2×10^8	US Bureau of Reclamation	1,390

Dam	Diversion Capacity (m^3/s)	
Angostura	0.18	Middle Rio Grande Conservancy District
Isleta	0.30	Middle Rio Grande Conservancy District
San	0.08	Middle Rio Grande Conservancy District
Percha	ND	US Bureau of Reclamation
Leasburg	ND	US Bureau of Reclamation
Mesilla	ND	US Bureau of Reclamation

Note: ND indicates that the information was unavailable.

2.4.3.2 Colorado-New Mexico Border to Cochiti Lake

In the section between the Colorado-New Mexico border to Española, the river flows naturally without anthropogenic interference. Between Española and Cochiti Lake, water is diverted through numerous small acequias for irrigation. Native American Pueblos in this area also divert small quantities of water for irrigation.

2.4.3.3 Middle Rio Grande: Cochiti to Elephant Butte Reservoir

The nineteenth-century irrigation networks influenced by the Spanish still operate today in this region, although with major modification. The Middle Rio Grande Conservancy District (MRGCD) was established in 1928 and began construction two years later on an extensive irrigation network to control flooding, drainage and irrigation [*NRC*, 1938]. By 1935, the MRGCD constructed four diversion dams: Cochiti, Angostura, Isleta and San Acacia [*MRGCD, 2003*]. These diversion dams route Rio Grande water into the irrigation networks for application to agricultural fields. At

the northernmost end of this region, the U.S. Army Corps of Engineers (USACE) installed Cochiti Reservoir in 1975. With a capacity of 50,000 acre-feet (7.2×10^7 m^3), this earthfilled dam was built to control the spring floodwaters and sediment [*USACE*, 2003]. The reservoir is basically a flow-through system in both winter and summer [*Mills, 2003*]. A schematic of the current Middle Rio Grande irrigation network is presented in Figure 2.7.

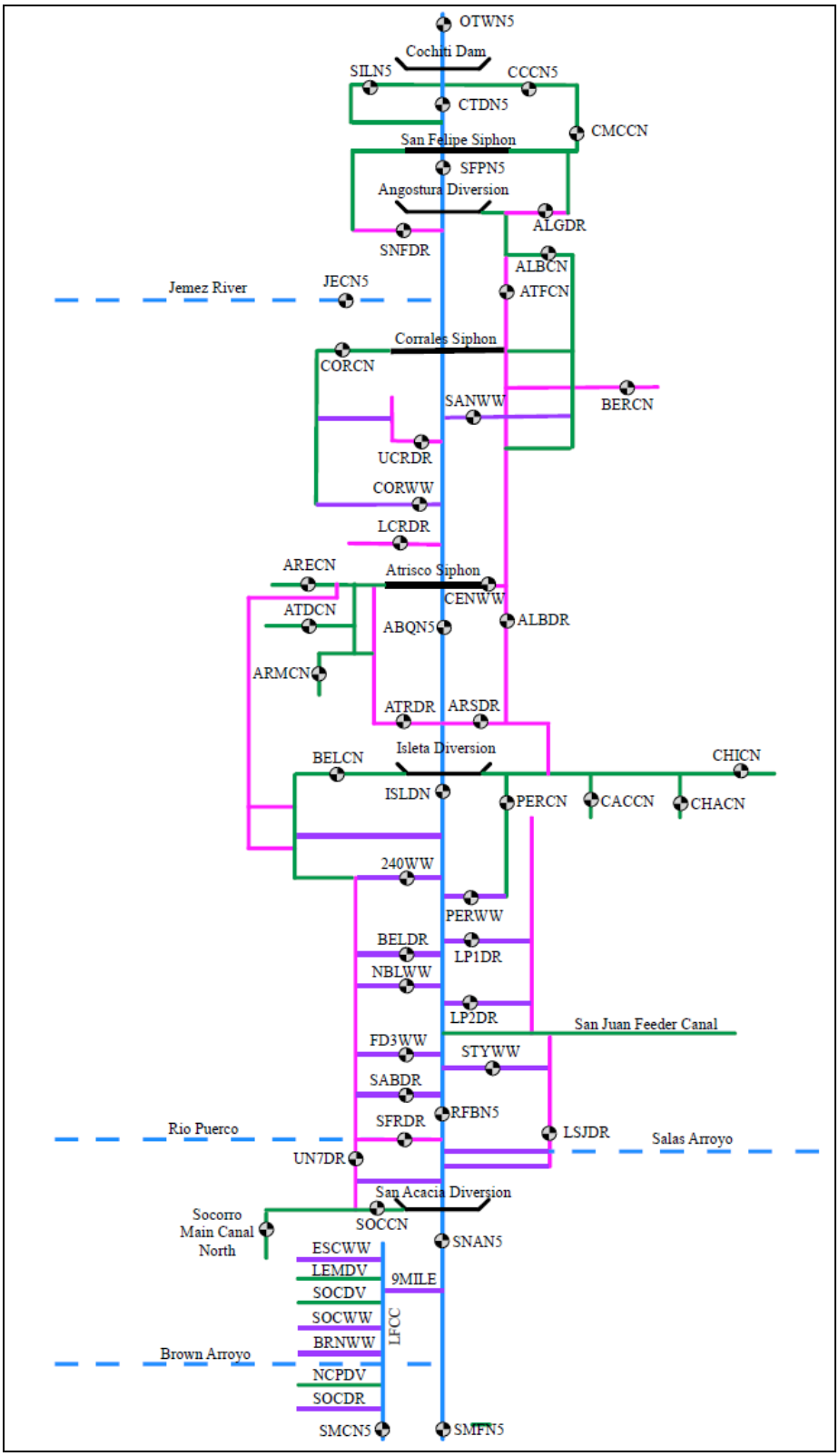

Figure 2.7a. Generalized schematic of the Middle Rio Grande irrigation network. [*Papadopulos and Associates*, 2002b]. Symbol identifications are presented in Figure 7b.

Existing and Planned Gaging Stations for Monitoring Key MRGCD Irrigation System Flows

Table 3.3 Cochiti Division

Gage Name	Gage ID	Operator	Gage Purpose	Period of Record
Cochiti East Side Main Canal	CCCN5	USGS	Canal Heading	1954 - present
Sili Main Canal	SILN5	USGS	Canal Heading	1954 - present
Approximately 10 - 14 return flow points	--------	---------	Returns to River	TBD
Cochiti Main at San Felipe	CMCCN	MRGCD	mid-reach	(1954) 1974 - present

Table 3.4 Albuquerque Division

Gage Name	Gage ID	Operator	Gage Purpose	Period of Record
Albuquerque Main Canal	ALBCN	MRGCD	Canal Heading	1974 - present
Atrisco Feeder Canal	ATFCN	MRGCD	Canal Heading	1974 - present
Algodones Riverside Drain	ALGDR	MRGCD	Return from Cochiti Div.	1974 - present
Arenal Main Canal	ARECN	MRGCD	Central Ave. X-Section	1974 - present
Armijo Acequia	ARMCN	MRGCD	Central Ave. X-Section	1958 - present
Atrisco Ditch	ATDCN	MRGCD	Central Ave. X-Section	1958 - present
Albuquerque Riverside Drain @ Central Avenue	ALBDR	MRGCD	Central Ave. X-Section	1954 - present
Corrales Main Canal	CORCN	MRGCD	Secondary Canal	1974 - present
Upper Corrales Riverside Drain	UCRDR	MRGCD	Drain to River	2001 - present
Corrales Main Canal Wasteway	CORWW	MRGCD	Wasteway to River	1997 - present
Central Avenue Wasteway	CENWW	MRGCD	Wasteway to River	2000 - present
Atrisco Riverside Drain	ATRDR	MRGCD	Drain to River	1997 - present
Lower Corrales Riverside Drain	LCRDR	MRGCD	Drain to River	2000 - present
Albuquerque Riverside Drain	ARSDR	MRGCD	Drain to River	1997 - present
Sandia Lakes Wasteway	SANWW	MRGCD	Wasteway to River	2000 - present
Bernalillo Acequia	BERCN	MRGCD	Secondary Canal	2001 - present

[1]This gage also forms the basis for estimating return flow to the river from this drain.
[2] Diversions from the Low Flow Conveyance Channel gaged intermittently by USGS.
[3] MRGCD has a new gage here beginning 2001.
TBD - the installation date has not yet been established.

Figure 2.7b. Middle Rio Grande drains and abbreviations used in Figure 7a. [*Papadopulos and Associates*, 2002b].

The Low-Flow Conveyance Channel (LFCC) was built in 1959 and extends from San Acacia to Elephant Butte Reservoir. Built in a time of extreme drought, the LFCC was designed to more effectively transport New Mexico Rio Grande water into Elephant Butte Reservoir and ultimately to fulfill Rio Grande Compact obligations to Texas [*Towne*, 2007]. The narrow and deep LFCC decreased evaporation by reducing surface area and draining shallow ground water, especially in the years following installation, and thereby increased the quantity of water entering Elephant Butte. Diversions of river water in the LFCC at San Marcial began in 1953 and at San Acacia in 1960 [*Towne*, 2007]. The LFCC also served to drain waterlogged agricultural areas

in the 1950's and 1960's when the LFCC became the hydraulic low point in the area. This flushing of shallow ground water into the Rio Grande affected historic Rio Grande chemistry as reflected in decadal average data for this time period. By the 1980s, diversion from the Rio Grande into the LFCC was halted. Presently the Conveyance Channel carries only agricultural return flow and shallow ground water into Elephant Butte Reservoir. However, due to installation of the LFCC, the natural hydraulic gradient is reversed at certain locations pulling water away from the river. To assure survival for specific aquatic life, especially the Rio Grande Silvery minnow, water is pumped from the LFCC back into the Rio Grande during periods of low river stage [*Mills*, 2003].

2.4.3.4 Elephant Butte Reservoir to El Paso

Designed to store runoff for irrigation, the Bureau of Reclamation completed Elephant Butte Reservoir in 1916. This reservoir, the largest man-made structure impeding natural flow along the Rio Grande, stands 91.7 meters high, 510 meters long and has the capacity to hold 2,210,290 acre-ft ($2.7x10^9$ m^3) of water [*USBR*, 2008,]. Elephant Butte Reservoir is supplied by both the main channel of the Rio Grande and the LFCC where flow is captured, stored, and released for irrigation on a strict schedule monitored by the USBR. The large surface area created by the reservoir greatly enhances the amount of water lost through evaporation each year. On average approximately 100,000 acre-feet ($1.2x10^8$ m^3) of water were lost from Elephant Butte Reservoir each year between 1934 and 2005. Rio Grande discharge below the dam, controlled almost entirely by reservoir releases, is the measured quantity of water

delivered to Texas under the Rio Grande Compact. The U.S. Bureau of Reclamation, under the Rio Grande Project, added Caballo Reservoir to the river in 1938. The 29.3 meter high, 1,399 meter wide structure has a maximum capacity of 343, 9000 acre-feet ($4.2x10^9$ m^3) [*USBR*, 2008]. Caballo reservoir created additional storage for irrigation in the El Paso Valley, provided increased control over releases from Elephant Butte, and regained the storage lost from sediment accumulation within Elephant Butte. Under current conditions, Elephant Butte is used for power generation through the winter with Caballo as a holding tank until summer when the water is released for irrigation [*USBR*, 2008]. Both reservoirs also serve as recreational parks.

The amount of time water is held within a reservoir may affect the quantity and quality of the released water. *Mills* [2003] calculated a stored residence time of 22 days (based on data from 1974-2002), 1.33 years (1915-2002) and 46 days (1939-2002) for Cochiti, Elephant Butte and Caballo respectively. Cochiti and Caballo are considered flow-through reservoirs meaning the residence time spent in the reservoir is relatively short, with entering water likely released that same season. Residence times on average are markedly shorter during the summer than the winter because higher volumes of water are released during the April-October irrigation season. In contrast, water remains stored in Elephant Butte reservoir for multiple seasons, impacting Rio Grande chemistry downstream of the dam. The effects of Elephant Butte Reservoir on Rio Grande chemistry are discussed in Chapter 5.

2.4.4 Wastewater Treatment Plants

The Rio Grande accepts wastewater discharge from cities, towns and industries (Table 2.3). Only a few of these discharges contribute significant flow to the river. Of the highest discharging entities, only four directly emit into the Rio Grande: the Rio Rancho wastewater treatment plant, the Southside Water Reclamation Plant of Albuquerque (ABQ WWTP), the Jacob Hands wastewater treatment plant in Las Cruces and the Northwest Wastewater Treatment Plant in El Paso. The other waste discharges enter through tributaries or agricultural drains which eventually meet the Rio Grande. Due to a lack of chemical data and relatively small discharges, the Rio Rancho and Las Cruces treatment plants were omitted from this analysis. The El Paso treatment plants were not included as they lie outside the study area south of Sunland Park USGS gaging station. Thus only the ABQ WWTP will be discussed and is included in subsequent analyses.

The ABQ WWTP traces installation back to 1885 [*Lucero*, 2008]. By 1923, the plant capacity was 2 million gallons per day. From 1919 to 1927, after removal of any solid waste, remaining water was discharged directly into the Rio Grande. In 1961, a second plant was constructed and both plants operated at a combined capacity of 52 million gallons per day [*Lucero*, 2008]. Currently the plant operates under a National Pollutant Discharge Elimination System (NPDES) permit from the U.S.EPA, which allows effluent discharge to the Rio Grande when water quality requirements are met.

Table 2.3. Wastewater Dischargers

Elephant Butte SP
Gadsden School
Bosque Farms
Los Lunas Pen
LA County White Rock
Rio Communities
Hatch
Taos Ski Valley
Red River
Santa Teresa
El Paso Elec
Anthony
Rio Rancho no. 3
LANL
LA County Bayo
Socorro
Sunland Park
T or C
Belen
Española
Los Lunas
Taos
PNM Reeves
Rio Rancho no. 2
Santa Fe
Las Cruces
Albuquerque Southside WWTP
El Paso Northwest WWTP
El Paso Haskell Street WWTP
El Paso Roberto Bustamante WWTP

2.5 Summary

Human activity has utilized and impacted the water flow of the Rio Grande since the early seventeenth century. Present day main channel discharge is significantly diverted in numerous locations along the river from the headwaters in Colorado to the southern end of the study area in El Paso. Manipulations consist of dams and reservoirs, the irrigation network and wastewater discharges. Each of these anthropogenic alterations impact the chemistry and hydrologic system of the Rio Grande. Hydrologically the structures raise or lower the ground water table, increase evaporation, increase possible soil interactions and affect the residence time within the basin. These structural modifications continue to influence the behavior of major cations and anions within the Rio Grande. Over the past century, many studies have investigated salinization of the Rio Grande with the conclusion that anthropogenic structures have contributed to the salt increase with distance downstream. In particular, irrigated agriculture was widely cited as the primary cause of salinization.

CHAPTER 3
PREVIOUS SALINIZATION STUDIES

Salinization of the Rio Grande and the surrounding farmlands has been a documented concern since the late eighteen hundreds when poorly drained agricultural soils became unusable. For the better part of the twentieth century, researchers have noted and hypothesized explanations for the increased salinization with distance downstream. Much of the early research [*NRC*, 1938; *Lippincott*, 1939, *Wilcox*, 1957; *Trock et al*., 1978] named effects of irrigated agriculture as the primary cause for the salinity increases. In contrast, more recent studies [*Moore and Anderholm*, 2002; *Mills*, 2003; *Lacey*, 2006] attributed salinization to a suite of factors including wastewater treatment plant effluent, natural tributary influxes and deep saline brine as well as the contribution from irrigated agriculture.

3.1 Pre-Elephant Butte Reservoir

During the period from 1905-1907 the United States Geological Survey (USGS) collected water, chemistry and discharge data at two Rio Grande locations, San Marcial and El Paso [*Stabler,* 1911]. This dataset is invaluable, as it provides discharge and chemistry prior to the major anthropogenic river alterations of Elephant Butte Reservoir and the current extended drainage network. Analyses were conducted on samples from these locations for TDS, chloride, bicarbonate, sulfate, calcium, magnesium, and a combined value of sodium and potassium approximately 10 times each month.

Concentrations were multiplied by the discharge in order to compute the average discharge-weighted solute load. (For definition of discharge-weighted average solute load, see Chapter 4). Solute results are presented in Table 3.1. At many Rio Grande locations, significantly higher discharge was measured during the 1900s compared to recent discharges (illustrated for Lobatos in Figure 3.1). The increased discharge can be caused by climatic conditions, specifically larger storm events or greater precipitation during these years. In addition, higher Rio Grande flows could be attributed to the absence of flood control structures such as Elephant Butte Reservoir and the extended irrigation canal network.

Table 3.1. Major ion concentration (calcium, magnesium, sodium, sulfate, bicarbonate and chloride) comparison between *Stabler* [1911] (data from 1905-1907), *NRC* [1938] (data from 1931-1936) and *Wilcox* [1957] (split into 3 decades: 1934-39, 1940-49, and 1950-59). Values are in units of mg/L.

Ca	Stabler (1911)	NRC (1938)	Wilcox (1934-1939)	Wilcox (1940-1949)	Wilcox (1950-1959)
Lobatos		28		26	
Otowi		44	40	37	43
San Marcial	52	84		58	78
EBD		75	64	63	64
El Paso	78	106	91	87	84

Mg	Stabler (1911)	NRC (1938)	Wilcox (1934-1939)	Wilcox (1940-1949)	Wilcox (1950-1959)
Lobatos		7		6	
Otowi		8	8	7	7
San Marcial	11	18		13	13
EBD		16	14	14	17
El Paso	12	23	20	20	19

Na	Stabler (1911)	NRC (1938)	Wilcox (1934-1939)	Wilcox (1940-1949)	Wilcox (1950-1959)
Lobatos		23		19	
Otowi		23	19	18	19
San Marcial	44	98		69	72
EBD		93	76	80	81
El Paso	61	187	153	155	144

SO4	Stabler (1911)	NRC (1938)	Wilcox (1934-1939)	Wilcox (1940-1949)	Wilcox (1950-1959)
Lobatos		48		47	
Otowi		62	58	54	51
San Marcial	101	244		155	175
EBD		187	181	162	175
El Paso	129	316	266	269	258

HCO3	Stabler (1911)	NRC (1938)	Wilcox (1934-1939)	Wilcox (1940-1949)	Wilcox (1950-1959)
Lobatos		48		89	
Otowi		70	60	53	70
San Marcial	128	89		81	123
EBD		91	74	88	77
El Paso	184	122	103	109	99

Cl	Stabler (1911)	NRC (1938)	Wilcox (1934-1939)	Wilcox (1940-1949)	Wilcox (1950-1959)
Lobatos		11		7	
Otowi		10	9	6	6
San Marcial	31	64		40	53
EBD		54	48	56	57
El Paso	46	169	136	130	125

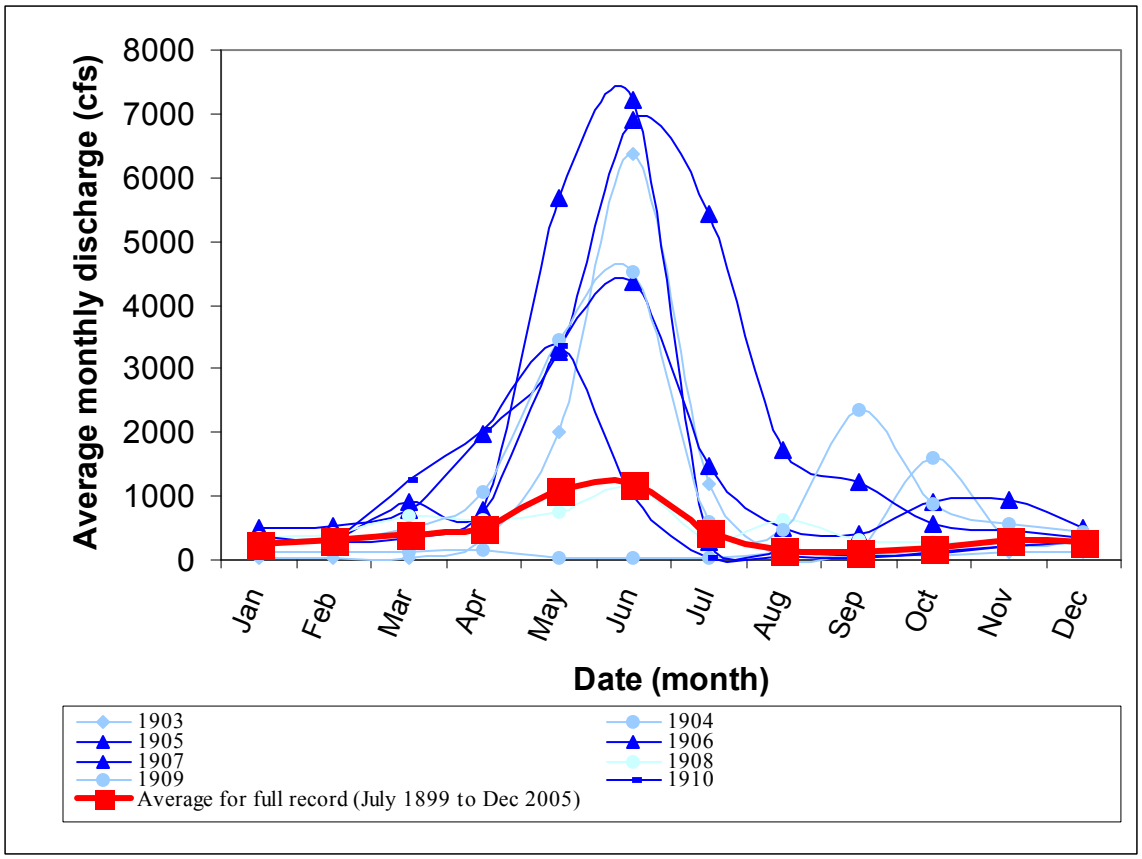

Figure 3.1. Discharge comparison between 1900's and full record average (1899 to 2005) at the Lobatos USGS gage. Discharge units are labeled cfs to represent ft^3/s.

3.2 River Chemistry: Post-Drainage Network

Two data sources contained discharge and chemistry information from decades after the installation of the more complex drainage network completed in 1928. The National Resources Committee (NRC) [1938] reported on water-related issues in the Upper Rio Grande. The report included data for the period from 1931-1936 at many Rio Grande locations between Lobatos and Fort Quitman, of which five are within the study area for this thesis: Lobatos, Otowi, San Marcial, Elephant Butte and El Paso. Chemical data are shown in Tables 3.1 and 3.2. The authors attributed salinity to irrigation-enhanced flushing of shallow ground water. Salinity increases above San

Acacia were said to be from natural tributaries and concentration through evaporation, although tributary chemistries were not investigated as part of this report.

Lippincott [1939] presented TDS data at four locations (Table 3.2). Sampling details were ambiguous as to whether these data represent long-term averages or were collected in a single sampling event. Total dissolved solids increased down the river from Del Norte, Colorado to Ft. Quitman, Texas. According to *Lippincott* [1939], these increases could be explained by agricultural recycling of Rio Grande water.

Over the span of 30 years from 1934-1963, the U.S. Salinity Laboratory [*Wilcox, 1957*] collected chemical data at Otowi, San Marcial, Elephant Butte Dam, Caballo, Leasburg, El Paso and Fort Quitman. Water samples were taken daily by USBR employees and poured into a gallon jug; at the end of the month the composite of all daily samples was sent to Salinity Laboratory for analysis. Discharge, TDS, calcium, sodium, magnesium, chloride, sulfate and bicarbonate data from both studies are presented in Tables 3.1 and 3.2. Higher solute concentrations were observed in the Rio Grande during the 1930's and 1940's. The *NRC* concentrations were on average 50% higher than those from 1905-1907 and were usually higher than the data collected by *Wilcox* [1957]. Prior to 1930, an extensive drainage network was installed resulting in stored solutes being flushed from soil and the shallow aquifer [*Hendrickx*, 1998]. *Wilcox* [1959] replicated the ideas described by the *NRC* [1938], and later corroborated by *Hendrickx* [1998], that downstream salinization was due to lower flow rates in the 1930's and flushing of built-up salt from agricultural lands. After 1945, solute loads decreased because the accumulated salts had been flushed from the system and the ground water table had already been lowered, such that less ground water entered the

drainage network [*Hendrickx*, 1998]. In addition, *Hendrickx* [1998] noted low chloride concentrations near El Paso during the mid-1950s with a sudden concentration peak in 1958. He concluded the low concentrations in the 1950s where caused by low irrigation due to drought conditions and that accumulated salt was subsequently flushed in 1958. *Hendrickx* [1998] also stated that sufficient leaching had occurred in the 25 years following drain installation such that fossil salts have little effect on current salinity behavior in the Leasburg and El Paso regions. The hypothesis that flushed salts contributed to the observed solute increases will be explored further in Chapter 5.

Cation and anion concentrations increased from Otowi to El Paso; however, the chemical composition changed significantly. The relative percent of calcium and magnesium dropped significantly, with sodium becoming the dominant cation by El Paso. Similarly, bicarbonate percentages dropped with distance downstream as well. The bicarbonate dropped at roughly the same rate as calcium and magnesium, in terms of equivalents. Therefore, *Wilcox* [1957] concluded calcium and magnesium carbonates were precipitating. Unfortunately, he did not speculate on where the proposed precipitation might occur. Discharge and chemical data comparisons are discussed in further detail in Chapters 4 and 5.

Table 3.2. Total dissolved solids (mg/L) at various locations along the Rio Grande.

Source:	Stabler [1911]	NRC [1938]	Lippincott [1939]	Wilcox [1957]	EPA [1978]
Years Studied:	1905-1907	1931-1936	1939	1934-1953	1918-1973
Del Norte	N/A	81	110	N/A	below 100
Otowi	N/A	253	N/A	221	200-300
San Marcial	340	610	427	449	482
EB Dam	N/A	595	N/A	478	N/A
Caballo Dam	N/A	N/A	N/A	515	504
Leasburg	N/A	640	N/A	551	558
El Paso	451	897	832	787	802
Ft Quitman	N/A	2023	2120	1691	1851

Note: N/A = no data was available

The U.S. Environmental Protection Agency (EPA) provided discharge weighted average annual TDS from 1918-1973 (Table 3.2) [*Trock et al*, 1978]. The authors identified a three-fold increase in TDS concentration from 504mg/L at Caballo to 1851mg/L at Ft Quitman. *Trock et al* [1978] also noted that TDS was high in agricultural drains. The authors attributed the salt increase to evaporative concentration from irrigation and shallow ground water flushing.

3.3 Irrigation Drainage Network Chemistry

Also reported in the *NRC* [1938] data is the average annual electric conductivity (ET) measured for drains within the Cochiti/Albuquerque, Belen and Socorro areas (Table 3.3). Electrical conductivity data was presented for irrigation canals, interior drains and riverside drains. The interior drains had the highest conductance, almost double that of the irrigation samples, which suggests a flushing of accumulated salt and shallow ground water as well as concentration due to evaporation.

Additional chemical data from drain samples was collected in 1930-1931 and was published in the University of New Mexico Bulletin by *Clark and Mauger* [1932].

In this study, 169 samples were collected over a two-year period from June 1930 to August 1931. The dates and number of samples collected are shown in Table 3.4. Chemical data from interior drains which directly transport irrigation tail water to the Rio Grande, are shown in Table 3.5. This data corroborated the EC results from *NRC* [1938], where it was noted that interior drains consistently contained higher concentrations of all major solutes than their counterpart riverside drains. High solute concentrations in the interior drains implied large amounts of salts in valley soils [*Clark and Mauger, 1932*]. Chemical variations between drains of the same type were speculated to be from land type (cultivated, uncultivated or swamp), drainage area, and/or the amount of water flowing within each drain. For example, the Isleta drain, which contained lower solute concentrations, traveled a greater distance through mainly cultivated lands in comparison to the Alameda and the Bosque drains, which had shorter flow paths and flowed through swamp and uncultivated lands. Riverside drains carried larger quantities of water, which diluted concentrations and damped evidence of salt flushing. Moreover, the rising ground water table discussed in the previous chapter was lowered by ground water removal through the drainage system [*Clark and Mauger, 1932*].

Table 3.3. Electrical conductivity values from irrigation drains, data from 1931-1936 [*NRC*, 1939].

	Mean Conductance K * 10^5 at 25 degrees C		
Divisions	Irrigation Water	Riverside Drains	Interior Drains
Cochiti and Albuquerque	37.9	52.7	88.5
Belen	53.2	71.1	163
Socorro	89	110.7	155

Table 3.4. Riverside and interior drains of the Middle Rio Grande: sample information. [*Clark and Mauger*, 1932]

Riverside Drains	Sample Dates: Start	Sample Dates: End	Number of Samples
Algodones	8/11/1930	7/13/1931	12
Bernalillo	8/11/1930	8/13/1931	13
Corrales	2/26/1931	8/17/1931	6
Albuquerque	6/7/1930	8/13/1931	16
Albuquerque Barr	7/7/1930	8/13/1931	11
Atrisco	2/26/1931	3/13/1931	7
Peralta	9/12/1930	8/15/1931	12
Belen	10/13/1930	8/13/1931	9
San Juan	10/9/1930	8/17/1931	11
Lemitar	8/14/1930	8/14/1931	12
San Antonio	8/14/1930	8/14/1931	11
Interior Drains:			
Alameda	9/10/1930	6/23/1931	9
Isleta	7/9/1930	8/13/1931	15
Bosque	8/12/1930	8/14/1931	13

Table 3.5. Riverside and interior drains of the Middle Rio Grande: chemistry. [*Clark and Mauger*, 1932]

Riverside Drains	TDS (mg/L)	Cl (mg/L)	SO_4 (mg/L)	Na+K (mg/L)	Mg (mg/L)	Ca (mg/L)	HCO_3 (mg/L)	CO_3 (mg/L)
Algodones	380	15	88	40	20	56	166	19
Bernalillo	374	30	103	33	21	55	160	18
Corrales	352	28	84	53	14	55	160	6
Albuquerque	349	21	91	37	14	49	144	16
Albuquerque Barr	431	33	126	42	20	65	195	8
Atrisco	436	28	120	71	21	59	157	18
Peralta	422	30	118	59	22	59	182	14
Belen	425	28	141	44	22	66	181	7
San Juan	383	29	125	62	25	62	160	15
Lemitar	550	63	186	83	20	76	177	17
San Antonio	608	72	167	109	20	64	201	16
Interior Drains:								
Alameda	941	96	305	145	33	131	272	5
Isleta	680	51	247	125	21	99	230	11
Bosque	1756	236	605	298	40	160	261	7

3.4 River Chemistry: Recent

In 2001, *Williams* [2001] compiled historic data for the time period from approximately 1930-1995 from various sources (*Wilcox* [1957], *USGS* [2008] and *USBR* [2008]) on the Rio Grande between San Marcial and Ft. Quitman gaging stations. Supported statistically, *Williams* [2001] utilized an ion/TDS ratio to fill in months where solute concentration data was missing. In a few instances, a straight-line interpolation was used to fill in locations without data [*Williams, 2001*]. Salt-balance calculations were made for the following river reaches: San Marcial to Elephant Butte Dam, Elephant Butte Dam to Caballo, Caballo to Leasburg, Leasburg to El Paso, and El Paso to Ft Quitman. Results are presented for each reach in Figures 3.2, 3.3, 3.4 and 3.5 respectively; I have omitted the graph from El Paso to Ft Quitman as it is outside the focus area of this thesis. Salt balances were computed such that a positive balance indicated higher quantities at the upstream location. The salt balance was generally positive from San Marcial to Elephant Butte, which indicated an accumulation of salt in Elephant Butte Reservoir; however no evidence of salt minerals had been found in or around Elephant Butte [*Williams*, 2001]. *Williams* [2001] offered no explanation for the positive salt balance other than possible ground-water outflows that he classified as unlikely to be large enough to account for the magnitude of salt observed. Data from Elephant Butte Dam to Caballo (Figure 3.3) showed a negative salt balance for all constituents, except sulfate, which indicated that more solutes exited Caballo than entered the reach at Elephant Butte Dam. *Williams* [2001] suggested the trend might be explained by tributary inflow from storm runoff.

In the early to mid-1950s, the TDS balance remained constant, coinciding with a period of drought, which suggested that Caballo was basically a flow-through system. *Williams* [2001] noted but did not offer any explanation for the observed sulfate balance increase. From Caballo to Leasburg, the salt balance remained negative except for bicarbonate, which had a positive balance. The negative trend was ascribed to solute flushing from valley soils into the Rio Grande, and the positive mass balance for bicarbonate was theorized to be from precipitated carbonate minerals in local soils [*Williams*, 2001]. Between Leasburg and El Paso, the salt balance oscillated between positive and negative based on drought conditions. The lack of available surface water in the 1950s forced farmers to irrigate with ground water. The ground water, containing higher solute concentrations, was considered to have caused the observed spike in the TDS balance as well as lowered the flow in the drainage network [*Williams*, 2001]. A positive salt balance was first observed in the 1950s. Recent data from 1980 to 1995 also showed a positive mass balance, which may remain positive because of continued ground-water pumping for irrigation and municipal use [*Williams*, 2001]. Data compiled by *Williams* [2001] have been incorporated into the dataset for this thesis, thus these chemical results will be presented and further discussed in greater spatial and temporal detail in this work in Chapter 5.

Figure 3.2. Salt balance from San Marcial to Elephant Butte Dam. [*Williams, 2001*]

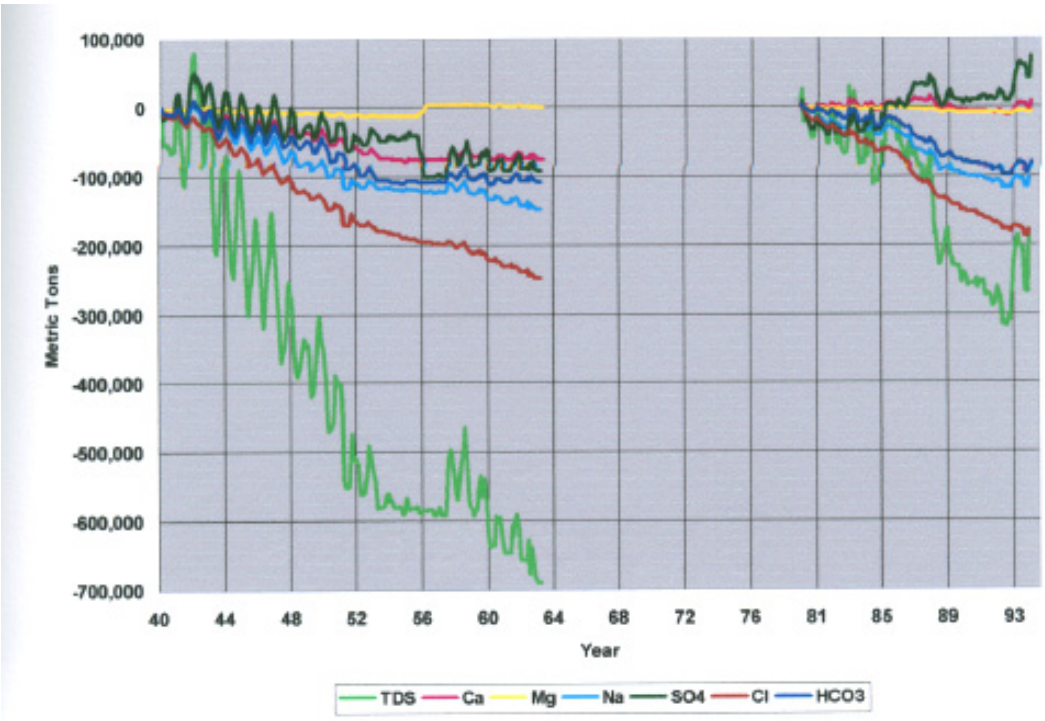

Figure 3.3. Salt balance from Elephant Butte Dam to Caballo. [*Williams, 2001*]

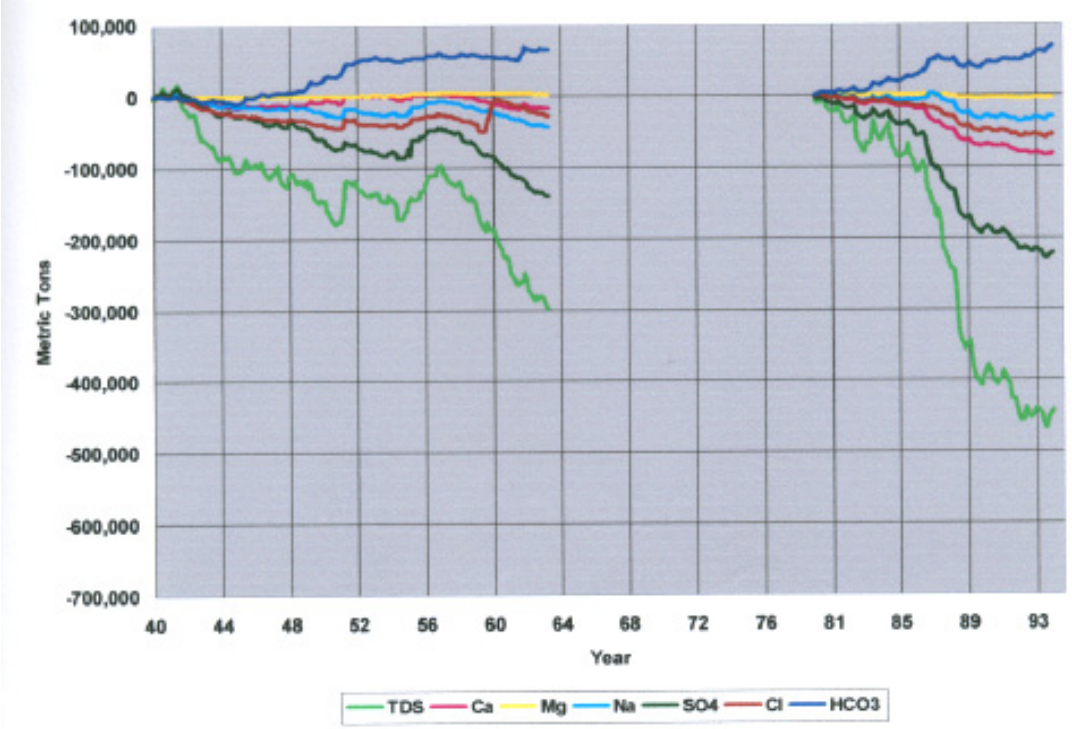

Figure 3.4. Salt balance from Caballo to Leasburg. [*Williams, 2001*]

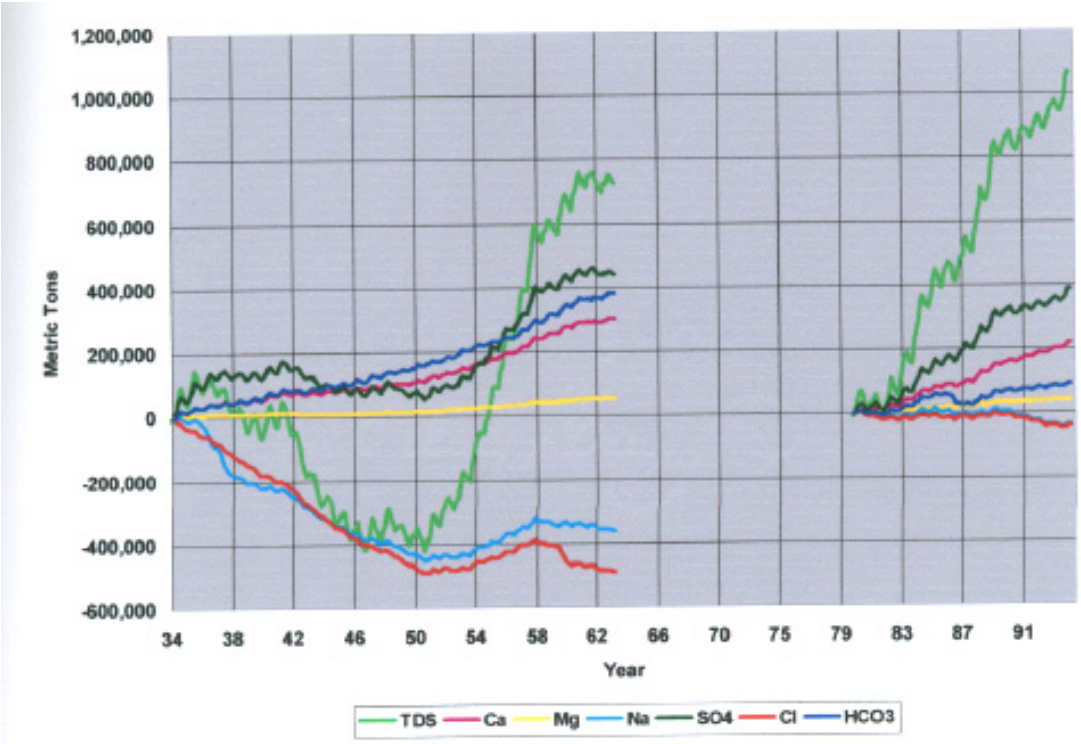

Figure 3.5. Salt balance from Leasburg to El Paso. [*Williams, 2001*]

Moore and Anderholm [2002] collected discharge and chemical data under the National Water Quality Assessment (NAWQA) program for the period between 1993 and 1995 from 12 USGS gaging stations and tributaries along the Rio Grande. Recent average TDS values paralleled with previous studies (Table 3.6). Salinity trends observed in the headwater regions were attributed to additions from the Closed Basin Canal, whereas the increase from Del Norte to Otowi was ascribed to natural tributaries, particularly the Rio Chama [*Moore and Anderholm*, 2002]. Although these salinity sources were not quantified, *Moore and Anderholm* [2002] suggested several factors that might have caused the observed increase in TDS load below Otowi, including wastewater treatment plant effluent, agricultural evapotranspiration, reservoir evaporation (Elephant Butte and Caballo), tributary contributions and saline groundwater seepage.

Table 3.6. Total dissolved solids load (kg/month).

Source:	NRC [1938]	Wilcox [1957]	Moore and Anderholm [2002]
Years Studied:	1931-1936	1934-1953	1993-1995
Del Norte	3.88E+06	No Data	3.83E+06
Otowi	2.18E+07	2.41E+07	2.65E+07
San Marcial	6.65E+07	3.87E+07	No Data
Elephant Butte Dam	4.62E+07	3.83E+07	No Data
Caballo Dam	No Data	4.08E+07	No Data
Leasburg	4.83E+07	4.15E+07	3.06E+07
El Paso	4.76E+07	4.19E+07	3.58E+07
Ft. Quitman	3.53E+07	3.48E+07	No Data

Previous studies agreed that salinity increased from the headwaters of the Rio Grande in Colorado through El Paso, Texas. Most of the studies concluded the increases were caused by evaporation and/or flushing of shallow groundwater, both of which are enhanced by irrigation of agricultural acreages. Salinity load and concentration both increased downstream, suggesting that evaporation was not the sole

source of the observed trend. *Hendrickx* [1998] reported that the accumulated salts should have been removed 30-40 years ago, concluding that it was unlikely that shallow ground water flushing was still dominant.

Mills [2003] postulated another explanation for this observed chemical trend. Focusing mainly on chloride and utilizing various natural chemical tracers including stable isotopes, the elemental ratio of chloride to bromide, and chlorine isotopes, *Mills* [2003] characterized and quantified salinization sources to the Rio Grande. *Mills* [2003] supported a hypothesis presented by *Phillips et al.* [2003], which stated that a significant portion of river salinization is derived from geologically controlled brine.

Mills [2003] compiled historic discharge, chloride and TDS data for 12 main-channel gaging stations and several tributaries along the Rio Grande from Lobatos, Colorado to Ft. Quitman, Texas. Gaging stations where data was collected are presented in Table 3.7. Historic data highlighted significant salinity increases at specific intervals between the most upstream (Lobatos) and downstream (Ft Quitman) stations (Figure 3.6). The interval increase in the chloride burden between Lobatos and San Felipe was credited to tributary inflow [*Mills, 2003*]. Chloride load doubled between San Felipe and Bernardo, which *Mills* [2003] attributed to inflows from the Jemez River and the Albuquerque wastewater treatment plant. The load increases from Bernardo to San Acacia were ascribed to an "unknown low-volume, high-chloride concentration source" [*Mills, 2003*]. Tributary flows from the Rio Puerco and Rio Salado, and discharges from the Low Flow Conveyance Channel increased the chloride load at Elephant Butte. As there are no natural tributaries in the section from Elephant Butte to Ft. Quitman, specific known sources could not be identified to account for this

load increase. In order to investigate the unknown salt sources and to characterize any component from geologic brine, high resolution sampling data was collected.

Table 3.7. Gaging stations with distance downstream. *Mills* [2003].

Label	Location	Distance (km)
A	Lobatos	256.9
B	Taos Junction	359.3
C	Otowi	430.9
D	San Felipe	496.4
E	Bernardo	630.7
F	San Acacia	655.3
G	San Marcial	731.1
H	Elephant Butte Dam	801.3
I	Caballo Dam	841.0
J	Leasburg	919.5
K	El Paso	1013.8
L	Ft. Quitman	1149.0

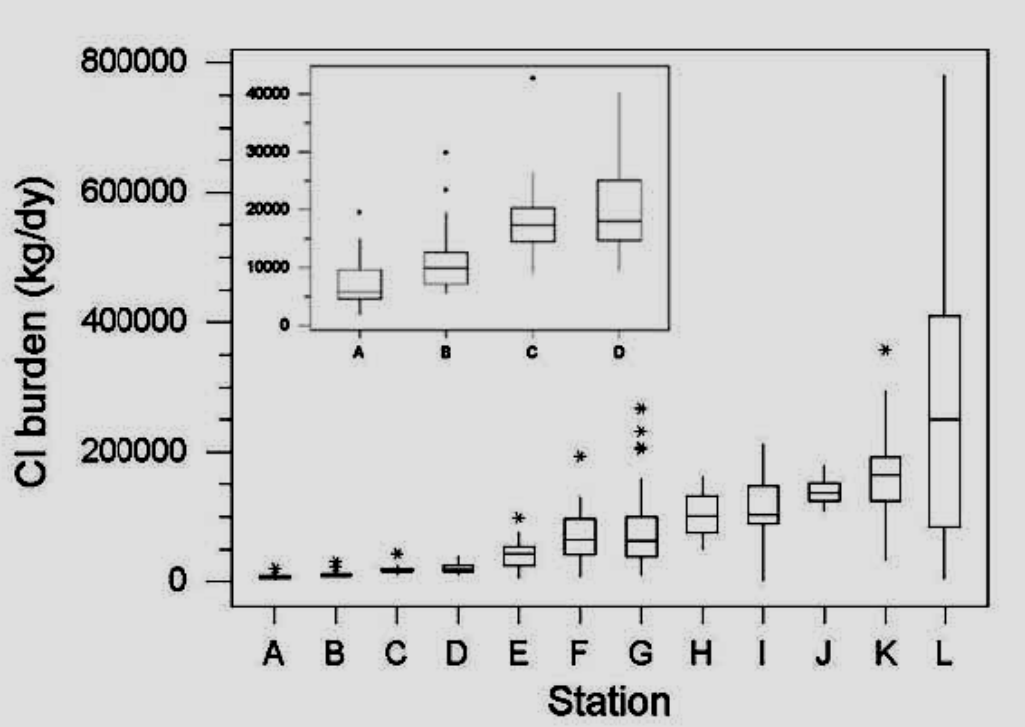

Figure 3.6. Average yearly chloride load from compiled historic data for main channel stations on the Rio Grande. A letter is assigned for each station and can be found in Table 7. The inset shows "the full extent of the data including outliers. Each box extends across the interquartile range from the 25th to the 75th percentile of the data. The line across the inside of the box represents the median. Whiskers extend to 1.5 times the interquartile range; outliers are shown by asterisks. Heavy black dots represent recent conditions from data collected . . . August 2001 or January 2002". [*Mills, 2003*]

To find additional salinity sources, graduate students at New Mexico Tech and the University of Arizona collected synoptic sampling data as a collaborative effort. The synoptic sampling was funded through SAHRA (Sustainability of semi-Arid Hydrology and Riparian Areas), a research organization funded by the National Science Foundation. Samples were collected biannually, each summer (mid-August) and winter (early January) from the summer of 2000 to the summer of 2006. Data was collected from 30-80 locations approximately every 100 km along the Rio Grande from Del Norte, Colorado to Fort Quitman, Texas, depending on the year. Sampling locations included the main channel of the Rio Grande, tributaries, drains and the Albuquerque wastewater treatment plant. Rio Grande locations were chosen to match the USGS gages and tributary locations. Drain, tributary and ABQ WWTP samples were collected at their point of entry into the Rio Grande. Only a limited number of river samples from early sampling data (2000 – 2002) were analyzed. Beginning in the summer of 2002, a number of drains and tributaries were added to the sampling campaign. The Albuquerque wastewater treatment plant was also added in later years. Each biannual sampling trip, the locations and chemical data remained consistent with the exception of slight variability due to weather conditions (frozen or dry water body or accessibility, i.e. flooding). Samples were analyzed for major anions and cations, TDS, pH, and dissolved oxygen as well as chlorine-36 and stable isotopes of hydrogen and oxygen. *Mills* [2003] analyzed data from two of these high-spatial-resolution sampling trips, August 2001 and January 2002. Chloride burdens from sampling trips were consistent with data from previous studies, namely the *NRC* [1938] dataset (Figure 3.7).

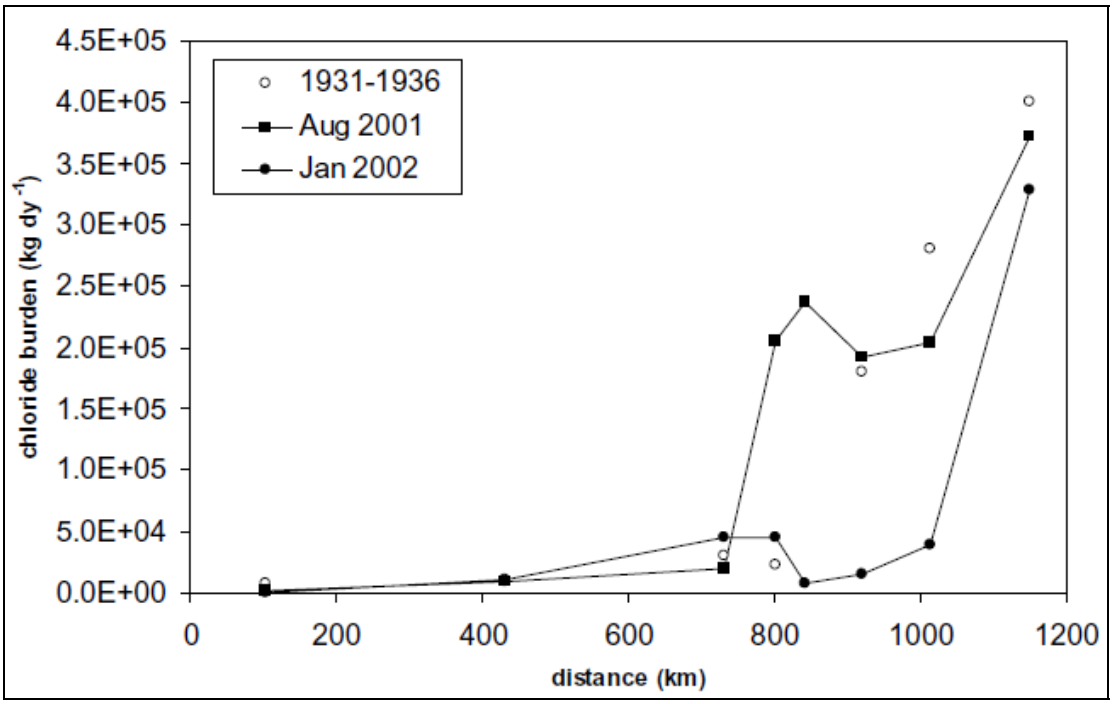

Figure 3.7. Chloride load from synoptic sampling trips in August 2001 and January 2002, in comparison with burdens from the *NRC* [1938] dataset for 1931-1936. [*Mills, 2003*]

In addition to chloride, bromide was also among the solutes analyzed and reported for each sampling trip. The chemical ratio between chloride and bromide was used as a tool for water source identification (Figure 3.8). *Mills* [2003] calculated a simple chloride and bromide mass-balance model from August 2001 data that was utilized to identify locations where water had high ratios of Cl/Br. Based on the assumption that all salinity increases were from evaporation and/or deep saline ground water, the model used chloride and bromide concentrations, discharge, tributary and evaporation contributions, and an estimate of deep brine chloride and bromide concentrations to compute the quantity of brine entering the Rio Grande within each river section. Ground water typically had higher Cl/Br ratios than surface water and deep geologic brine was characterized by an even higher ratio. Model results indicated significant brine additions at the following locations: Alamosa, Albuquerque, San

Acacia, narrows above Elephant Butte Reservoir, Seldon Canyon and El Paso [*Mills, 2003*]. The Closed Basin Canal registered a higher Cl/Br ratio than samples from other northern locations. The higher Cl/Br ratio was explained by noting that the Closed Basin Canal water is derived from a groundwater source and ground water Cl/Br ratios are typically higher than those found in surface waters. The Albuquerque ratio was increased due to wastewater treatment plant inflows. The termini of the four sedimentary basins within the Rio Grande rift correlated to the other four peaks in the Cl/Br ratio. Basin termini were areas where the bedrock nears the surface and may allow deep ground water to escape into the Rio Grande (Figure 3.9). Additional evidence was derived from the ratio between chlorine-36 and chloride. Areas that had low $^{36}Cl/Cl$ ratios identified locations with ground water components. Thus *Mills [*2003] concluded that a source water with a high Cl/Br ratio and low $^{36}Cl/Cl$ ratio enters the river system at geologically controlled locations.

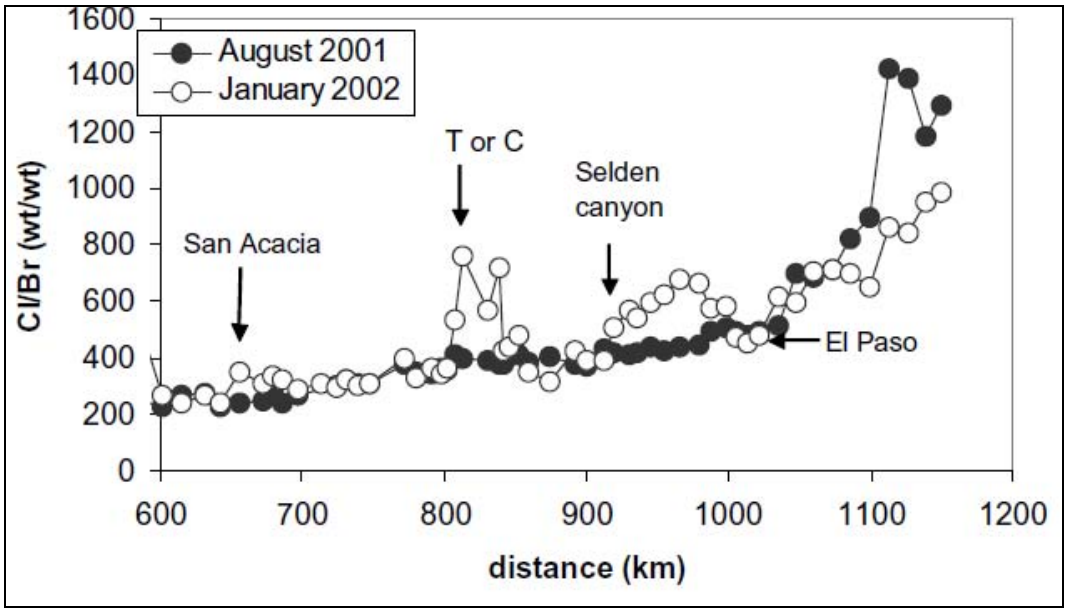

Figure 3.8. Chloride bromide ratio with distance downstream from the headwaters of the Rio Grande. [*Mills, 2003*]

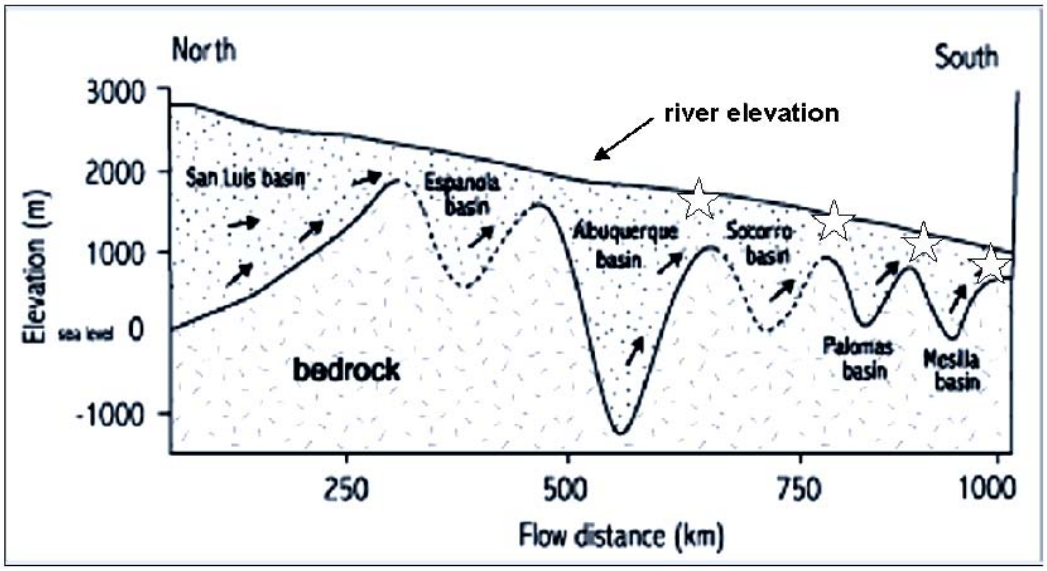

Figure 3.9. Generalized geologic cross-section of sedimentary basins in the Rio Grande rift. Arrows indicate estimated ground water flow lines, dashes represent areas where basin depth was inferred and stars indicate locations with brine inflow (from north to south): San Acacia, Elephant Butte, Selden Canyon and El Paso correlating to basin termini. [*Mills, 2003*]

More extensive modeling ensued to quantify and further characterize geologically controlled brine. This model contained mass-balance calculations for water, chloride and bromide utilizing Rio Grande, tributaries and wastewater measurements from August 2001 and January 2002. *Mills* [2003] calculated the water balance between USGS gaging stations, however solute balances were computed at synoptic sampling locations. Agricultural diversions and returns, riverbed seepage, tributary inflow, evaporation and wastewater inflow were all incorporated into the mass balances. Reach evaporation was estimated from reservoir evaporation, calculated from pan evaporation studies and stable-isotope data. The model accounted for all chloride and bromide from known sources such that any remaining quantities were assumed to be from brine seepage. Based on this mass balance model, *Mills* [2003] estimated the quantity of brine entering the Rio Grande during the summer of 2001 and the winter of

2002 at the four previously discussed locations: San Acacia, Truth or Consequence Seldon Canyon and El Paso. Results are presented in Figure 3.10.

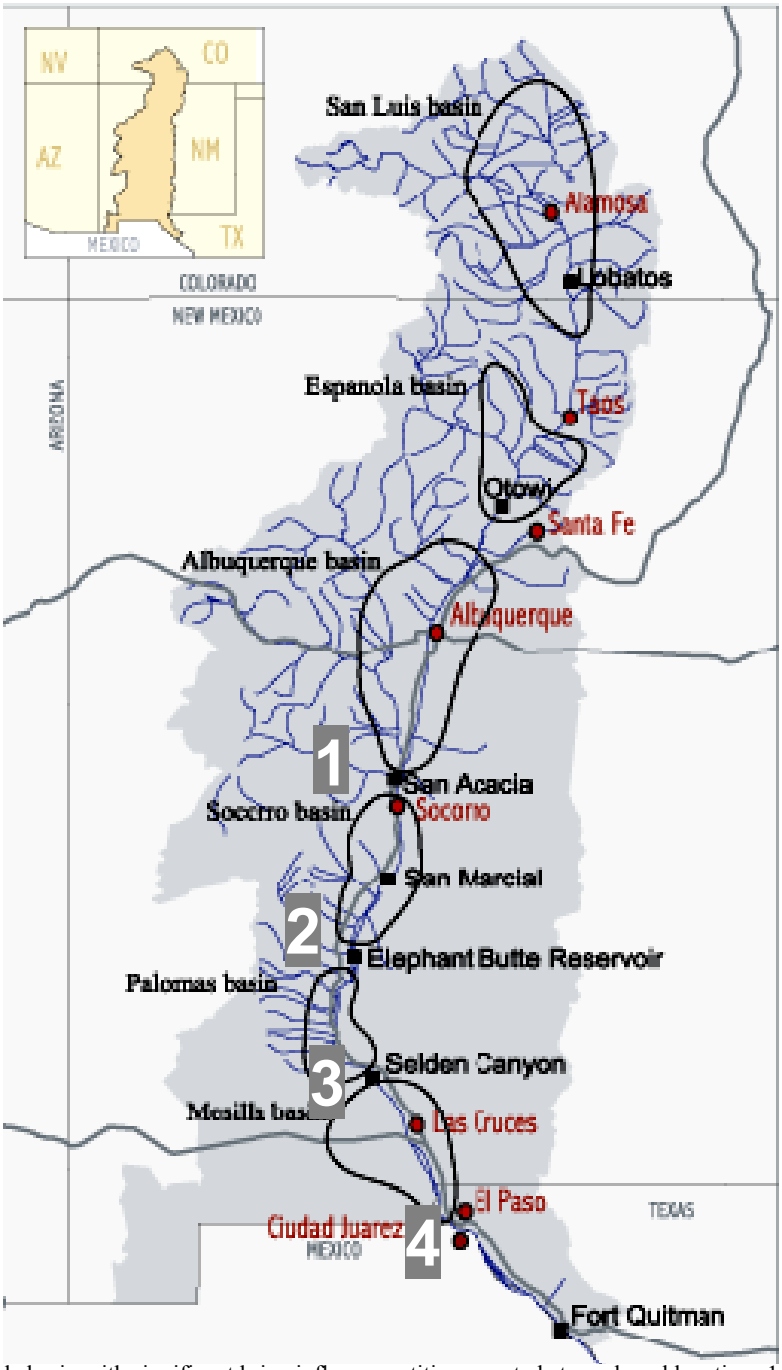

Figure 3.10. Rio Grande basin with significant brine inflow quantities reported at numbered locations 1-4. [*Mills*, 2003]

Chloride load quantity from brine: (in kg/day)

1- San Acacia = 2,000 in August 2001 and 42,000 in January 2002
2- T or C = 29,000 in August 2001 and 60,000 in January 2002
3- Seldon Canyon = 150 - 6,000 in January 2002
4- El Paso = 2,900 in August 2001 and 16,000 in January 2002

In order to support and build upon *Mills* [2003] brine computations, another thesis was devoted to characterizing and quantifying geologically controlled brine inflow over an extended time period. A dynamic simulation model was utilized to compute a mass balance model for chloride and bromide. *Lacey* [2006] incorporated chloride and bromide historical data from 1975-2005 into an existing water balance model, Upper Rio Grande Water Operations Model (URGWOM). Information regarding the URGWOM model can be found at http://www.spa.usace.army.mil/urgwom/default.asp. The URGWOM model accounts for all water entering or exiting the Rio Grande, including agricultural drains, evaporation, transpiration, ground-water seepage (calculated from a MODFLOW ground-water model), tributaries and wastewater. The chloride (or bromide) information was multiplied by each discharge term in order to create a chloride mass-balance model. Figure 3.11 illustrates *Lacey's* [2006] chloride model from San Felipe to Albuquerque. The model parallels historic data in Figure 3.12 where chloride loads are compared to modeled loads at Otowi for the period from 1975-2005. *Lacey's* [2006] model reasonably captured the historic chloride load. Also presented were modeled cumulative contributions from major chloride sources in the basin including geologic brine (Figure 3.13).

In addition, *Lacey* [2006] investigated the impacts of Elephant Butte Reservoir on the chloride balance of the Rio Grande. Utilizing data from 1905-1907 [*Stabler, 19*11] a pre-Elephant Butte Reservoir chloride model was constructed (Figure 3.14). As mentioned previously, the river chloride burden increased between San Marcial and El Paso both prior to and post Elephant Butte Reservoir construction. Comparing the pre-

Elephant Butte model to modern modeled data (1975-2005) suggested a 362% increase in brine inflow between San Marcial and El Paso (Figure 3.15) [*Lacey, 2006*]. Due to Rio Grande system changes between 1907 and 1975 (including reservoir installation and the extended irrigation network), the chloride load and concentration at El Paso increased by 28% and 70% respectively. This difference is probably accentuated by the unusually large discharge in 1905-1907.

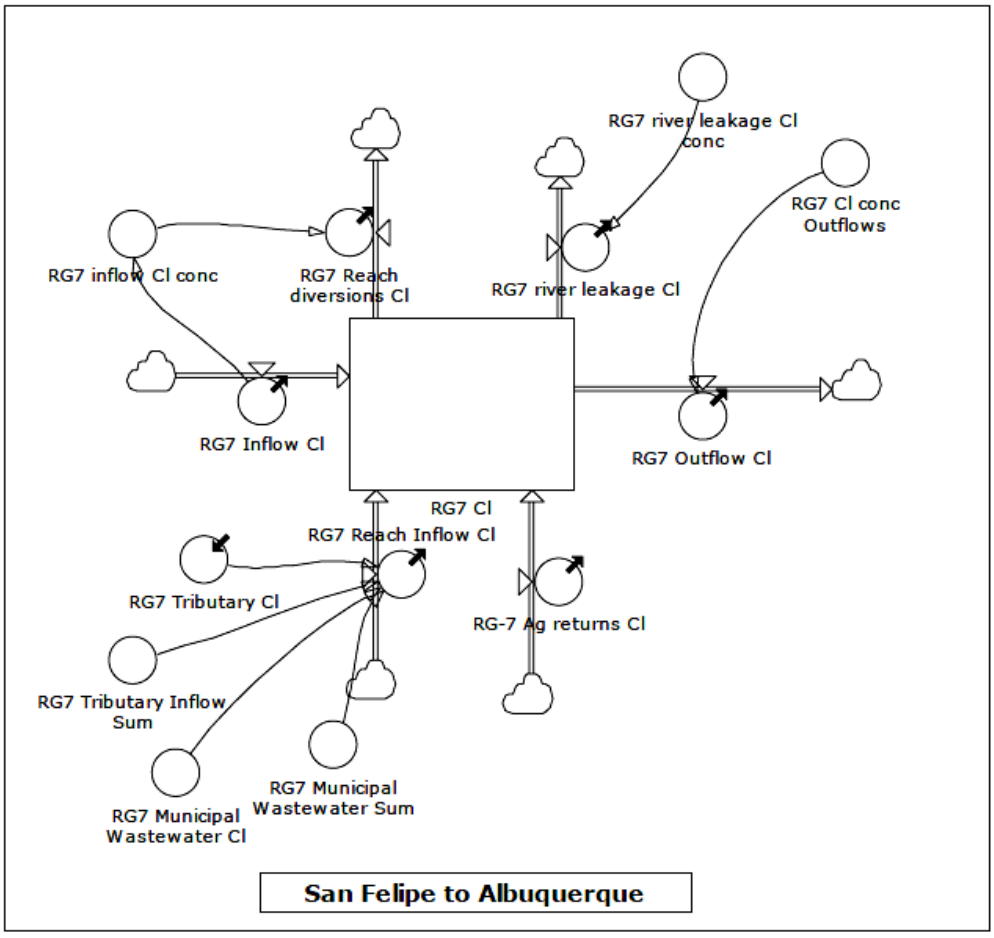

Figure 3.11. Chloride mass balance model (in Powersim) for the Rio Grande reach from San Felipe to Albuquerque. [*Lacey*, 2006]

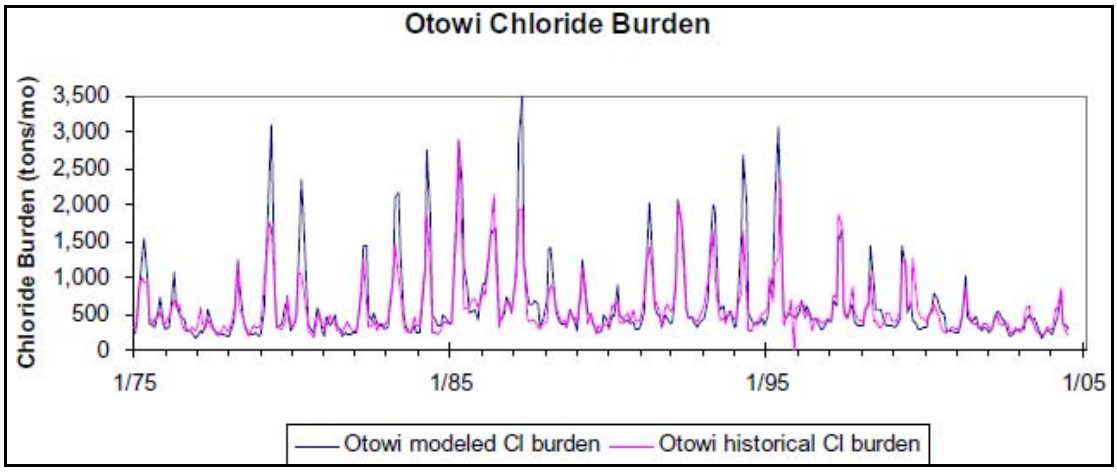

Figure 3.12. Chloride burden comparison between *Lacey's* [2006] model (using URGWOM water balance) and historic data. [*Lacey*, 2006]

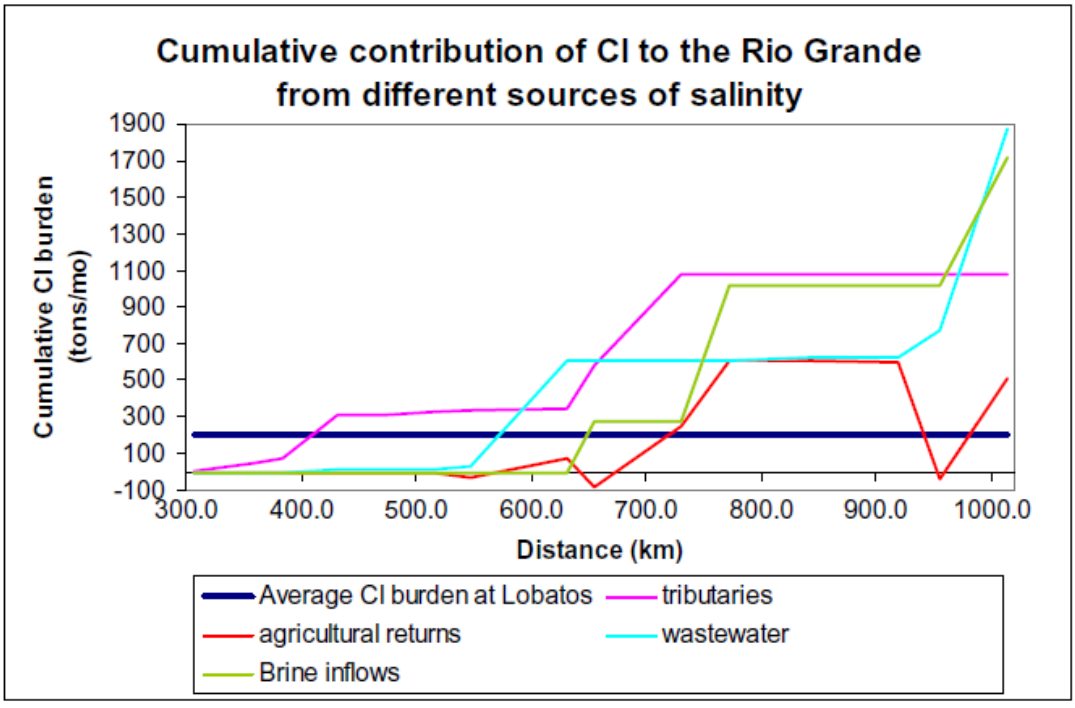

Figure 3.13. Cumulative chloride load from various sources (agricultural returns, tributaries, wastewater, and brine. [*Lacey*, 2006]

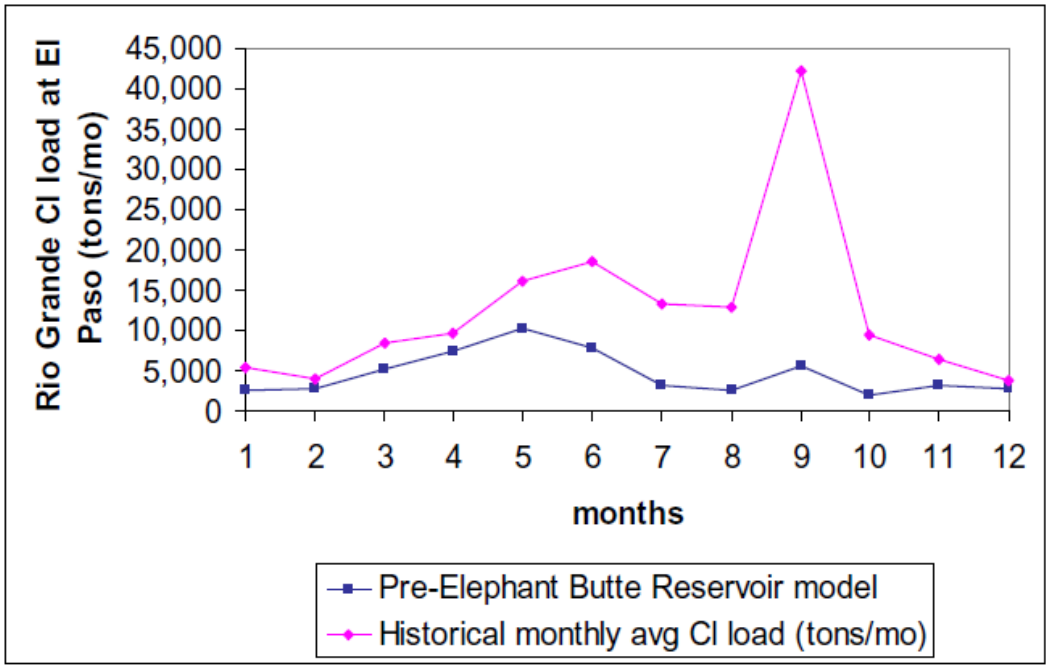

Figure 3.14. Chloride burden at El Paso, comparing historic data from 1905-1907 [*Stabler*, 1911] to modeled pre-Elephant Butte Reservoir. Months are listed in numerical format, such that January is indicated by the number 1. [*Lacey*, 2006]

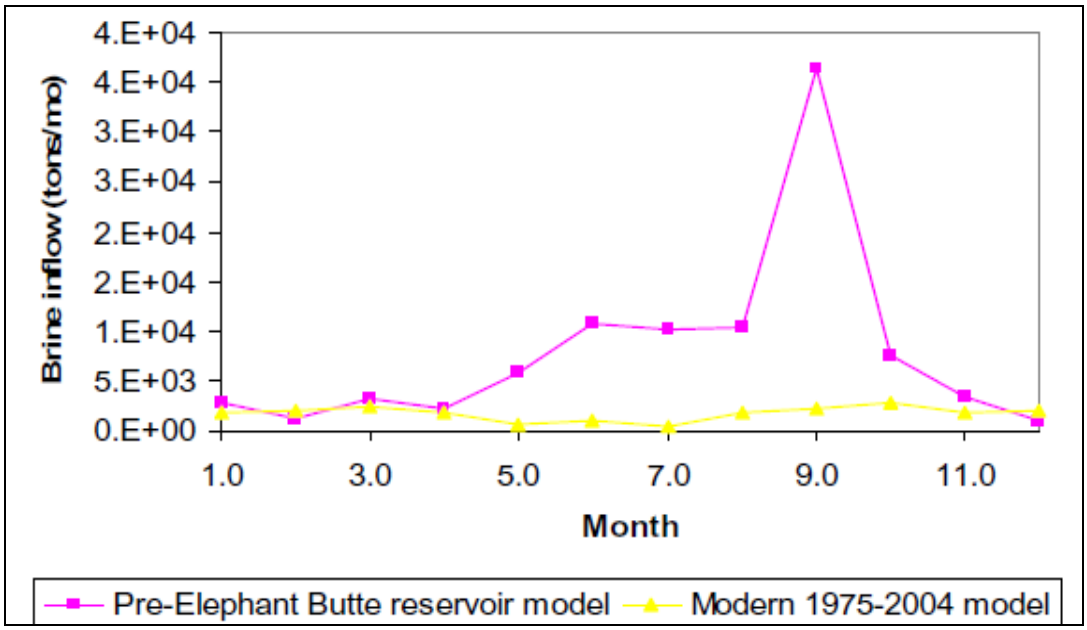

Figure 3.15. Modeled temporal brine comparison between the pre-Elephant Butte Reservoir model and the modern model. [*Lacey*, 2006]

3.5 Conclusions

All previous research agreed that the Rio Grande increased in salinity with distance downstream. Early water quality studies [*Lippincott*, 1939] attributed the solute load increase to evaporative concentration due to irrigation practices and storage in reservoirs. The majority of studies ascribed solute increases to a flushing of shallow ground water enhanced by installation of an extensive drainage network [*NRC*, 1938; *Wilcox*, 1957; *Trock et al*., 1978]. Furthermore, recent studies provided evidence for the significance of geologically controlled brine inflow [*Phillips et al*., 2003; *Mills*, 2003; *Lacey*, 2006]. More recent studies presented estimates that quantified brine seepage between 1975 and 2005 [*Mills*, 2003; *Lacey*, 2006], along with chloride and bromide additions. Moreover, *Lacey* [2006] computed brine inflows during the early twentieth century (1905-1907). Neither of these studies investigated solute trends over the entire period of record nor considered all major ions. *Williams* [2001] presented a solute budget including the entire available record for the southern half of the Upper Rio Grande basin (San Marcial to Ft. Quitman), however, solute trends observed in the budget were not fully examined nor explained. This thesis will expand upon the temporal range and chemical breadth data presented by *Mills*, [2003] and *Lacey* [2006] as well as broaden the spatial scope of *Williams* [2001], while developing a mechanistic interpretation of solute behavior in the Rio Grande.

CHAPTER 4
AVAILABILITY OF DATA AND SOLUTE BUDGET METHODOLOGY

Government agencies such as the Interstate Stream Commission, the Middle Rio Grande Conservancy District (MRGCD), the United States Geological Survey (USGS) and the United States Bureau of Reclamation (USBR) monitor water quality from over 50 gaging stations on the Rio Grande. Daily discharge and various chemical species are recorded. Monthly discharge data is available at most of the gaging stations and some locations have data from as early as the late nineteenth century. However, the water quality data is sporadic. Certain sampling locations have many years of consecutive monthly chemical data, whereas other stations have only a few samples for a fifty-year period. The discharge and solute data utilized in this study can be found in Appendix A. This chapter will discuss the quantity and quality of data utilized in the solute budget and modeling analyses.

4.1 Main Channel

Eleven USGS gaging stations on the main channel of the Rio Grande contain a usable amount of flow and chemical data and thus the locations included the following: Lobatos, CO; Taos Junction Bridge, NM; Otowi, NM; San Felipe, NM; Albuquerque, NM; Bernardo, NM; San Acacia, NM; San Marcial, NM; Elephant Butte Dam, NM; Caballo, NM; El Paso TX. The discharge record at each of these stations is almost complete. Illustrated in Table 4.1, the river stations typically had a monthly discharge

record available. Monthly discharge values were calculated from daily mean values collected by the USGS. In contrast, water quality data were less abundant; solute concentrations were generally available monthly to semi-monthly, although a few locations had large sections of missing data. Availability of average monthly solute data is presented in Table 4.2. Monthly solute concentrations from USGS data were calculated by averaging daily sample concentrations per month. Water samples were collected once a day, representing an instantaneous view of water quality for a variable number of days within the month. For any given month, the average monthly concentration may represent anywhere from 1 to 30 daily samples. The monthly concentration represents a best-estimate of the concentration based on the limited solute information available. Table 4.3 shows a detailed estimate of the number of samples available for each solute during each decade.

Station chemistries were compiled into discharge-weighted monthly concentrations and burdens. The solute burden or solute load describes the amount of solute mass flowing past a particular location at a given rate and is defined as the concentration multiplied by the discharge. Both discharge and concentration affect the amount of solute that is carried downstream. In order to compute the monthly burden, each monthly concentration is multiplied by the respective monthly discharge. Monthly loads were averaged over each decade yielding average decadal discharge-weighted solute burdens. The average discharge-weighted concentration is calculated by dividing the summation of the burden by the cumulative discharge for each decade. By weighting the values against discharge, a more accurate decadal chemistry estimate was

achieved. All subsequent chemical interpretations were derived from these discharge-weighted concentrations.

Table 4.1. Monthly discharge record quality for Rio Grande and tributaries.

Station Type	Station ID	Discharge Quantity	Discharge Quality	Data Source
Rio Grande	Lobatos	1930-2005	~ All months have data	USGS Station 08220000
Rio Grande	Taos Jct	1930-2005	~ All months have data	USGS Station 08251500
Rio Grande	Otowi Bridge	1930-2005	~ All months have data	USGS Station 08263500
Rio Grande	San Felipe	1930-1999	~ All months have data	USGS Station 08276500
Rio Grande	ABQ	1942-2005	~1/2 months have data	USGS Station 08279500
Rio Grande	Bernado	1958-2005	~2/3 months have data	USGS Station 08313000
Rio Grande	San Acacia	1940-2005	~ All months have data except 1956-1958	USGS Station 08317400
Rio Grande	San Marcial	1934-2005	~ All months have data	USGS Station 08319000
Rio Grande	Elephant Butte Dam	1934-2005	~ All months have data	USGS Station 08330000
Rio Grande	Caballo Dam	1940-2005	~ All months have data	USGS Station 08332010
Rio Grande	El Paso	1930-2005	~ All months have data	USGS Station 08354900
Major Tributary	Rio Chama	1930-2005	~ All months have data	USGS Station 08358400
Major Tributary	Jemez river	1943-2005	~ All months have data	USGS Station 08361000
Major Tributary	Rio Puerco	1940-2005	Almost all months	USGS Station 08362500
Major Tributary	Rio Salado	1948-1984	~1/3 of months have data (this record was extended with regression against precipitation at Grants, NM)	USGS Station 08364000
Minor Tributary	Costilla Creek	1941-2007	~ All months have data	USGS Station 08255500
Minor Tributary	Red River	1979-2007	~ All months have data	USGS Station 08266820
Minor Tributary	Rio Hondo	1935-2007	~ All months have data	USGS Station 08267500
Minor Tributary	Rio Pueblo de Taos	1957-2007	~ All months have data	USGS Station 08276300
Minor Tributary	Embudo Creek	1924-1955, 1963-2007	~ All months have data	USGS Station 08279000
Minor Tributary	Santa Cruz River	1933-2007	~ All months have data	USGS Station 08291000
Minor Tributary	Santa Fe River	1970-1999, 2005-2007	~ All months have data	USGS Station 08317200
Minor Tributary	Galisteo Creek	1970-2007	~ All months have data	USGS Station 08317950

Table 4.2. Quantity of solute data at main channel locations, prior to regression.

Station Type	Station ID	Dates of Available Data	Solute Data Quality	Data Source
Rio Grande	Lobatos	1947-1960, 1970-2005	~1/2 of months have data, with a few missing sections of 12 months consecutively	USGS Station 08220000
Rio Grande	Taos Jct	1975-2003	~1/3 of months have data, with some missing sections	USGS Station 08251500
Rio Grande	Otowi Bridge	1934-1981, 1982-2005	Full monthly record, ~1/2 of months have data, with a few missing sections	[*Wilcox,* 1957] [*USGS*, 2008] USGS Station 08263500
Rio Grande	San Felipe	1975-1980, 1981- 2005	Full monthly record, ~1/3 of months have data, with a few missing sections	USGS Station 08276500
Rio Grande	ABQ	1970-1995	~1/5 of months have data, data is sporadically spaced throughout the record	USGS Station 08279500
Rio Grande	Bernado	1965-1998	~1/4 of months have data, data is sporadically spaced throughout the record	USGS Station 08313000
Rio Grande	San Acacia	1940-1956, 1980-2003	~1/5 of months have data, data is sporadically spaced throughout the record	USGS Station 08317400
Rio Grande	San Marcial	1934-1963 and 1975-1983, 1964-1974 and 1983-2003	Full monthly record, ~1/3 of months have data	[*Wilcox,* 1957] *[Williams,*2001] [*USGS*, 2008] USGS Station 08319000
Rio Grande	Elephant Butte Dam	1934-1963 and 1979-1994	Full monthly record	[*Williams,* 2001] [*Wilcox,* 1957] [*USGS*, 2008] USGS Station 08330000
Rio Grande	Caballo Dam	1940-1967 and 1980-1994	Full monthly record	[*Williams,* 2001] [*Wilcox,* 1957] [*USGS*, 2008] USGS Station 08332010
Rio Grande	El Paso	1934-1994, 1995-2004	Full monthly record, ~2/3 of months have data	[*Williams,* 2001] [*Wilcox,* 1957] [*USGS*, 2008] USGS Station 08354900

Note: The column titled 'Solute Quality' describes the number of months, which have measured data meaning the data came directly from the reporting source, no regressed values were included. A few locations have many months of missing data consecutively, these time periods are noted by one of the following attached statements: (1) some missing sections indicating there are more than 10 sections missing data or (2) a few missing sections indicating that there are less than 10 time periods which have more than 6 months of missing data. For locations with limited months of data, an indication is also given for the data spacing, i.e. data is sporadically spaced. The spacing of data is given to suggest that

although, the location may have a very limited record the data may still yield a representative decadal average.

Table 4.3. Rio Grande stations: number of solute samples, prior to regression.

Station Name	Decade	Number of Samples for Ca, Mg, Na, Cl, SO4	Number of Samples for K	Number of Samples for HCO3
Lobatos	1947-49	low	low	low
Lobatos	1950-60	low	low	low
Lobatos	1970-79	medium	medium	low
Lobatos	1980-89	medium	medium	low
Lobatos	1990-99	medium	medium	low
Lobatos	2000-04	low	low	No Data
Taos Jct	1975-79	low	low	low
Taos Jct	1980-89	medium	medium	low
Taos Jct	1990-99	medium	medium	medium
Taos Jct	2000-05	low	low	very low
Otowi Bridge	1960-69	high	high	high
Otowi Bridge	1970-79	high	high	medium
Otowi Bridge	1980-89	medium	medium	very low
Otowi Bridge	1990-99	medium	medium	low
Otowi Bridge	2000-05	medium	medium	low
San Felipe	1970-79	low	low	low
San Felipe	1980-89	low	low	very low
San Felipe	1990-99	low	low	very low
San Felipe	2000-05	low	low	very low
ABQ	1970-79	low	low	extremely low
Bernado	1960-69	low	very low	low
Bernado	1970-79	medium	low	medium
Bernado	1980-89	low	very low	very low
Bernado	1990-99	low	very low	very low
San Acacia	1980-89	low	low	very low
San Acacia	1990-99	low	low	low
San Marcial	1960-69	medium	low	medium
San Marcial	1970-79	medium	medium	medium
San Marcial	1980-89	low	low	very low
San Marcial	1990-99	low	low	low
San Marcial	2000-05	very low	very low	very low
El Paso	1970-79	medium	medium	low
El Paso	1980-89	medium	medium	very low
El Paso	1990-99	medium	medium	low
El Paso	2000-05	low	low	low

Note: These are subjective estimates, where very low = < 15 samples, low = ~30 samples, medium = ~50 samples, high = ~70 samples, very high = ~100 samples. Data is from [*USGS*, 2008].

4.2 Regression Analysis

Tables 4.2 and 4.3 illustrate that important sections of solute data were unavailable for main channel Rio Grande stations. In order to fill these missing sections, solute concentrations were generated by regression against electrical conductivity and discharge. The solutes were first regressed against electrical conductivity (or TDS when EC was unavailable) over the entire period of record at each location. The total dissolved solids (TDS) record also had missing sections, which were filled by regression against electrical conductivity. The TDS record at Albuquerque was particularly limited, thus the regression equation from EC vs TDS at San Felipe was utilized to fill in TDS at Albuquerque. Remaining gaps in monthly chemical data were filled with a regression against discharge. In order to achieve improved regression coefficients, discharge regressions were run by decade. Table 4.7 shows the total solute data record for each station including measured and regressed data. The discharge and electrical conductivity equations can be found in Appendix B.

A statistical test was performed to determine the benefit of utilizing a regression against discharge. The regression-filled data based on discharge resulted in a representative decadal average solute load. Chloride concentrations and discharges from the Otowi Bridge USGS gaging station were utilized to calculate monthly average chloride loads. To simulate a decade with contiguous data filling every month, 120 months were chosen from the period 1959-1976, where each monthly average concentration was computed from at least three daily samples. Utilizing all the 120 months, an “actual” decadal average chloride load was calculated (actual decadal average chloride load = 540,000 kg/month). The analysis consisted of simulating

missing data by randomly deleting a month of data and comparing the new average load (now with 119 data points) to the actual average load. This process was repeated until only 1 data point remained. Results are shown in Figure 4.1, where the blue diamonds represent an average computed from measured data with missing data points left empty. In order to assess the worth of regression against discharge, chloride monthly loads were plotted against monthly discharges yielding two reasonable regression equations: a power law (r^2= 0.717) and a natural log (r^2= 0.6519). Each regression equation was used to fill the simulated decade. Average computed chloride load where missing data were filled with a power-law regression equation (pink squares) or a natural-log regression equation (yellow triangles) are shown in Figure 1. The results clearly show that using a regression to fill missing data achieves a better estimate of the actual decadal average load compared to simply omitting months without data. The decade average was almost always over estimated when missing data was left out. Similarly, the regression using a natural-log equation also over estimated the average load when 100-40 months of data remain. In contrast, the power-law regression closely estimated the actual average load consistently until approximately 40 months of measured data remained, after which the power law began to significantly underestimate the actual average. Thus a power law regression against discharge was utilized to fill in solute chemical records.

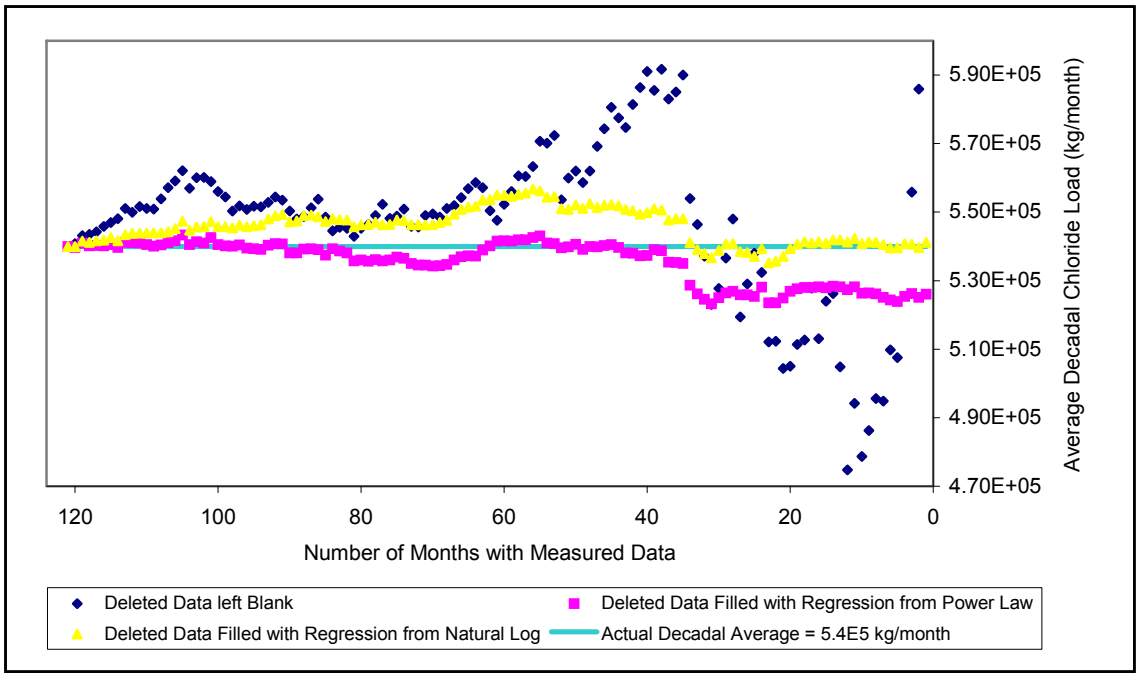

Figure 4.1. Discharge regression test and method comparison.

4.3 Sampling Technique Comparison

Various sources have contributed data to this project. Data from ~1960-2005 was collected utilizing a sampling protocol similar to that of recent data collection (which can be found on the USGS website at http://water.usgs.gov/owq/FieldManual/Factsheet.pdf or http://pubs.usgs.gov/of/1997/223/). However, the older datasets (*Wilcox* [1957] and *Stabler* [1911]) collection methods varied in technique. *Wilcox* [1957] combined daily water samples throughout each month and the combined sample (assumed to be homogenous) was analyzed. Due to this variation in collection technique, some difference was noticed among the data. Figures 4.2, 4.3, 4.4, 4.5, 4.6 and 4.7 illustrate variations in discharge, salinity (TDS and EC), chloride, calcium and sodium, magnesium, and sulfate between *Wilcox* [1957] and the *USGS* [2008] dataset. The figures plot data collected by the *USGS* [2008] and *Wilcox* [1957] over the same

sampling time period of October 1959 to December 1963 at the Otowi USGS gage. The data collected with the various techniques result in minor variation. Slightly more variation was observed at downstream stations (i.e. San Marcial or El Paso), where river concentrations are more variable. On the decadal scale, these issues of sampling technique and regression filled data become minimal. Therefore, the included data is a reasonable representation of the chemical history of the Rio Grande.

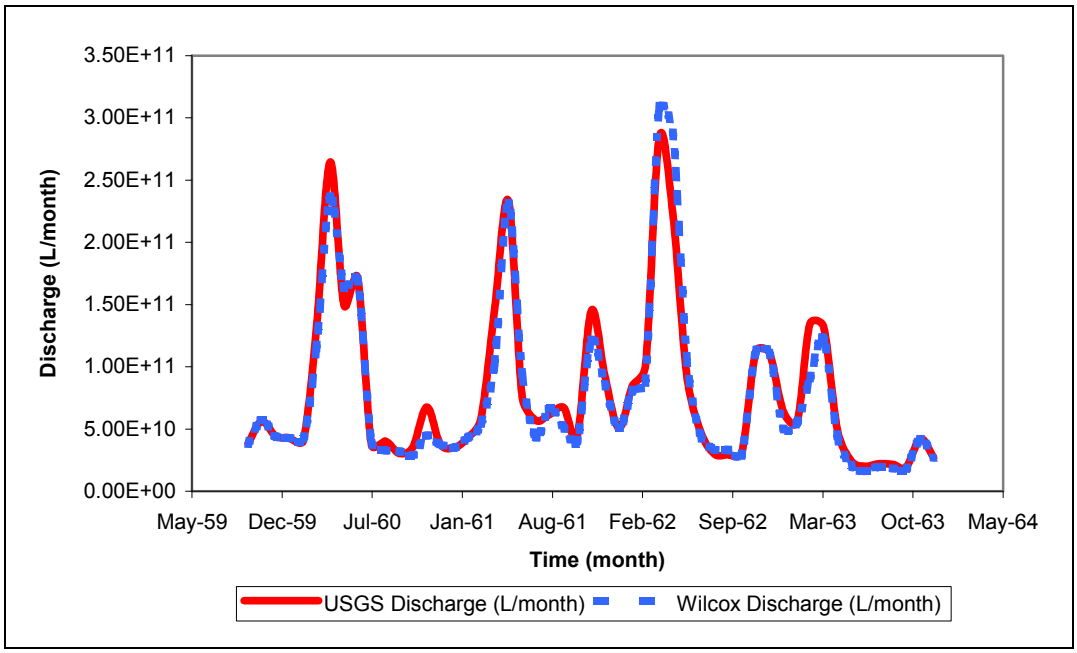

Figure 4.2. *Wilcox* [1957] and *USGS* [2008] sampling technique comparison: discharge. Data collected during the period October 1959 to December 1963 at the Otowi gaging station.

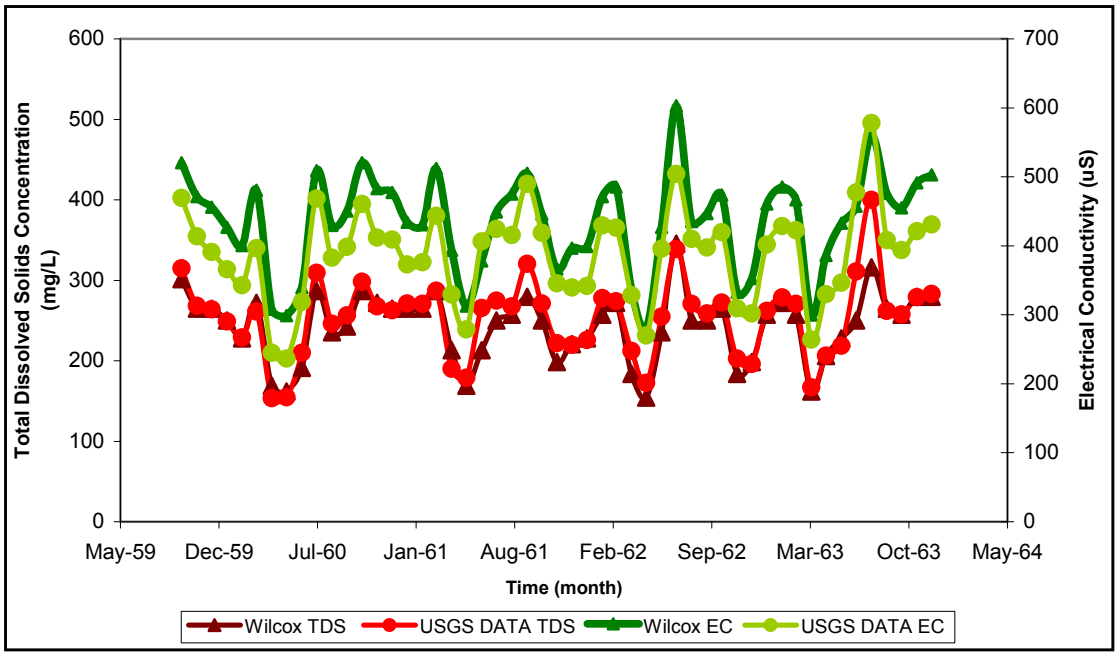

Figure 4.3. *Wilcox* [1957] and *USGS* [2008] sampling technique comparison: salinity. Data collected during the period October 1959 to December 1963 at the Otowi gaging station.

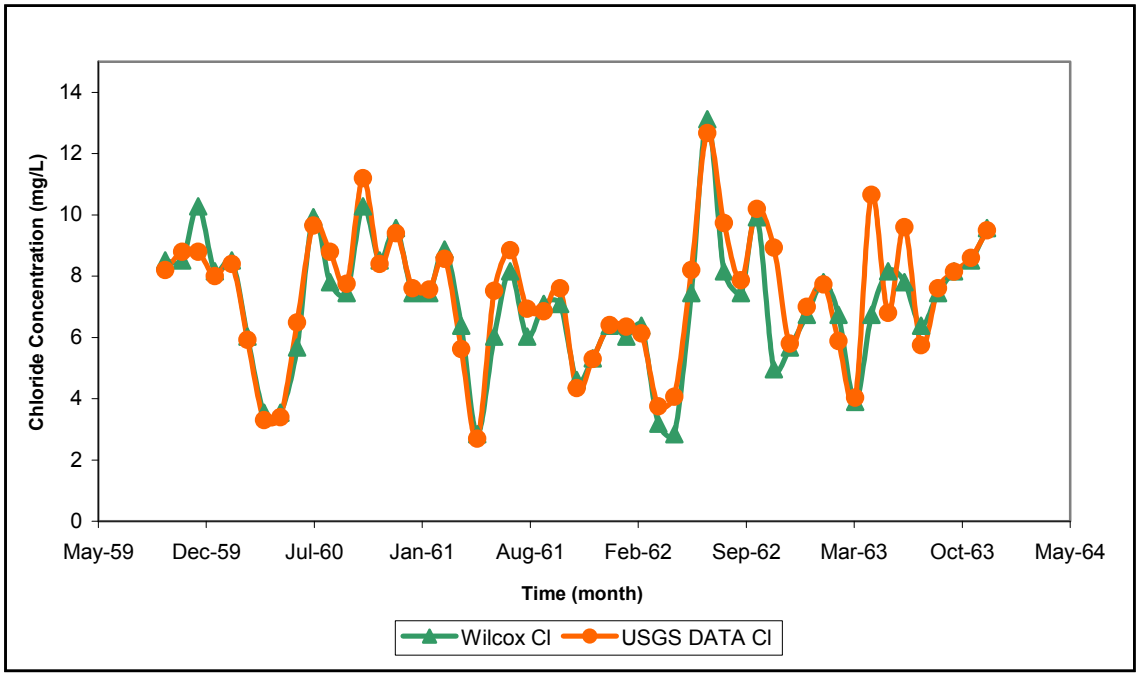

Figure 4.4. *Wilcox* [1957] and *USGS* [2008] sampling technique comparison: chloride. Data collected during the period October 1959 to December 1963 at the Otowi gaging station.

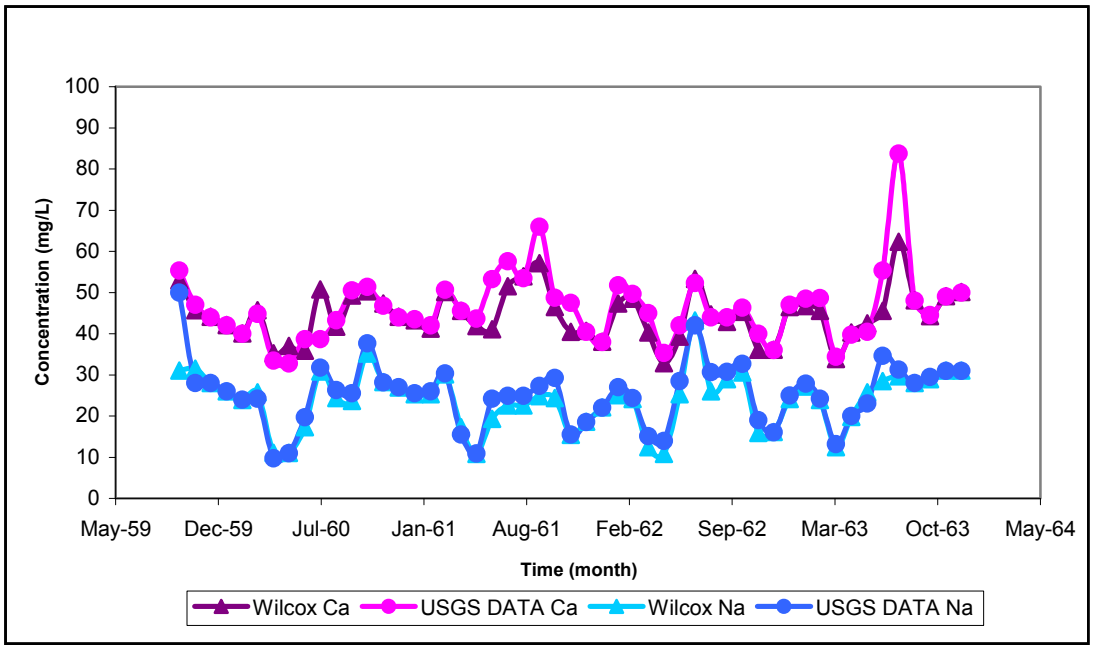

Figure 4.5. *Wilcox* [1957] and *USGS* [2008] sampling technique comparison: calcium and sodium. Data collected during the period October 1959 to December 1963 at the Otowi gaging station.

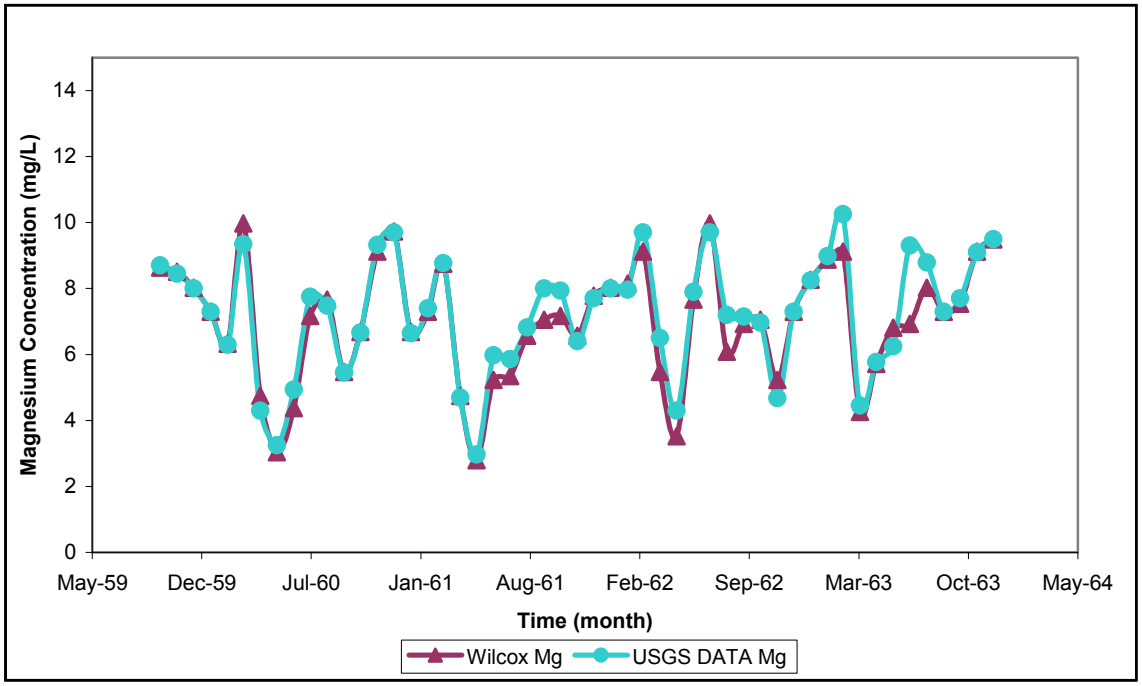

Figure 4.6. *Wilcox* [1957] and *USGS* [2008] sampling technique comparison: magnesium. Data collected during the period October 1959 to December 1963 at the Otowi gaging station.

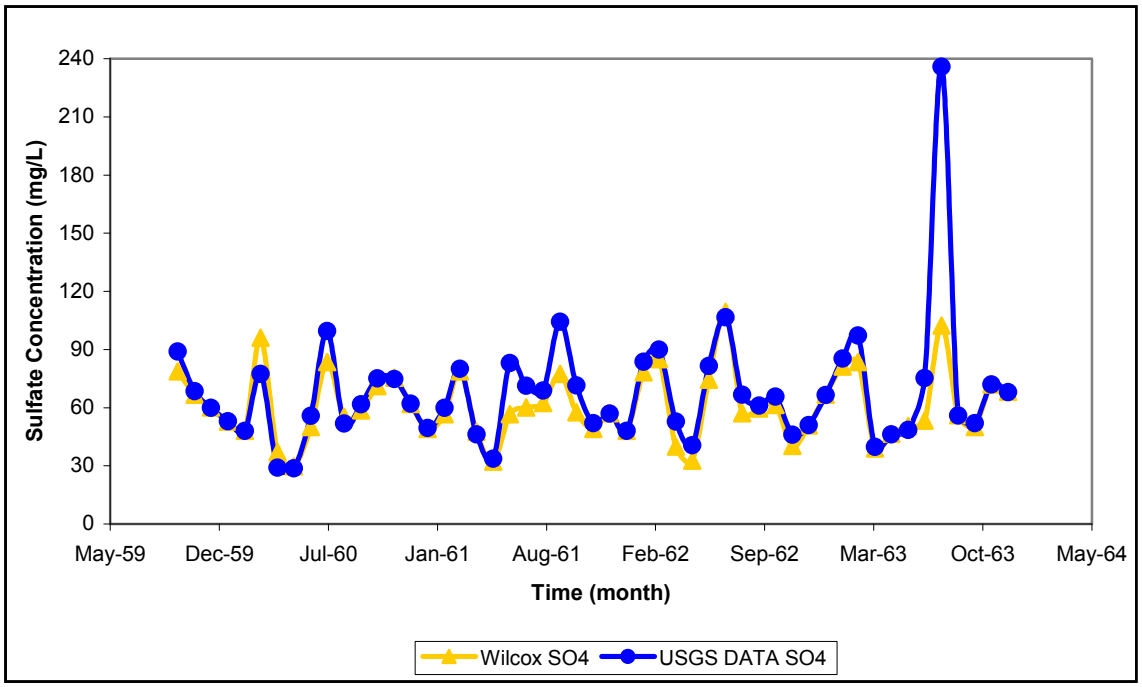

Figure 4.7. *Wilcox* [1957] and *USGS* [2008] sampling technique comparison: sulfate. Data collected during the period October 1959 to December 1963 at the Otowi gaging station. The high concentration in August 1963 reported by the USGS is unrepresentative for the month; likely this average was computed from a minimal number of daily samples.

4.4 Tributaries

Tributaries contribute a significant percentage of flow and solutes to the Rio Grande. As discussed for the main channel stations, discharge and chemical data have been collected for many tributaries along the Rio Grande. The discharge record was monthly to semimonthly for most of the tributaries (Table 4.1); however, the chemical data are extremely sparse. The tributaries were separated into categories: major and minor, based on the TDS load contributed to the Rio Grande (Table 4.4). The tributaries considered minor include the following: Costilla Creek, Red River, Rio Hondo, Rio Pueblo de Taos, Embudo Creek, Santa Cruz River, Santa Fe River, and Galisteo Creek. These rivers collectively contribute a significant amount of flow to the Rio Grande, however, the solute record is sporadic and sparse. For this reason, one average value

was computed from all available samples and utilized as an estimate for all decades. The remaining four tributaries were categorized as major: Rio Chama, Jemez River, Rio Puerco and Rio Salado. These rivers had sufficient chemical data to justify handling them as described in the main channel section; that is, using a regression against EC and discharge to fill data gaps. Tributary data quantity and sources can be found in Tables 4.1, 4.5, 4.6 and 4.7 that contain discharge, solute data availability, the number of solute samples collected in each decade (major tributaries only) and all available chemical data (measured and regressed values) respectively.

Table 4.4. Tributary category determination.

River Reach	Category Type	Tributary Name	Discharge (L/month)	TDS Conc. (mg/L)	TDS Load (kg/month)
Lobatos - Taos	Minor	Costilla Creek	4.13E+09	10.8	4.46E+04
Lobatos - Taos	Minor	Red River	6.05E+09	145.6	8.81E+05
Lobatos - Taos	Minor	Rio Hondo	2.78E+09	99.6	2.77E+05
Lobatos - Taos	Minor	Rio Pueblo de Taos	6.16E+09	233.8	1.44E+06
Taos - Otowi	Minor	Embudo Creek	7.52E+09	174.3	1.31E+06
Taos - Otowi	Minor	Santa Cruz	3.03E+09	56.8	1.72E+05
Otowi - SF	Minor	Santa Fe river	7.72E+08	378.7	2.92E+05
Otowi - SF	Minor	Galisteo Creek	4.09E+08	No Data	No Data
Taos - Otowi	Major	Rio Chama	5.0E+10	215.6	2.25E+11
SF-ABQ	Major	Jemez	6.4E+09	481.8	3.07E+12
Bernardo-SA	Major	Rio Puerco	2.5E+09	1429.2	3.59E+12
Bernardo-SA	Major	Rio Salado	6.6E+07	586.5	3.88E+10

Table 4.5. Quantity of solute data at tributary locations, prior to regression.

Station Type	Station ID	Solute Quantity	Solute Quality	Data Source
Major Tributary	Rio Chama	1964-1974, 1987-2004	~2/3 of months have data, ~1/3 of months have data with some missing sections	USGS Station 08358400
Major Tributary	Jemez river	1966-1988	~1/3 of months have data	USGS Station 08361000
Major Tributary	Rio Puerco	1960-1980, 1981-2004	~1/3 of months have data, ~1/5 of months have data, data is sporadically spaced throughout the record	USGS Station 08362500
Major Tributary	Rio Salado	1966-1984	~1/4 of months have data with some missing sections	USGS Station 08364000
Minor Tributary	Costilla Creek	July 1966-1976	~3/4 of months have data	USGS Station 08255500
Minor Tributary	Red River	1978-1986	~3/4 of months have data	USGS Station 08266820
Minor Tributary	Rio Hondo	1986-July 1995	~1/2 of months have data	USGS Station 08267500
Minor Tributary	Rio Pueblo de Taos	1985-1998	~1/3 of months have data	USGS Station 08276300
Minor Tributary	Embudo Creek	1971-1978, 1979-1995	~1/2 of months have data, ~1/3 of months have data	USGS Station 08279000
Minor Tributary	Santa Cruz River	2 values, June 1974, Feb 1975	2 months have data	USGS Station 08291000
Minor Tributary	Santa Fe River	1981-1999	~1/3 of months have data	USGS Station 08317200
Minor Tributary	Galisteo Creek	No Data		

Note: The column titled 'Solute Quality' describes the number of months, which have data measured data meaning the data came directly from the reporting source, no regressed values were included. The listed fraction indicates an approximate number of months over the time period listed under 'Solute Quantity' that have reported concentration values. A few locations have many months of missing data consecutively, these time periods are noted by one of the following attached statements (1) some missing sections indicating there are more than 10 sections missing data or (2) a few missing sections indicating that there are less than 10 time periods which have more than 6 months of missing data. For locations with limited months of data, an indication is also given for the data spacing, i.e. data is sporadically spaced. The spacing of data is given to suggest that although, the location may have a very limited record, the data may still yield a representative decadal average.

Table 4.6. Major tributaries: number of solute samples, prior to regression.

Station Name	Decade	Number of Samples for Ca, Mg, Na, Cl, SO4	Number of Samples for K	Number of Samples for HCO3
Rio Chama	1960-69	Low	Low	Low
Rio Chama	1970-79	Low	Low	Low
Rio Chama	1980-89	very low	very low	very low
Rio Chama	1990-99	Low	Low	Low
Rio Chama	2000-04	very low	very low	very low
Jemez	1966-69	Low	very low	very low
Jemez	1970-79	Low	Low	Low
Jemez	1980-89	Low	Low	No Data
Jemez	1990-99	very low	very low	No Data
Rio Salado	1960-69	Low	very low	Low
Rio Salado	1970-79	Low	Low	Low
Rio Salado	1980-89	very low	very low	No Data
Rio Puerco	1960-69	Low	very low	Low
Rio Puerco	1970-79	Medium	Low	Low
Rio Puerco	1980-89	Low	Low	No Data
Rio Puerco	1990-99	Low	very low	very low
Rio Puerco	2000-05	very low	very low	very low
San Acacia CC	1980-89	very low	very low	No Data
San Marcial CC	1960-69	High	Low	High
San Marcial CC	1970-79	Medium	Low	Low
San Marcial CC	1980-89	very low	very low	very low
San Marcial CC	1990-99	Low	Low	Low

Note: These are subjective estimates, where very low = < 15 samples, low = ~30 samples, medium = ~50 samples, high = ~70 samples, very high = ~100 samples. Data is from [USGS, 2008]

Table 4.7. Total solute dataset including measured and regression-filled data.

Station Type	Station ID	Solute Quantity	Solute Quality	Data Source
Rio Grande	Lobatos	1947-1960 and 1969-2005	Filled with Regression	USGS Station 08220000
Rio Grande	Taos Jct	1975-2005	Filled with Regression	USGS Station 08251500
Rio Grande	Otowi Bridge	1934-2005	Filled with Regression	*Wilcox* [1957]/ *USGS* [2008] USGS Station 08263500
Rio Grande	San Felipe	1970-2005	Filled with Regression	USGS Station 08276500
Rio Grande	ABQ	1970-2003	Mostly filled with a few large sections of missing	USGS Station 08279500
Rio Grande	Bernado	1960-2003	Mostly filled with a few large sections of data are missing	USGS Station 08313000
Rio Grande	San Acacia	1940-1956, 1980-2003	Filled, a few months in 1970, Mostly filled with a few large sections missing 1980-2003	USGS Station 08317400
Rio Grande	San Marcial	1934-1963 and 1963-2003	Filled with Regression	*Wiliams* [2001]/*Wilcox* [1957]/ *USGS* [2008] USGS Station 08319000
Rio Grande	Elephant Butte Dam	1934-1963 and 1975-1994	Filled with Regression	*Wiliams* [2001]/*Wilcox* [1957]/ *USGS* [2008] USGS Station 08330000
Rio Grande	Caballo Dam	1940-1967 and 1980-1994	Filled with Regression	*Wiliams* [2001]/*Wilcox* [1957]/ *USGS* [2008] USGS Station 08332010
Rio Grande	El Paso	1934-2004	Filled with Regression	*Wiliams* [2001]/*Wilcox* [1957]/ *USGS* [2008] USGS Station 08354900
Major Tributary	Rio Chama	1960-2005	Filled with Regression	USGS Station 08358400
Major Tributary	Jemez river	1960-1999	Filled with Regression	USGS Station 08361000
Major Tributary	Rio Puerco	1960-2005	~Filled with Regression	USGS Station 08362500
Major Tributary	Rio Salado	1960-1984	~1/3 filled	USGS Station 08364000

Note: The column titled 'Solute Quality' describes the number of months which have data reported, including all measured and regressed data. Filled with Regression = all months have a measured or regressed value, Mostly filled = over ¾ of months have data, ~1/3 filled =~1/3 of months have data. Occasionally there is a note such as "a few large sections of missing data" which means that this time period has more than 6 months of missing data consecutively.

4.5 Irrigation Canals and Drains

At certain locations, a significant portion of Rio Grande flow travels in canals and drains that flow alongside the main channel. At these locations, the USGS gage in the river does not measure the discharge flowing in the irrigation network. The total amount of water and dissolved solids passing each location was calculated as a summation of main channel flow and irrigation network flow. Discharge from these canals and drains that by-pass the main channel USGS gage were included in order to account for the total flow and chemistry passing the river cross-section. The following canals and drains bypass the main channel gage:

- Albuquerque cross-section: Atrisco, Arenal, Armijo Drains and Albuquerque Riverside drain.
- Bernardo cross-section: Lower San Juan Riverside Drain, Bernardo Conveyance Channel, and Bernardo Interior Drain.
- San Acacia cross-section: Low Flow Conveyance Channel (LFCC), and Socorro Main Canal.
- San Marcial cross-section: Low Flow Conveyance Channel.

The drains and canals were organized into groups of those with chemical data and those without. With measured data reported in approximately one-third of months, the Low Flow Conveyance Channel at San Acacia and San Marcial were classified as having sufficient chemical data to be included in the analysis as the main channel stations. Electrical conductivity and discharge regressions were used to fill in many of the missing data sections. Furthermore, the LFCC carried significantly higher solute concentrations than to the main river channel. Therefore, the LFCC burdens at San Acacia and San Marcial are computed separately and added to the main channel burden.

The other drains do not have sufficient chemical data to support regression or calculate representative averages. Due to this lack of chemical data in the remaining

drains, the solute concentrations were assumed to be the same as the main channel of the river such that the discharge-weighted burden was computed with the multiplication of the total cross-section discharge (main-channel discharge plus any bypass drains) and the main-channel discharge-weighted average concentration. A comparison between conveyance system and river chemistry suggested it was reasonable to estimate canal and drain chemistry with river chemistry. Figures 4.8, 4.9, and 4.10 illustrate chemical agreement between the main channel of the Rio Grande and drains bypassing at that location. A comparison was made at Albuquerque, Bernardo and San Acacia using average concentrations of available data collected during the NMT/UA biannual synoptic sampling campaign (Summer 2004-Winter 2006).

The total cross-section decadal average load or concentration was calculated for each station as is described below for the cross-section San Acacia. The San Acacia discharge is the summation of discharges from the main-channel gage, the conveyance channel, and the Socorro Main Canal North. Solute burdens were calculated from the main channel concentration multiplied by discharge at the main-channel and the Socorro Main Canal; this load was then added to the Low Flow Conveyance Channel solute load at San Acacia (concentration multiplied by discharge from the San Acacia Conveyance Channel). Table 4.8 contains the quantity and sources of data for drain discharge. The drain chemical data availabilities are shown in Table 4.9. The total cross-section discharge, burden or concentration will be referred to by its river location. Thus the station locations refer to the total flow and an estimate of the total chemistry passing each location.

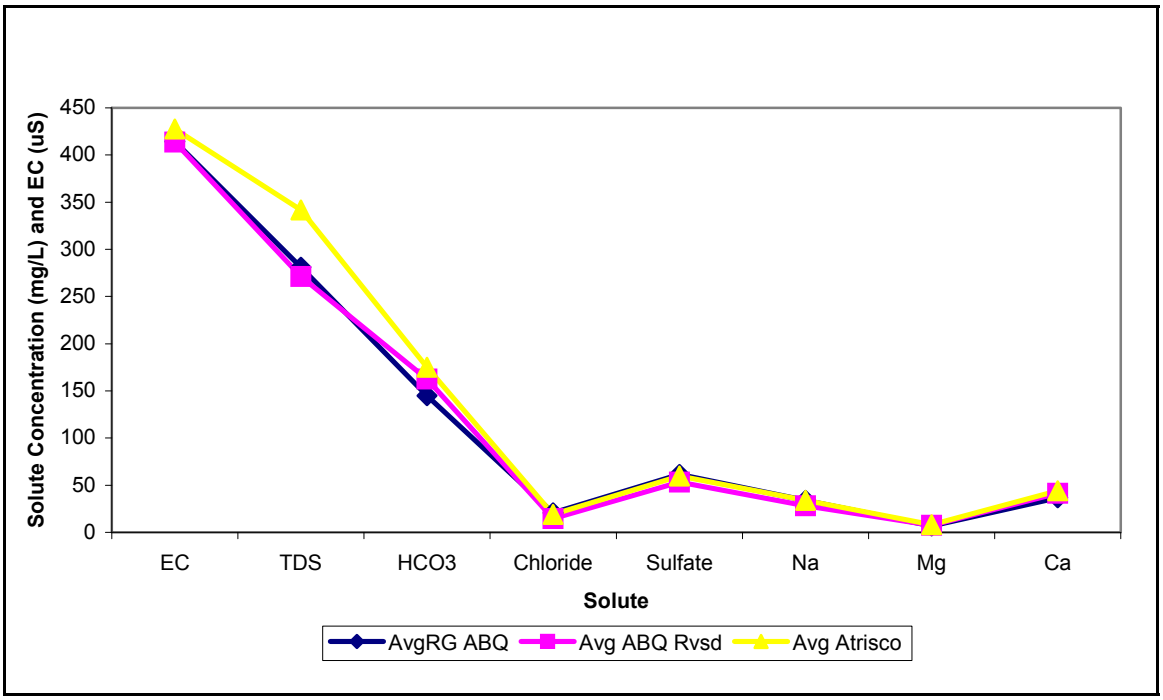

Figure 4.8. River-to-drain chemical comparison at the Albuquerque cross-section. Sample labels indicate 'Avg' for average, 'RG' for Rio Grande main-channel sample, 'Rvsd' for riverside drain and the name of the location or drain, i.e. Atrisco.

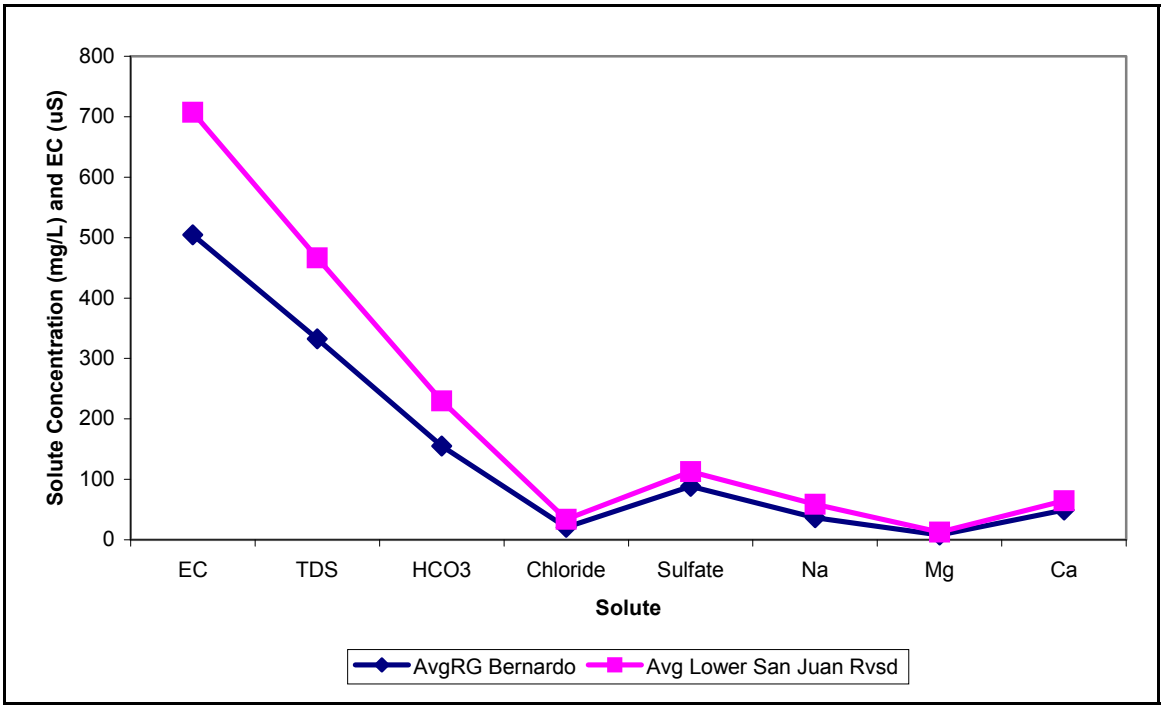

Figure 4.9. River-to-drain chemical comparison at the Bernardo cross-section. Sample labels indicate 'Avg' for average, 'RG' for Rio Grande main-channel sample, 'Rvsd' for riverside drain and the name of the location or drain, i.e. Bernardo.

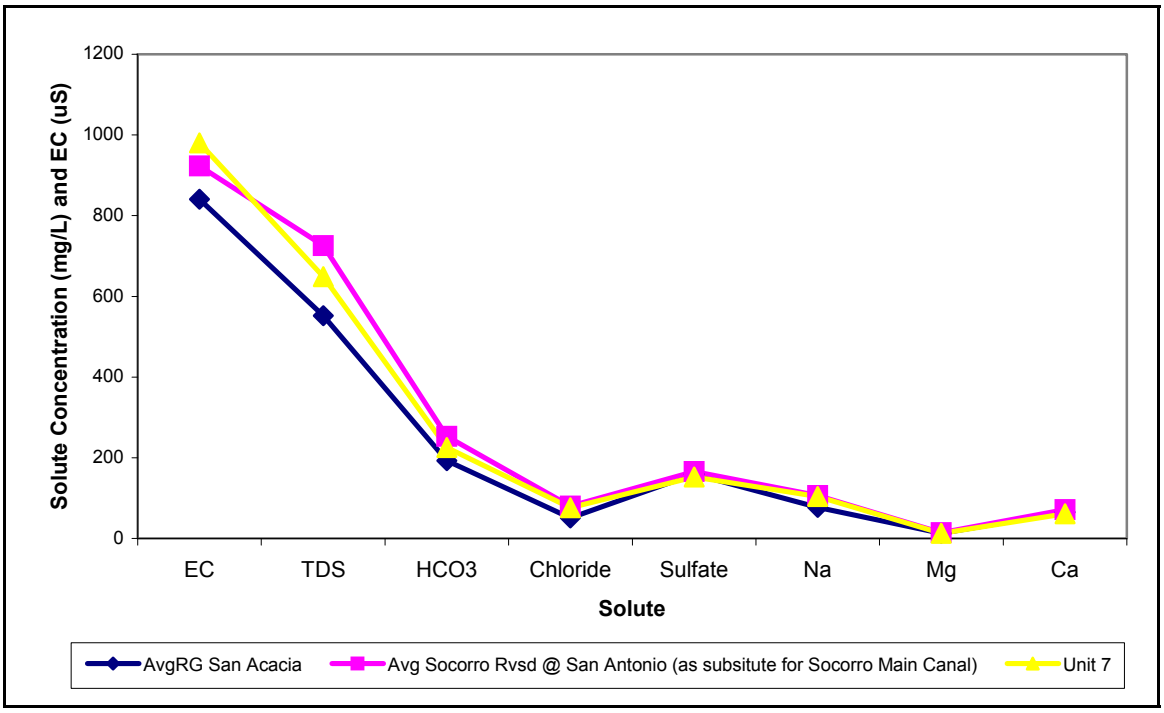

Figure 4.10. River-to-drain chemical comparison at the San Acacia cross-section. Sample labels indicate 'Avg' for average, 'RG' for Rio Grande main-channel sample, 'Rvsd' for riverside drain and the name of the location or drain, i.e. Unit 7.

4.6 Wastewater Treatment Plant

Only the Albuquerque wastewater treatment plant has been included in this analysis. Other wastewater treatment plants were not included based on smaller discharges and limited chemical data. Discharge data was collected by the New Mexico State Environment Department. The discharge record was sufficient, with data available approximately monthly for the most recent period of 1980-2007 (Table 4.8). The solute information however was extremely limited (Table 4.9). Solute data was estimated based on an average between a few samples collected by the U.S. Fish and Wildlife Service in 2002 and four samples collected during a synoptic sampling by New Mexico Tech and the University of Arizona in 2005-2006. The total chloride load entering at Albuquerque was much higher than the load leaving at Bernardo. Chloride is a conservative ion and cannot be lost downstream. Because the wastewater treatment

plant was based on a very small amount of data, it was deemed most likely to be incorrect. Thus, the solute concentrations were decreased by sixty percent in an effort to better match the total chloride load at Bernardo.

Table 4.8. Drain and WWTP: discharge quantity and data source.

Station Type	Station ID	Discharge Quantity	Discharge Quality	Data Source
Drain at RG x-sect	ABQ Riverside	1996-1999 (used for pre-2000 decades) and 2000-2006 (used for decade 2000-2007)	~All Months have data	David Gensler MRGCD personal communication May 2008
Drain at RG x-sect	Arenal	1996-1999 (used for pre-2000 decades) and 2000-2004 (used for decade 2000-2007)	~All Months have data	David Gensler MRGCD personal communication May 2008
Drain at RG x-sect	Armijo	1996-1999 (used for pre-2000 decades) and 2000-2004 (used for decade 2000-2007)	~All Months have data	David Gensler MRGCD personal communication May 2008
Drain at RG x-sect	Artisco	1996-1999 (used for pre-2000 decades) and 2000-2004 (used for decade 2000-2007)	~All Months have data	David Gensler MRGCD personal communication May 2008
Drain at RG x-sect	Lower San Juan Riverside	1996-1999 (used for pre-2000 decades) and 2000-2006 (used for decade 2000-2007)	~All Months have data	David Gensler MRGCD personal communication May 2008
Drain at RG x-sect	Low Flow Conveyance Channel @ Bernardo	1964-2004	~ All Months have Data	USGS Station 08317950
Drain at RG x-sect	Bernado Interior	1954-2004	~ All Months have Data	USGS Station 08332050
Drain at RG x-sect	LFCC @ San Acacia	1958-1986, 1986-2004	~ All Months have Data	USGS Station 08354800
Drain at RG x-sect	Socorro Main Canal North	1964-2003	~ All Months have Data	USGS Station 08354500
Drain at RG x-sect	LFCC @ San Marcial	1951-1975, 1978-2005	~ All Months have Data	USGS Station 08358300
Wastewater Treatment Plant	Albuquerque WWTP	1981-2007	~Monthly, a few missing months	NM Environment Department (Personal Communication with Sandra Gabaldon)

Table 4.9. Drain and WWTP: chemical data quantity and source.

Station Type	Station ID	Solute Quantity	Solute Quality	Data Source
Drain at RG x-sect	Cochiti Eastside Main Canal	No Data	No Data	Substituted with Rio Grande Chemistry
Drain at RG x-sect	ABQ Riverside	No Data	No Data	Substituted with Rio Grande Chemistry
Drain at RG x-sect	Arenal	No Data	No Data	Substituted with Rio Grande Chemistry
Drain at RG x-sect	Armijo	No Data	No Data	Substituted with Rio Grande Chemistry
Drain at RG x-sect	Artisco	No Data	No Data	Substituted with Rio Grande Chemistry
Drain at RG x-sect	Lower San Juan Riverside	No Data	No Data	Substituted with Rio Grande Chemistry
Drain at RG x-sect	Low Flow Conveyance Channel @ Bernardo	1965-1974	~1/2 filled	USGS Station 08317950
Drain at RG x-sect	Bernado Interior	1965-1968	~1/3 filled	USGS Station 08332050
Drain at RG x-sect	Low Flow Conveyance Channel @ San Acacia	1980-1989	sparse, ~1/2 filled with Regression	USGS Station 08317950
Drain at RG x-sect	Socorro Main Canal North	1 value, May 1974	1 value	USGS Station 08354500
Drain at RG x-sect	Low Flow Conveyance Channel @ San Marcial	1960-1974, 1975-1995	~1/2, ~All filled with Regression	USGS Station 08317950
Wastewater Treatment Plant	Albuquerque WWTP	Biannual 2002, 2005, 2006	Discharge Weighted Decadal Average, decreased by 60%	U.S. Fish and Wildlife samples (2002) [U.S. Fish and Wildlife, 2004] and NMT and UA samples (2005-2006) [Mills, 2003; Lacey, 2006]

4.7 Ground Water

Ground-water seepage and chemistry were available for many of the river reaches. Ground-water seepage rates and chemical data were taken from estimates in reference material, source and data quantity presented in Table 4.10. Ground water chemistry data quantity is in Table 4.11. Due to a lack of data and based on the assumption that groundwater chemistry remains constant, the data was not separated on

a decadal basis. All available data was lumped into a single seepage and a single solute value, which were used for all decades. A regression cannot be used to fill data gaps, because neither seepage nor solute information were available; thus, missing ground water data was filled by spatial extrapolation from nearby river reaches. For example, ground-water chemistry could not be found for the reach between Elephant Butte Dam and Caballo, therefore ground-water chemistry from San Acacia to San Marcial was used.

Table 4.10. Ground water: discharge quantity and data source.

Station Type	Rio Grande Reach	Discharge Quantity	Data Source
Ground Water	Lobatos - Taos	1 value used	[Ellis et. al., 1993]
Ground Water	Taos - Otowi	As an estimate, the seepage value from Otowi to San Felipe was used	[*Papadopulos and Associates*, 2000]
Ground Water	Otowi - SF	1 value used	[*Papadopulos and Associates*, 2000]
Ground Water	SF-ABQ	1 value used	[*Papadopulos and Associates*, 2000]
Ground Water	ABQ - Bernardo	1 value used	[*Papadopulos and Associates*, 2000]
Ground Water	Bernardo-SA	1 value used	[*Papadopulos and Associates*, 2000]
Ground Water	SA-SM	1 value used	[*Papadopulos and Associates*, 2000]
Ground Water	SM-EBD	1 value used	[*Papadopulos and Associates*, 2000]
Ground Water	EBD-Caballo	As an estimate the value from SM – EBD was used	[*Papadopulos and Associates*, 2000]
Ground Water	Caballo - El Paso	1 value used	[*Wilson*, 1981]

Table 4.11. Ground water: solute quantity and data source.

Station Type	Rio Grande Reach	Solute Quantity	Data Source
Ground Water	Lobatos - Taos	1 value used	Well # 13, from [*Anderholm* 2002]
Ground Water	Taos - Otowi	Median from 16 samples	Area #1 from [*Bexfiled and Anderholm*, 1996]
Ground Water	Otowi - SF	Average from 18 samples	Area #1, 11 from [*Bexfiled and Anderholm*, 1996] and data from [*Plummer et. al*, 2004]
Ground Water	SF-ABQ	Average from 26 samples	Area #1, 2, 3, 5, 8 from [*Bexfiled and Anderholm,* 1996]
Ground Water	ABQ - Bernardo	Average from 273 samples	Area #3, 4, 5, 8, 9, 10, 12 from [*Bexfiled and Anderholm*, 1996]
Ground Water	Bernardo-SA	Average from 8 samples	Area #7, 13 from [*Bexfiled and Anderholm*, 1996]
Ground Water	SA-SM	Average from 4 samples	from [*Plummer et. al*, 2004]
Ground Water	SM-EBD	1 value used	from [*Plummer et. al*, 2004]
Ground Water	EBD-Caballo	As an estimate the Caballo to El Paso (30 sample average) was used	From [*Anderholm* 2002]
Ground Water	Caballo - El Paso	Average from 30 samples	Avg. from Rincon Valley Wells in [*Anderholm* 2002]

4.8 Evapotranspiration

Evapotranspiration was included in each river reach. Data sources are shown in Table 4.12. The evapotranspiration number includes evaporation (from open water on the Rio Grande and reservoirs) and evapotranspiration (riparian and crop). Open-water evaporation was estimated by multiplying the channel area and the potential evaporation rate. Crop and riparian ET amounts were reported in *Lacey* [2006] and in *Papadopolous and Associates* [2000]. ET data quality and quantity varied with river

section. For the section from Lobatos to Taos and Taos to Otowi, open-water evaporation (calculated as described above) and an estimate of riparian ET (from Otowi to San Felipe) were included. *Papadopolous and Associates* [2000] calculated open-water evaporation and crop and riparian ET for sections between Otowi and San Marcial and Caballo to El Paso. The ET values presented by *Papadopolous and Associates* [2000] provide average values for crop and riparian ET from 1985-1998. ET for the remaining three river sections San Marcial to Elephant Butte Dam and Elephant Butte Dam to Caballo included Elephant Butte and Caballo reservoir evaporation [USBR unpublished data from personal communication with *Grajeda*, 2008], open-water river-channel evaporation and crop and riparian ET [*Lacey*, 2006]. One ET value was used for all decades except for the Elephant Butte-to-Caballo reach and the Caballo-to-El Paso reach. In the two southernmost reaches, ET data was sufficient to justify decadal separation. It is important to note that the ET data contains significant uncertainty, estimations were obtained or calculated from limited data and simplified equations.

Table 4.12. Evapotranspiration data quantity and source.
ET equation 1: ET = ET_{rate}*length*width (referenced in 'Solute Quantity' column as Eq. 1)

Station Type	Station ID	Solute Quantity	Solute Quality	Data Source
Evapotranspiration	Lobatos - Otowi	Same 1 value used for all decades	Open water ET calculated from (Eq. 1), Riparian ET estimated from Otowi – SF, No crop ET	[*Winograd*, 1960]
Evapotranspiration	Taos - Otowi	Same 1 value used for all decades	Open water ET (Eq 1), Riparian ET estimated from Otowi – SF, No crop ET	[*Winograd*, 1960]
Evapotranspiration	Otowi - SF	Same 1 value used for all decades	Value includes ET from crops, riparian, and open water.	[*Papadopulos and Associates*, 2000]
Evapotranspiration	SF-ABQ	Same 1 value used for all decades	Value includes ET from crops, riparian, and open water.	[*Papadopulos and Associates*, 2000]
Evapotranspiration	ABQ - Bernardo	Same 1 value used for all decades	Value includes ET from crops, riparian, and open water.	[*Papadopulos and Associates*, 2000]
Evapotranspiration	Bernardo-SA	Same 1 value used for all decades	Value includes ET from crops, riparian, and open water.	[*Papadopulos and Associates*, 2000]
Evapotranspiration	SA-SM	Same 1 value used for all decades	Value includes ET from crops, riparian, and open water.	[*Papadopulos and Associates*, 2000]
Evapotranspiration	SM-EBD	1 value used per decade	Riparian and crop data from S.S. Papadopulos 2000. EB Lake Evap. separated by decade from monthly samples.	[*Papadopulos and Associates*, 2000] USBR Unpublished data from personal communication with Jesus Grajeda
Evapotranspiration	EBD-Caballo	Same 1 crop and riparian value used for all decades 1 value used per decade	Open water ET (Eq 1), Riparian ET estimated from Otowi – SF, No crop ET Caballo Reservoir Evaporation separated by decade from monthly samples.	[*Farnsworth et. al.,* 1982] USBR Unpublished data from personal communication with *Jesus Grajeda*, 2008
Evapotranspiration	Caballo - El Paso	1 value used per decade	Open water ET (Eq 1), Riparian ET estimated from Otowi – SF, Crop ET	[*Farnsworth et. al.,* 1982]

CHAPTER 5
SOLUTE BUDGET AND CHEMICAL TRENDS

The following chapter presents graphics and discussion regarding decadal variations in chemical data with space and time. Concentrations, discharge and burdens are presented for the eleven station locations, from Lobatos, CO to El Paso, TX. Data from 1905-1907, 1931-1936, 1934-1939, 1940-1949, 1950-1959, 1960-1969, 1970-1979, 1980-1989, 1990-1999 and 2000-2005 is presented for all major solutes: calcium, sodium, magnesium, potassium, bicarbonate, sulfate and chloride. Recall that a lack of chemical data is an appreciable source of uncertainty for many decades at various locations. Early datasets were compiled from monthly data over only a few years, whereas the modern data were sporadically spaced throughout the decade. The modern data therefore tend to yield a more representative average over the decade, depending which location was considered. For purposes of visual clarity, data are occasionally reduced to the decades with the most complete chemical record (1960-1990).

5.1 Chemical Composition

The chemical composition of the Rio Grande relates molar equivalents of the dominant cations and anions. The relative percentage of each ion is independent of discharge. A trilinear diagram or Piper plot is used to capture the type of water at each river location. The 1980's decade is utilized to represent typical spatial variation in

chemistry. Figure 5.1 illustrates the linear trend from a calcium-bicarbonate water near Lobatos to a sodium-sulfate-chloride water at El Paso. The compositional linear trend is reversed at Lobatos and Otowi. Many tributaries join the Rio Grande between Lobatos and Otowi. These tributaries affect the chemical composition of the river. Figure 5.2 illustrates the tributary and brine sway over modern data, illustrated for 1980-1989. The Rio Chama cations plotted directly on top of the Rio Grande at Otowi cations and near the average minor tributary chemistry. Thus the Lobatos-to-Otowi compositional reversal is due to tributary influence, particularly the Rio Chama. After San Marcial, the compositional trend is strongly influenced by geologic brine seepage (Figure 5.2). The brine data are taken from ground waters near San Antonio [*Newton, 2005*] and El Paso [*Moore et al, 2008]*. Sodium is the dominant cation in all brine samples, but the dominant anion varies with spatial location. The brine collected near San Marcial has a strong sulfate signature, such that locations below San Marcial veer to the upper right in the anion triangle of Figure 5.2. Elephant Butte, Caballo and El Paso appear to be affected by the San Marcial brine. The El Paso brine is heavy in chloride and thus the Rio Grande samples at El Paso are pulled toward chloride.

Temporal variations in chemical composition are illustrated at select locations in Figure 5.3 and specifically at El Paso in Figure 5.4. Cation compositions remain constant through time, spatially trending toward brine composition from calcium dominated (northern) toward sodium dominated (southern). However the anion compositions vary significantly, trending historically from sulfate-chloride water toward bicarbonate in modern decades (2000-2005). San Marcial data from 1905-1907 fit this trend, plotting inline with the other decades at San Marcial. Interestingly, the

1905-1907 data at El Paso compositionally matches the other decades at San Marcial. Storage within Elephant Butte Reservoir may be the reason behind this deviation (Figure 5.4). Elephant Butte Reservoir did not exist during 1905-1907. Prior to the reservoir, water flowed freely from San Marcial to El Paso without any residence time spent in Elephant Butte Lake. Samples from 1905-1907 at El Paso are compositionally similar to those at San Marcial because of an absence of solute precipitation in Elephant Butte Reservoir. Calcium and bicarbonate are lost to mineral formation and the compositions of sodium, sulfate and chloride increase due to a greater inflow of brine seepage derived from the presence of Elephant Butte Reservoir. Due to the hydrologic connection, less water in the river leads to more water entering the channel from brine and ground water sources. This deviation between modern and historic chemistry at El Paso indicates that Elephant Butte Lake influences the composition of the Rio Grande. In addition, low lake levels in Elephant Butte during the 1970's may have driven larger quantities of brine into the river system, which strongly influenced chemical compositions at Elephant Butte Dam.

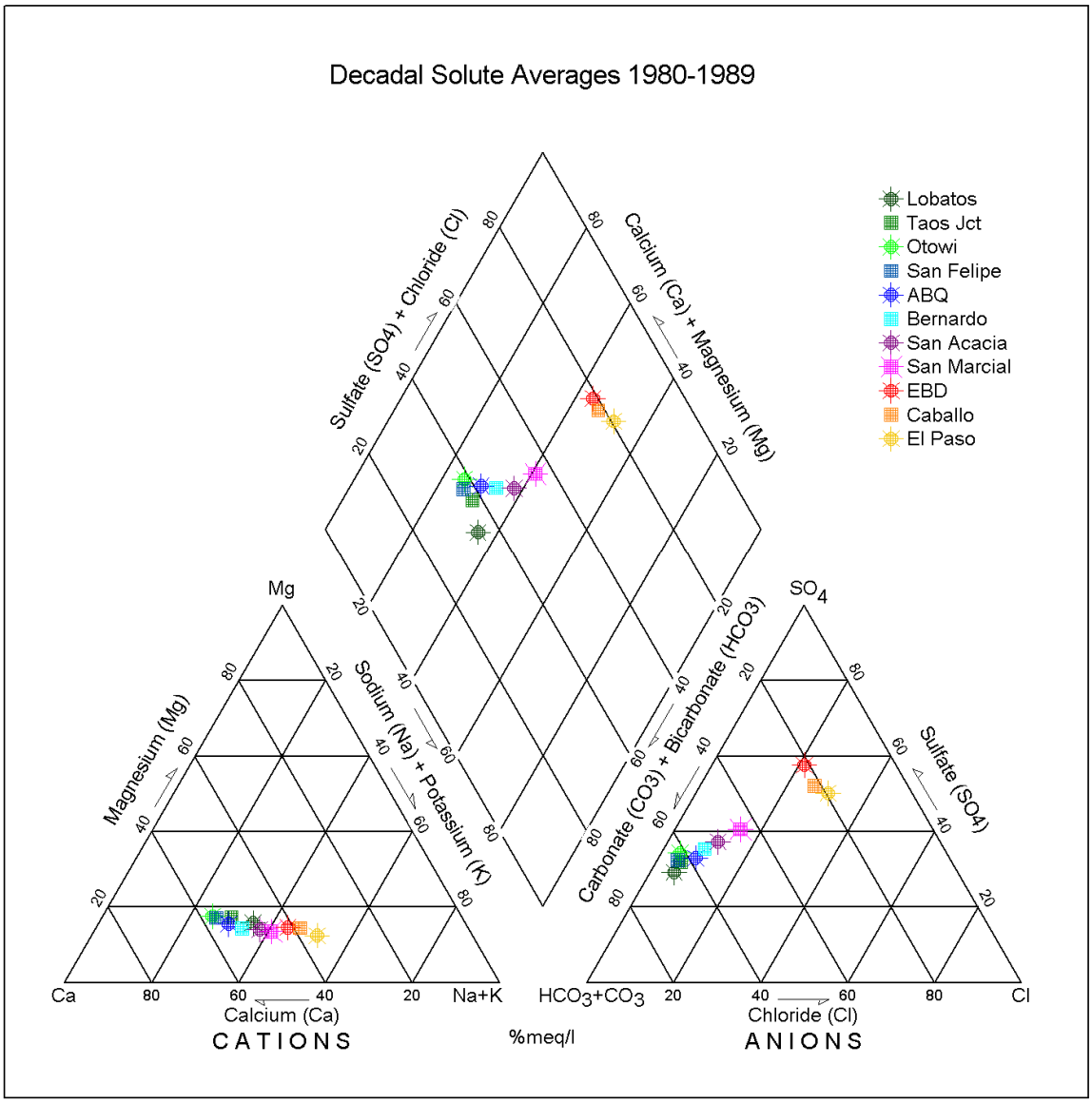

Figure 5.1. Trilinear diagram of average decadal chemistry from the 1980's for all Rio Grande locations.

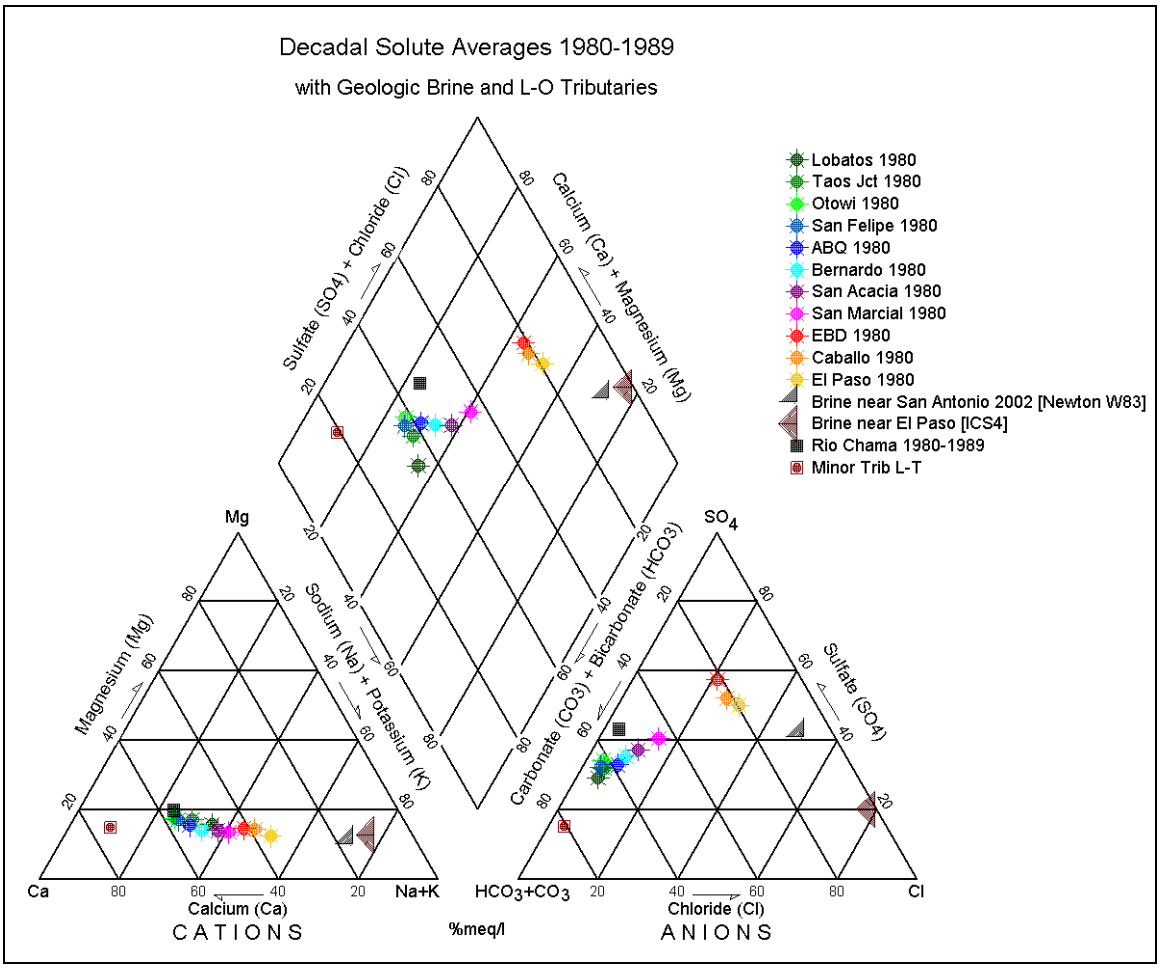

Figure 5.2. Trilinear diagram of average decadal chemistry from the 1980's at all Rio Grande locations, for comparison with geologic brine and Lobatos to Otowi tributaries, specifically the Rio Chama. Circles represent Rio Grande cross sections, triangles represent geologic brine at San Antonio and El Paso, squares represent average minor tributary chemistry between Lobatos to Taos and Rio Chama chemistry from 1980-1989.

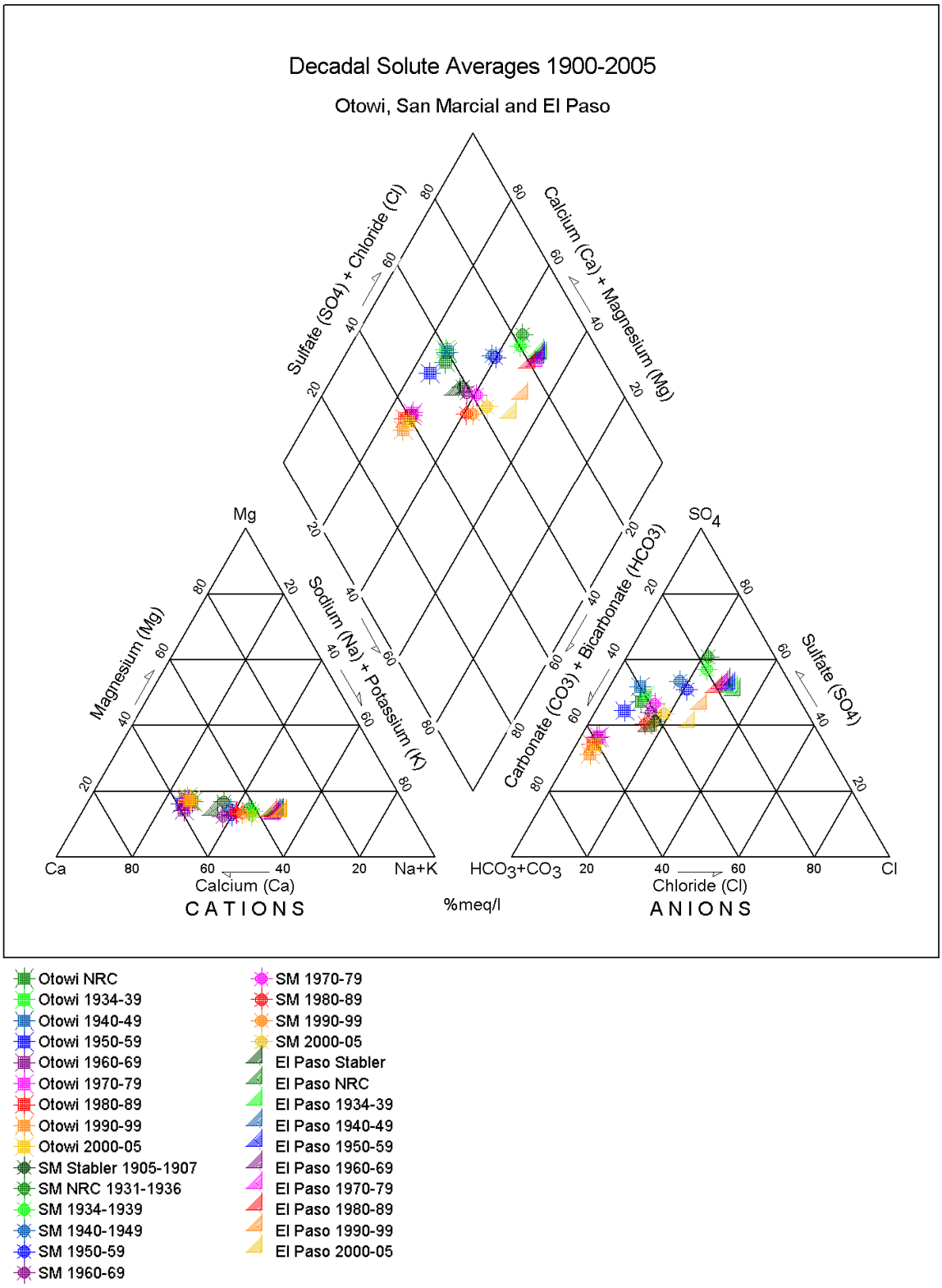

Figure 5.3. Trilinear diagram of average decadal chemistry from the decades between 1905-2000 for three Rio Grande stations: Otowi, San Marcial, and El Paso.

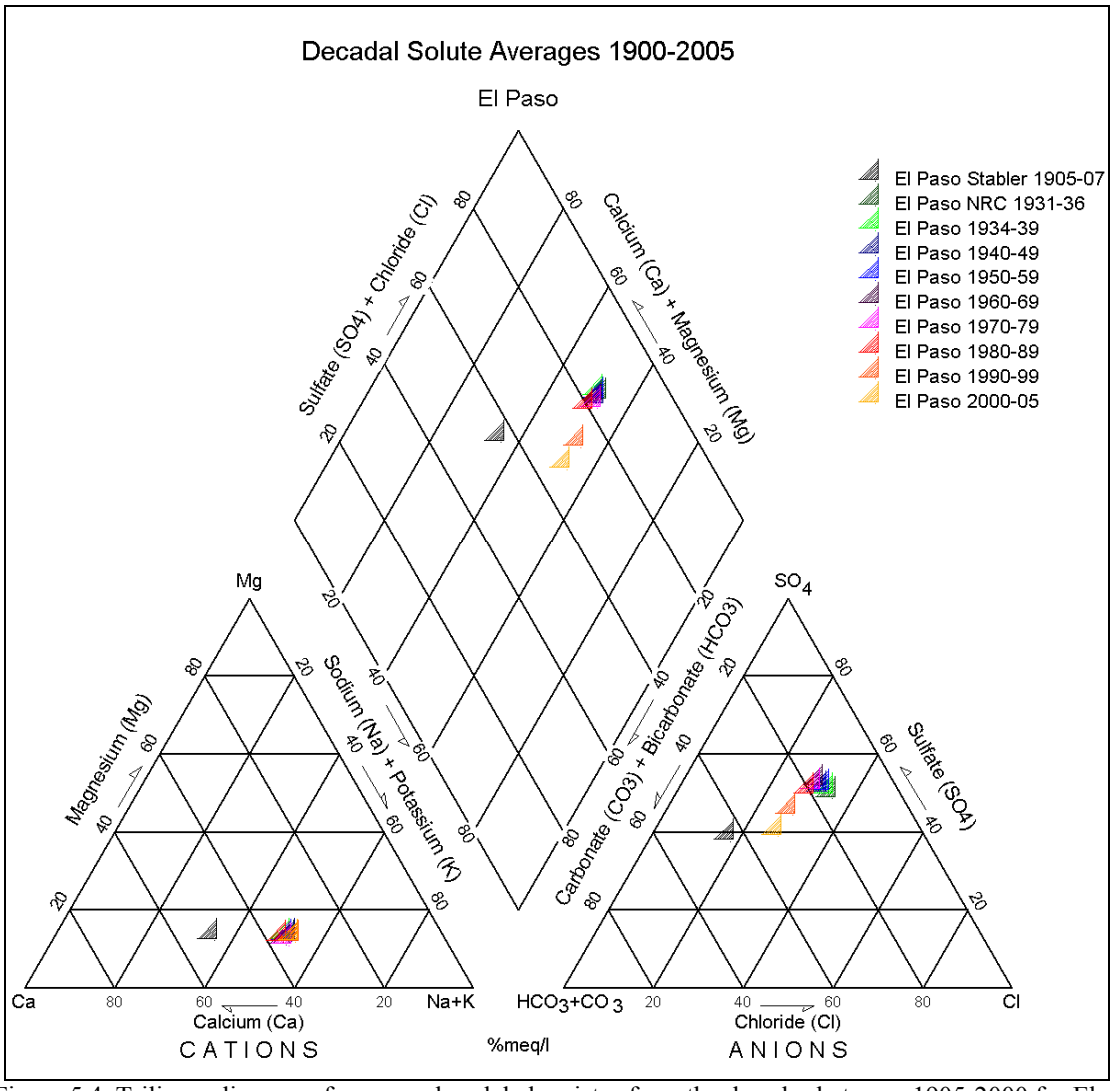

Figure 5.4. Trilinear diagram of average decadal chemistry from the decades between 1905-2000 for El Paso.

5.2 Discharge Comparison

The Rio Grande transports flow from winter snowmelt, summer monsoon rain, ground water, and tributaries. Variations in climate affect the amount of snow, rain and runoff, which affects the discharge carried in the river at any given location. The total discharge is the total amount of water in the Rio Grande system flowing past a particular location, i.e., water from drains that by-pass the main channel gage are included in these discharge calculations. All decades show increased discharges with

distance downstream from Lobatos to Otowi, constant flow from Otowi until San Marcial where the discharge declines as the Rio Grande enters El Paso (Figure 5.5). The increase between Lobatos and Otowi is controlled by a wetter climate and higher elevations, which lead to increased runoff generation and larger discharge contributions from tributaries (Table 5.1). Discharge remained relatively constant between Otowi and San Marcial due to increased evapotranspiration, fewer tributary contributions and seepage loss to the aquifer as compared to the northern section. Storage released from the reservoirs and diversion dams directly affected the quantity of water in the Rio Grande below Elephant Butte Dam.

The wettest periods were 1905-1907, 1980-1989 and 1990-1999 based on Rio Grande discharge. In order of highest-to-lowest discharge, the periods were ranked: 1905-1907, 1980-1989, 1940-1949, 1990-1999, 1934-1939, 1970-1979, 1950-1959, and 2000-2005. The high discharge in 1905-1907 can be attributed to weather patterns, less irrigation diversion and no reservoir storage. The 1905-1907 data was particularly high during the snowmelt/runoff and monsoon season months of March through July. Monthly trends are presented at San Marcial (Figure 5.6) and El Paso (Figure 5.7) comparing 1905-1907 data to modern data (1986-1990). These dates were utilized to represent typical modern behavior, specifically utilizing the 1980's because modeling efforts (to be discussed in Chapter 6) were focused on this decade. The discharge transition between San Marcial and Elephant Butte Dam is greatly controlled by storage within Elephant Butte Reservoir. When the volume of water stored in the reservoir increases, the flow at Elephant Butte Dam decreases. During the 1980's, Elephant Butte Reservoir was in a refilling stage (Figure 5.8), such that more water entered at San

Marcial than exited at the Elephant Butte dam. Notice the large dip in discharge between San Marcial and Elephant Butte (Figure 5.5). In 2000, the reservoir entered an emptying period (Figure 5.8); notice the discharge increase between San Marcial and Elephant Butte Dam (Figure 5.5). The amount of water stored in Elephant Butte is dependent on the amount of water that enters the reservoir at the northern narrows because a specified amount of water must leave Elephant Butte to ensure that the Rio Grande Compact is met. The quantity of water stored within Elephant Butte carries a certain mass of each solute, such that the solute mass balance calculations must account for this stored quantity may be impacted. For this reason, the amount of solutes that remained stored in Elephant Butte reservoir in the 1980's was computed. Discussion of the stored solute load calculation can be found in Chapter 6.

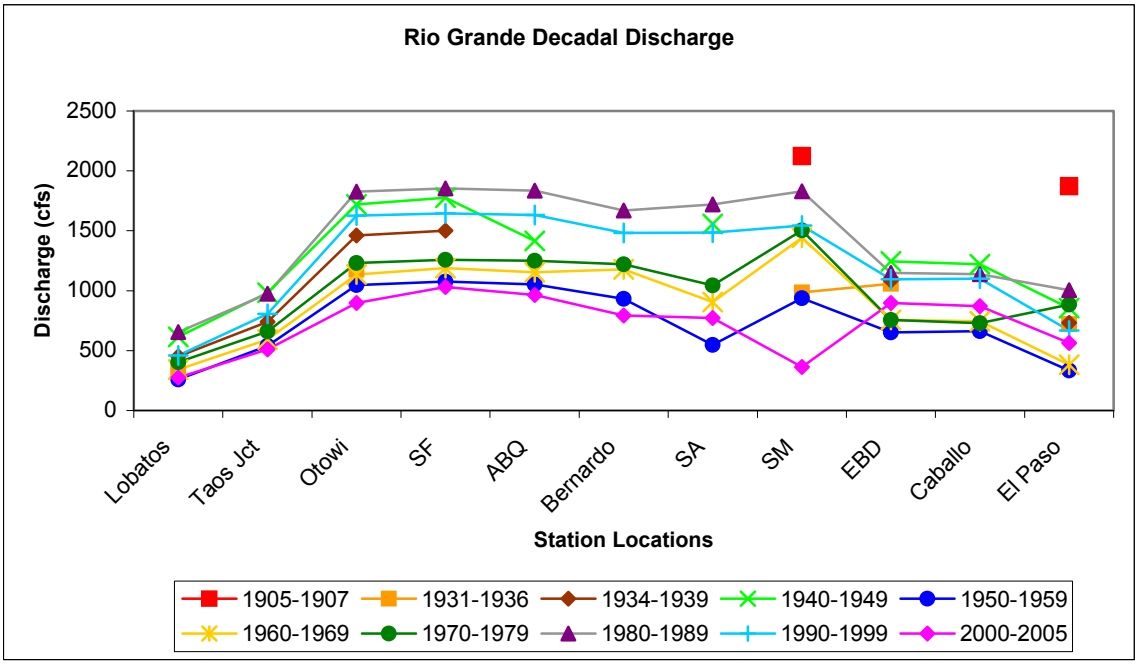

Figure 5.5. Discharge data from 1905-1907 (Stabler), 1931-1934 (NRC), and 1934-2005 compiled by decade from various sources (Wilcox, USGS, USBR).

Table 5.1. Combined tributary discharge (L/month).

	Lobatos - Taos	Taos - Otowi	Otowi - SF	SF – ABQ	Bernardo - SA
1934-1939	2.8E+09	5.2E+10	No Data	No Data	No Data
1940-1949	7.3E+09	5.4E+10	No Data	4.3E+09	4.4E+09
1950-1959	1.1E+10	3.6E+10	No Data	3.2E+09	4.3E+09
1960-1969	8.1E+09	3.9E+10	No Data	4.2E+09	3.0E+09
1970-1979	1.5E+10	4.1E+10	1.1E+09	4.9E+09	2.6E+09
1980-1989	1.9E+10	6.1E+10	1.2E+09	6.4E+09	2.6E+09
1990-1999	1.9E+10	6.0E+10	1.6E+09	5.2E+09	2.5E+09
2000-2005	1.2E+10	3.9E+10	7.8E+08	3.4E+09	9.2E+08

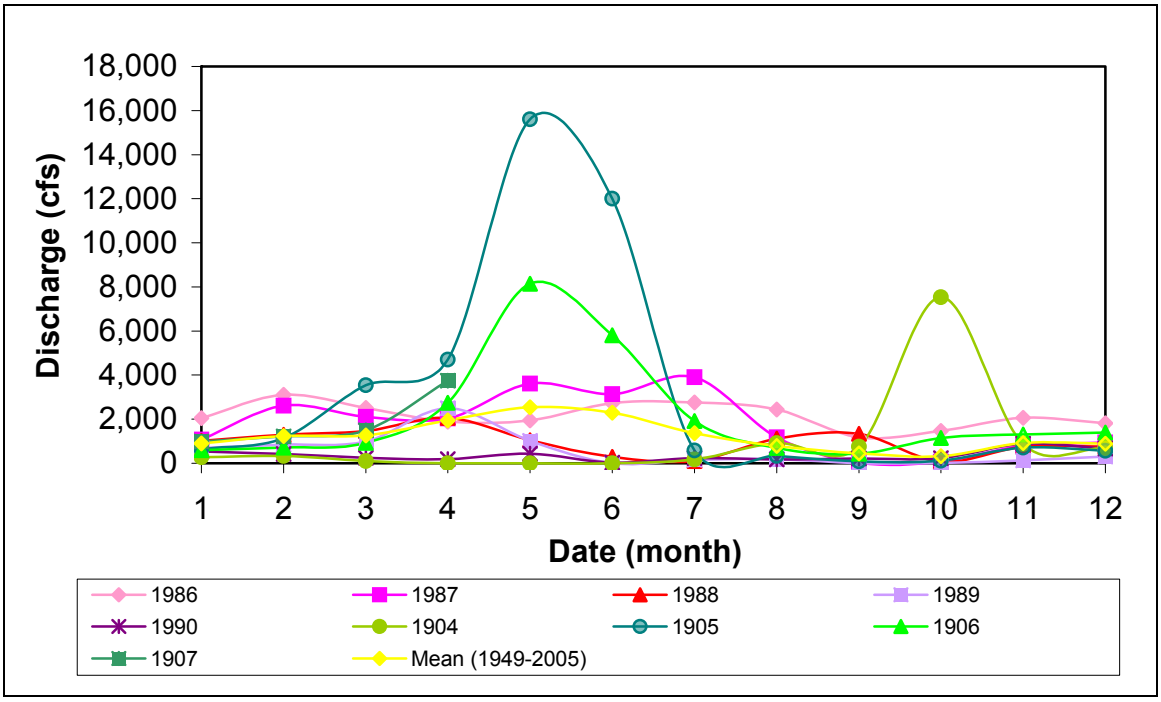

Figure 5.6. Monthly average discharge comparing 1905-1907 to modern (1986-1990) at San Marcial. Note: only main channel discharge is presented (LFCC at San Acacia and LFCC at San Marcial have not been included). The unit cfs = ft^3/s.

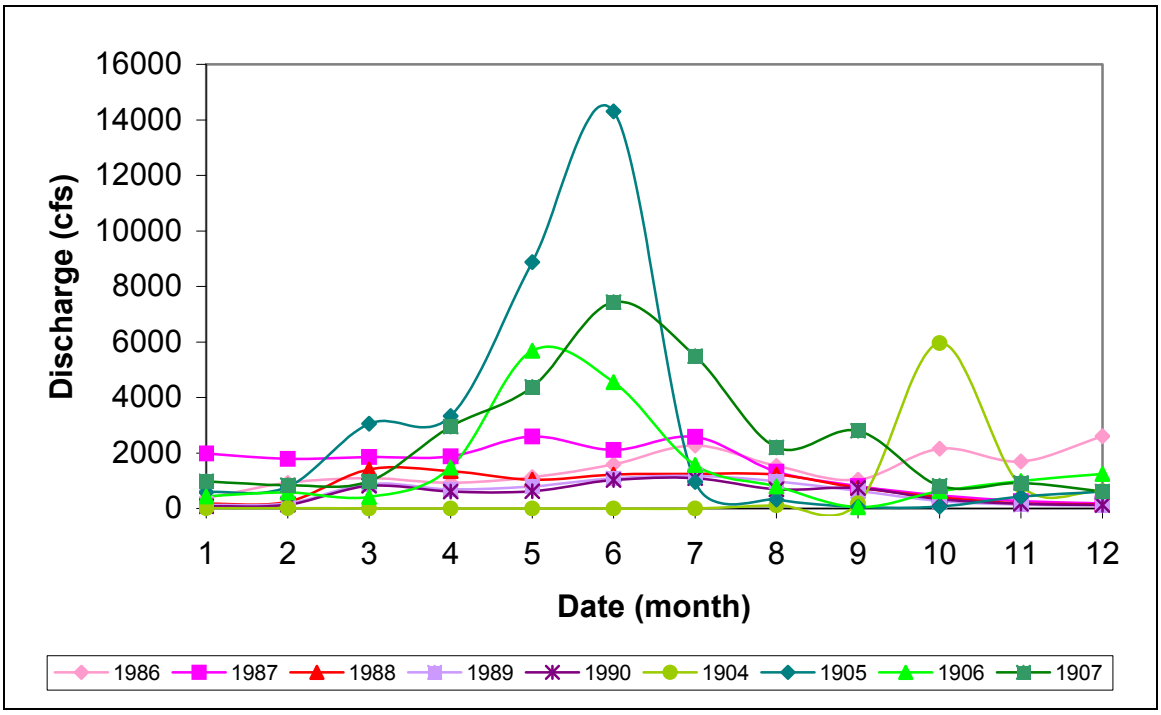

Figure 5.7. Monthly average discharge comparing 1905-1907 to modern (1986-1990) at El Paso. Note: only main channel discharge is presented (LFCC at San Acacia and LFCC at San Marcial have not been included). The unit cfs = ft^3/s.

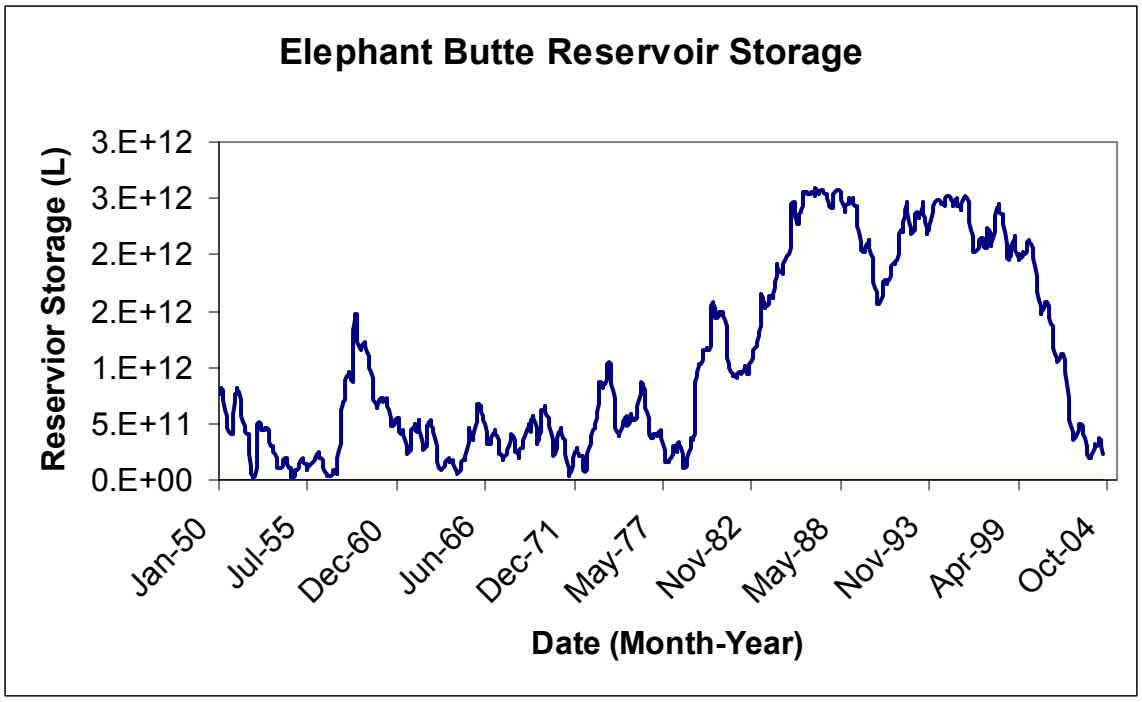

Figure 5.8. Monthly average storage volume in Elephant Butte Reservoir from January 1950-July 2004.

5.3 Solute Concentrations

Chemical concentrations for reactive and conservative solutes as well as TDS are presented with respect to time and space. Chloride is considered a conservative solute as it rarely interacts with other solutes or mineral phases. Chloride and TDS are discussed collectively due to similar behavior in the Rio Grande system. The reactive solutes (sodium, calcium, magnesium, potassium, sulfate and bicarbonate) are discussed collectively. These solutes may or may not interact with mineral phases along the flow path from the irrigation canal through agricultural soil, mixing with ground water and flowing back to the Rio Grande.

5.3.1 TDS and Cl

Total dissolved solids (TDS) continually increased from the headwaters near Lobatos to El Paso during all decades (Figure 5.9). The Rio Grande TDS increased from dilute source waters (200 mg/L) to 900 mg/L near El Paso. The chloride decadal average concentration also steadily increased with distance downstream (Figure 5.10). The increasing trend occurred in a stepwise fashion at key locations, specifically San Acacia, Elephant Butte, and El Paso. These intervals coincide with the termini of sedimentary basins, where brine inflows entered the river [*Mills 2003, Lacey 2006*]. Low concentrations of chloride in the range of 3-10 mg/L in the headwaters increase to up to 130mg/L by El Paso.

Temporal variability in TDS and chloride data existed among decades. The Rio Grande valley experienced water shortages during the 1950's, which likely caused the higher concentrations during this decade at all reported locations. The 1960's and 1970's deviated from other decadal data at Albuquerque and San Acacia. An

unrepresentative data record due to limited chemical information at Albuquerque during these decades likely created the concentration spikes. Much of the chemical data for this decade was generated from a regression against discharge. It is possible that the Albuquerque decadal solute averages could have been affected by the percentage of ground water entering the Rio Grande. As the population of Albuquerque increased, the city progressively utilized increasing quantities of ground water to offset the municipal demand, which eventually flushed through the wastewater treatment plant and into the Rio Grande. The high TDS and chloride concentrations at San Acacia in the 1970's were a function of high chloride in the Low-Flow Conveyance Channel, where the record for both decades was derived almost entirely from EC/TDS regression.

There was some inter-decadal variability among modern (1960-2000) and historical concentrations (1905-1907 and 1931-1936). The *Stabler* [1911] solute concentrations from 1905-1907 were similar to modern concentrations at San Marcial and El Paso. The data published by the *National Resources Committee* [1938] for 1931-1936 significantly deviated from modern data. The *NRC* [1938] reported a much higher TDS and chloride concentration than any other decade. The compiled data for 1934-1939 also had higher solute concentrations than modern decades, thus suggesting that greater concentrations of salt flushed through the Rio Grande basin during the 1930's. The increased salt concentration in the Rio Grande during the 1930's related to irrigation of agricultural lands, poorly drained soils, and the installation of a proper drainage network. Interior drain data from the 1930's captured these high concentration waters indicative of agricultural solute flushing. Chemical data from interior drains and riverside drains is shown in Table 5.2 [*Clark and Meager*, 1932]. Riverside drains flow

along the river carrying river water, ground water and water intercepted from interior drains. The interior drains branch from the riverside drains, directly drain agricultural land, then empty back into riverside drains or in a few cases empty into the Rio Grande. The interior drain labeled Bosque carried a TDS concentration of 1756 mg/L, more than double that of the nearby riverside drain in Belen with a concentration of 425 mg/L. Solute concentrations from this dataset suggest that agricultural drains transmitted large concentrations of solutes to the river during the 1930's and 1940's, following the installation of an extensive drainage network.

Chemical data collected by *Clark and Meager* [1932] were compared to current drain concentrations (data from biannual synoptic sampling 2000-2006) in the same general area (Table 5.3). Higher TDS and chloride concentrations were found in the interior drains of the 1930's than current drain conditions; notice the Bosque TDS in 1930 was 1756 mg/L compared to an average 371 mg/L from 2000-2005. At a few locations, current drains carry higher concentrations than 1930's drains. The average concentration from current data might be unrepresentative since samples were collected on one day during the summer of the consecutive years, whereas the 1930's data was an average of multiple samples collected over an irrigation season. Other major solute concentrations are also presented in Tables 5.3b and 5.3c. Calcium, sodium, magnesium, potassium, sulfate and bicarbonate concentrations from the 1930's were generally similar or slightly higher than current drain conditions, supporting the idea that accumulated salts had been flushed from the drains. This salt source no longer significantly affects Rio Grande chemistry.

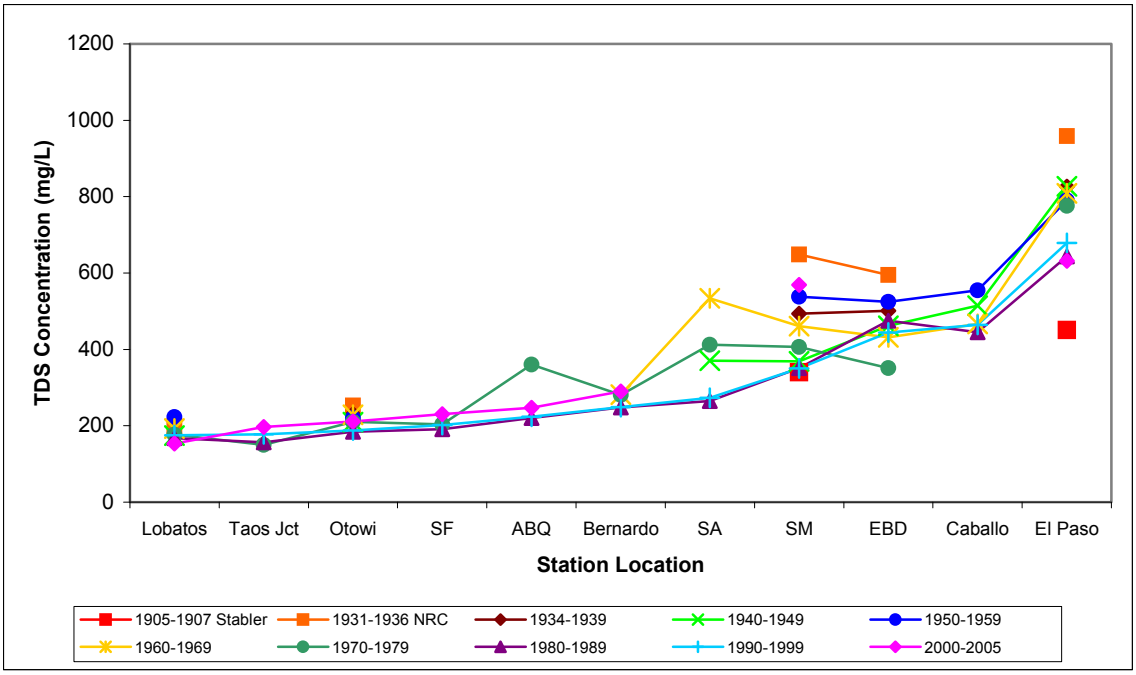

Figure 5.9. Total dissolved solids concentration at each station for the decades 1905-1907 from *Stabler* [1911], 1931-1936 from *National Resources Committee* [1938], the compiled data for 1934-1939, and decades between 1940 and 2000.

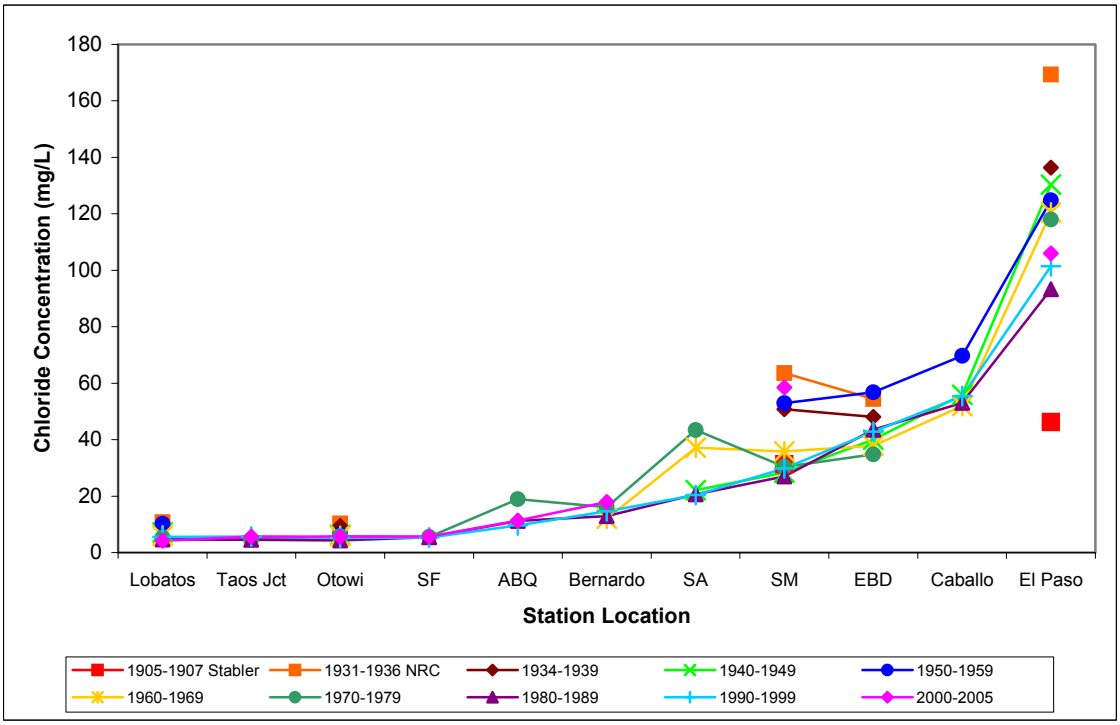

Figure 5.10. Chloride concentration at each station for the decades 1905-1907 from *Stabler* [1911], 1931-1936 from *National Resources Committee* [1938], compiled data for 1934-1939, and decades between 1940 and 2000.

Table 5.2. Riverside and interior drains of the Middle Rio Grande: chemistry. [*Clark and Mauger*, 1932]

Riverside Drains	TDS (mg/L)	Cl (mg/L)	SO_4 (mg/L)	Na +K (mg/L)	Mg (mg/L)	Ca (mg/L)	HCO_3 (mg/L)	CO_3 (mg/L)
Algodones	380	15	88	40	20	56	166	19
Bernalillo	374	30	103	33	21	55	160	18
Corrales	352	28	84	53	14	55	160	6
Albuquerque	349	21	91	37	14	49	144	16
Albuquerque Barr	431	33	126	42	20	65	195	8
Atrisco	436	28	120	71	21	59	157	18
Peralta	422	30	118	59	22	59	182	14
Belen	425	28	141	44	22	66	181	7
San Juan	383	29	125	62	25	62	160	15
Lemitar	550	63	186	83	20	76	177	17
San Antonio	608	72	167	109	20	64	201	16
Interior Drains:								
Alameda	941	96	305	145	33	131	272	5
Isleta	680	51	247	125	21	99	230	11
Bosque	1756	236	605	298	40	160	261	7

Table 5.3. Comparing modern (from Rio Sampling 2000-05) to 1930-1931 drain study (from UNM Bulletin) chemistry: a) TDS, b) major cations, c) major anions.

a)	TDS	TDS
	1930-1931	2000-2005
Corrales Rvsd	352	245
Atrisco Drain	436	256
ABQ Rvsd	349	283
Peralta Rvsd	422	371
San Juan Rvsd	383	501
Socorro Rvsd in San Antonio	608	628
Bosque Interior Drain and Feeder 3 WW	1756	371

b)	Na +K (mg/L)	Na +K (mg/L)	Ca (mg/L)	Ca (mg/L)	Mg (mg/L)	Mg (mg/L)
	1930-1931	2000-2005	1930-1931	2000-2005	1930-1931	2000-2005
Corrales Rvsd	53	25	55	39	14	7
Atrisco Drain	71	32	59	41	21	7
ABQ Rvsd	37	40	49	44	14	8
Peralta Rvsd	59	49	59	57	22	10
San Juan Rvsd	62	67	62	65	25	13
Socorro Rvsd in San Antonio	109	116	64	74	20	14
Bosque Interior Drain and Feeder 3 WW	298	47	160	53	40	9

c)	Cl (mg/L)	Cl (mg/L)	SO_4 (mg/L)	SO_4 (mg/L)	HCO_3 (mg/L)	HCO_3 (mg/L)
	1930-1931	2000-2005	1930-1931	2000-2005	1930-1931	2000-2005
Corrales Rvsd	28	9	84	45	160	150
Atrisco Drain	28	13	120	58	157	163
ABQ Rvsd	21	17	91	60	144	178
Peralta Rvsd	30	26	118	91	182	203
San Juan Rvsd	29	37	125	124	160	225
Socorro Rvsd in San Antonio	72	84	167	171	201	259
Bosque Interior Drain and Feeder 3 WW	236	20	605	76	261	200

5.3.2 Reactive Solutes

The reactive solutes consist of calcium, sodium, magnesium, potassium, bicarbonate, and sulfate. These constituents, considered reactive due to the likelihood of interacting with mineral phases, also vary with distance downstream. The sodium concentration presented in Figure 5.11, shows a similar trend to that of Rio Grande TDS and chloride. Sodium increased from 16 mg/L (Lobatos) to approximately 150 mg/L (El Paso). Varying slightly from sodium, the calcium, magnesium and potassium ions shared similar chemical trends. The concentrations increased with distance downstream from 20mg/L to 85 mg/L for Ca, 5-20 mg/L for Mg, 3-7 mg/L for K, 30-270 mg/L for SO_4, see Figures 5.12, 5.13, 5.14 and 5.15, respectively. The reactive solutes as a group moderately increased downstream, although the trend was less pronounced than the stepwise concentration increases visible in the TDS, Cl and Na trends (Figures 5.9, 5.10 and 5.11). As with TDS and chloride, the 1931-1936 [*NRC*, 1938] concentrations remain consistently high. Noted previously, the *NRC* [1938] data was high due to flushing of salts from high concentration vadose zone pore water or directly dissolving mineralized salt from previously undrained acreages. The peak

observed at San Acacia during the 1960's and 1970's, more dominant with the reactive solutes, was likely caused by brine inflow, although it is important to note that 1970's data was limited. Sulfate and bicarbonate concentrations increased more rapidly than the other reactive solutes. The concentration of sulfate is greatly affected by geologic brine inflow, as the typical brine is a sodium-sulfate-chloride water. In contrast, the bicarbonate concentration (Figure 5.16) decreased below Elephant Butte and below Caballo. The bicarbonate (as well as the other solute) data suggest that the solutes may be precipitating in Elephant Butte. Reactive solute behavior will be further examined in Chapters 6 and 7.

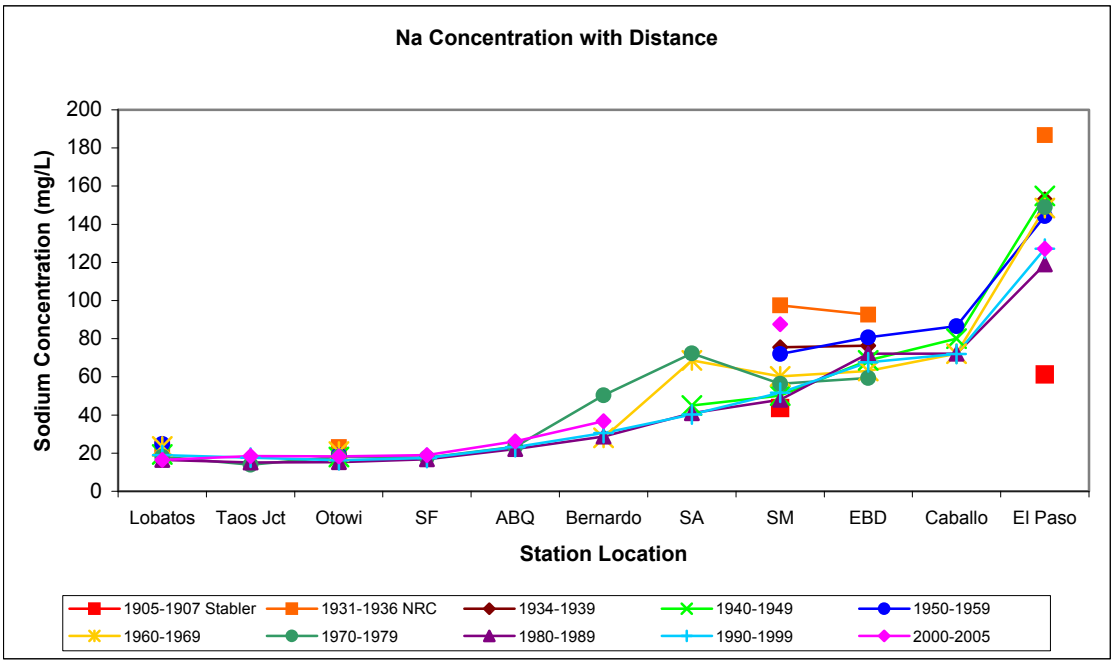

Figure 5.11. Sodium concentration at each station for the decades 1905-1907 from *Stabler* [1911], 1931-1936 from *National Resources Committee* [1938], the compiled data for 1934-1939, and decades between 1940 and 2000.

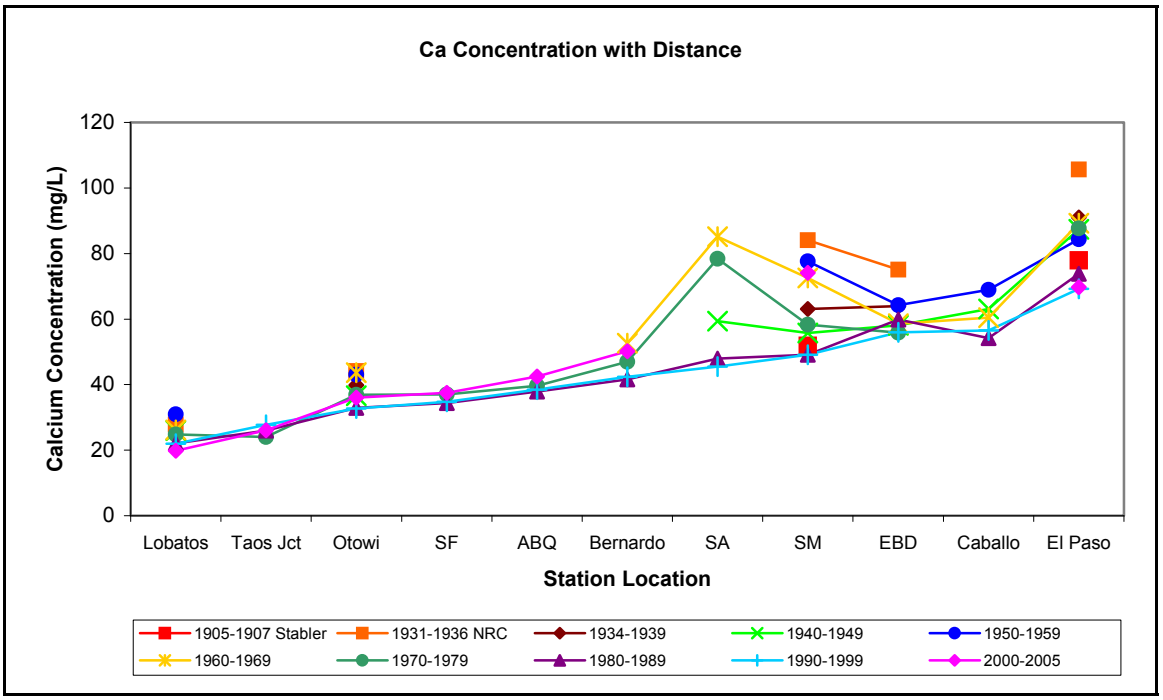

Figure 5.12. Calcium concentration at each station for the decades 1905-1907 from *Stabler* [1911], 1931-1936 from *National Resources Committee* [1938], the compiled data for 1934-1939, and decades between 1940 and 2000.

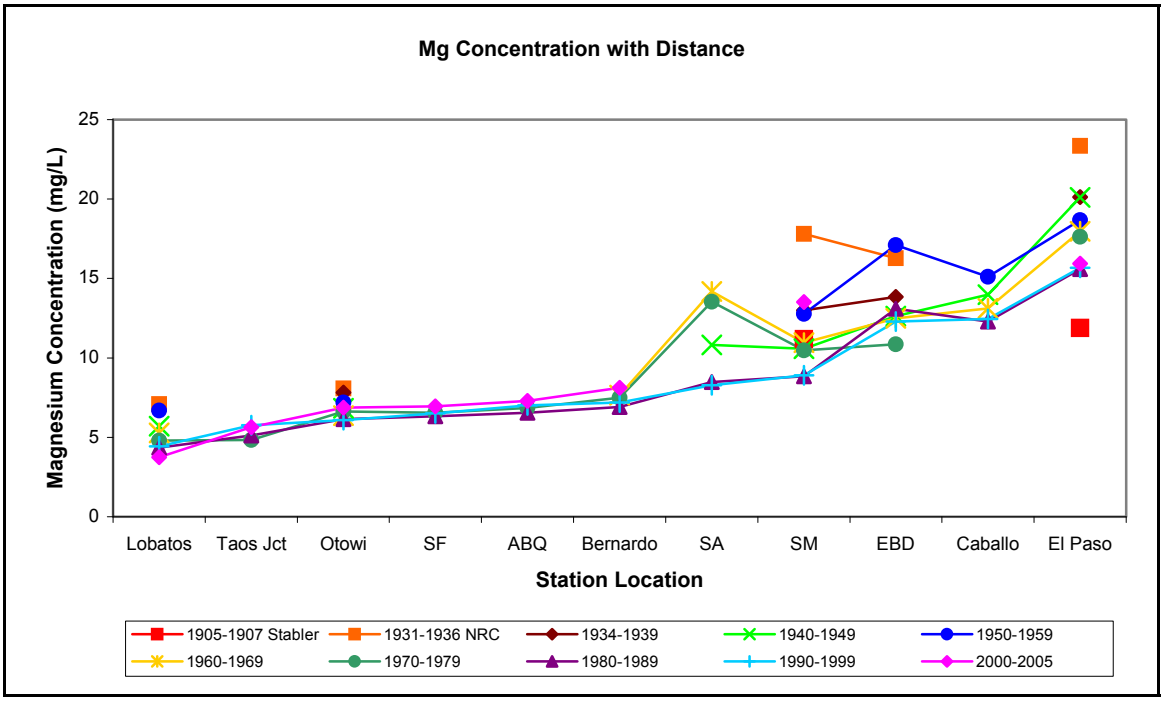

Figure 5.13. Magnesium concentration at each station for the decades 1905-1907 from *Stabler* [1911], 1931-1936 from *National Resources Committee* [1938], the compiled data for 1934-1939, and decades between 1940 and 2000.

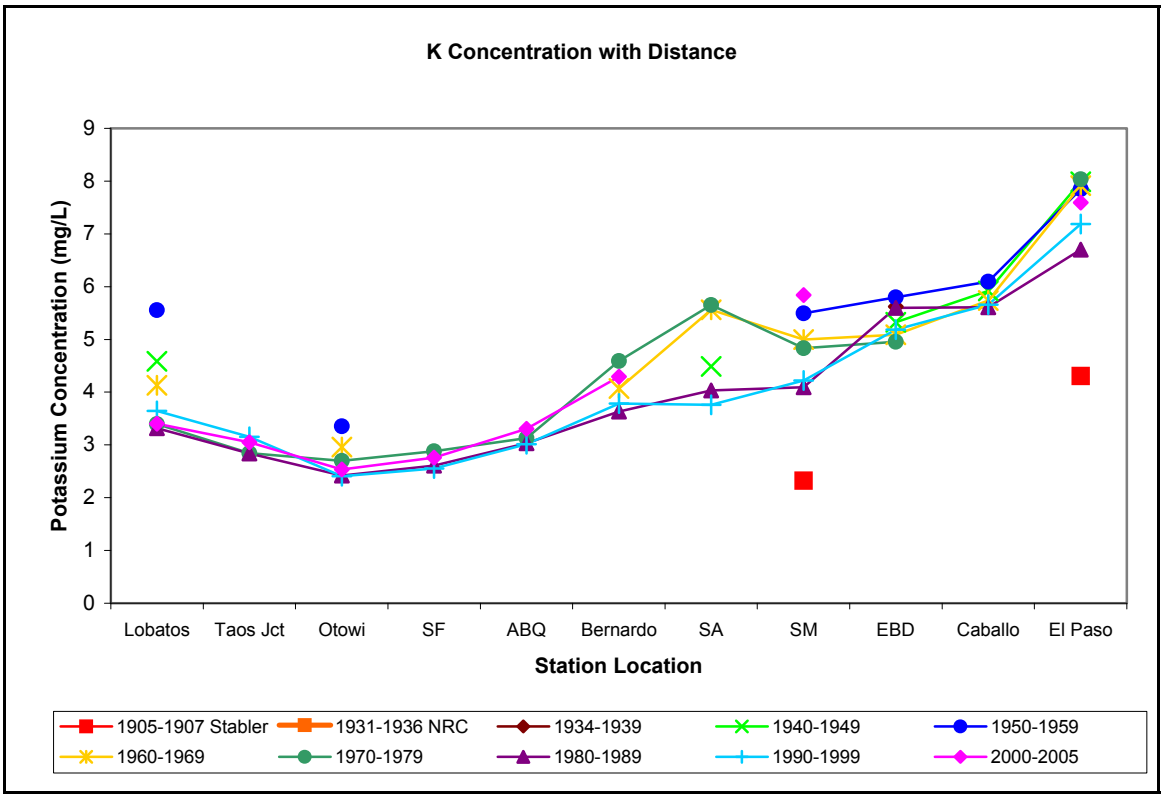

Figure 5.14. Potassium concentration at each station for the 1905-1907 from *Stabler* [1911], 1931-1936 from *National Resources Committee* [1938], the compiled data for 1934-1939, and decades between 1940 and 2000.

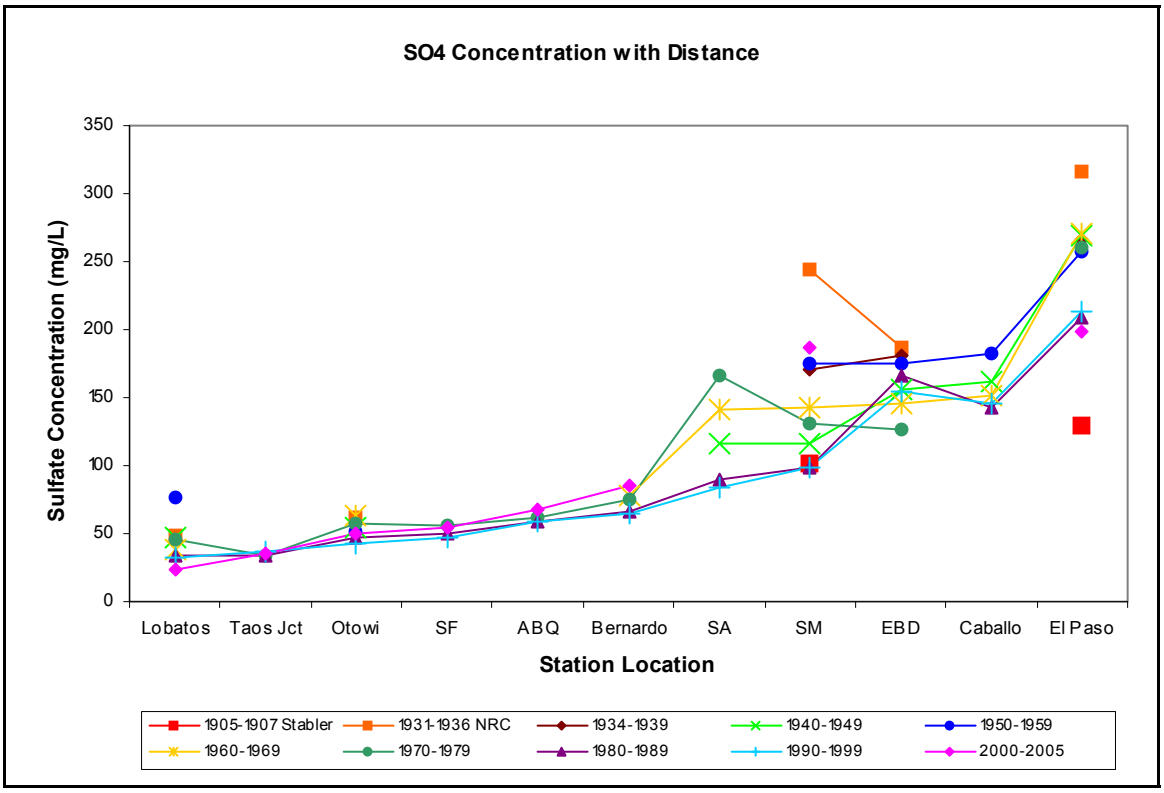

Figure 5.15. Sulfate concentration at each station for the decades 1905-1907 from *Stabler* [1911], 1931-1936 from *National Resources Committee* [1938], the compiled data for 1934-1939, and decades between 1940 and 2000.

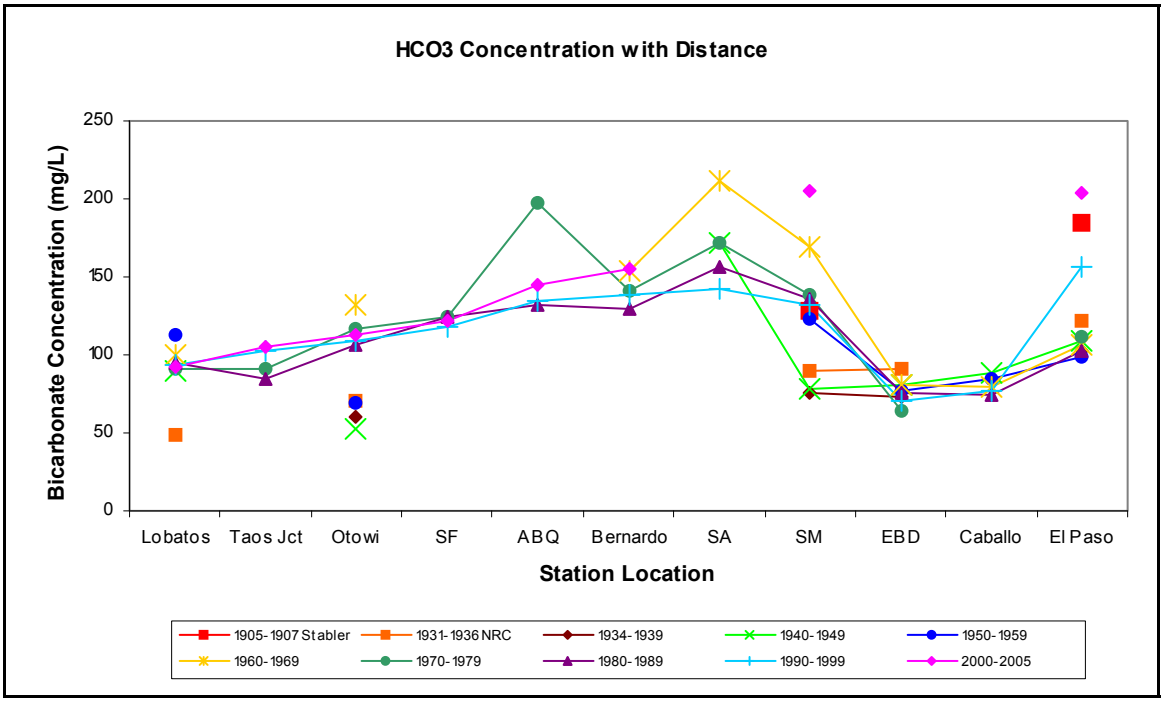

Figure 5.16. Bicarbonate concentration at each station for the decades 1905-1907 from *Stabler* [1911], 1931-1936 from *National Resources Committee* [1938], the compiled data for 1934-1939, and decades between 1940 and 2000.

5.4 Solute Loads

Defined as the concentration multiplied by the discharge, the solute load is the mass of solute passing a location in a given time period. Load comparisons allow for the assessment of solute fluxes both spatially and temporally. The Rio Grande solute loads follow similar spatial trends to the concentration variations.

TDS, chloride and sodium (Figures 5.17, 5.18 and 5.19) loads increased steadily downstream just as the concentration did. There was very little data available from the Low Flow Conveyance Channel at San Acacia. Calcium, magnesium, potassium, sulfate, and bicarbonate (Figures 5.20, 5.21, 5.22, 5.23 and 5.24 respectively) were also dominated by the concentration trend, increasing until Elephant Butte Dam where there was a slight decline. Recall that the discharge decrease below Elephant Butte is due to reservoir storage and flow regulation. Since both concentration and discharge increased between Lobatos and Otowi, the load also increased during this stretch for all constituents. Between Otowi and Elephant Butte, the concentration increased but the discharge remained essentially constant, thus the load increased at a slightly shallower rate than the concentration. Below Elephant Butte solute behavior varied. Chloride and sodium continued to increase due to high chloride and sodium brines merging with river water. Reactive solute loads decreased slightly after Elephant Butte due to decreased discharge and possibly precipitation of minerals within Elephant Butte Lake. The bicarbonate load showed the largest decrease below Elephant Butte. Modern decades of 1960, 1970, 1980 and 1990 are compared temporally in Figures 5.19 – 5.24. Solute loads from the 1980's and 1990's illustrated similar downstream trends, due to

the similarly high discharges experienced during both decades. Typically the 1960's showed the smallest loads, which again correlates to the discharge.

Spatial and temporal solute loads for the entire period of record are presented in summary plots, Figures 5.25 (5.25a is TDS prior to regression and 5.25b is post regression), 5.26, 5.27, 5.28, 5.29, 5.30, 5.31 and 5.32. Historical solutes loads present a sinusoidal pattern with high loads in the early 1900's, 1930's and 1940's, and 1980's. The 1905-1907 and 1931-1936 data showed much higher loads for all solutes as compared to other decades. The discharge during 1905, 1906 and 1907 was exceptionally high (see Figures 5.6 and 5.7); probably from the lack of anthropogenic flood control features, i.e. the lack of Elephant Butte. Higher loads in the 1930's were due to flushing of vadose-zone and ground water solutes from previously undrained soils. Loads generally decreased over recent decades from the 1980's to the present. The 1970's and 1980's also showed high loads, particularly at El Paso. This is due in part to the 1980's being the wettest decade. Fairly high discharge flowed during the 1970's, which may create the higher loads or this increase could be from a smaller scale salt flushing which accumulated during drought periods in the 1950's and 1960's.

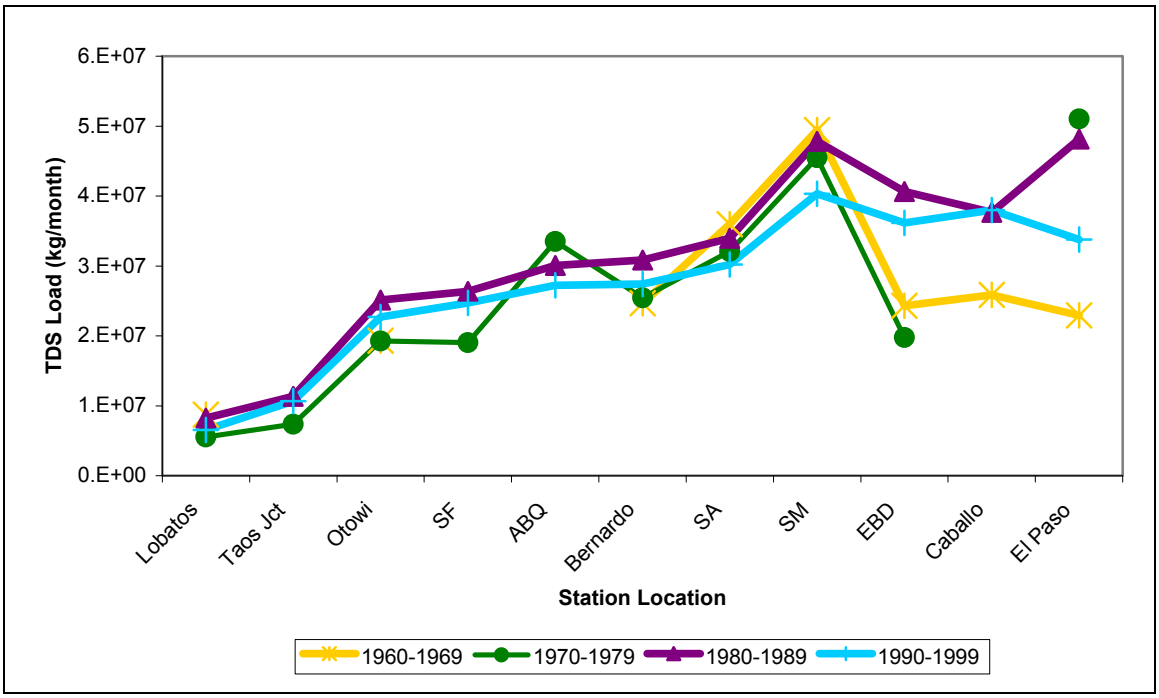

Figure 5.17. Total dissolved solids load at each station for the decades between 1960 and 1990.

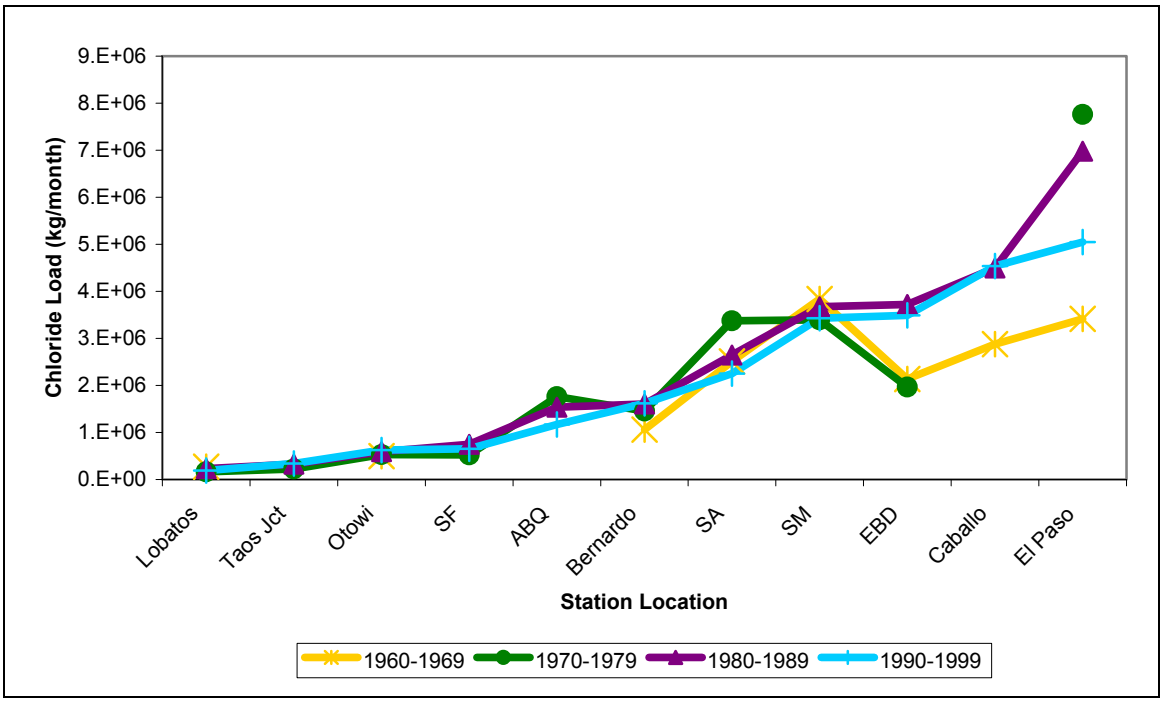

Figure 5.18. Chloride load at each station for the decades between 1960 and 1990.

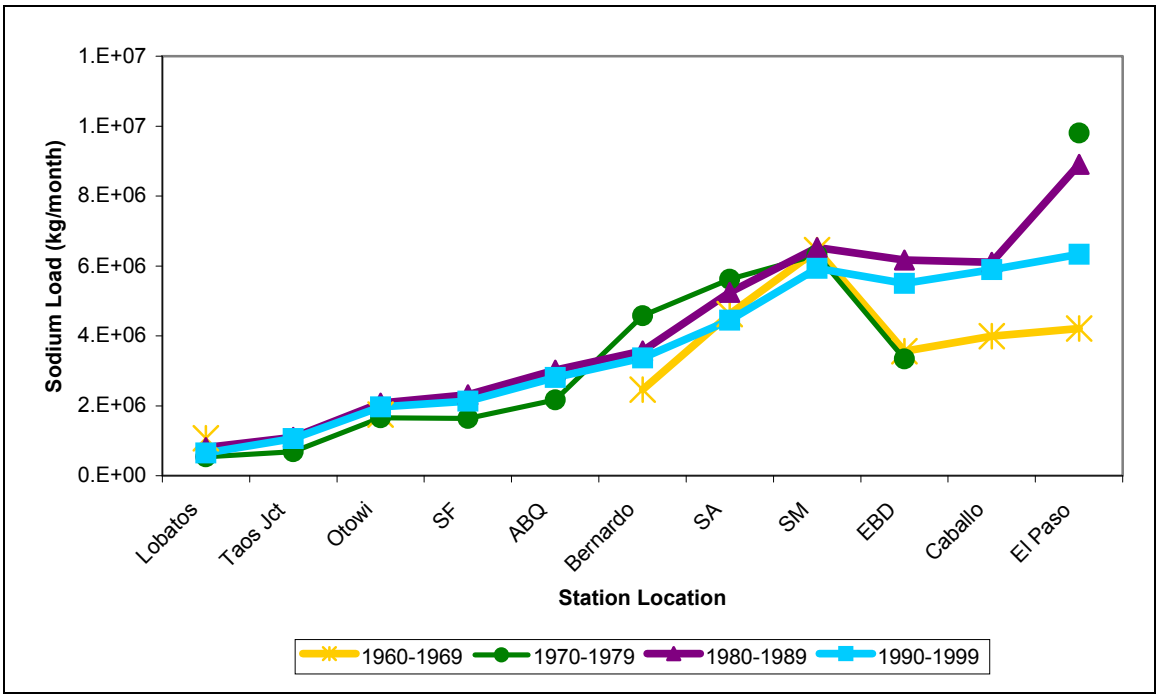

Figure 5.19. Sodium load at each station for the decades between 1960 and 1990.

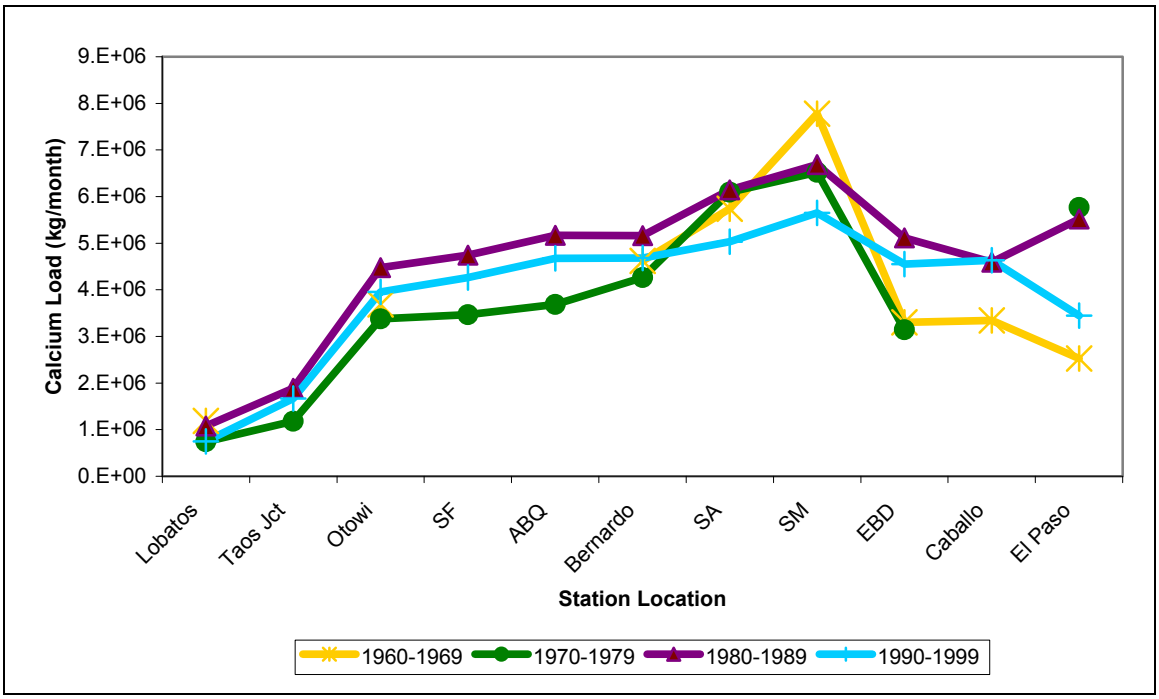

Figure 5.20. Calcium load at each station for the decades between 1960 and 1990.

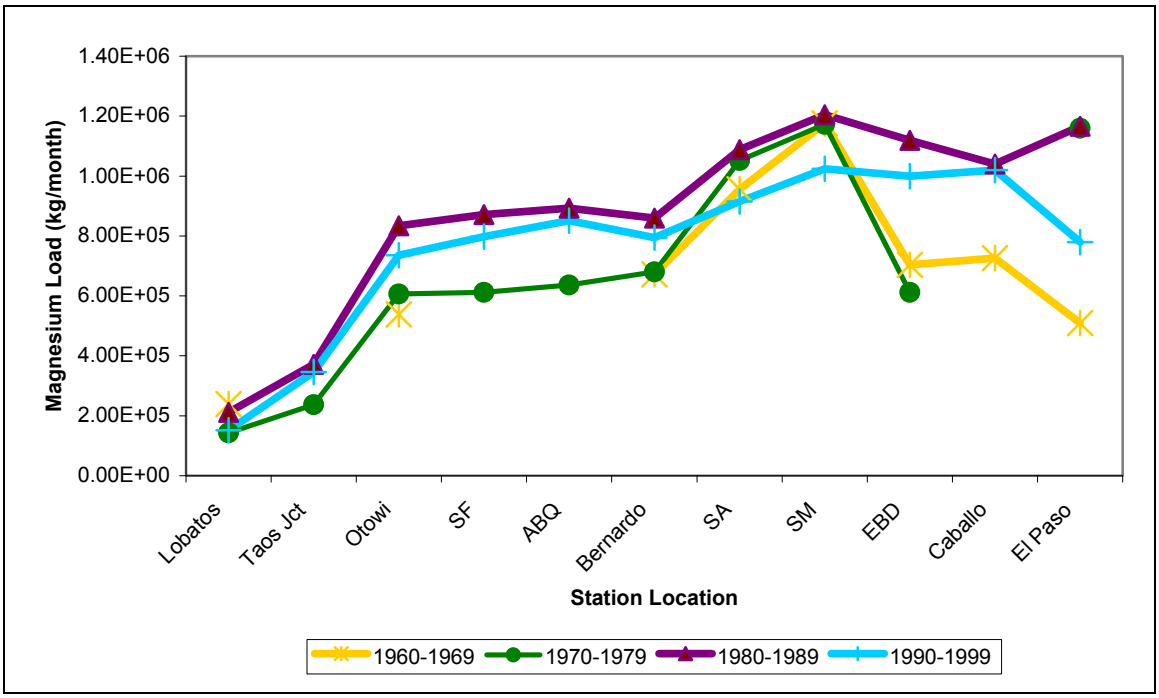

Figure 5.21. Magnesium load at each station for the decades between 1960 and 1990.

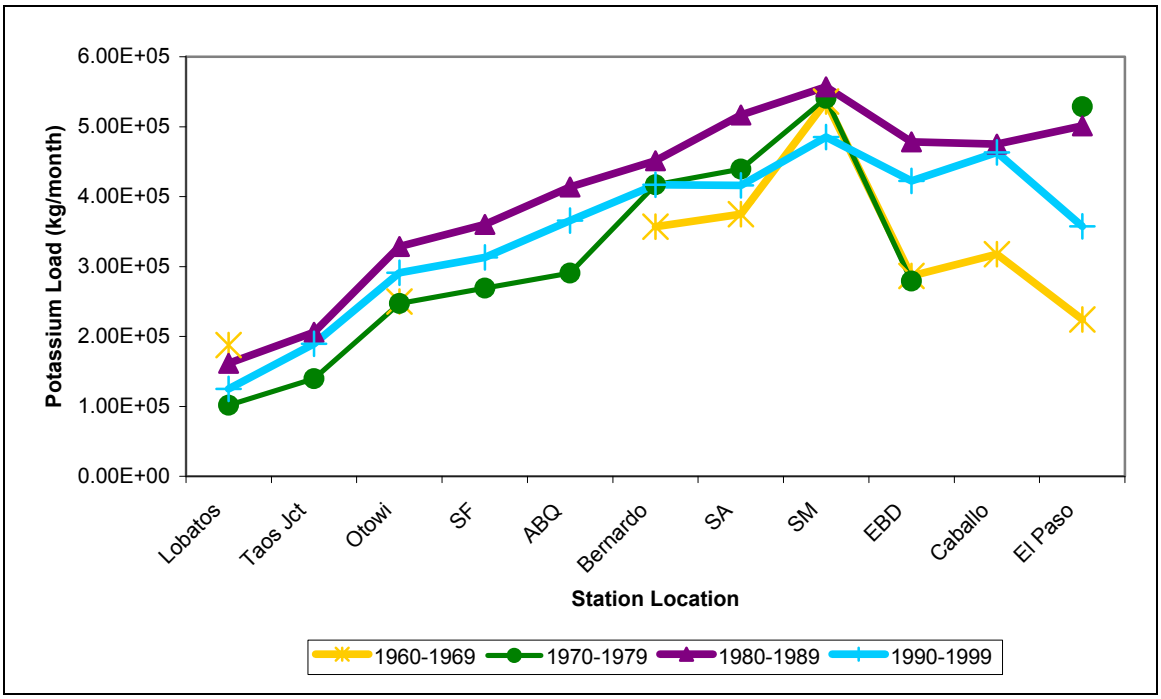

Figure 5.22. Potassium load at each station for the decades between 1960 and 1990.

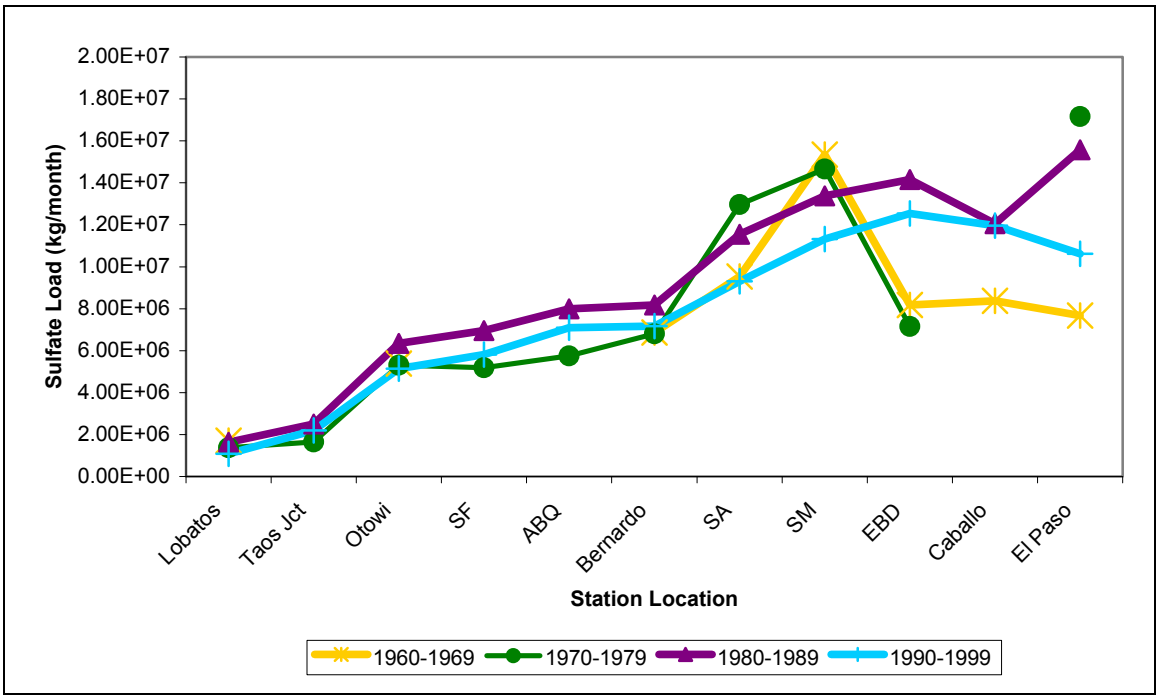

Figure 5.23. Sulfate load at each station for the decades between 1960 and 1990.

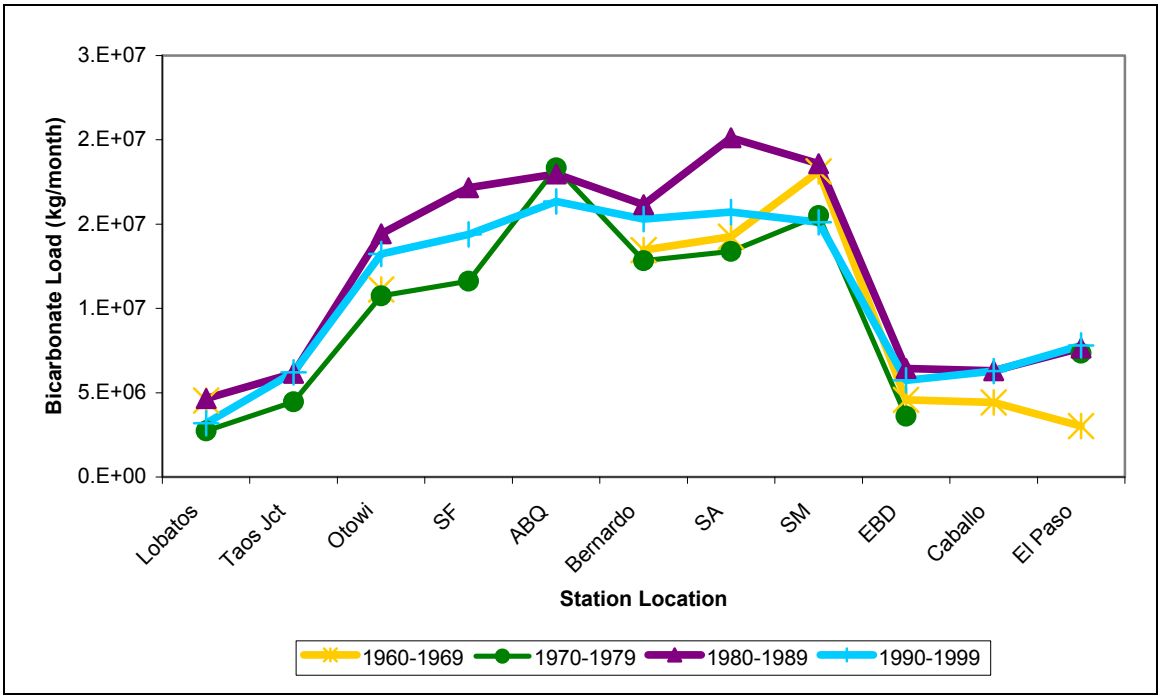

Figure 5.24. Bicarbonate load at each station for the decades between 1960 and 1990.

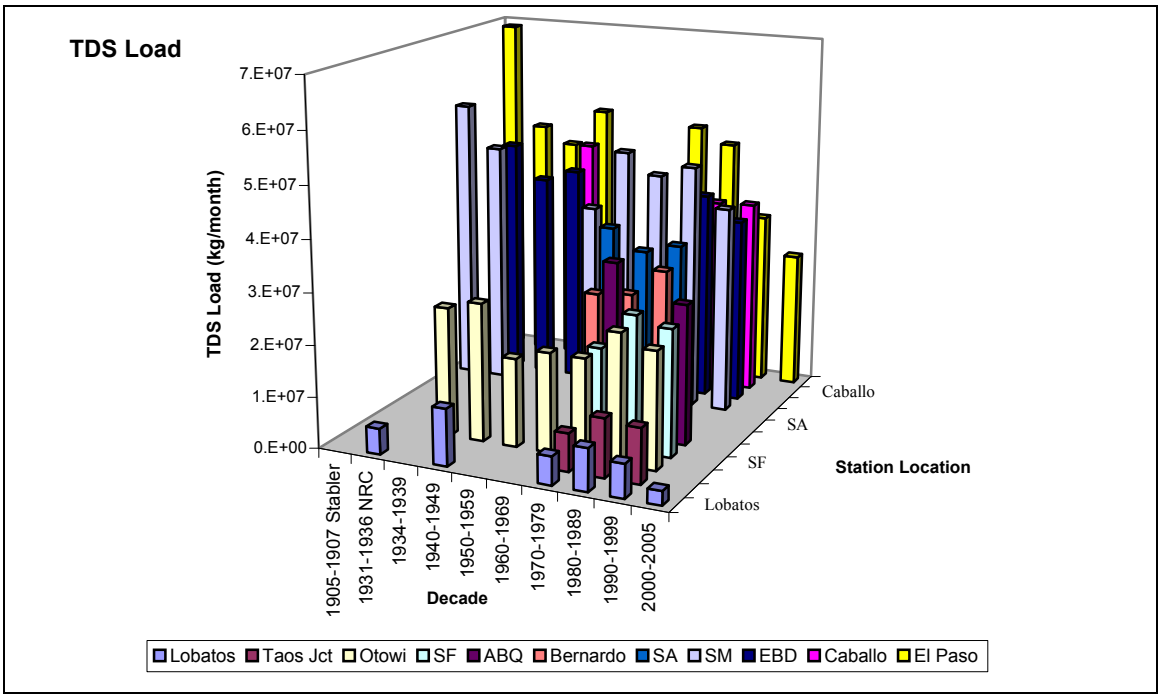

Figure 5.25a. Total dissolved solids load at each station for all decades, plotted spatially and temporally. Data are presented prior to any addition of regressed-data.

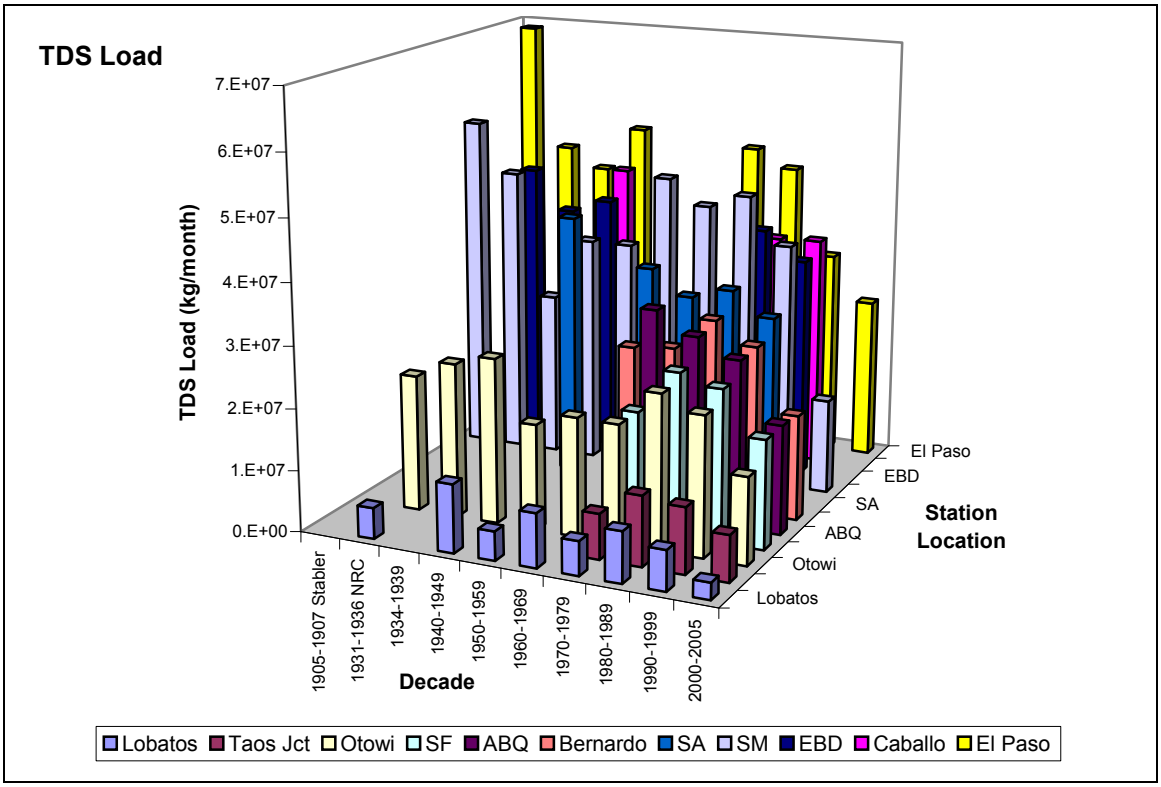

Figure 5.25b. Total dissolved solids load at each station for all decades, plotted spatially and temporally. Data are presented with additional regressed-data.

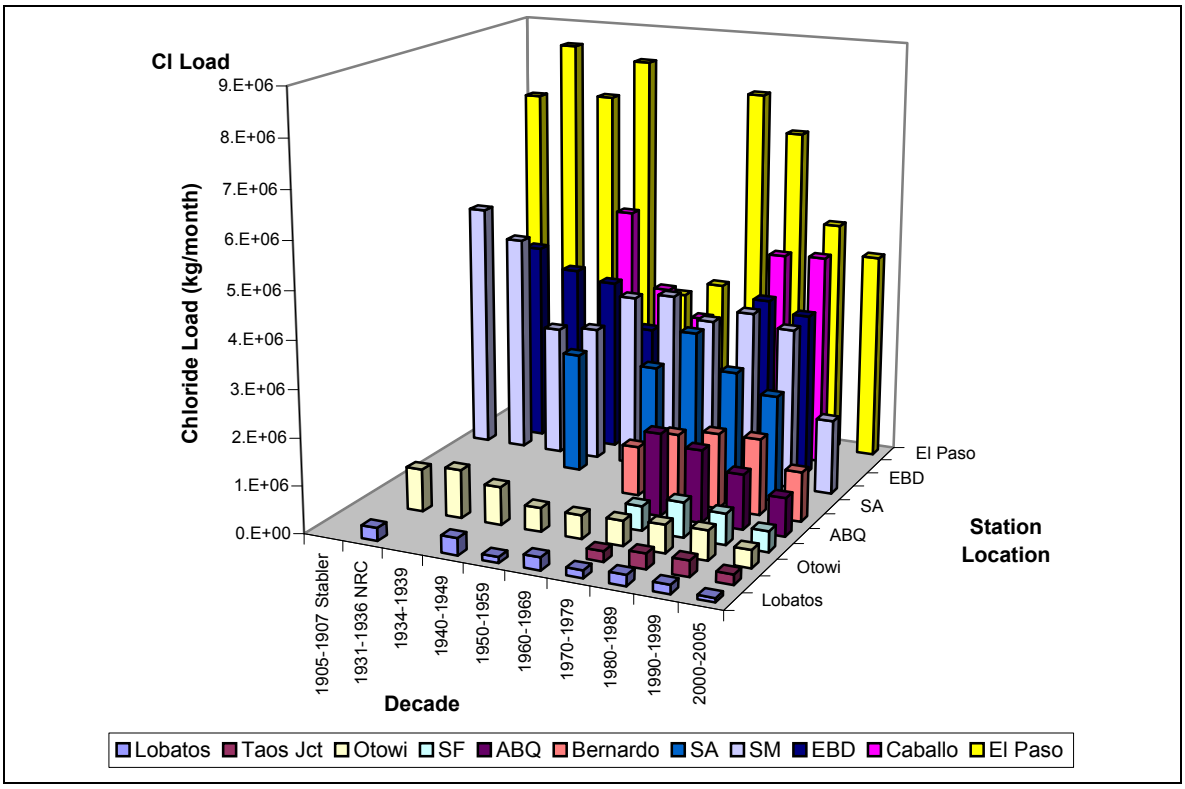

Figure 5.26. Chloride load at each station for all decades, plotted spatially and temporally.

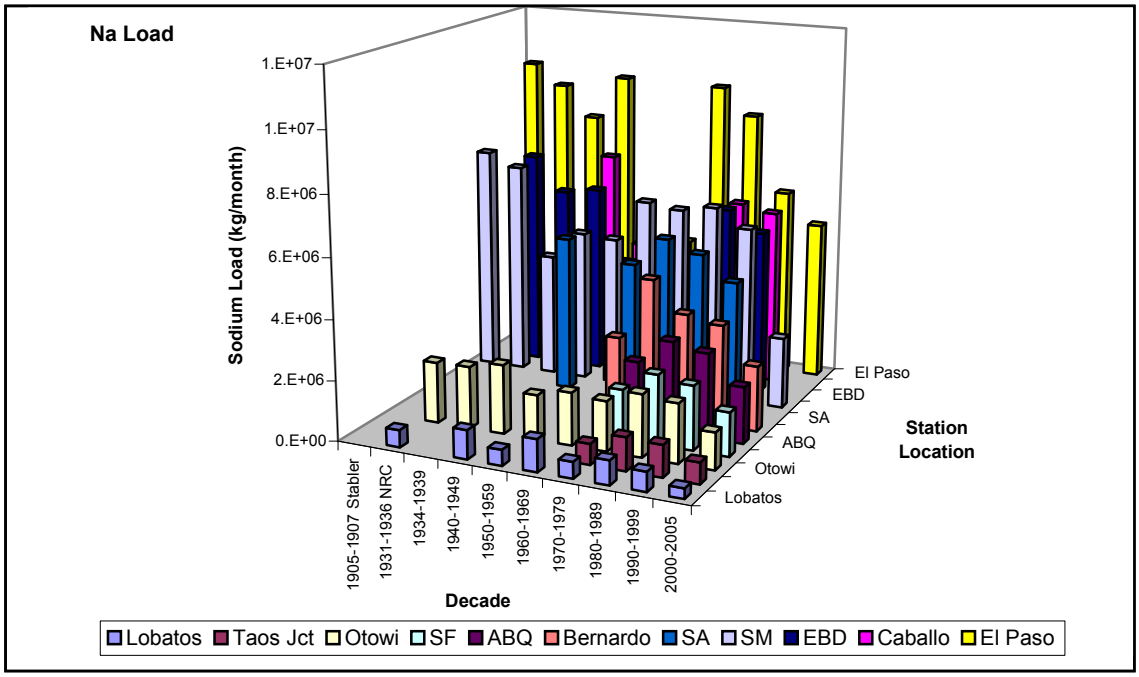

Figure 5.27. Sodium load at each station for all decades, plotted spatially and temporally.

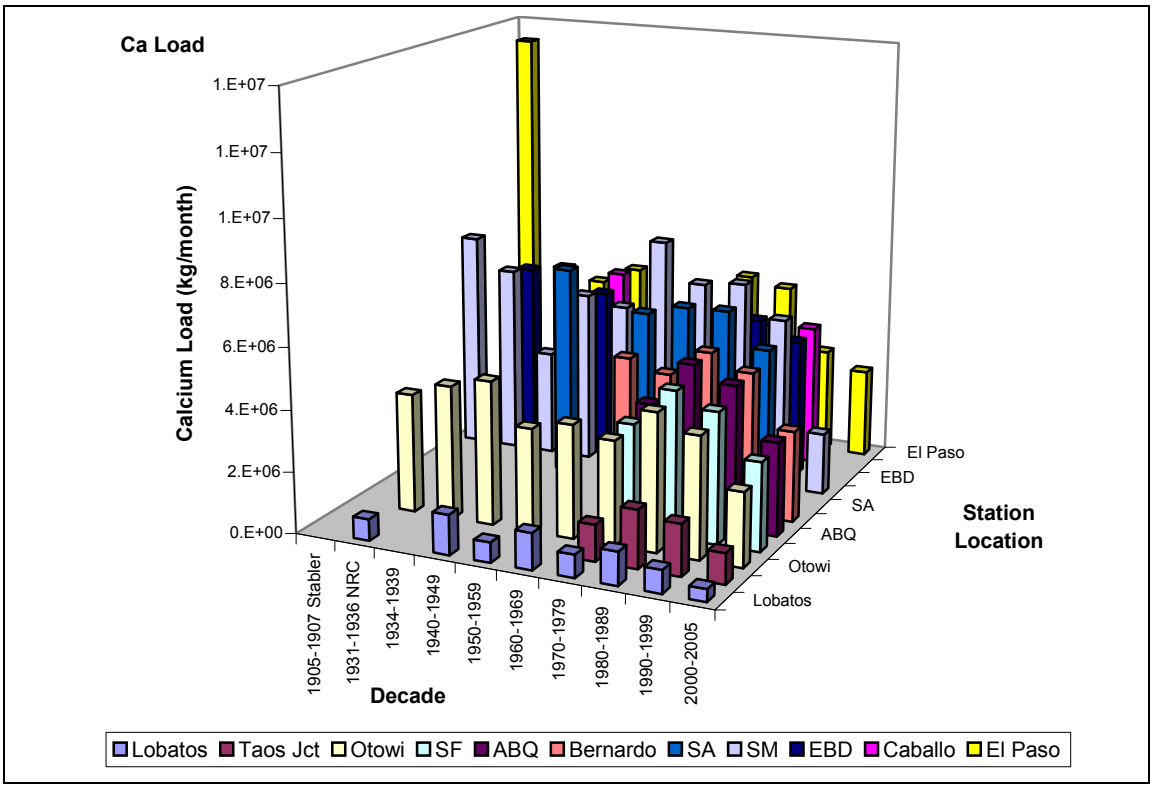

Figure 5.28. Calcium load at each station for all decades, plotted spatially and temporally.

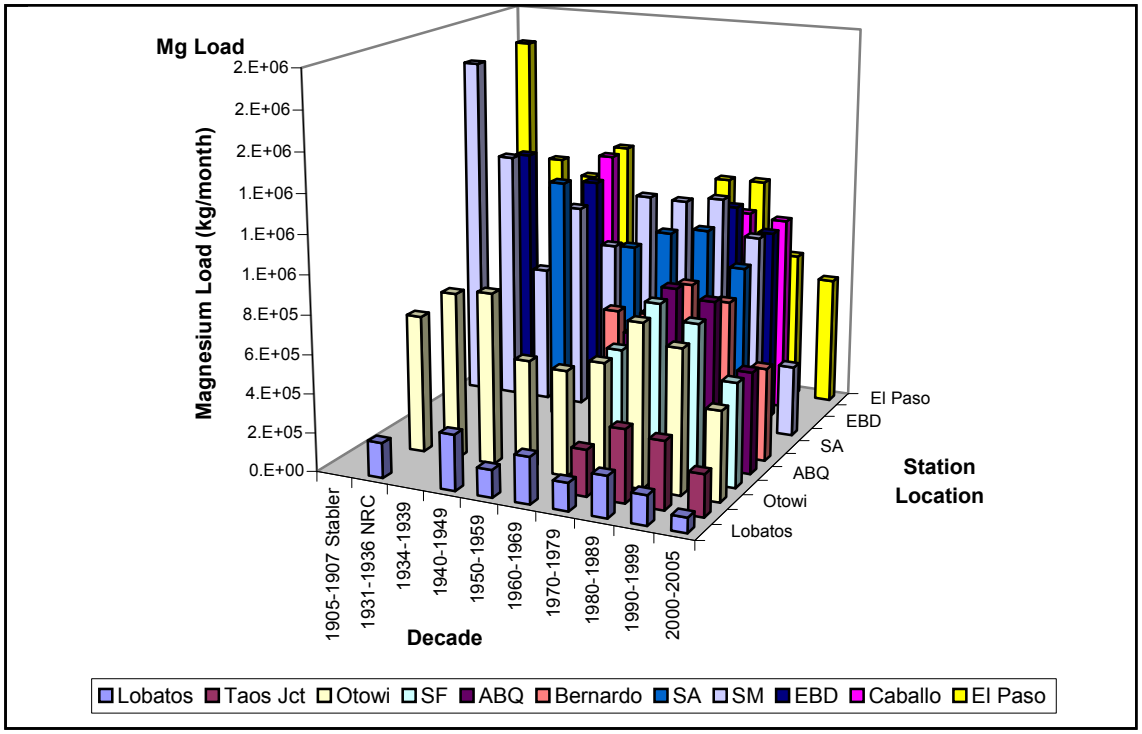

Figure 5.29. Magnesium load at each station for all decades, plotted spatially and temporally.

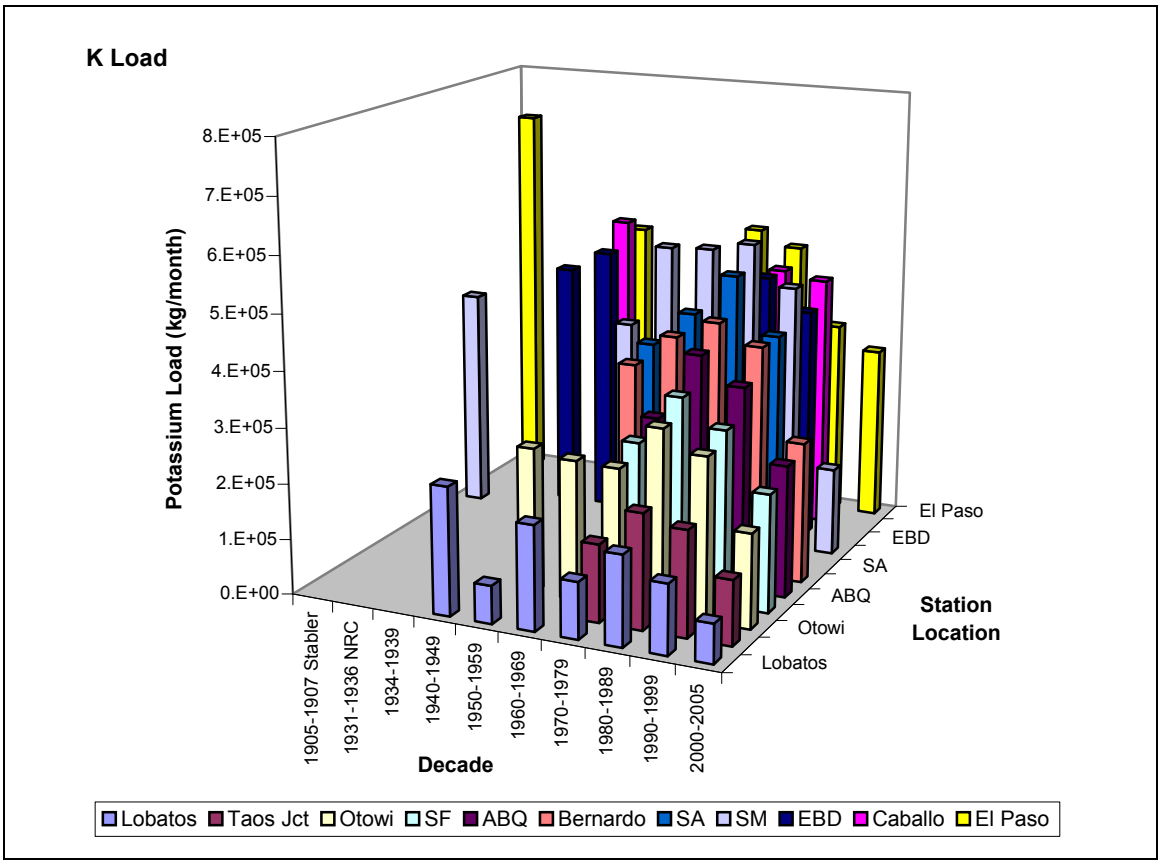

Figure 5.30. Potassium load at each station for all decades, plotted spatially and temporally.

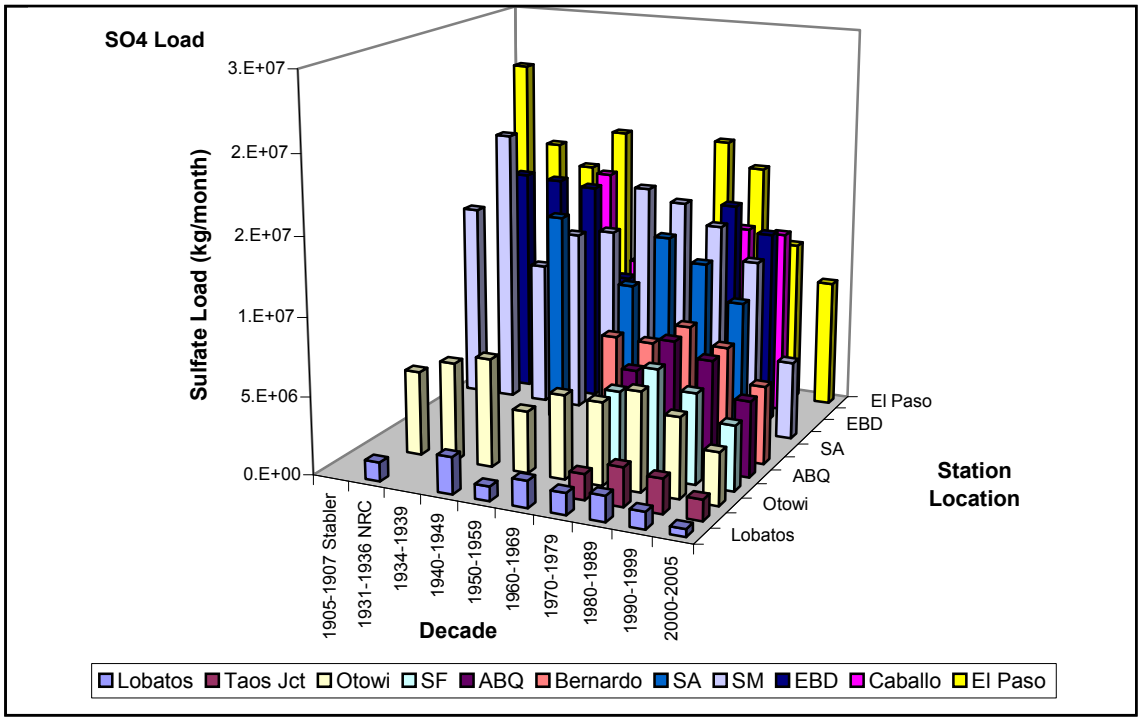

Figure 5.31. Sulfate load at each station for all decades, plotted spatially and temporally.

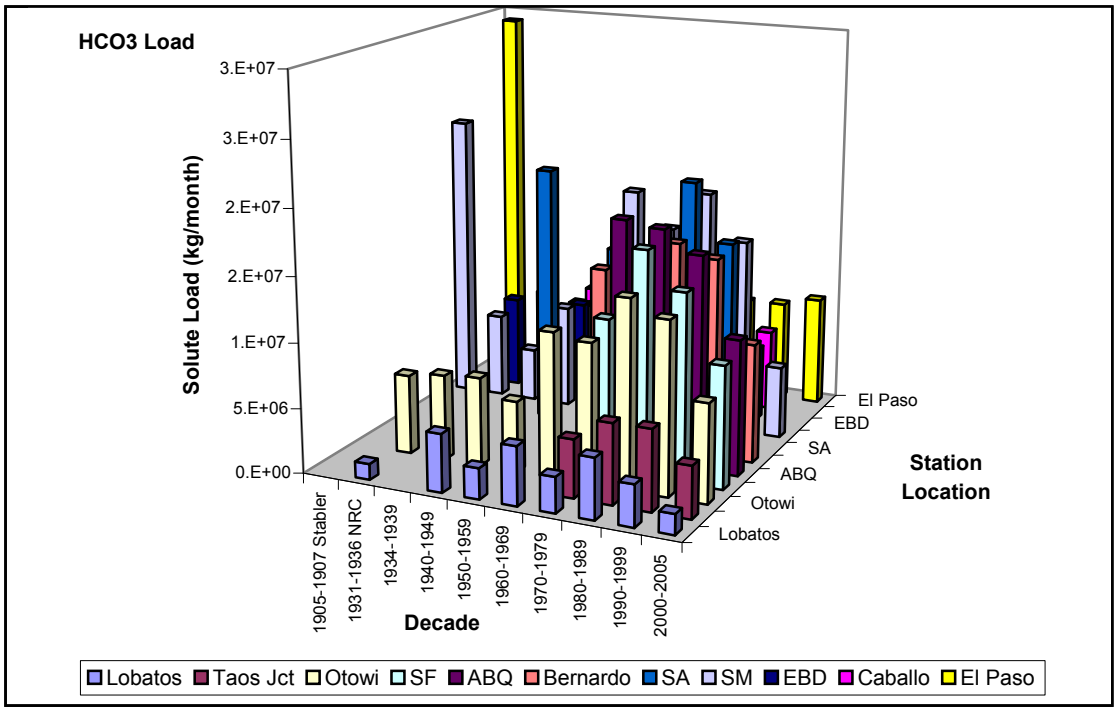

Figure 5.32. Bicarbonate load at each station for all decades, plotted spatially and temporally.

5.5 Conclusions

Solute loads and concentrations vary spatially and temporally. Concentrations increase with distance downstream. However, certain river reaches lost or gained quantities of reactive solutes due to additions from various sources. Additions from tributaries, ground water, wastewater treatment plant and brine as well as concentration from evapotranspiration affected river chemistry and led to increased concentrations with downstream distance. The Rio Grande transformed from a calcium bicarbonate water (Lobatos) to a sodium-sulfate-chloride dominated water near El Paso. Geologic brine seepage near San Acacia and El Paso and northern tributaries altered the chemical composition of the river. In addition, pre-Elephant Butte Dam sampling suggested that Rio Grande chemical constituents were affected within Elephant Butte Reservoir or by the extended irrigation network. A mass-balance model was employed to further

understand these chemical patterns and to quantify the effect of each known solute source.

CHAPTER 6
MASS BALANCE MODEL

6.1 Methodology

6.1.1 Introduction and Theory

Investigation of the Rio Grande solute budget revealed chemical variations among river locations. In order to understand the sources that contributed to these chemical changes, a mass balance calculation was computed for each solute and each river reach. A summation (by load, in units of kg/month) of the upstream station chemistry and all known solute sources (referred to as upstream+) was computed to estimate the chemistry of the downstream station. If the mass-balance calculation could account for all downstream chemical changes, then the chemical changes were attributed to the following: ET, brine addition, tributaries and/or ground water. However, if the mass balance could only partially account for the chemical changes between any main stem river stations, then the remaining chemical changes were attributed to soil-water interactions. This section will describe mass-balance solute models for each river reach: data compilation, calculations, and results. The water and solute mass-balance models have been included in Appendix C.

6.1.2 Total Discharge

6.1.2.1 Cross-Sectional Discharge

All data for the solute budget calculation was compiled for each decade from available data as discussed in Chapter 4. The total discharge passing each location was calculated by adding the main-channel Rio Grande station average decadal discharge to the discharge bypassing the main gage through the irrigation network. Figure 6.1 shows a river schematic with the included tributaries and bypassing irrigation canals.

6.1.2.2 Evapotranspiration

The evapotranspiration number included evaporation (from open water, the Rio Grande and reservoirs) and riparian and crop evapotranspiration. Open-water evaporation was estimated by multiplying the channel area and the evaporation rate. Crop and riparian ET amounts were reported in *Lacey* [2006] and *Papadopolous and Associates* [2002]. One ET value was used for all decades except for the Elephant Butte-to-Caballo reach and the Caballo-to-El Paso reach. In the two southernmost reaches, decadal ET data was sufficient to justify including data for each decade separately.

6.1.2.3 Upstream+ Discharge

The total discharge estimate for the outflow at the downstream station was calculated from the upstream cross-sectional discharge plus the combined tributary discharge, the brine discharge and ground-water seepage, and subtraction of evapotranspiration.

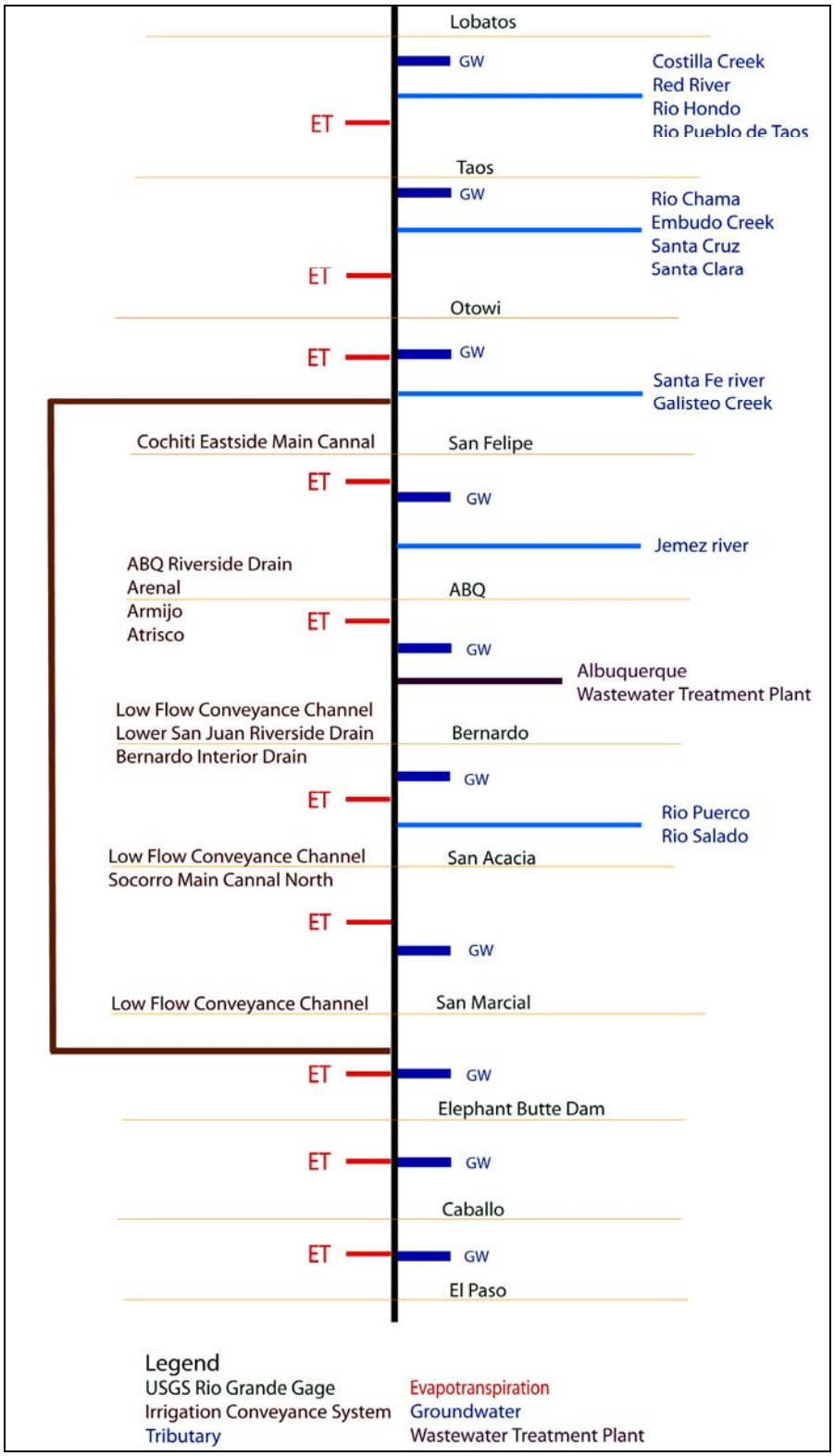

Figure 6.1. Mass-balance river schematic. Black centerline represents the Rio Grande. River reaches are delineated with orange horizontal lines. River gages, irrigation bypasses, tributaries, wastewater treatment plant, evaporation and groundwater are labeled with colors as in the legend.

6.1.3 Total Solute Load

Solute loads were calculated based on the average decadal discharge and concentration. The monthly concentrations were calculated from the solute load such that the concentrations were weighted by the discharge during that month.

6.1.3.1 Discharge-Weighted Decadal Average

The solute mass-balance calculations were made using decadal averages for both discharge and concentration. The average decadal solute concentration was calculated by weighting the monthly concentrations against their respective discharges (i.e. solute burdens were computed). The solute burdens (or solute loads, i.e. concentration multiplied by the discharge) were summed over each decade and divided by the cumulative discharge for each decade. Thus, the solute concentrations were discharge-weighted such that a high discharge leads to the estimation of an appropriate amount of solute across a location.

6.1.3.2 Cross-Section Solute Load and Concentration

Discharge and monthly concentration data were used to obtain the monthly load by multiplying the Rio Grande discharge-weighted decadal-average concentration by the total cross-sectional discharge. As mentioned previously, appreciable quantities of water and solutes flow in the irrigation network alongside the main-channel of the Rio Grande. These quantities of water and the solutes they carry bypass the main-channel sampling location, however, their discharge and chemistry are vital to understand the mass balance of the river. The chemistry of these canals and drains was necessary to

evaluate Rio Grande basin processes and to calculate an accurate mass balance. Due to a lack of chemical data for the by-passing conveyance system, canal and drain chemistry was estimated from main-channel river chemistry. Conveyance system discharge was included in the total cross-section discharge and multiplied by the main channel Rio Grande station concentration. As discussed in Chapter 4, river chemistry provided a reasonable estimate for certain canal and drain chemistry. However, the locations along the LFCC have significantly higher solute concentrations than the river as well as sufficient chemical data available to characterize them. Thus, solute loads from the conveyance channel at San Acacia (SACC) and San Marcial (SMCC) were calculated. The discharge and monthly concentration from the SACC and SMCC were used to get the monthly solute load by multiplying the respective concentration and discharge.

6.1.3.3 Tributaries

Major and minor tributary calculations were handled differently. Major tributary loads were computed in the same manner as the main stem stations, which was described in Chapter 4. Discharge and monthly concentration were used to get the monthly load by multiplying the concentration by the discharge. Minor tributary solute concentrations were averaged differently due to low availability of data. All available concentration data was averaged for each station, each station average concentration was then averaged with the other tributaries in that section. The average tributary concentration for each river reach was multiplied by the combined minor tributary discharge for each decade to estimate the solute load for that reach.

6.1.3.4 Albuquerque Wastewater Treatment Plant

Only the Albuquerque wastewater treatment plant was included in the analysis. Other wastewater treatment plants were not included based on smaller discharges and a lack of chemical data. Discharge data was available from 1980 to 2007; an average decadal discharge was calculated for these 3 decades. Data from the 1980's was utilized to extrapolate a decadal discharge for the 1950's, 1960's and 1970's based on population. The solute information was estimated with an average between a few samples collected by the U.S. Fish and Wildlife Service in 2002 and four samples collected during a synoptic sampling by New Mexico Tech and the University of Arizona in 2005-2006. Chemical loads were calculated for the six samples and a discharge-weighted concentration was estimated. In order to more appropriately estimate the decadal effluent concentration the discharge-weighted solute concentrations were reduced by sixty percent. The effluent concentrations were reduced until the effluent chloride load during the 1980's was consistent with total cross-section outflow results at Bernardo. The treatment plant concentrations were a major source of uncertainty for the mass balance calculations. Because the six water quality samples were all from recent data, the year 2000 or later, these calculations neglected any solute variation through time.

6.1.3.5 Ground Water

Seepage information was gathered from multiple sources and multiplied by the average of all available concentration data. The availability of data varied with river station location. Seepage and concentration information came from different sources

and different time periods, such that discharge weighting the concentrations was not possible. Due to a lack of data, and based on the assumption that groundwater chemistry remains constant; data was not calculated separately such that the same ground water values were used for all decades. Based on a ground water study in the Middle Rio Grande Valley, *Plummer et al.* [2004] reported that Santa Fe Group aquifer sediments mainly consist of unreactive sands and gravels, which only slightly alter ground water solute concentrations. All available data was lumped into a single seepage and a single solute value, which were used for all the decades.

6.1.3.6 Elephant Butte Reservoir Storage

Drought in the 1970's decreased the stored quantity of water within Elephant Butte Reservoir. This storage deficit was erased when the reservoir refilled in the wetter 1980's. While the reservoir was filling, more Rio Grande water and solute mass entered Elephant Butte Lake than left at the dam. Since more solute mass was entered than leaving, the mass-balance calculations needed to account for the mass stored during this decade. In order to account for solute storage, a storage component was computed. The stored load for each constituent was based on the difference between the load at San Marcial and the load at Elephant Butte Dam. The amount of solute stored in Elephant Butte was added to the total load at Elephant Butte Dam so that the San Marcial+ load could be compared to the amount of solute flowing out of Elephant Butte Reservoir. Table 6.1 contains the added quantity of each solute due to storage within the reservoir.

Table 6.1. Quantity of solute stored in Elephant Butte Reservoir during 1980-1989.

Solute	Solute Amount Stored in Elephant Butte Reservoir between 1980-1989 (Tons)
Cl	6.4E+04
Ca	6.8E+04
Na	1.0E+05
Mg	1.7E+04
K	6.4E+03
HCO_3	9.4E+04
SO_4	2.4E+05
TDS	6.0E+05

Note: The TDS value is a sum of stored ions.

6.1.4 Brine Discharge and Load

Previous work by *Mills* [2003] and *Phillips et al*. [2003] documented geologic brine seepage into the river. Their work reported the presence and locations for brine upwelling. In order to close the solute mass balance, brine chemistry and flow rate were calculated. To access the quantity of brine entering each river reach, the chloride load was used under the assumption that all chloride entering the system comes from a known source already included in the model. Chloride is a conservative solute, hence all chloride found in the Rio Grande system must be attributed to some source water. Chloride load was calculated from the upstream location, tributaries, drains, wastewater treatment plant, ground water, and evaporative increases such that all known chloride sources were included, except the amount from brine. Thus, any discrepancy between this calculated upstream+ chloride load and the downstream load was attributed to brine seepage.

From the previous calculations, the amount of chloride entering the river due to brine seepage is estimated. However, in order to calculate a mass-balance for all major

ions as well as a water mass-balance, the seepage rate and the reactive solute load are required. To complete the water balance, the rate at which brine discharges into the river was calculated using the mass flux of chloride derived from brine. Recall that the chloride load from brine is equal to the brine seepage rate multiplied by the chloride concentration in the brine. If the chloride load from brine is divided by the concentration of chloride in brine, the result yields the brine discharge rate. Two brine samples were utilized to represent the chemistry of saline ground water. Samples were chosen based on their high Cl/Br ratios, high chloride concentrations and their location. Tables 6.2 present the seepage rate for each river reach, also indicating the source of the brine samples. The concentration of major ions in brine is presented in Table 6.3. For reference, these brine samples are presented in on a trilinear diagram in Figure 5.2.

The brine discharge was multiplied by the concentration of each solute of interest in the brine such that a brine solute load was calculated. With the discharge and solute load from brine computed, all known sources were quantified. Thus any remaining residual solute load between the upstream+ and the downstream locations was attributed to chemical reactions, with a caveat regarding uncertainty of the chemical data.

Table 6.2. Brine data sources for each river reach.

River Reach	Brine Chemistry Source	Modeled Seepage Rate (L/month) 1980-1989
Lobatos - Taos	[*Newton*, 2005]	7.14E+06
Taos – Otowi	[*Newton*, 2005]	0.00E+00
Otowi – SF	[*Newton*, 2005]	2.24E+07
SF-ABQ	[*Newton*, 2005]	8.08E+07
ABQ - Bernardo	[*Newton*, 2005]	1.78E+06
Bernardo-SA	[*Newton*, 2005]	1.49E+08
SA-SM	[*Newton*, 2005]	2.44E+08
SM-EBD	[*Newton*, 2005]	8.24E+06
EBD-Caballo	[*Moore et. al*., 2008]	6.09E+07
Caballo - El Paso	[*Moore et. al*., 2008]	1.11E+08

Table 6.3. Brine solute concentrations.

	[*Newton*, 2005]	[*Moore et. al*., 2008]
Location	Bosque del Apache, south of San Antonio	El Paso Narrows
Date Collected	Jun-02	Jan-05
Well ID	W-83.98-1	ISC4
Ca (mg/L)	770	840
Mg (mg/L)	296	670
Na (mg/L)	3900	7700
K (mg/L)	146	33
CO_3 (mg/L)	0	4
HCO_3 (mg/L)	1070	180
SO_4 (mg/L)	4500	6200
Cl (mg/L)	4100	18000
Br (mg/L)	3.8	25
Cl/Br ratio	1079	720

6.2 Mass Balance Results

6.2.1 Discharge

The water mass balance accounted for major diversions and returns of water to the Rio Grande on an average decadal basis. Each reach was separated into an upstream and downstream location (e.g., Lobatos-to-Taos). The upstream total cross-section

discharge (main channel + bypass drains) was converted into an upstream+ discharge by summing the discharge from major and minor tributaries, ground water, wastewater treatment plant and subtracting water lost through evapotranspiration. Tables 6.4 and 6.5 illustrate these results from the water balance at each river reach for 1934-1939 and 1980-1989 respectively. The results for all considered decades can be found in Appendix D. Discharge percentages from the various sources are included in Table 6.6 at all locations during the 1980's. For each source water, the discharge percentage was calculated by dividing its average decadal discharge by the total modeled discharge leaving that river reach (RG In+). Thereby the calculation presents the percentage of discharge leaving the reach that was derived from each source. Tributaries accounted for as much as forty five percent of the flow in northern reaches. The highest percentage of ground water entered in the Lobatos-to-Taos reach. Between San Felipe and Bernardo the Rio Grande discharged to the aquifer, becoming a losing reach on average over the decade. In the Caballo-to-El Paso region, low river flows caused a substantial amount of ground water to flow into the river. The highest evapotranspiration rates occured in reaches with heavy irrigation and those containing reservoirs. Caballo-to-El Paso lost the highest percentage of water to ET in 1980-1989. Due to filling of Elephant Butte reservoir, less water entered the Caballo-to-El Paso reach and thus more water evaporated.

Table 6.4. Modeled discharge 1934-1939 (L/month).

Discharge 1934-1939	Lobatos – Taos	Taos - Otowi	Otowi - SF	SF-ABQ	ABQ - Bernardo	Bern.- SA	SA-SM	SM-EBD	EBD-Caballo	Caballo - El Paso
RG In	3.4E+10	5.5E+10	1.1E+11	1.1E+11	No Data	No Data	No Data	No Data	8.07E+10	No Data
Total Tributary (Major and Minor)	2.8E+09	5.2E+10	No Data	No Data	N/A	No Data	N/A	N/A	N/A	N/A
Wastewater Treatment Plant	N/A	N/A	N/A	N/A	No Data	N/A	N/A	N/A	N/A	N/A
GW	7.1E+09	1.5E+09	1.5E+09	-1.5E+09	-1.5E+09	1.0E+09	7.2E+08	7.2E+08	7.2E+08	3.8E+09
Brine	No Data	No Data	No Data	No Data	No Data	No Data	No Data	No Data	No Data	No Data
RG In+ (Modeled Reach Input)	4.1E+10	No Data	1.1E+11	1.0E+11	No Data	No Data	No Data	No Data	7.9E+10	No Data
RG Out	5.5E+10	1.1E+11	1.1E+11	No Data	No Data	No Data	No Data	8.1E+10	No Data	5.5E+10

Note: The N/A indicates locations that do not have enough data to complete the calculation.

Table 6.5. Modeled discharge 1980-1989 (L/month).

Discharge 1980-1989	Lobatos - Taos	Taos - Otowi	Otowi - SF	SF-ABQ	ABQ - Bernardo	Bern.- SA	SA-SM	SM-EBD	EBD-Caballo	Caballo - El Paso
RG In	4.9E+10	7.3E+10	1.4E+11	1.4E+11	1.4E+11	1.2E+11	1.3E+11	1.4E+11	8.6E+10	8.5E+10
Total Tributary (Major and Minor)	1.9E+10	6.1E+10	1.2E+09	6.4E+09	No Data	2.6E+09	N/A	N/A	N/A	N/A
Wastewater Treatment Plant	N/A	N/A	N/A	N/A	4.9E+09	N/A	N/A	N/A	N/A	N/A
GW	7.1E+09	1.5E+09	1.5E+09	-1.5E+09	-1.5E+09	1.0E+09	7.2E+08	7.2E+08	7.2E+08	3.8E+09
Brine	7.1E+06	0.0E+00	2.2E+07	8.1E+07	1.8E+06	1.5E+08	2.4E+08	8.2E+06	6.1E+07	1.1E+08
RG In+ (Modeled Reach Input)	7.2E+10	1.3E+11	1.4E+11	1.4E+11	1.2E+11	1.3E+11	1.2E+11	1.2E+11	8.2E+10	6.2E+10
RG Out	7.3E+10	1.4E+11	1.4E+11	1.4E+11	1.2E+11	1.3E+11	1.4E+11	8.6E+10	8.7E+10	7.5E+10

Table 6.6. Source percent discharge of total modeled discharge, 1980-1989.

	Lobatos - Taos	Taos - Otowi	Otowi - SF	SF - ABQ	ABQ - Bernardo	Bern. - SA	SA-SM	SM-EBD	EBD-Caballo	Caballo - El Paso
Total Tributary (Major and Minor)	26	46	0.88	4.7	N/A	2.1	N/A	N/A	N/A	N/A
Wastewater Treatment Plant	N/A	N/A	N/A	N/A	4.2	N/A	N/A	N/A	N/A	N/A
GW	9.7	1.2	1.1	-1.1	-1.3	0.8	0.6	0.62	0.88	6.2
ET	3.4	1.8	3.0	4.6	19	2.4	9.2	18	5.8	44
Brine	0.01	0.00	0.02	0.06	0.00	0.12	0.21	0.01	0.07	0.18

Note: A negative discharge indicates water is lost from the Rio Grande and enters the shallow aquifer.

6.2.2 Water Mass Balance Test

During modern decades, the modeled upstream+ discharges matched the downstream discharges reasonably well. A residual discharge calculation was made in order to quantify model output. Residual discharge was defined as the upstream+ discharge subtracted from the downstream discharge such that negative residuals indicated that the model was under-predicting discharge and positive residuals indicated the model over-predicted the downstream discharge. Residual discharge is shown in Figure 6.2, where the upstream+ discharge was subtracted from the downstream discharge, revealing discrepancies. Discharge discrepancies increased with distance downstream.

Discharge residuals varied with time. Most decades had random variations, which could be attributed to relatively high levels of uncertainty associated with the basic data. However, notice the systematic decrease in discharge residuals for the San Acacia to San Marcial reach. The high historic residuals decreased through time, indicating an increasingly representative discharge calculations moving forward in time from 1960 to 2000. The monotonic temporal improvement at San Acacia to San Marcial suggested that either there is an error in the modeled quantities or that an additional source of water entered the river but was not included in the model.

Additionally, the estimated historic evapotranspiration may be unrealistic. Recall that historic ET was estimated with modern (1985-1998) ET values for the river reaches between Lobatos and San Marcial. Evapotranspiration in this section of the river may have varied over time. The Bosque del Apache Wildlife Refuge, created in 1939, has undergone transitions from farmland to floodplain to salt cedar to marshland [U.S. Fish and Wildlife Service, 2008]. These transitions likely affected the overall ET within the reach, which could explain the decreases in the residual discharge over time. Ground water that entered the Low-Flow Conveyance Channel might also have affected the discharge residual calculation. The Low-Flow Conveyance Channel was constructed 1959 in order to improve agricultural drainage and facilitate delivery to Elephant Butte [*Towne*, 2007], see Chapter 3 for further discussion. Water was diverted into the San Acacia diversion dam depending on the river flow at San Acacia. During the 1960's, ground water filled the LFCC until gradually, over time, the local water table dropped to near-steady-state conditions. Ground water that entered the conveyance channel was not included in the model. Thus, additional groundwater entering the conveyance channel after San Acacia but before San Marcial may have resulted in higher discharges, which were not captured in the model, as the data shows (Figure 6.2). Over time, the amount of ground water that entered the conveyance system decreased as a new steady state was reached, which could explain the temporal linear improvement in the model in this reach.

The water balance models of the 1980's and 1990's seem to capture historic decade averages, the discharge residuals are relatively low indicating that modeled upstream+ discharge was close to the measured average discharge. In Table 6.7, percent

differences were calculated. They are as small as 0.08 % and as large as only 36 % between the 1980's model and the average historic Rio Grande data, whereas the 1960's and 1970's models had percent differences of over 80%. Because the 1980's water balance model matched historic average discharge reasonably well, this decade was utilized for subsequent reactive solute modeling.

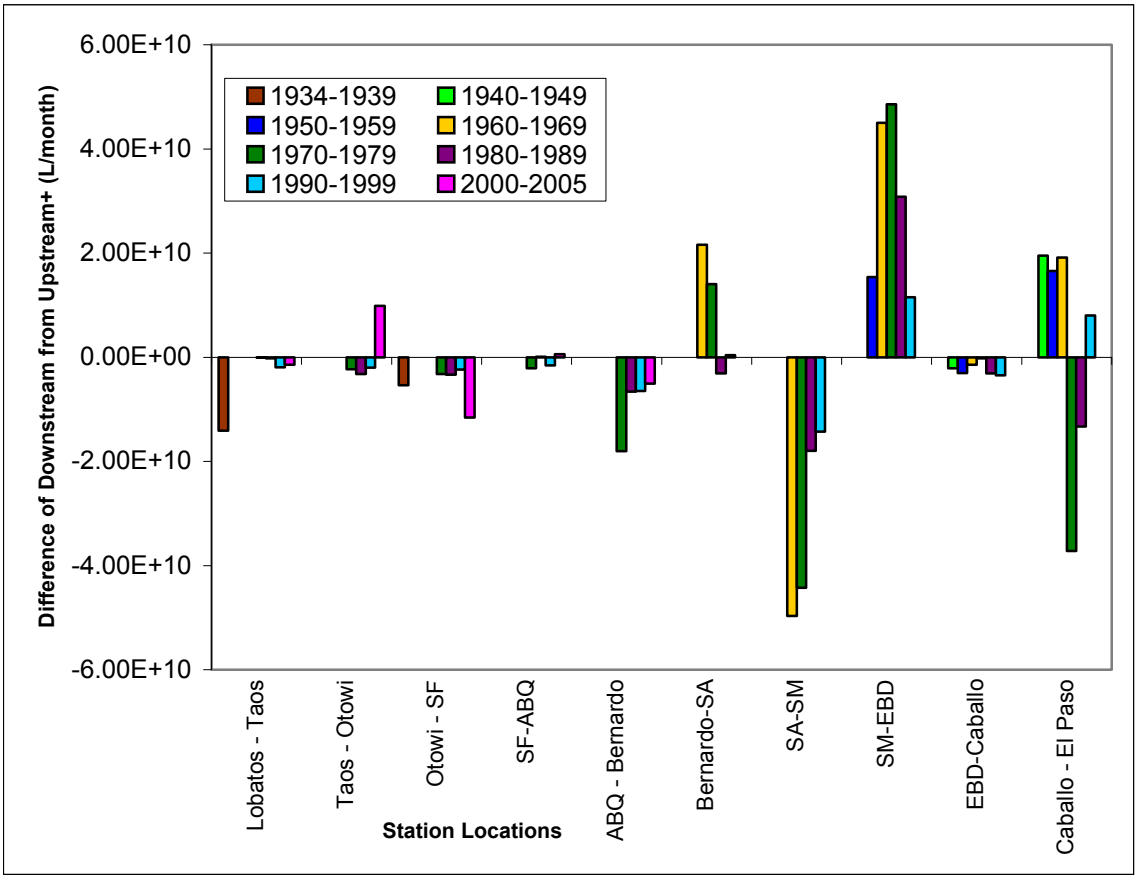

Figure 6.2. Residual discharge calculated from downstream discharge – upstream+ such that negative residuals indicate the model is under-predicting and positive residuals indicate the model over-predicts the downstream discharge.

Table 6.7. Discharge percent difference at modeled locations, upstream+ (L/month).

	Lobatos+	Taos+	Otowi+	SF+	ABQ+	Bernardo+	SA+	SM+	EBD+	Caballo+
1934-1939	-26	ND	-4.8	ND	ND	ND	ND	ND	ND	ND
1940-1949	ND	ND	ND	ND	ND	ND	ND	ND	-2.3	31
1950-1959	ND	ND	ND	ND	ND	ND	ND	32	-6.2	67
1960-1969	ND	ND	ND	ND	ND	32.07	-46	80	-2.7	68
1970-1979	-0.21	-2.5	-3.5	-2.3	-19.9	18.10	-40	86	-0.45	-57
1980-1989	-0.27	-2.4	-2.4	0.08	-5.3	-2.41	-13	36	-3.7	-18
1990-1999	-3.3	-1.65	-1.9	-1.3	-5.9	0.34	-12	14	-4.2	16
2000-2005	-3.8	15	-15	0.79	-8.6	ND	ND	ND	ND	ND

Note: ND = No Available Data

6.2.3 Chloride Mass Balance Model

Chloride is a non-reactive solute, therefore the mass balance model should account for all chloride sources. Chloride enters the system from tributaries, wastewater treatment plant, ground water, and geologic brine (*Mills, 2003*). The summation of these sources quantifies the chloride load within the system (Table 6.8). However, the amount of chloride entering from brine was not independently quantified on a decadal scale for all decades. Without a chloride load from brine the model was unable to match the measured load outflow. Thus, as described above, brine was used to close the chloride mass balance. Therefore, the chloride residuals are usually zero except in a few locations where the model over-predicted the chloride load prior to brine addition. Figure 6.3a presents the upstream+ modeled loads and the downstream measured data for 1970, 1980, 1990, 2000 (darker shade of each color is the modeled upstream+ value). The model mass-balance residuals are smallest during 1980's and 1990's. Presumably, this is because modern decades have the most data available. Detailed modeling was therefore performed on decade of the 1980's and this decade will serve as the basis for the detailed subsurface investigation with NETPATH. Figure 6.3b presents modeled and measured average chloride loads for the 1980's. The decade from

1980-1989 was chosen based on availability of chemical data for all sources (tributaries, wastewater treatment plant, etc). Bicarbonate availability was a significantly limiting factor in all the analyses, however the record was fairly complete during the 1980's.

Table 6.8. Modeled chloride load 1980-1989 (kg/month).

	Lobatos - Taos	Taos - Otowi	Otowi - SF	SF-ABQ	ABQ - Bernardo	Bern. - SA	SA-SM	SM-EBD	EBD-Caballo	Caballo - El Paso
RG In	2.3E+05	3.3E+05	5.9E+05	7.5E+05	1.5E+06	1.6E+06	2.6E+06	3.67E+06	3.3E+06	4.5E+06
Minor Trib	6.6E+04	2.5E+04	3.7E+04	N/A	N/A	N/A	N/A	N/A	N/A	N/A
Major Trib (including WWTP)	N/A	2.4E+05	N/A	5.0E+05	1.4E+05	6.8E+03	N/A	N/A	N/A	N/A
GW	3.5E+03	8.7E+03	2.3E+04	-4.2E+04	-8.0E+04	2.5E+05	2.9E+04	1.5E+04	9.1E+04	4.8E+05
Brine	2.9E+04	0.0E+00	9.2E+04	3.3E+05	7.3E+03	6.1E+05	1.0E+06	3.4E+04	1.1E+06	2.0E+06
Storage in EBD	N/A	N/A	N/A	N/A	N/A	N/A	N/A	4.16E+05	N/A	N/A
RG In+ (Modeled Reach Input)	3.3E+05	6.0E+05	7.5E+05	1.5E+06	1.6E+06	2.6E+06	3.7E+06	3.7E+06	4.5E+06	7.0E+06
RG Out	3.3E+05	5.9E+05	7.5E+05	1.5E+06	1.6E+06	2.6E+06	3.7E+06	3.7E+06	4.5E+06	7.0E+06

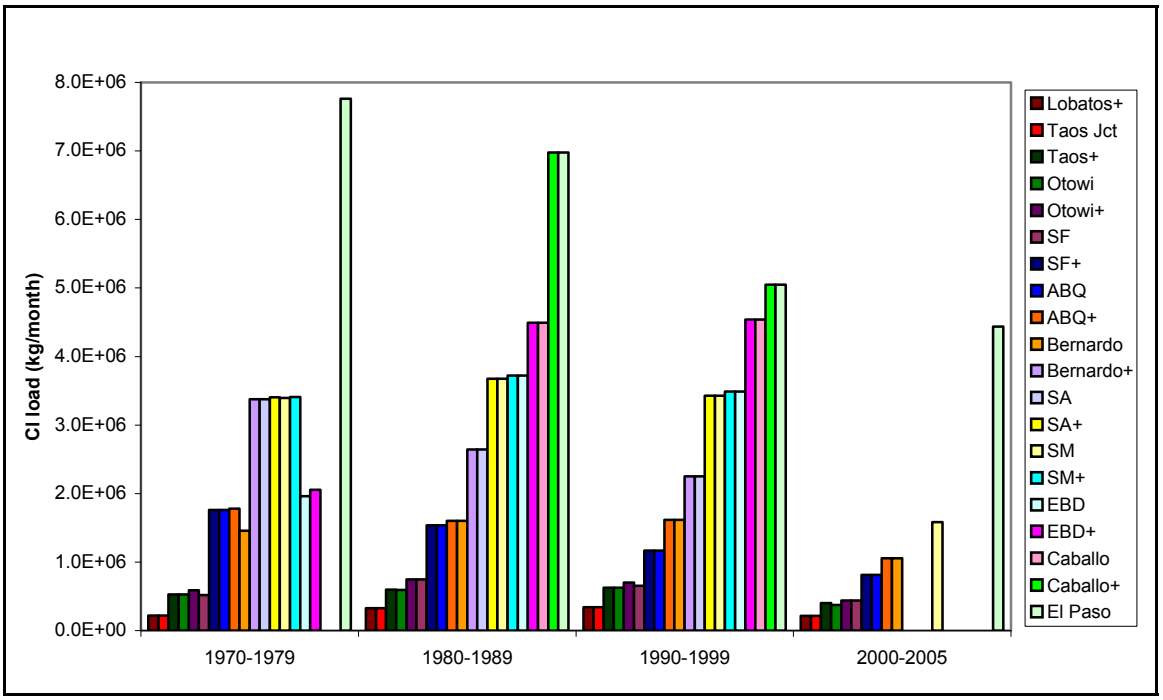

Figure 6.3a. Chloride load comparison between modeled (upstream+) and measured values at all locations during the 1970's, 1980's, 1990's and 2000.

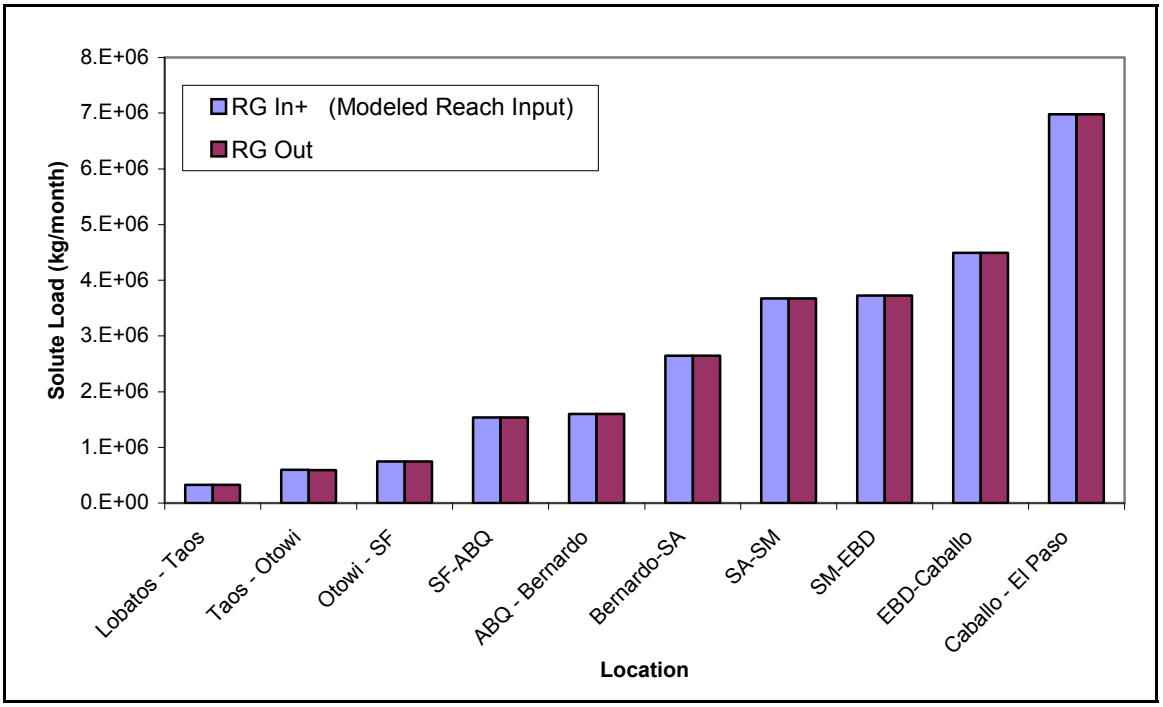

Figure 6.3b. Chloride load comparison between modeled (upstream+) and measured values at all locations during the 1980's.

6.2.4 Geologic Brine Calculation

In order to test the chloride mass balance, the amount of chloride load from brine seepage was compared to previous estimates by *Mills* [2003]. *Mills* [2003] identified significant amounts of brine seeped into the river system at San Acacia, San Marcial, Leasburg and El Paso Narrows. *Mills* [2003] quantified the brine seepage by reporting chloride burden within each reach as presented in Table 6.9 and illustrated in Figure 6.4. Figure 6.4 compares average chloride load from brine calculated from *Mills'* [2003] model and from the decadal mass-balance model. Differences are likely caused by variations in methodology. The calculations by *Mills* [2003] each used only two samples collected during biannual synoptic sampling campaigns in August 2001 and January 2002. In addition to the limited chloride information, *Mills* [2003] brine values included all brine entering the system, including brine that entered the river through an indirect pathway, e.g. tributaries or drains. Contrastingly, the decadal average method accounted for brine that entered the river directly or through certain drains where chemical data could not be included due to availability. Although some methodological differences contributed to variations, both models presented similar results. This comparison tends to support the accuracy of the brine inflow estimates from the decadal chloride model.

Table 6.9. Comparison of chloride load from brine (kg/month).

River Reach	1980s Average	*Mills* [2003] Aug 2001	*Mills* [2003] Jan 2001
Lobatos - Taos	2.9E+04		
Taos - Otowi	-4.6E+03		
Otowi - SF	9.2E+04		
SF-ABQ	3.3E+05		
ABQ - Bernardo	7.3E+03		
Bernardo-SA	6.1E+05		
SA-SM	1.0E+06	6.0E+04	1.3E+06
SM-EBD	3.4E+04		
EBD-Caballo	1.1E+06	8.7E+05	1.8E+06
Caballo - El Paso	2.0E+06	4.8E+05	2.7E+05

Note: Locations from Mills are San Acacia, T or C, Seldon Canyon and El Paso which match to the decadal model reaches of San Acacia to San Marcial, Elephant Butte Dam to Caballo, Caballo to El Paso, respectively.

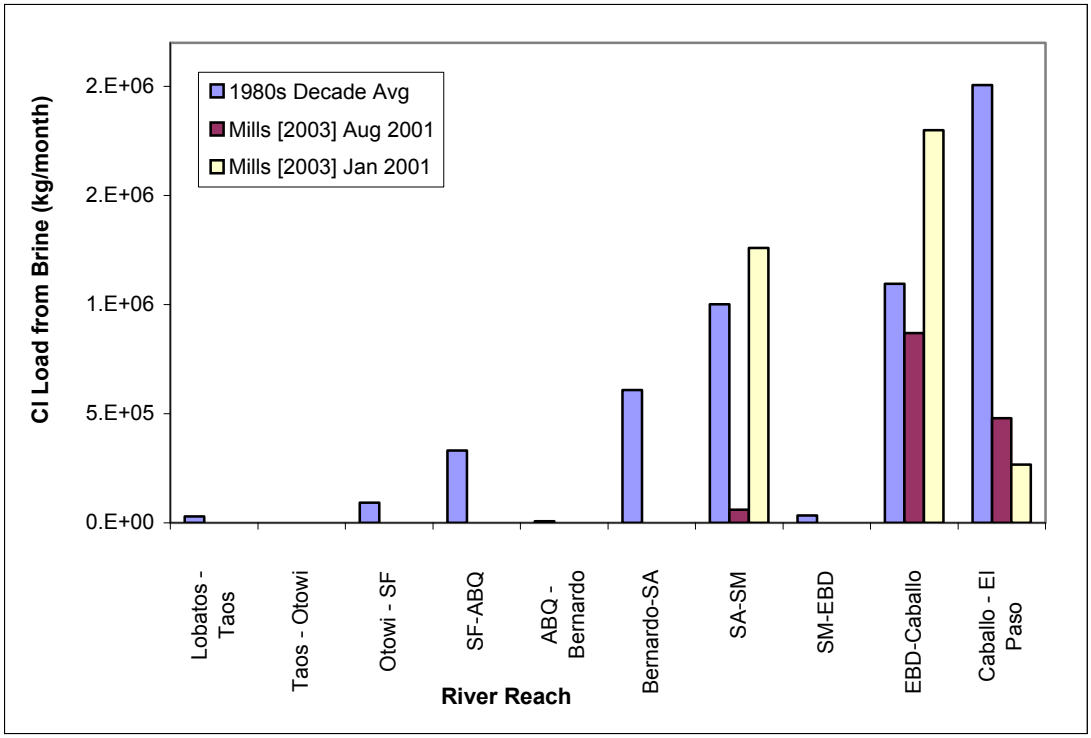

Figure 6.4. Chloride addition from brine, a comparison between the decadal mass balance model for the 1980s and *Mills* [2003] instantaneous model for August 2001 and January 2002 and. The negative brine inflow at San Marcial to Elephant Butte is attributed to data errors and assumed to mean that no brine enters the river in that reach.

6.2.5 Reactive Solutes

The upstream+ chloride model was used to compute the amount of brine entering the river in each reach; the chloride load from brine was converted into a brine seepage rate by dividing the chloride load by the chloride concentration found in brine samples. Wells sampled by *Newton* [2005] and *Moore et al.* [2008] from the Socorro and El Paso regions, respectively, were used to estimate brine chemistry (Table 6.3). Samples from the Socorro area were used in the river reaches between San Acacia to Elephant Butte and the *Moore et al.* [2008] samples were used in river reaches below Elephant Butte Dam (Table 6.2). In order to determine the quantity of each solute derived from brine, the brine seepage rate was multiplied by each respective solute concentration. The quantity of solute attributed to brine seepage was then included in the mass-balance model calculated for each solute.

Reactive solutes have been modeled as described previously for chloride, including the following solute sources and factors affecting concentration: tributaries, drains, wastewater treatment plant, groundwater and concentration from water lost through evapotranspiration. In contrast to the discharge and chloride models, the reactive models were not expected to match the historic measured data because the mass-balance models do not include chemical reactions. The reactive solute models may or may not account for all solutes that enter the Rio Grande within a particular reach. The following diagrams compare upstream+ model results to downstream data for the 1980's. TDS, calcium, sodium, magnesium, potassium, sulfate and bicarbonate are displayed in Figures 6.5, 6.6, 6.7, 6.8, 6.9, 6.10, and 6.11. Each reactive solute had residual loads that could not be attributed to the known sources listed above. Residual

loads for all locations and each solute during the 1980's are presented in Figure 6.12. These solute load residuals are ascribed to chemical interactions with mineral phases.

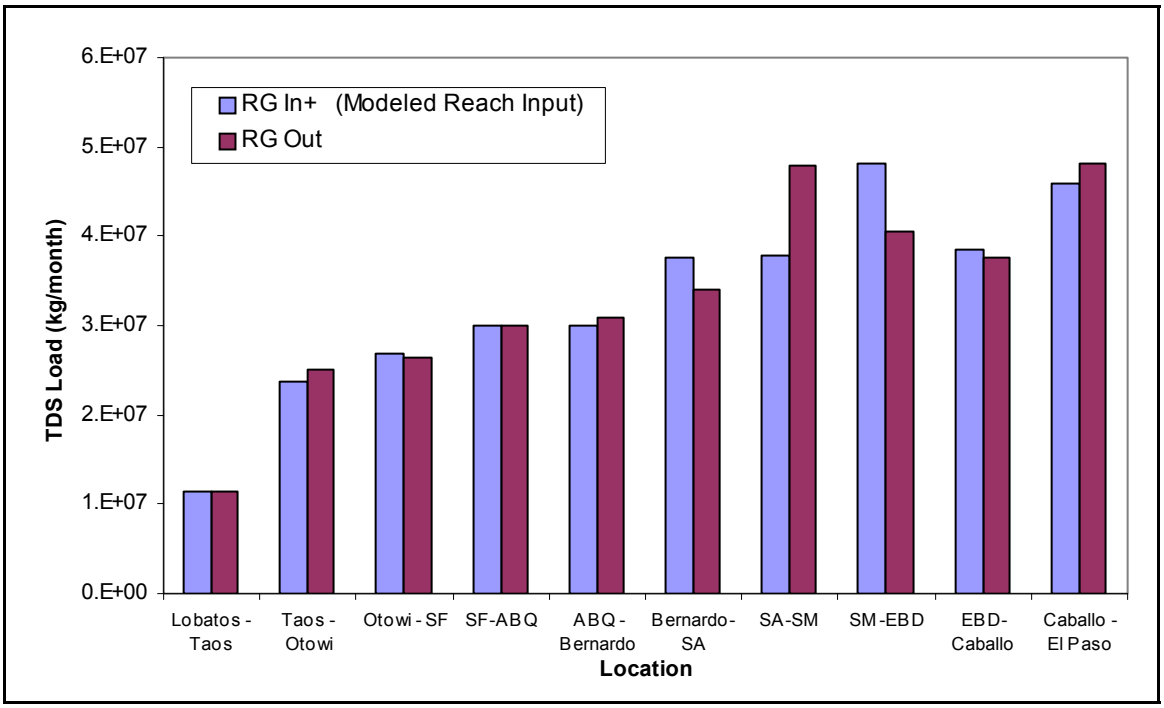

Figure 6.5. Total dissolved solids load at all locations during the 1980's.

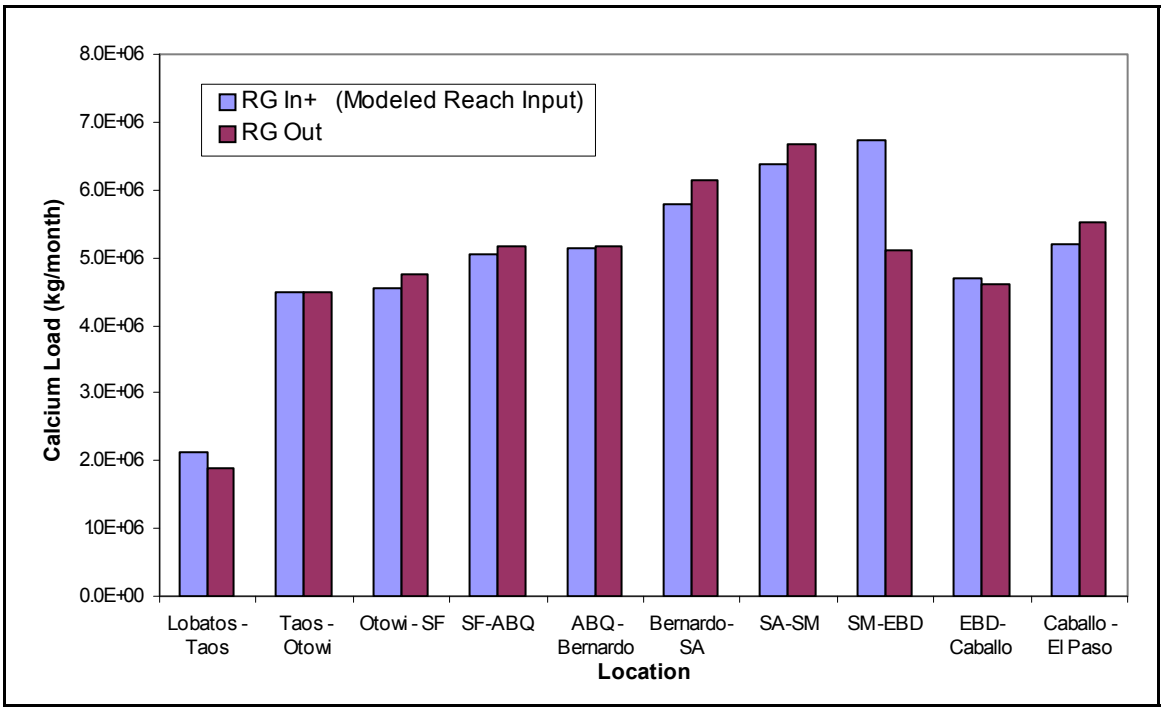

Figure 6.6. Calcium load at all locations during the 1980's.

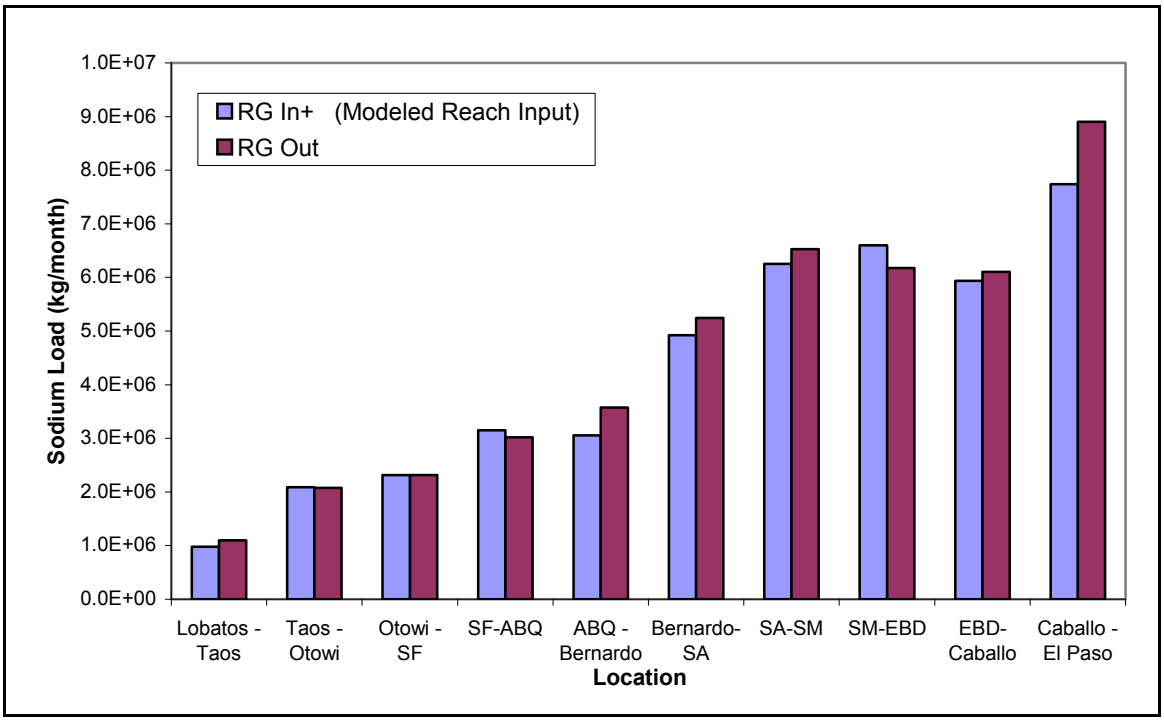

Figure 6.7. Sodium load at all locations during the 1980's.

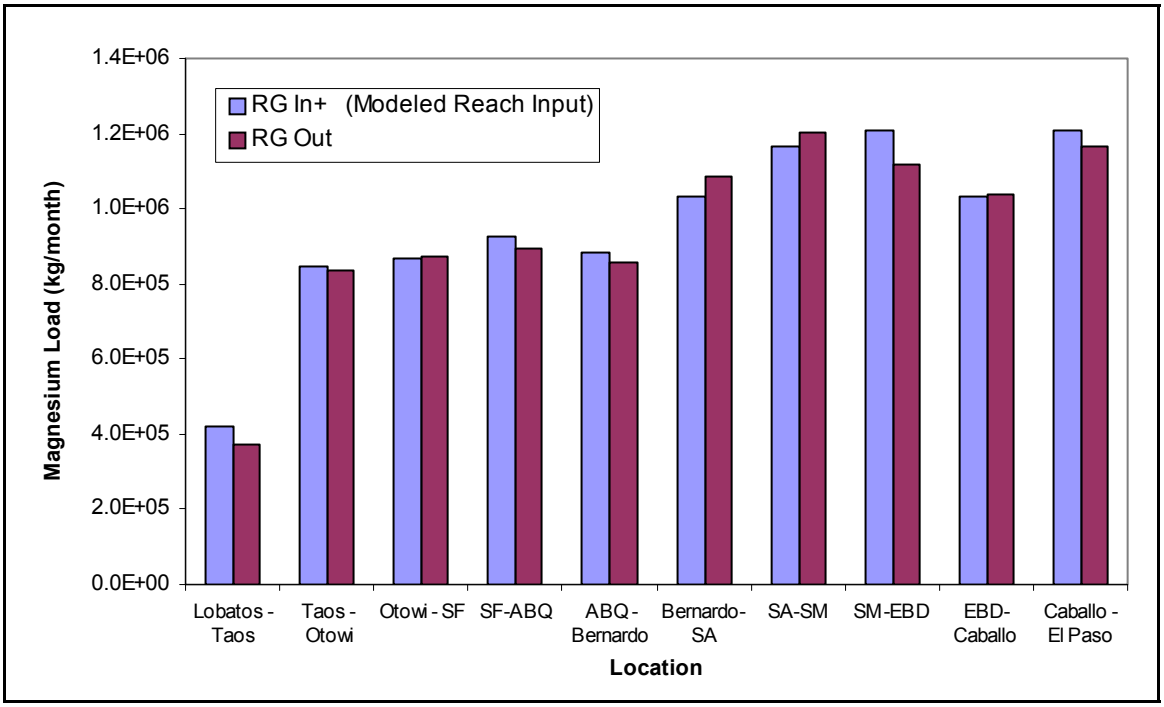

Figure 6.8. Magnesium load at all locations during the 1980's.

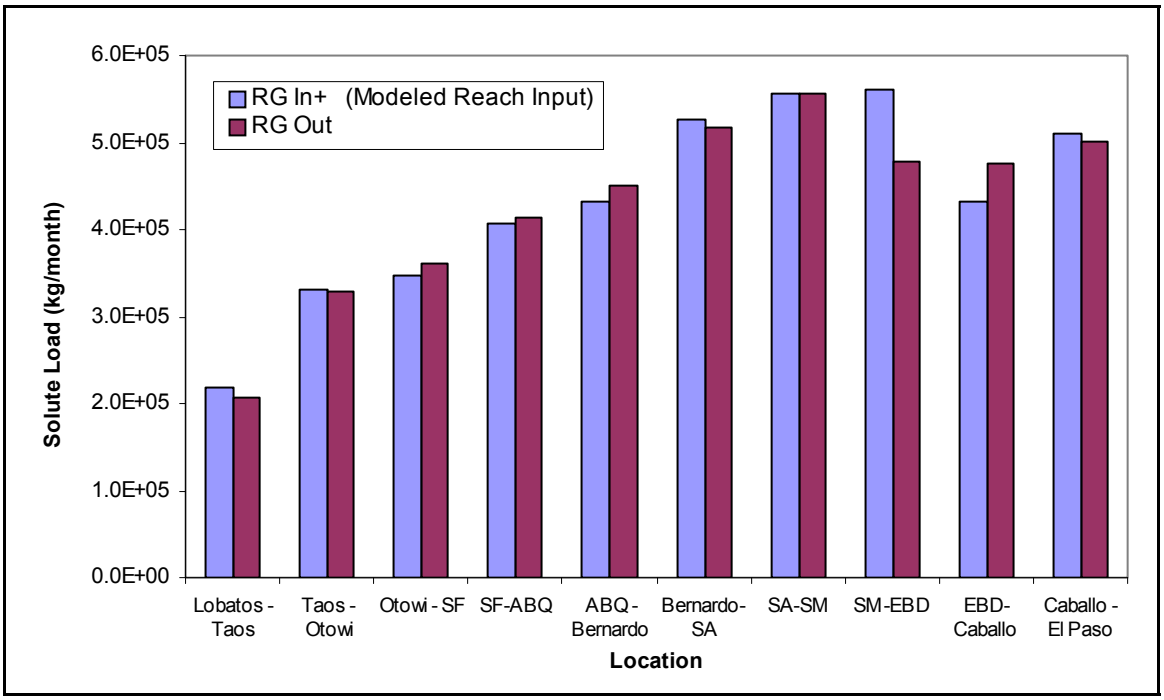

Figure 6.9. Potassium load at all locations during the 1980's.

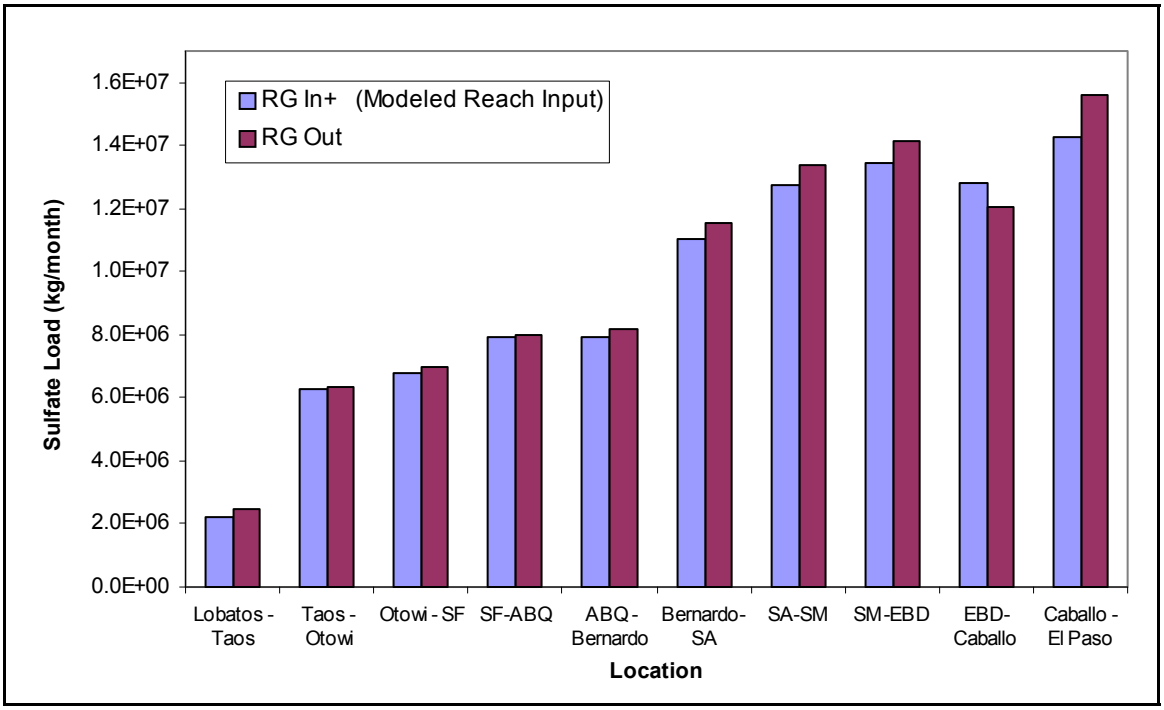

Figure 6.10. Sulfate load at all locations during the 1980's.

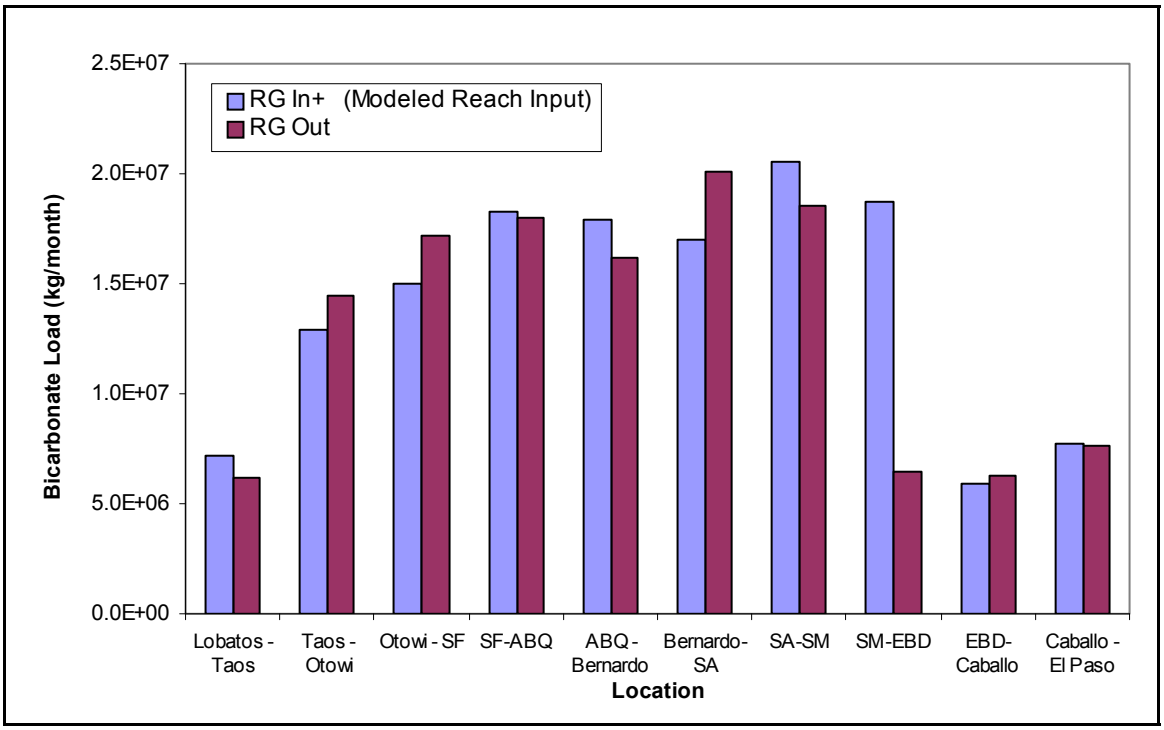

Figure 6.11. Bicarbonate load at all locations during the 1980's.

The residual loads varied through time and space; compare Figure 6.12, 1980's to Figure 6.13, 1990's. It is important to recall that the 1980's and 1990's were both relatively wet decades. During drier decades (e.g. 1950's), residuals solute loads would likely be smaller due to less water flowing in the Rio Grande. In addition, drier conditions would mean a greater proportion of water was derived from ground water, tributaries and deep brine. These solute sources would be accounted for within the mass balance model, which would most likely lead to smaller solute residuals. Further, lower flows in the river generally indicate higher solute concentrations, which equates to fewer solute residuals (i.e., mineral interactions).

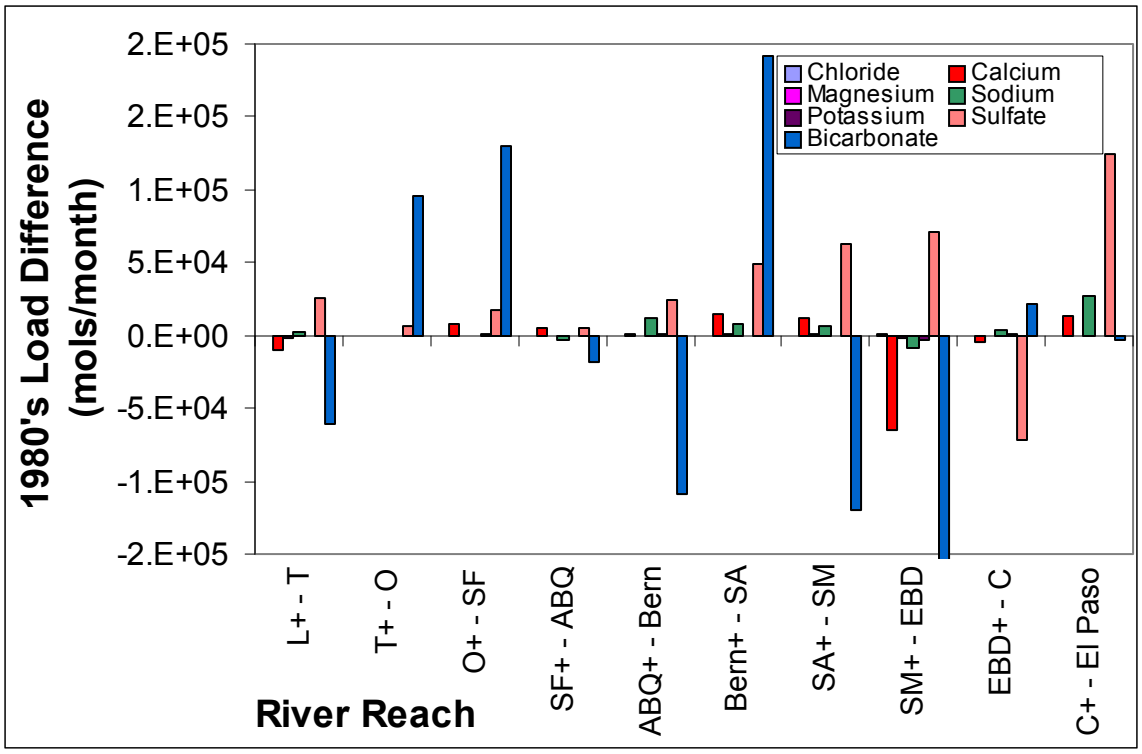

Figure 6.12. Residual solute load for all solutes and river reaches during the 1980's. Negative values present locations where the upstream+ modeled load has under-predicted the amount of solute entering within that reach. The bicarbonate residual for SM to EBD is -7.5×10^5 mols/month.

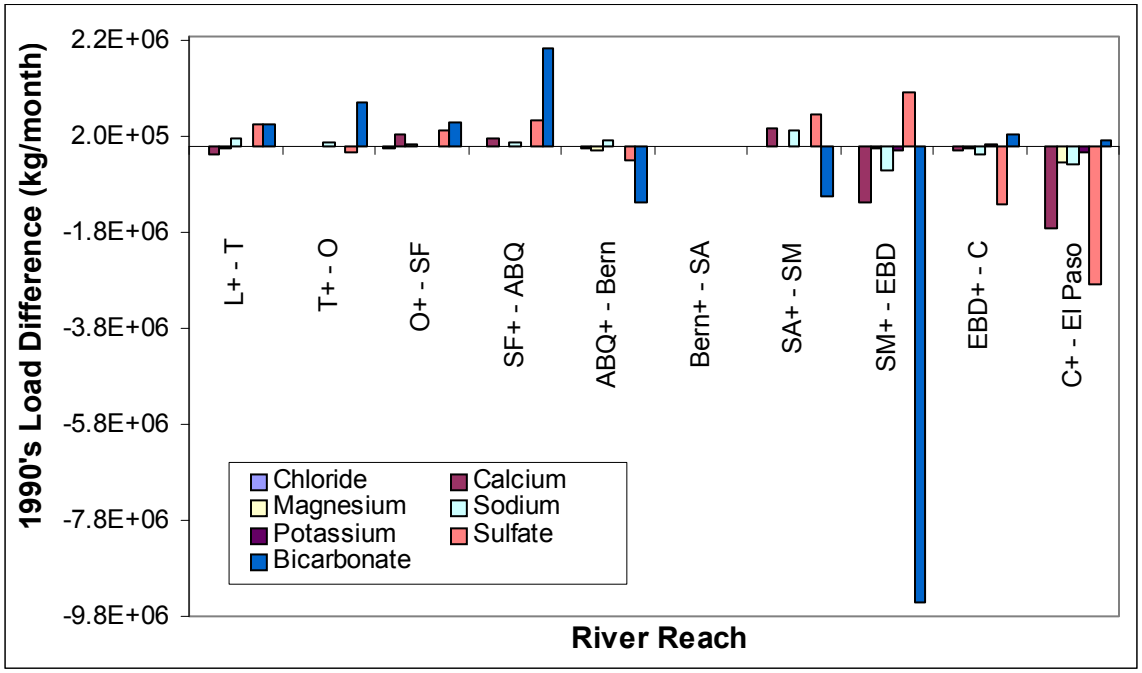

Figure 6.13. Residual solute load for all solutes and river reaches during the 1990's. Negative values present locations where the upstream+ modeled load has under predicted the amount of solute entering within that reach.

6.3 Uncertainty

There are many sources of uncertainty associated with the load and load difference calculations. Each component of the load calculation carries an associated uncertainty that is derived from both systematic and random error. For example, a single discharge measurement is based on the USGS gage or stage recorder and a rating curve computation utilized to convert the stage measurement into a discharge reading. The stage recorder output and the rating curve each include an approximately known random uncertainty, meaning that on any particularly day one collects a measurement; the observer or the instrument will record an answer that varies randomly from the true value. In addition, the process carries a systematic error or bias that would affect all measurements the same. For instance, if the rating curve contained a calculation error, all the discharges reported using that rating curve might be 5% too high, thus all the discharge data would, on average, be biased 5% high.

The standard method for calculating uncertainty is error propagation. For any one load calculation, the discharge is multiplied by the concentration in order to achieve the flux of solute mass through the river cross section. The uncertainty in the load for one sample can be computed by uncertainty propagation as follows: $U = \sqrt{U_D{}^2 + U_{SC}{}^2 + U_{SL}{}^2}$ where $U_D{}^2$ is the uncertainty in the discharge, U_{SC} is a random uncertainty associated with the ability of a single collected sample to represent a time and spatial interval and U_{SL} is the uncertainty in the solute lab analysis. From a USGS publication on uncertainty in stream gaging [*Harmel et. al*., 2006], a discharge measurement typically includes 6-19% random uncertainty based on propagation of uncertainty from the continuous stage measurement device and the rating curve utilized

to extrapolate the stage reading into a discharge. To determine the uncertainty in a solute-load calculation, the uncertainty associated with the solute concentration must also be evaluated. The solute concentration uncertainties from sample collection from lab analysis are in the range of 4-48% and 5-21% respectively [*Harmel et. al*., 2006]. Thus, $U = \sqrt{(0.19)^2 + (0.48)^2 + (0.21)^2}$, giving a worst-case scenario uncertainty of 56%. However, this uncertainty applies only to one daily sample pair of concentration and discharge information. For the purpose of this thesis, solute-load data was averaged monthly and then on a decadal basis. The approach to quantifying uncertainty that is outlined above is not actually applicable to calculations of long-term average load.

When the loads are averaged over long time periods such as decades, the random error becomes negligible. As long as errors due to random uncertainty are normally distributed, high and low errors will cancel each other. As the number of averaged measurements grows large, the average will approach the "true" mean (plus any systematic uncertainty). Because results are presented as decadal averages, the uncertainty derived from random errors becomes negligible, thus leaving only uncertainty derived from systematic error. Unfortunately, systematic error is difficult to identify and even harder to quantify. Thus, the standard method for evaluating uncertainty (i.e., error propagation) severely overestimates the uncertainty of long-term averages. The error propagation method is inappropriate for this long-term analysis.

In addition, recall that much of the solute concentration data was interspersed with regressed data. Utilizing regressed data adds additional uncertainty. In this case, it seems that the regressed data add only a minimal amount of uncertainty. Based on the statistical test (Chapter 4), intermixing regressed values yielded a relative percent

difference of approximately 3%. In fact, utilizing the regressed data provides a better estimate of the true decadal average load than to leaving the months without data out of the analysis.

Further issues for estimating uncertainty arose in the mass-balance calculations. Recall that each mass balance was computed from the summation of solute load additions to the river from the upstream river station, major and minor tributaries, wastewater treatment plant, ground water and brine. Each of these sources contributes an uncertainty to the average decadal load. Much of this uncertainty cannot be expressly quantified. For example, ground water seepage rates were taken from one reference paper and utilized as an estimate for multiple river reaches. Evapotranspiration data was also estimated from very limited data and extrapolated to near-by river reaches. The use of these generalized values was necessary to obtain chemical balances, but quantification of the error (bias) associated with them is very difficult or impossible to estimate. In light of these considerations I have not presented a formal uncertainty analysis, however, the reader should be aware that results that show small residuals between large solute loads could be unrepresentative in both direction and magnitude. Relatively large differences in load are probably more robust.

6.4 Conclusions

I have formatted a mass-balance model to calculate masses of water and solutes in the Rio Grande. Comparisons with river gaging data for water masses and *Mills* [2003] brine calculations support the results of the mass-balance model. Reactive solute mass balance models for calcium, sodium, magnesium, potassium, bicarbonate, and

sulfate do not account for all observed downstream changes. I ascribe most of the model residuals to mineral interactions.

CHAPTER 7
CHEMICAL REATIONS – SITE STUDY LEMITAR, NM

The overall Rio Grande mass balance, presented above, indicated that chemical reactions significantly influence river chemistry. In order to interpret trends in system behavior, the nature of the chemical reactions and how and where the reactions occur must be understood. Previous studies have suggested that irrigation practices caused the observed Rio Grande solute increase with distance downstream [*Lippincott*, 1939]. Additional studies support the hypothesis that drainage water flushed accumulated salt from agricultural areas in the 1930's. Thus, it seems logical to assume that chemical reactions may occur on agricultural lands irrigated with Rio Grande water. During irrigation, water is evaporated and percolated through many layers of soil, where the water encounters soluble mineral phases. In order to better understand the effect of irrigation agriculture on the water quality of the Rio Grande, a representative site was chosen for a small-scale, subsurface investigation near the middle of the basin. Solute mass-balance calculations and subsurface reaction modeling results from this small-scale study will be extrapolated into macro-scale implications for the Rio Grande within the San Acacia to San Marcial river reach.

7.1 Background and Geology

The site rests in the Middle Rio Grande Valley (see Figure 7.1 for location within Upper Rio Grande Basin). This section of the Rio Grande hosts many acres of

irrigated farmland and an extensive irrigation network. Rio Grande water is diverted at many locations into the canal system, first into larger canals such as the Socorro main canal and then allocated into the smaller laterals and canals for distribution. Landowners are allotted river water equally regardless of their water rights, since the region has not been adjudicated. The owners operate their own turnouts for irrigation. The soil consists of mainly clay and sandy loams, classified as Armijo, clay-Glendale, and sand-Glendale *[Johnson, 1984]* in the Soil Survey of Socorro County Area, New Mexico.

The experimental site is located north of the Lemitar exit on I-25, property marker 786 on state road north 408. The specific site, belonging to Dr. Robert Bowman, (referred to as the Lemitar site) is a small farm growing mainly Kentucky-31 fescue pasture grass that covers approximately eighty percent of the acreage. Property records show water rights extend back to 1850 with irrigation beginning prior to that date. Information regarding agriculture is limited; according to personal communication with Dr. Bowman, the area was a vineyard until the vines were destroyed during Prohibition. The land was subsequently converted to crop production including alfalfa, oats, chile, melons, and pasture grass. The Bowman property consists of 9.7 acres with 7.9 acres of irrigated farmland. Figure 7.2 contains a picture of the location indicating sampling locations. Groundwater flows North West (10 degrees West of North) toward the Rio Grande with a hydraulic gradient of 0.0072 determined with a triangulation method using monitoring wells and distance. The Bowman property was specifically chosen because there are no drainage structures to drain excess water after irrigation. Thus, all applied irrigation water is either evaporated, transpired by plants or infiltrates

into the subsurface. The site was further chosen for its known lack of ground water mixing, particularly with deep brines. As was discussed in Chapter 6, deep brine waters contribute significant quantities of solutes to the Rio Grande in many locations. Deep brines have a characteristic chloride/bromide ratio of over 1000. Table 6.3 from Chapter 6 shows the chloride/bromide ratio for the brine samples used in the mass balance, both have a Cl/Br > 1000. The Lemitar site ground water contains no evidence to suggest mixing with deep brine, as it has a chloride/bromide ratio less than 350 (Table 7.1).

Figure 7.1. Map of middle Rio Grande, with Lemitar, NM highlighted in pink.

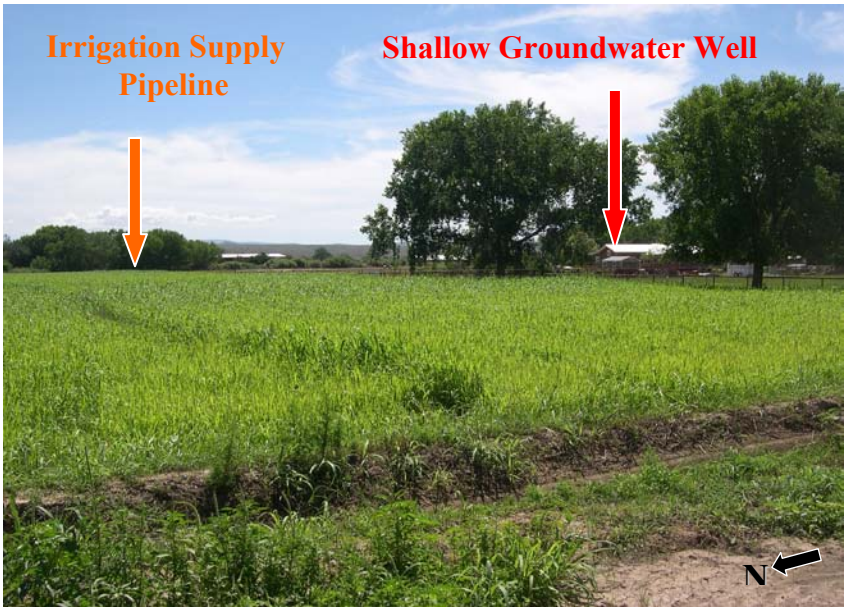

Figure 7.2. Picture indicating layout of the Lemitar, NM site (Bowman property) with canal and shallow ground water locations labeled.

7.2 Water Balance

In order to quantify the effects of irrigation on Rio Grande chemistry, the amount of irrigation water applied, seepage rate of ground water to the river and the solute concentrations are required. The water balance is extremely important in understanding the rate and ultimate amount of solutes being transported to the Rio Grande. Thus a water mass balance was calculated at the Lemitar site so that it might be extrapolated to the San Acacia-San Marcial reach, as well as the entire upper Rio Grande.

Two water balances were computed; one using information from outflow data calculated with Darcy's Law, the other was based on inflow rates that were estimated from applied irrigation minus evapotranspiration. For both calculations it was assumed that any vadose zone and aquifer storage was negligible, thus the amount of water that entered must be equal to the amount of water that exited the system. The calculations

are illustrated in Equation 7.1 and 7.2. The seepage results shown in equations 7.1 and 7.2 did not yield the same flux but were close. Qualitative uncertainty estimates were used to resolve this discrepancy. To calculate flow from Darcy's Law, the cross-sectional area, hydraulic conductivity and hydraulic gradient were needed. The hydraulic gradient was computed based on water-level information collected from monitoring wells at various locations on the Lemitar property and the distance between them. Uncertainty exists in both the water-level measurements and the land survey measurements. The cross-sectional area was difficult to determine, being calculated from the multiplication of the aquifer saturated thickness and the width across the property. Although the water table remains reasonably constant at approximately 3.1 meters (10 ft) below the ground surface, the bottom of the aquifer could not be determined and was estimated to be 15.3 m (50 ft). Finally, uncertainty exists in the computation of hydraulic conductivity as well. The hydraulic conductivity was calculated from an aquifer pump test. Results were analyzed using the Jacob-Cooper method, which carries significant uncertainties in the assumptions that define the method. The Jacob-Cooper method assumes an infinite aquifer of homogenous and isotropic material. None of the Jacob-Cooper assumptions are strictly valid for the Lemitar site.

The alternative method for determining the amount of water flushed through the aquifer at the Lemitar site also involved significant uncertainties. The applied irrigation method utilized an estimate of the amount of irrigation water applied to the land surface and the amount of water lost from the site to evapotranspiration. The quantity of applied irrigation water was estimated from 30 months of data collected by the property

owner over the period from June 2004 to March 2006. The quantity of water lost to evapotranspiration was taken from the ratio of irrigation to ground water chloride concentrations. Consideration of these factors indicated that the applied irrigation estimate was probably more accurate than the Darcy's Law calculation, due mainly to the larger number of assumptions required for the Darcy's Law computation.

Equation 1. Darcy's Law applied to the Lemitar site.

$$Q = KA\left(\frac{dh}{dl}\right)$$

$$Q = \left(1\times10^{-4}\ {}^{m}\!/_{s}\right)\left(418 m^2\right)\left(0.0072\right) \qquad \text{[Equation 7.1]}$$

$$Q = 3.0\times10^{-4}\ {}^{m^3}\!/_{s}$$

where Q is the seepage rate, K is the hydraulic conductivity (estimated based on aquifer test results), A is the cross sectional area (A=saturated thickness*cross sectional length) and hydraulic gradient (dh/dl) was found with distance and depth to water table.

Equation 2. Amount of irrigation applied to the Lemitar site.

$$Q_{effective} = Q_{applied} - Q_{evaporated}$$

$$Q_{effective} = \left(1.06\,{}^{\mathrm{m}}\!/_{\mathrm{yr}}\times31933 m^2\right) - \left(0.69\,{}^{\mathrm{m}}\!/_{\mathrm{yr}}\times31933 m^2\right)$$

$$Q_{effective} = \left(34066\,{}^{\mathrm{m}^3}\!/_{\mathrm{yr}}\right) - \left(22034\,{}^{\mathrm{m}^3}\!/_{\mathrm{yr}}\right) \qquad \text{[Equation 7.2]}$$

$$Q_{effective} = 12,032\,{}^{\mathrm{m}^3}\!/_{\mathrm{yr}} = 3.8\times10^{-4}\ {}^{\mathrm{m}^3}\!/_{\mathrm{s}}$$

where $Q_{applied}$ is an estimated on amount of water applied based on 30 months of data from June 2004-March 2006. $Q_{evaporated}$ is the amount of water lost to evaporation based on the ground water to irrigation water chloride ratio.

The water balance is closed using the $Q_{effective}$ for both the effective inflow (accounting for evapotranspiration) and outflow. Thus the estimated amount of water that was effectively applied to the field from the canal, percolated through the soil and flowed underground back to toward the river was $3.8\text{x}10^{-4}$ m^3/s. This seepage rate coupled with

the solute concentrations will reveal chemical implications for the Rio Grande and downstream users.

7.3 Hydrogeochemistry

Chemistry data were collected in order to assess the role of subsurface reactions; samples were analyzed both before irrigation (from the supply canal) and after (from a well sampling the shallow ground water). Sampling locations are visible in Figure 7.2. Samples were collected approximately twice a month during the irrigation season from May through September of 2005. The chemical results are presented in Table 7.1 and Figure 7.3, in which Stiff diagrams show the general chemistry for a few of the irrigation and ground-water samples. Solute concentrations are presented in milli-equivalents per liter. Concentrations of major ions were higher in the ground-water samples than the irrigation samples. The relative chemistry and concentrations in the ground water and irrigation water samples remained nearly constant during the 5-month sampling period. Figure 7.4 illustrates a comparison between the various samples for irrigation chemistry (top) and ground-water chemistry (bottom) collected in May, August, and September 2005. Notice the sample labeled Irr-GW515 w corrected pH, the pH of this sample was corrected to the field-measured pH. The field measured pH was taken the following year during the same time period. The remaining ground water samples from May report lab-measured pH. The lab-measured values drastically alter the chemistry and likely do not represent field conditions. The corrected samples collected in May 14 from the canal and from the ground water on May 15, 2005 were chosen to represent typical irrigation and ground water chemistry at

this site during the irrigation season. These two samples were utilized in the solute budget calculations and to assess the ultimate solute burden of agriculture on the Rio Grande in this area.

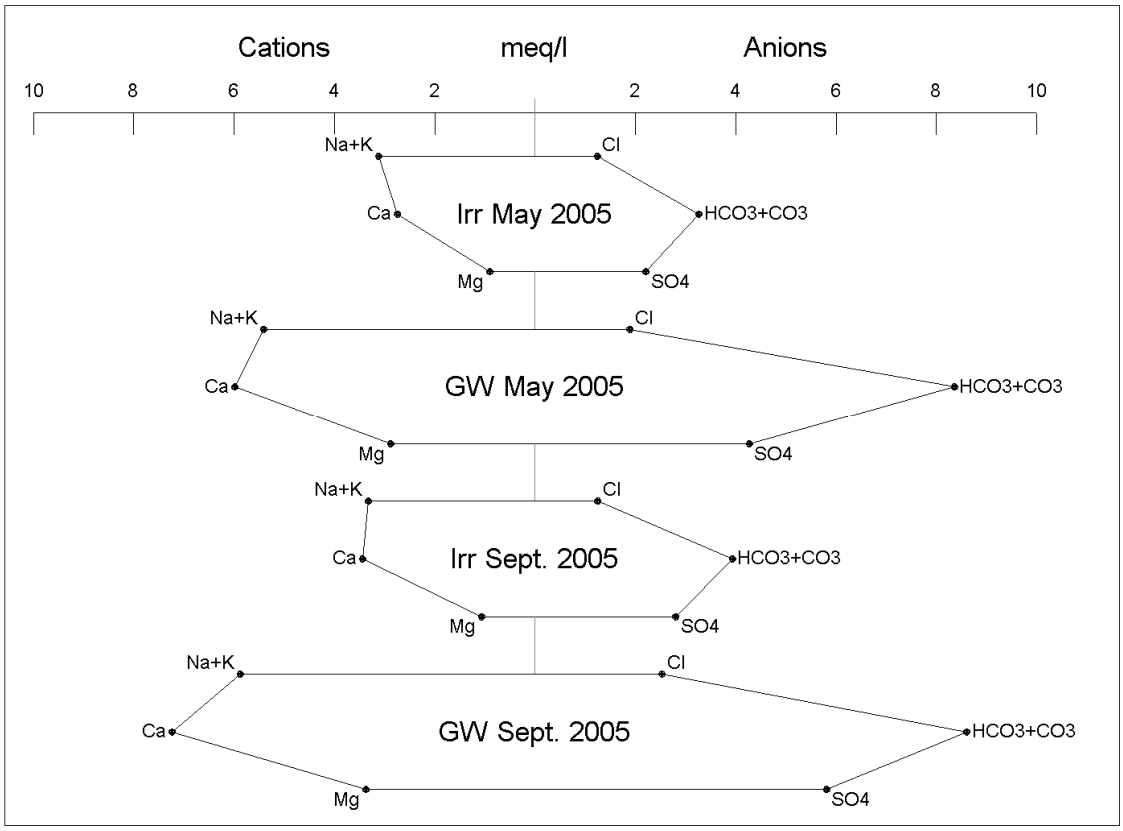

Figure 7.3. Stiff diagram illustrating general chemistry at site in Lemitar, NM. Irrigation water and groundwater samples from May 2005 were used in the mass balance analysis.

Table 7.1. General chemistry for irrigation and ground water samples at Lemitar, New Mexico.

Sample ID	pH	Ca	Mg	Na	K	Cl	SO_4	HCO_3	F	Br	pCO2 (Atm)	Charge Balance %
Irrigation water 20050514	8.3	55	11	69	4.7	44	106	185	0.38	0.11	7.2E-04	2.1
Ground Water 1 20050515	7.02	120	35	120	7.7	67	205	510	0.94	0.3	3.6E-02	-1.1
Ground Water 2 20050516	7.9	120	36	120	8.8	67	220	510	0.95	0.24	4.7E-03	-1.8

Ground Water 3 20050517	7.9	120	35	125	10	67	220	510	0.95	0.25	4.7E-03	-1.2
Ground Water 4 20050518	7.8	125	35	115	7.4	67	220	510	0.95	0.23	5.9E-03	-2.1
Ground Water 5 20050519	7.8	120	36	115	7.3	67	220	510	0.95	0.24	5.9E-03	-2.8
Ground Water 6 20050520	7.8	120	35	115	7.4	67	220	510	0.95	0.23	5.9E-03	-3.1
Ground Water 9 20050523	7.8	125	37	110	7.3	68	225	510	0.93	0.23	5.9E-03	-2.8
Ground Water 10 20050524	7.7	125	36	115	7.3	68	220	510	0.94	0.24	7.5E-03	-2
Irrigation water 20050810	7.92	53	9.7	51	6.1	29.8	91.36	195	0.59	0.11	1.9E-03	-2.5
Ground Water 20050810	6.92	140	39	125	8.1	86.85	273.85	485	1.45	0.26	4.3E-02	-1.3
Irrigation water 20050827	8.1	63	12	67	7	39.97	134.68	225	0.64	0.13	1.4E-03	-4.7
Ground Water 20050827	6.82	140	42	115	8.1	82.33	261.82	500	1.49	0.25	5.6E-02	-1.5
Irrigation water 20050905	7.58	62	12	57	4.5	33.11	115.51	210	0.59	0.08	4.4E-03	-6
Ground Water 20050905	6.74	145	42	125	8.5	87.36	274.71	530	1.43	0.26	7.1E-02	-2.1
Irrigation water 20050918	7.94	69	13	72	7.6	44.22	134.83	240	0.72	0.14	2.1E-03	-3.2
Ground Water 20050918	6.67	145	41	130	8.8	89.57	279.07	525	1.46	0.26	8.3E-02	-1.9

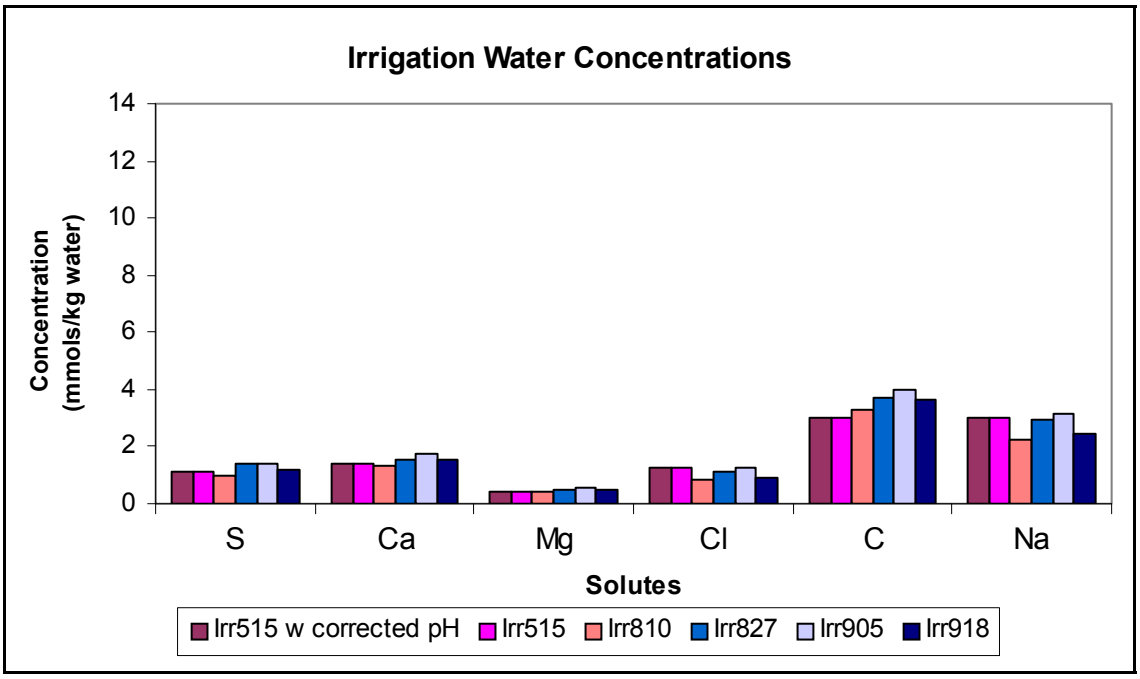

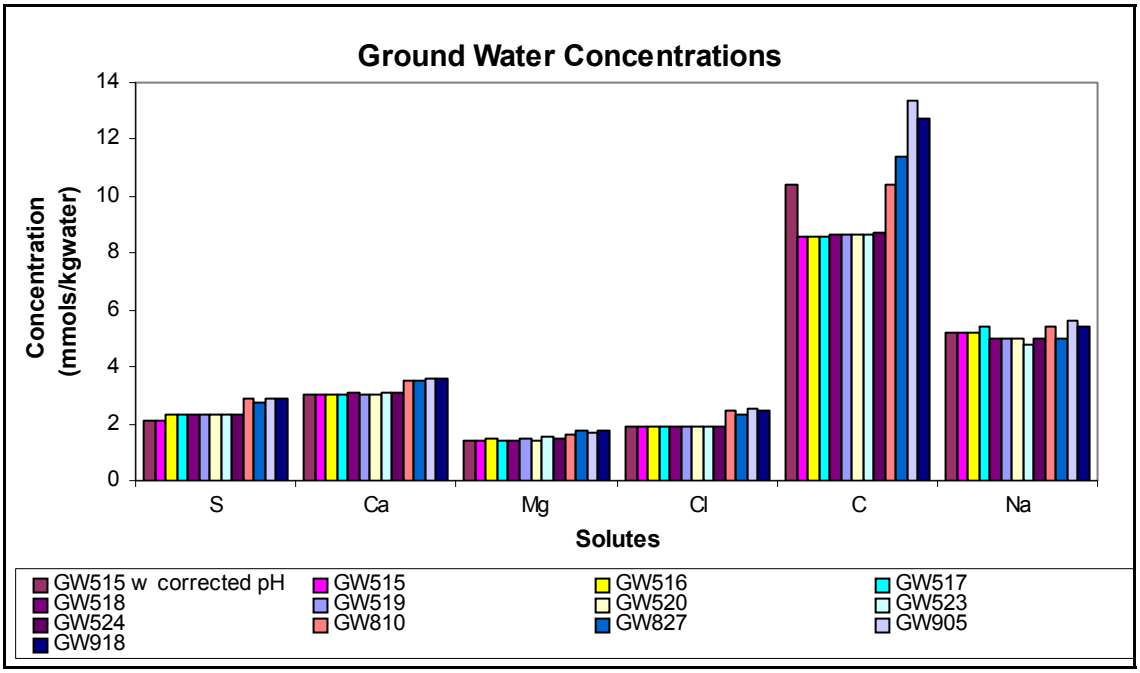

Figure 7.4. Elemental chemistry for irrigation and ground water samples at the site in Lemitar, NM. Irrigation chemistry (top) and ground water chemistry (bottom) for samples collected in May, August, and September 2005. Ground water samples from May have lab-measured pH which drastically alters the chemistry.

7.4 Preliminary Chemical Analysis

Utilizing the pH-corrected samples from May, Figure 7.5 illustrates a comparison between irrigation and ground water general chemistry. Previous studies [*Lippincott*, 1939] suggested that evapotranspiration was the principal source for salinization of the Rio Grande and thus caused the chemical variations between irrigation and ground water. To evaluate this hypothesis, Figure 7.5 also contains a calculated value called predicted groundwater. The predicted groundwater column is a calculated concentration derived from the ratio of irrigation to ground water chloride concentrations. The chloride concentration ratio provides the percentage of water remaining after evapotranspiration. At the Lemitar site, the ratio of irrigation to ground water chloride yields a value of 0.66, which means that 66% of the applied irrigation water infiltrates into the soil and 34% is lost to evapotranspirative processes. When 34% of the irrigation water is evaporated, all the major ion concentrations will increase proportionately. The solute concentrations derived from evaporated irrigation water were calculated by dividing each solute concentration by the percentage of water remaining after evaporation. This quantity was named the predicted ground water and the solute concentrations are presented in Figure 7.5. The predicted ground water chemistry represents solute concentrations from a hypothetical ground water sample that was created solely by evaporating the May 15th irrigation water sample. If evaporation was the only process affecting the transformation from irrigation water into ground water concentrations, the predicted ground water chemistry would be equal to the measured ground water concentrations. However, the measured ground water concentrations are much higher than the predicted ground concentrations. Because the

measured ground water concentrations are different from the predicted ground water concentrations, there must be other processes occurring that affect the chemistry of the irrigation and ground water at this site. As mentioned in the introduction to this section, the increase in groundwater concentration was most likely due to chemical reactions occurring in the soil.

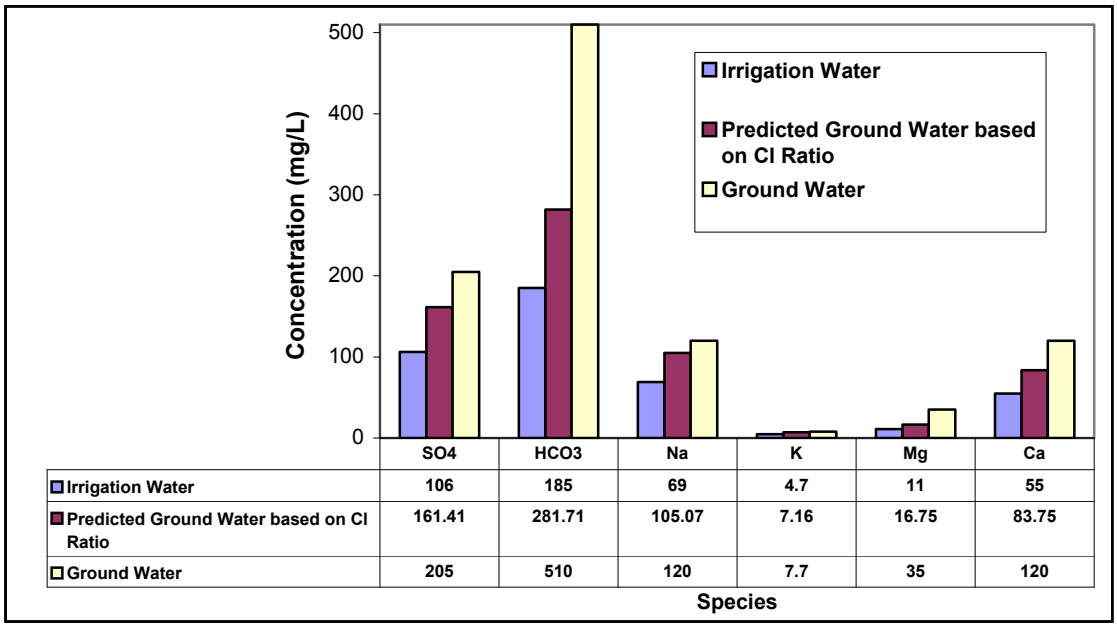

	SO4	HCO3	Na	K	Mg	Ca
Irrigation Water	106	185	69	4.7	11	55
Predicted Ground Water based on Cl Ratio	161.41	281.71	105.07	7.16	16.75	83.75
Ground Water	205	510	120	7.7	35	120

Figure 7.5. Comparison between irrigation, ground water and predicted ground water solute concentrations. Irrigation and groundwater concentrations are from May 2005 samples.

7.5 Mineral Mass Transfer Modeling

7.5.1 Theory

NETPATH, a computer program that calculates a geochemical mass-balance between initial and final waters was utilized to generate possible subsurface reaction combinations to account for chemical differences between irrigation and groundwater. The transformation from initial to final water can occur through various pathways: evaporation, subsurface reactions with multiple phases, or mixing with an additional source of water. Each of the possible water evolution mechanisms must be specified.

The user decides which chemical constituents are important, which phases are present and whether or not mixing or evaporation could play a role. NETPATH mathematically accounts for variations in solute mass between two waters along a single flow path, such that the final water is derived from the initial water through chemical reactions, source water mixing or evaporation. Kinetics and equilibria do not factor into the NETPATH calculations, nor does the plausibility of any designated factor. The results determined by NETPATH are based solely on the stoichiometry of the minerals and constraints specified. Each NETPATH output model is a set of reactions, which specify the amounts of the various phases that must precipitate or dissolve in order to transform the chemistry of the initial water (irrigation water in this case) into the chemistry of the final water (in this case groundwater). Positive values indicate dissolution and forward reaction (e.g. respective release of sodium or magnesium into the ground water by ion exchange), correspondingly a negative value indicates precipitation of a phase or the reverse exchange reaction. All NETPATH simulation results are quantified in millimoles per kilogram of water. Details on NETPATH can be found at the USGS website: http://wwwbrr.cr.usgs.gov/projects/GWC_coupled/netpath/. *[Plummer et al, 1991]*.

7.5.2 Lemitar Mass Transfer Methodology and Results

Water chemistries from 13 irrigation and groundwater samples were put into NETPATH. Samples were collected in May, August and September of 2005. Tandem irrigation and ground water samples were collected on the same day in August and September. Chemistry from the May sample set are shown in Table 7.2. Further inputs include the specified constraining elements calcium, magnesium, sulfur, sodium,

chloride and carbon (Table 7.2); as well as the specified phases calcite, dolomite, gypsum, carbon dioxide gas, Ca/Na exchanges and Mg/Na exchanges (Table 7.3). Evaporation was also included as a calculation based on chloride concentration differences. From these inputs, NETPATH suggested 4 possible reaction combinations (Figure 7.7). Each combination quantified a closed solute mass balance with chemical interactions between the irrigation water and specified minerals. In addition to the model results, NETPATH calculated the saturation index for each mineral phase.

Table 7.2. NETPATH model input: constraints, samples May 15, 2005.

	Irrigation Water	Ground Water
NETPATH Constraints	Initial (mmols/kg water)	Final (mmols/kg water)
Carbon	3.0	10
Calcium	1.4	3.0
Chloride	1.2	1.9
Sulfate	1.1	2.1
Magnesium	0.45	1.4
pCO_2	0.036	0.00072
Sodium	3.0	5.2
Charge Imbalance	2.1%	-1.1%

Table 7.3. NETPATH model input: phases.

Phases	Formulas	Notes
GYPSUM	$CaSO_4$	Positive = dissolution of gypsum
DOLOMITE	$CaMg(CO_3)_2$	Positive = dissolution of dolomite
Mg/Na EX	$MgX + Ca^{2+} \rightarrow CaX + Mg^{2+}$	Positive = releases Mg to solution (i.e. GW)
CO_2 GAS	$CO_{2(gas)} \rightarrow CO_{2(aq)}$	Positive = in gassing of CO_2
CALCITE	$CaCO_3$	Positive = dissolution of calcite
EXCHANGE	$Na_2X + Ca^{2+} \rightarrow CaX + 2Na^+$	Positive = releases Na to solution (i.e. GW)

Note: X = soil solid phase for ion exchange. GW = Ground Water.

MODEL 1	
CALCITE	0.016
GYPSUM	0.30
DOLOMITE	0.49
CO2 GAS	2.8
EXCHANGE	0.21
Evaporation factor:	1.5
656g H2O remain	

MODEL 2	
CALCITE	-0.41
GYPSUM	0.30
DOLOMITE	0.71
CO2 GAS	2.8
Mg/Na EX	0.21
Evaporation factor:	1.5
656g H2O remain	

MODEL 3	
CALCITE	1.0
GYPSUM	0.30
CO2 GAS	2.8
EXCHANGE	0.71
Mg/Na EX	-0.49
Evaporation factor:	1.5
656g H2O remain	

MODEL 4	
GYPSUM	0.30
DOLOMITE	0.50
CO2 GAS	2.8
EXCHANGE	0.21
Mg/Na EX	0.0081
Evaporation factor:	1.5
656g H2O remain	

Figure 7.6. NETPATH model results for the Lemitar site samples from May 2005. Constraints = Ca, Mg, S, C, and Cl. Phases = calcite, dolomite, gypsum, CO_2 gas and exchange reactions (Ca/Na and Mg/Na).

7.5.3 Soil Mineral Saturation State

Saturation calculations assess thermodynamic controls on the phase equilibria. The saturation index (SI) quantifies whether the solution is in equilibrium with the various minerals which may be reacting in the system. The SI is defined by equation 7.3:

$$SI = \log \frac{IAP}{K_T} \qquad \text{[Equation 7.3]}$$

where IAP is the ion activity product of the mineral/water reaction and K_T is the thermodynamic equilibrium constant adjusted to water temperature. The saturation indices were calculated in NETPATH from relevant thermodynamic data contained in WATEQFP *[Plummer et al, 1976]*. An SI value equal to 1 indicates a mineral at equilibrium, positive saturation indices indicate a state of oversaturation, and a negative indicates a state of undersaturation for a particular mineral. An uncertainty of ± 0.5 is generally accepted [*Plummer et al*, 1990]. The SI listed for pCO_2 is defined as above except that the K_T value is equal to the constant reference CO_2 fugacity of 1 atmosphere [Personal communication with David Parkhurst, USGS NETPATH contact]. The pCO2 was computed based on pH and bicarbonate information. Equilibrium with respect to

pCO_2 is reached at an SI of –3.5. Saturation indices are presented in Table 7.4 (for May 15 samples) and Figures 7.7 (all irrigation) and 7.9 (all ground water). Most of the irrigation samples are oversaturated with respect to calcite and aragonite. Gypsum and fluorite are both undersaturated. Dolomite is undersaturated in a few irrigation samples and oversaturated in others. The partial pressure of CO_2 for all the irrigation samples is very close to equilibrium or slightly undersaturated. Of greater importance to subsurface reactions were the saturation indices of minerals in ground water. Ground-water samples were near equilibrium to slightly undersaturated with respect to calcite; all other phases of interest were undersaturated (aragonite, dolomite, gypsum and fluorite). The pCO_2 was supersaturated. Gypsum is undersaturated in all samples in both irrigation and ground water, thus to be thermodynamically consistent, in the NETPATH solutions, gypsum must be dissolving. As visible in Figure 7.6, gypsum was computed to be undergoing dissolution in all four models (i.e. gypsum had a positive value in the models). Dolomite was always undersaturated in the ground waters. Therefore, the models should have dolomite dissolving. As shown in Figure 7.6, dolomite was positive in all models indicating dissolution. On the other hand, calcite reactions cannot be defined based solely on saturation. Calcite was oversaturated in irrigation samples but at equilibrium or undersaturated in ground water samples.

NETPATH offers no basis for discriminating between input phases or models. NETPATH presents all possible combinations of phases that mathematically meet the given constraints; it is the user who must evaluate each model. The four models presented cannot be narrowed to a smaller number based on saturation index alone. Further information about the system was necessary to interpret the NETPATH results.

Table 7.4. NETPATH model output: saturation index (SI), samples May 15, 2005.

Phases	Irrigation Water Saturation Index	Groundwater Saturation Index
GYPSUM	-1.7	-1.2
DOLOMITE	0.57	-0.53
CALCITE	0.57	-0.039
CO_2 GAS	-3.1	-1.4

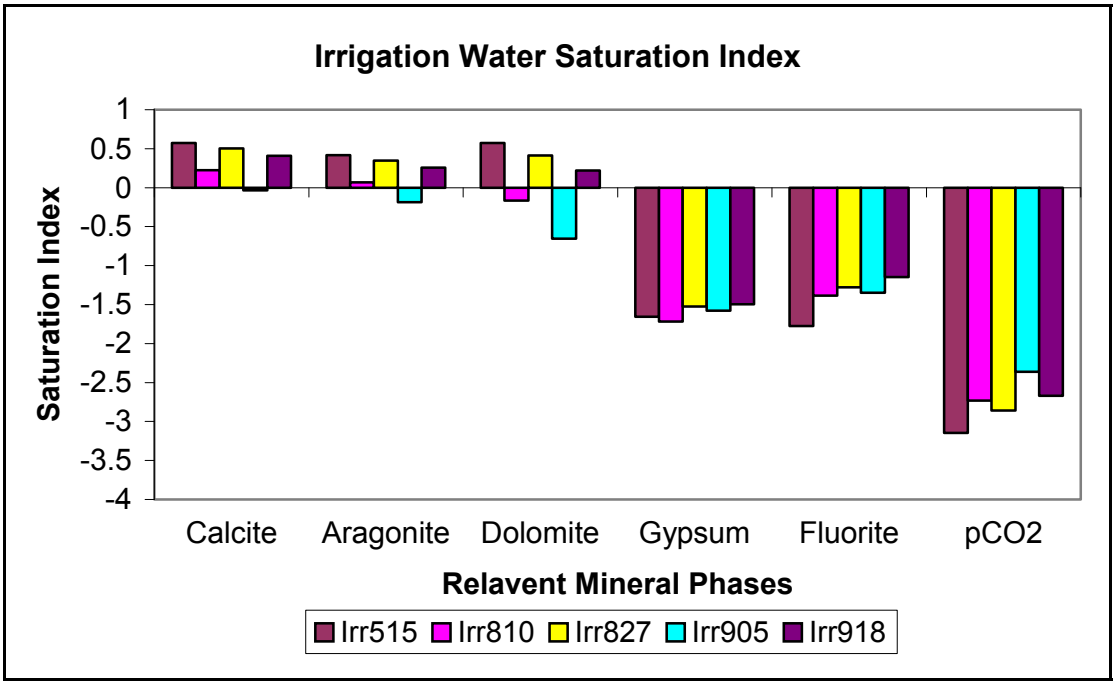

Figure 7.7. Solubility indices (SI) for relevant minerals in all irrigation water samples. Positive SI indicates the water is oversaturated for that mineral, negative SI refers to waters that are undersaturated.

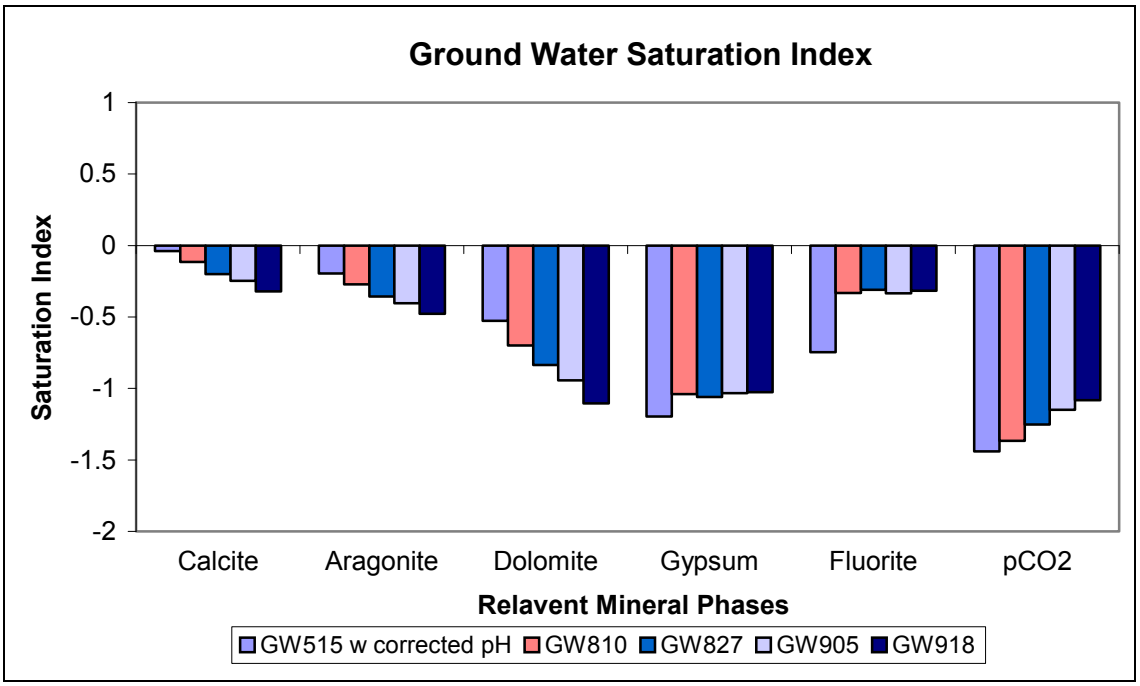

Figure 7.8. Solubility indices (SI) for relevant minerals in ground water samples. Positive SI indicates the water is oversaturated for that mineral, negative SI refers to waters that are undersaturated.

7.6 Supplemental Data

Additional data necessary to understand the geochemistry of the Lemitar site include confirmation of the mineral phases present in the soil, saturation indices, and cation-exchange properties. The following sections will discuss each of these interpretive datasets in detail. Chemical reaction mechanisms such as the process of dedolomitization were also investigated. Two soil analyses were completed to quantitatively assess the minerals present. Soil analysis also yielded important evidence to support the dedolomitization mechanism. A third analysis of the soil phases focused on ion exchange. The following sections will describe these analyses, results, and their implications for understanding mass transfer reactions identified by NETPATH.

7.6.1 Soil Analysis

In order to narrow the 4 NETPATH results to the most probable reaction scenario, a soil analysis was performed. Three boreholes were dug and a total of fifteen soil samples were collected. The borehole locations can be viewed in Figure 7.9. The borings were completed with a hand auger on June 1, 2006. Each boring contained alternating layers of sand and clay. A total of fifteen soil samples were collected at the interface between each soil type. Table 7.5 describes the soil samples.

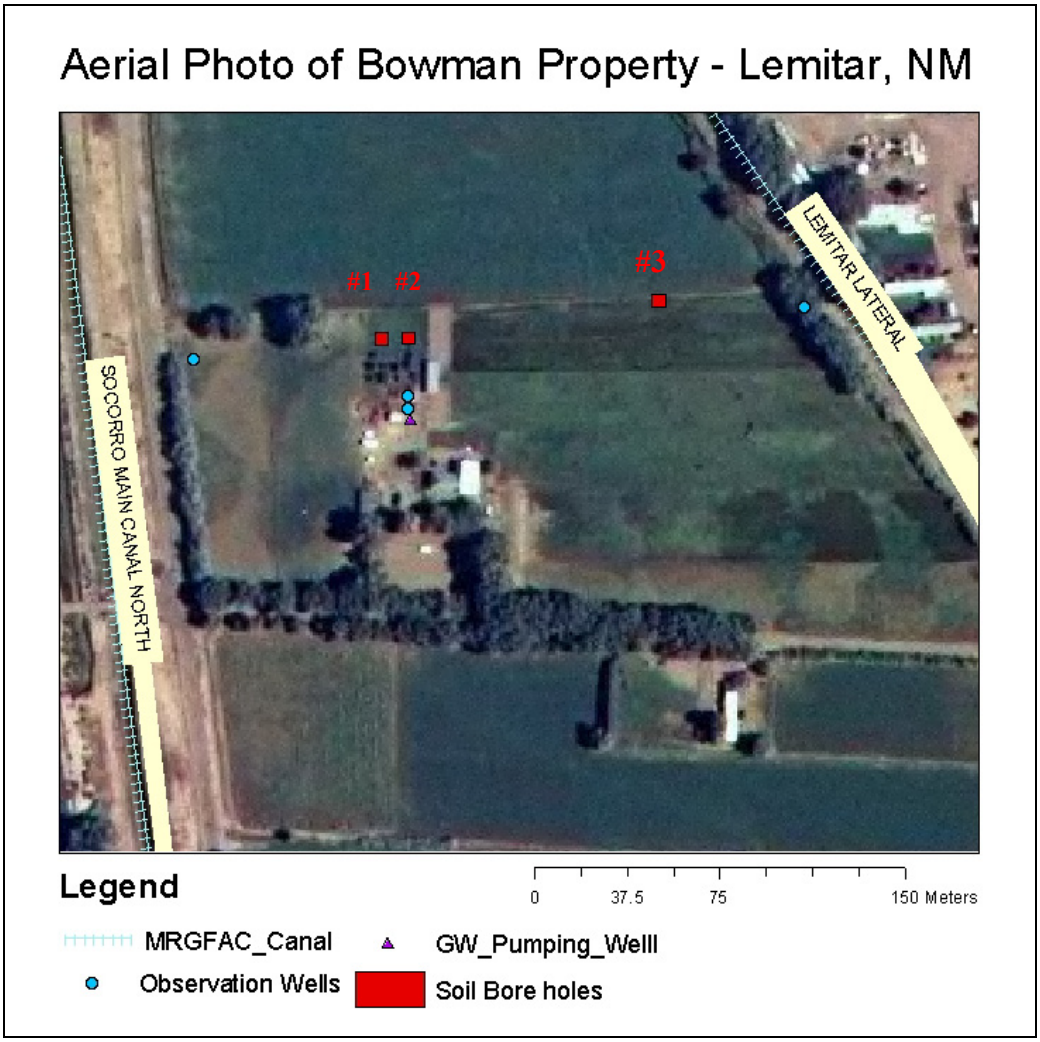

Figure 7.9. Aerial map of Lemitar site. Sample locations not to scale, only to illustrate relative locations of soil borings and piezometer locations. Soil samples were collected on June 1, 2006. Boreholes are numbered from west to east, with borehole 3 closest to the Lemitar Lateral (right side of the photo).

Table 7.5. Lemitar site soil profile.

Depth below Ground Surface (ft)	Borehole 1	Borehole 2	Borehole 3
1	Clay (E1-1)	Clay (E2-1)	
2			Sand (E3-2)
3	Sand (E1-3)	Sand (E2-3)	
4			Sand (E3-4)
5	Sand/Clay (E1-5)		
6			
7		Sand/Clay (E2-7)	
8	Clay (E1-8)		Sand (E3-8)
9	Black Clay (E1-9)	Clay/Sand (E2-9)	
10	Sand (E1-10)	Clay (E2-10)	
11 (~water table)		Black Clay (E2-11)	

Note: The parenthetical information is sample id numbers, the letter refers to the project, the first number indicates the borehole location and the second numbers indicates the depth of the soil sample.

7.6.1.1 Acid Dissolution

Each soil sample was analyzed by a carbonate release-and-capture method using a laboratory apparatus called Chittick. The method uses hydrochloric acid to dissolve the mineral carbonates, which causes release of carbon dioxide gas. The carbon dioxide gas is captured, measured and used to calculate the amount of carbonate present in the sample. The method is detailed in *Machette* [1986]. Analyses of the soils suggest that dolomite is likely present and confirm the presence of calcite. The quantity of calcium carbonate varied among the soil layers from approximately 0.4% (E2-10) to 9% (E1-9), whereas dolomite (if present) made up closer to 0.2%. The percentage of calcium and magnesium carbonate contained in each soil sample is shown in Table 7.6. These results were obtained based on the procedure previously mentioned, however, the validity of the magnesium carbonate analysis was questionable. The amount of magnesium carbonate was measured by the additional amount of carbon dioxide gas released after all the calcium carbonate had dissolved. During the procedure it was difficult to assess whether late-released carbon dioxide was from dissolution of magnesium carbonate or if it was

residual calcium carbonate. Part of this uncertainty might have been caused by the soil-sample grain size. Some of the soil was left coarser than the procedure recommends. A coarser sample might prevent the acid from reaching all of the calcium carbonate, thus allowing some calcium carbonate to be present during the dissolution of magnesium carbonate. Consequently, an additional analysis was completed to test these results.

Table 7.6. Percent carbonate (calcium, magnesium) calculated by a release and capture method using Chittick apparatus.

Sample ID	CaCO3 %	MgCO3 %
E1-1	3.4%	0.19%
E1-3	0.7%	<0.001
E1-5	1.8%	0.06%
E1-8	7.1%	0.36%
E1-9	8.9%	0.04%
E1-10	0.4%	0.07%
E2-1	1.8%	0.07%
E2-3	1.3%	0.04%
E2-7	1.8%	<0.001
E2-9	5.4%	0.20%
E2-10	0.4%	<0.001
E2-11	4.2%	0.20%
E3-2	5.7%	0.08%
E3-4	1.7%	<0.001
E3-8	3.5%	<0.001

7.6.1.2 Electron Microprobe Analysis

An electron microprobe analysis was performed on a few of the soil samples in order to affirm the results from the laboratory carbonate release-and-capture method. The following samples were made into thin sections (sent to National Petrographic Lab) and analyzed with a Cameca S x100 Electron Probe Microanalyzer: E1-1, E1-3, E1-8, E1-10, E2-7 and E2-11. This set of soil samples contained high percentages of calcium carbonate and magnesium carbonate based on the carbonate release-and-capture analysis. Two

electron microprobe analyses were completed. The first method (which is called image analysis) allowed the user to scan the thin section sample by hand. The user was able to visually identify grains by scanning for high calcium (or magnesium), low silica and low iron grains. Figures 7.10 and 7.11 show images of the grains analyzed by this method. Visual analysis of certain grains suggested that some of the minerals exhibit signs of dissolution, called dissolution veins (Figure 7.11). Dissolution may or may not have occurred in-situ. The calcite and dolomite grains appear to be weathered (rounded grains) and most likely detrital (physically weathered material probably transported by the Rio Grande). The additional analysis, conducted on the electron microprobe, is an elemental analysis, which located all areas containing a particular element. Results from one of the elemental analyses are shown in Figure 7.12. Areas containing calcium are shown in red, areas with magnesium are in blue, and purple areas highlight grains where both Ca and Mg are present. Beside carbonate minerals, silicate minerals such as feldspars were also common in the soil samples. However, for the purpose of this project, minerals containing small amounts of magnesium, calcium and/or high amounts of silica were ignored. These two electron microprobe analyses were used collectively to identify mineral grains of calcite and dolomite. Many grains in each of the samples were identified as calcite and dolomite. Figure 7.11 provides a visual comparison of calcite (red) and dolomite (purple) grains to all other minerals (the black section). Visually estimated from Figure 7.11, the relative abundance of these minerals parallels the Chittick results, where calcite ranges from 1-10% and dolomite ranges from 0.01-0.5%.

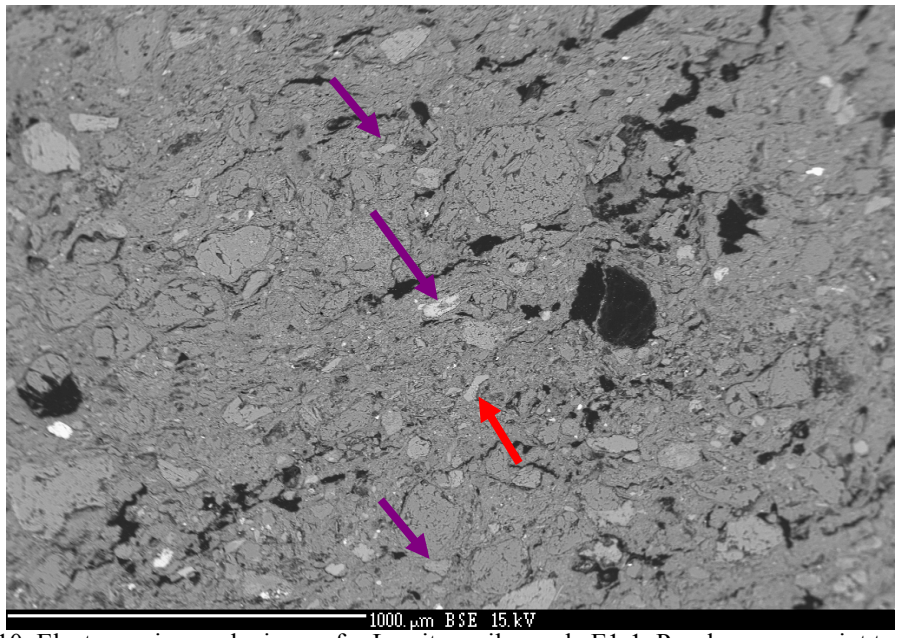

Figure 7.10. Electron microprobe image for Lemitar soil sample E1-1. Purple arrows point to dolomite grains and red arrows point to calcite grains.

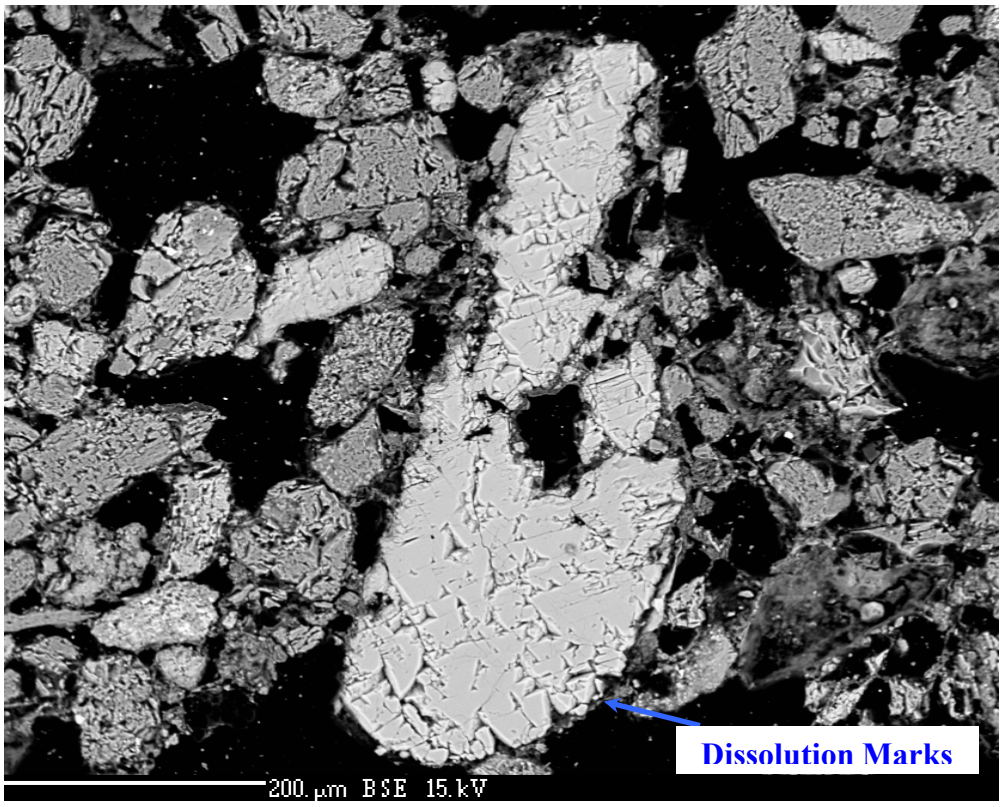

Figure 7.11. Electron microprobe image from sample E1-8. Blue arrow indicates points, which resemble dissolution veins on a calcite grain.

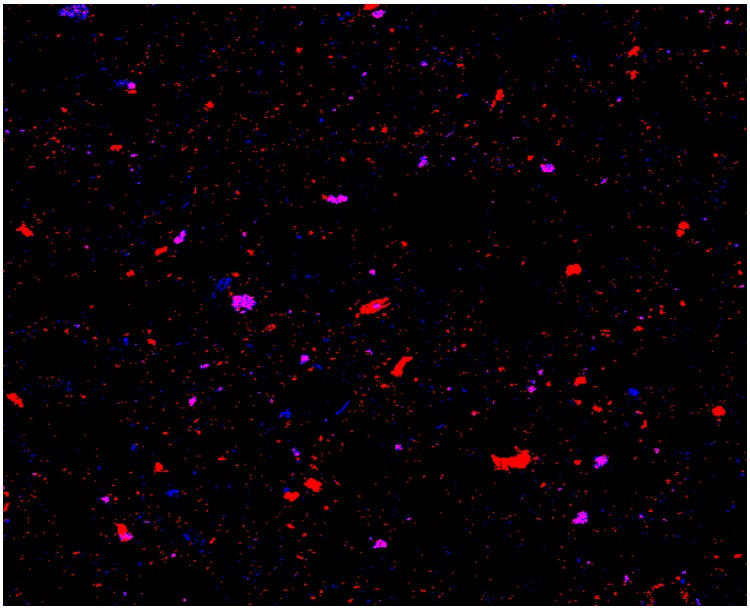

Figure 7.12. Electron microprobe element analysis for sample E1-1. Purple spots indicate areas with both magnesium and calcium, red spots are areas with high calcium, and blue spots are areas with magnesium. [Note: Same thin section view and area as Figure 7.11.]

The electron microprobe analysis suggested that calcite and dolomite were present in the soil. Utilizing this knowledge the NETPATH model results were narrowed. Since the soil contains calcite and dolomite, these phases must be present in the NETPATH model. Of the four possible models only models 1 and 2 have both calcite and dolomite, which means models 3 and 4 are probably not applicable (see Figure 7.6 for all 4 possible and Figure 7.13 for remaining models).

MODEL 1		MODEL 2	
CALCITE	0.016	CALCITE	-0.41
GYPSUM	0.30	GYPSUM	0.30
DOLOMITE	0.49	DOLOMITE	0.71
CO2 GAS	2.8	CO2 GAS	2.8
EXCHANGE	0.21	Mg/Na EX	0.21
Evaporation factor:	1.5	Evaporation factor:	1.5
656g H2O remain		656g H2O remain	

Figure 7.13. Narrowed NETPATH model results for the Lemitar site samples from May 2005. Remaining plausible models based on the criteria that both calcite and dolomite are present in soil.

7.6.1.3 Dedolomitization Evidence

In addition to supporting the presence of calcite and dolomite, the electron microprobe analysis also suggests dedolomitization as a major subsurface process in this system. Dedolomitization is a process where dolomite dissolves incongruently and calcite precipitates in its place. The term "dedolomite" was first used by von Morlot (1847), who recognized the replacement of calcite for dolomite during near-surface chemical reactions. The modern mechanistic understanding comes from laboratory, field and theoretical investigations mainly conducted in the 1970's and 1980's [*Plummer and Back*, 1981]. As currently understood, the mechanism begins with a solution supersaturated with respect to calcite flowing through an aquifer containing gypsum and dolomite (stoichiometric reactions: Equations 7.4 and 7.5). The solution is undersaturated with respect to gypsum and dolomite, thus both minerals undergo dissolution. The dissolution of these minerals release calcium ions to the solution (Equations 7.4 and 7.5, summary reaction in Equation 7.6). Gypsum remains undersaturated throughout the process and continues to dissolve, which leads to the continued saturation or supersaturation of calcite. With a sufficient carbonate supply (in this case from soil gas CO_2), the supersaturated calcite precipitates. Calcite formation removes bicarbonate from the solution, thereby decreasing the partial pressure of carbon dioxide (pCO_2) and enhancing the solubility of dolomite [*Back et al*, 1983].

Dissolution Equations:

Gypsum: $CaSO_4 \bullet 2H_2O \rightarrow Ca^{2+} + SO_4^{2-} + 2H_2O$ [Equation 7.4]

Dolomite: $2H_2CO_3 + CaMg(CO_3)_2 \rightarrow Ca^{2+} + Mg^{2+} + 4HCO_3^-$ [Equation 7.5]

Dedolomitization Reaction: [Equation 7.6

Dissolution of Gypsum and Dolomite $\rightarrow$ Precipitation of Calcite

$$2H_2CO_3 + CaSO_4 + CaMg\left(CO_3\right)_2 \rightarrow 2Ca^{2+} + SO_4^{2-} + Mg^{2+} + 4HCO_3^-$$
$$\rightarrow 2CaCO_3 + SO_4^{2-} + Mg^{2+} + 2H_2CO_3$$

Evidence for dedolomitization can be found in the soil and water chemistry at the Lemitar site. The electron microprobe image in Figure 7.14 captures a mineral grain undergoing dedolomitization. The illustrated grain is sample E1-1, which was collected from soil boring 1 at a depth of one foot below the ground surface. The red and purple arrows indicate portions of the grain that are calcite or dolomite respectively. For reference, the surrounding matrix is small feldspar fragments and epoxy. As the outer dolomite dissolves, calcite co-precipitates in its place on the edge of the grain. Dedolomitization could occur in the soil on the Lemitar site or may have been transported through historical Rio Grande flood deposition. The dissolution marks, the presence of other dedolomitized grains, and the fragile condition of the grain all support in situ dedolomitization rather than transportation of dedolomitized grains from elsewhere.

Saturation indices also indicated dedolomitization as a likely process. Recall from Table 7.4 and Figures 7.7 and 7.8 that gypsum is undersaturated in both irrigation and ground water, whereas dolomite is undersaturated in ground water and calcite is oversaturated in irrigation water but undersaturated in ground water. Based on the observed dedolomitization, one might expect calcite to be oversaturated indicating precipitation was likely. However, as previously discussed, calcite precipitation from dedolomitization depends on the availability of carbonate. Near the

soil surface, plant respiration and decaying organic matter supply carbon dioxide, such that mineral reactions have an abundant supply of carbonate. In contrast, as the irrigation water percolates further into the aquifer, available carbonate is removed by calcite precipitation.

Variations in chemical composition also contribute support to the hypothesis that dedolomitization occurs in the Lemitar subsurface. General chemistry data presented in Figure 7.5 (predicted ground water to measured ground water) and Figure 7.15 show higher concentrations of sulfate and magnesium, as well as increased pCO_2 and lower pH in the ground water. *Back et. al*. [1983] discuss the importance of the Mg/Ca ratio. For a 25 degree Celsius ground water that is in equilibrium with calcite and dolomite, the Mg/Ca ratio is equal to 1. At magnesium:calcium ratios greater than 1, dolomite can form; at lower ratios dissolution is observed [*Back et. al*., 1983]. The relative chemical percentages of anions and cations are presented in a trilinear diagram (Figure 7.15). The irrigation water samples from May through September are symbolized with red circles, the ground-water samples with green squares. The representative sample pair from May 15th, 2005 is depicted with a purple triangle (irrigation water) and a blue cross (ground water). Best visualized from the cation triangle of the trilinear diagram, the solution mixture increased in magnesium at a greater rate than calcium as water traveled from irrigation to ground water. The collected samples had a Mg/Ca ratio below 1; see the cation section of Figure 7.15. In a system dominated by dedolomitization, concentrations of magnesium and sulfate would increase, while bicarbonate and calcium would decrease or remain constant. The collected field data

illustrate this trend, although the constituent concentrations show some deviation where bicarbonate and calcium also increased from irrigation water to ground water. This deviation is likely due to the fact that irrigation and ground water samples are end-members along this flow path. Data does not exist in the vadose zone between the surface (where irrigation water enters, 0 meters) and the ground water (below the water table, 12.2 meters). Various degrees of dedolomitization may occur at intermediate depths. Assuming dedolomitization would be captured in the irrigation-to-ground water modeling, the NETPATH results contained in Figures 7.6 (all four models) and 7.13 (soils analysis narrowed, 2 models) can be summarized. NETPATH model 2 is the only model where calcite precipitated and thus the most plausible (Figure 7.17, model 2). Model 2 unites the formation of calcite, the dissolution of dolomite and gypsum with Mg/Na ion exchange reactions where carbon dioxide is available.

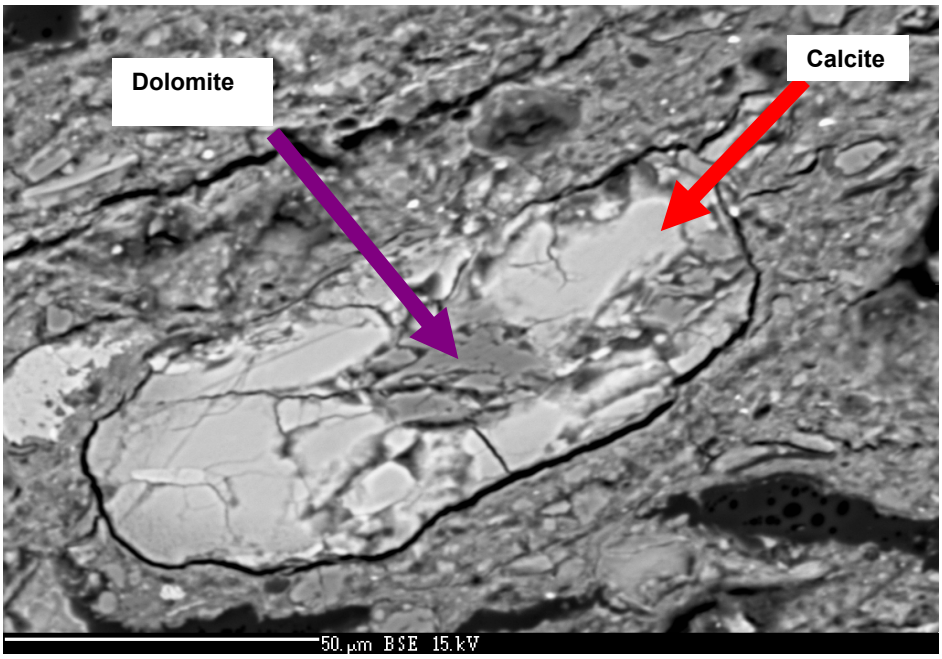

Figure 7.14. Electron microprobe image from sample E1-1, grain showing dedolomitization. Purple arrows point to dolomite grains and red arrows point to calcite grains.

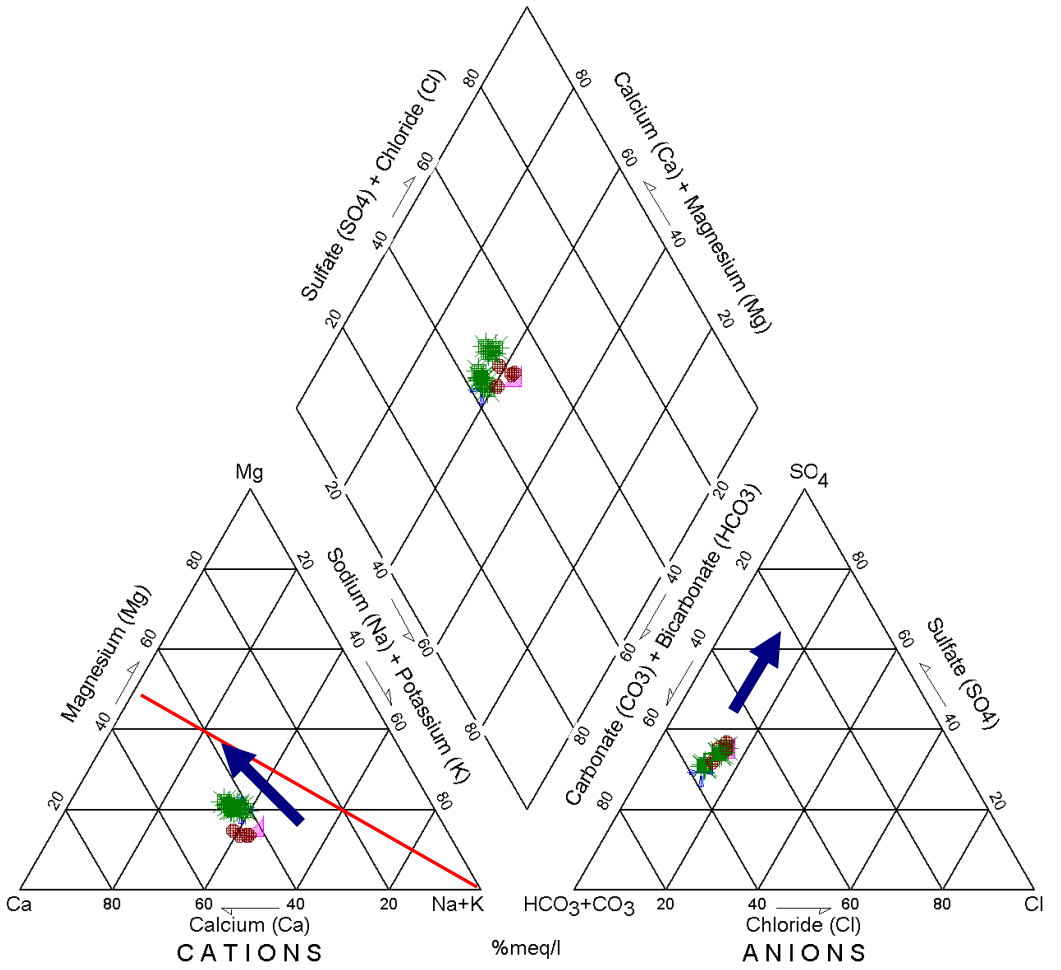

Figure 7.15. Piper diagram of irrigation and ground water samples from Lemitar site, May – September. Green squares = ground water, red circles = irrigation water, purple triangle = irrigation water May 15, blue cross = ground water May 15th. Red line represents the 1:1 Ca:Mg ratio and the blue arrows illustrate the direction of dedolomitization

7.6.1.4 Ion Exchange Reactions

The evidence presented thus far illustrates a clear argument for surface dedolomitization. Dedolomitization is a major process affecting the chemistry of irrigation water at the Lemitar property. However, dedolomitization was not the only process that affected the chemical changes observed in this system (based on Figure

7.15). The remaining NETPATH models (Figure 7.13) also include ion exchange. The following section will discuss the possibility of ion exchange processes and decipher the most likely ion exchange reaction: magnesium for sodium exchange as compared to calcium for sodium exchange.

Ion exchange data was measured for several of the soil samples at one borehole location. Five soil samples from borehole 1 (see aerial photographic, Figure 7.9) were sent to the Soil, Water and Air Testing Laboratory (SWAT) at New Mexico State University. The samples were analyzed for extractable cations (sodium, potassium, calcium and magnesium), saturated paste percent water, saturated paste extract (sodium, potassium, calcium and magnesium), and cation exchange capacity. The SWAT Lab used procedures from the National Laboratory Standard Methods [*USDA-SCS staff*, 1972], [*USDA staff*, 1954] and [*Agronomy Society of America*, 1965]. Soil data are presented in Tables 7.7, 7.8, and 7.9 along with a calculated value for the amount of exchangeable solutes. The exchangeable cation value represents the concentration of solute that was sorbed to the soil. The equivalents of soluble solute per unit volume of soil pore water are referred to as the saturated paste concentration. The extractable solute value is the combination of both soluble and exchangeable cations, in other words, the concentration of solute that was removed from the soil after saturating all ion exchange sites with ammonium acetate. Figure 7.16 is a schematic diagram of the extractable cation procedure. The saturated paste procedure was similar to Figure 7.16 except that water was added to saturate the field soil; the soil water was extracted and analyzed. Exchangeable ion concentrations were computed by subtracting the soluble cations from the extractable cations, thus leaving

the concentration of each solute that was adsorbed to the soil in the field. Analysis was also made of the cation-exchange capacity, which is the quantity of sites available for exchange. To determine the quality of the ion-exchange data, a comparison was made between the summations of the exchangeable cations and the cation exchange capacity. The summation of the exchangeable ions should be equal to the cation exchange capacity since both values measure the available sites held by cations Na, Ca, Mg. Table 7.10 illustrates that some of the data are suspect; samples E1-5 and possibly with E1-3 and E1-8 have excessively high percent differences of 177, 48 and 25% respectively. The percent difference was calculated assuming that the CEC was the correct value. One possible explanation for the discrepancy could stem from the analysis procedure. The ammonium acetate solution utilized in the saturated paste procedure has been documented to interfere with the extractable cation analysis through dissolution of carbonate minerals in the soil sample [*USDA-SCS Staff*, 1972; *USDA Staff*, 1954]. Since, an alternative procedure was not available, the data with reasonable reproduction (samples E1-1, E1-9, E1-3 and E1-8) were deemed acceptable.

Table 7.7. Lemitar site soil properties: extractable cations.

Sample ID	Sample Description	Sample Depth (ft)	Layer Thickness (ft)	Extractable Cations (meq/100g) Na	K	Ca	Mg	Sum
E1-1	clay	1	2	2.67	0.54	17.80	4.88	25.89
E1-3	sand	3	2	1.00	0.13	7.22	1.27	9.62
E1-5	sand/clay mix	5	3	0.16	0.10	5.99	0.51	6.76
E1-8	clay	8	1	0.60	0.38	11.60	2.87	15.45
E1-9	black clay	9	1	0.91	0.70	13.90	4.23	19.74

Note: Depths and descriptions are approximate, based on visual assessment

Table 7.8. Lemitar site soil properties: saturated paste percent and soluble concentration.

Sample ID	Sample Description	Sample Depth (ft)	Layer Thickness (ft)	Saturated paste percent (Volumetric %)	Saturated Paste Extract: soluble concentration (meq/L)			
					Na	K	Ca	Mg
E1-1	clay	1	2	64.42	17.70	0.19	7.89	2.81
E1-3	sand	3	2	20.67	28.50	0.27	15.60	6.49
E1-5	sand/clay mix	5	3	23.88	4.66	0.15	3.10	0.72
E1-8	clay	8	1	38.08	5.13	0.21	3.88	1.49
E1-9	black clay	9	1	50.75	5.57	0.31	4.08	1.87

Note: Depths and descriptions are approximate, based on visual assessment

Table 7.9. Lemitar site soil properties: exchangeable cations and cation exchange capacity (CEC).

Sample ID	Sample Description	Sample Depth (ft)	Layer Thickness (ft)	Exchangable Cations (meq/100g)				CEC (meq/100g)
				Na	K	Ca	Mg	
E1-1	clay	1	2	1.53	0.53	17.29	4.70	24.80
E1-3	sand	3	2	0.41	0.12	6.90	1.14	5.78
E1-5	sand/clay mix	5	3	0.05	0.10	5.92	0.49	2.36
E1-8	clay	8	1	0.40	0.37	11.45	2.81	12.02
E1-9	black clay	9	1	0.63	0.68	13.69	4.14	20.60

Note: Depths and descriptions are approximate, based on visual assessment

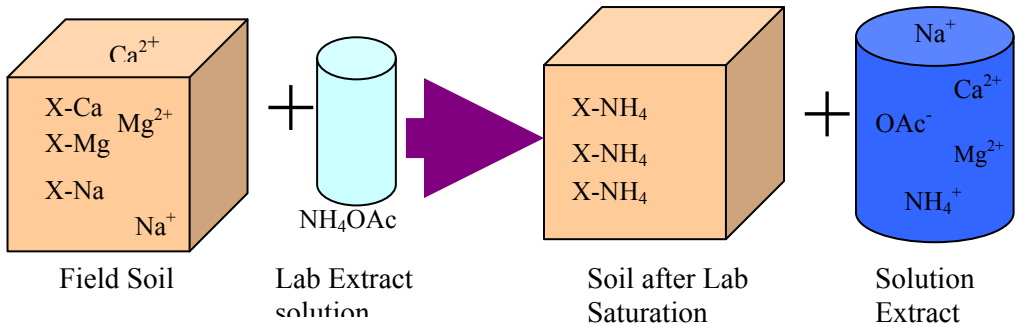

Figure 7.16. Extractable cation schematic of procedure.

Table 7.10. Lemitar site soil analysis data quality assessment: comparing CEC to exchangeable summation.

Sample ID	Sample Description	Sample Depth (ft)	Exchangeable Cation Total (meq/100g)	CEC (meq/100g)	% Difference
E1-1	clay	1	24.05	24.80	-3.03
E1-3	sand	3	8.57	5.78	48.3
E1-5	sand/clay mix	5	6.55	2.36	178
E1-8	clay	8	15.04	12.02	25.1
E1-9	black clay	9	19.14	20.60	-7.09

Note: The percent difference = (Exchangeable – CEC)/CEC, assuming that the CEC is a more reliable analysis.

In order to evaluate the likelihood of the two probable exchange reactions, a selectivity coefficient was calculated for each (recall the NETPATH models use Ca/Na and Mg/Na exchange). The Vaneslow Selectivity Coefficient is a conditional equilibrium constant that describes which of the ions will undergo exchange in the system based on properties of the soil and the solution; see Equation 7.7. The Vaneslow Selectivity was calculated for magnesium/sodium and calcium/sodium exchange, written as $k_v(C_{Mg^{2+}} - C_{Na^+})$ and $k_v(C_{Ca^{2+}} - C_{Na^+})$, for each of the five samples: E1-1, E1-3, E1-5, E1-8 and E1-9. The ion activity for each sample was based on the ionic strength of the pore-water solution, in which the cation concentration was taken from the saturated paste laboratory reported results and each anion concentration was estimated from an average of anion percentages in all the irrigation and groundwater samples. The mole fraction is the number of available sites for a particular cation (exchangeable cation value) compared to the total number of available sites (cation-exchange capacity) in a given soil sample. The selectivity results are presented in Table 7.11, where a higher k_v indicates a greater affinity for exchange with that ion pair. The soils collected from the Lemitar site all favor the ion

exchange reaction of calcium for sodium as compared to magnesium for sodium. The Kv calculations seem to suggest that calcium is most likely to be adsorbed while sodium is released and thus the NETPATH model should include Ca/Na exchange rather than Mg/Na exchange. However, the selectivity coefficient does not account for changing pore water concentrations with depth; recall that due to lack of data the anion concentration in the pore water is one composite value used at all depths. Further soil exchange analysis with depth is required.

$$k_v(C_2 - C_1) = \frac{\left[\gamma_{C_1} * m_{C_1}\right] * \bar{X}_{C_2}}{\left[\gamma_{C_2} * m_{C_2}\right] * \bar{X}_{C_1}} \qquad \text{[Equation 7.7]}$$

where k_v is the Vaneslow Selectivity Coefficient, C_1 and C_2 are the ions involved in exchange, γ is the activity for the respective ion, m is the molality (moles/kg) for the respective ion and $\bar{X}$ is the mole fraction of ion adsorbed to the soil.

Table 7.11. Vaneslow selectivity coefficient for soil from Lemitar, NM.

Sample ID	kv (Ca-Na)	kv (Mg-Na)
E1-1	37	26
E1-3	32	12
E1-5	40	14
E1-8	5.2	3.3
E1-9	8.0	5.2

The adsorbed fraction (Table 7.12) should match the cation-exchange reaction direction. For example, NETPATH model 2 calculated Mg/Na exchange such that sodium was released to the solution. Thus, the adsorbed fraction of sodium would decrease as the magnesium adsorption ratio increased with depth. The data exhibits a messy trend, but ignoring the E1-5 data, the result shows that, as expected, sodium decreased with depth as the magnesium increased with depth. Calcium and potassium adsorption ratios also increased with depth, although not as quickly as the

magnesium. The fact that the absorption ratio of magnesium increased more than calcium and potassium, suggested that magnesium exchanges more readily with sodium than the other two cations. Thus, the adsorbed-fraction data corroborate NETPATH model 2 from Figure 7.13.

Table 7.12. Adsorbed fraction of solute for soil from Lemitar, NM.

Sample ID	Na	K	Ca	Mg
E1-1	0.079	0.027	0.89	0.24
E1-3	0.055	0.017	0.93	0.15
E1-5	0.0080	0.016	0.98	0.081
E1-8	0.033	0.030	0.94	0.23
E1-9	0.042	0.046	0.91	0.28

Note: Adsorbed fraction is the fraction of exchangeable cations divided by the total sorbed cations.

7.7 Lemitar Geochemical Modeling Conclusions

In conclusion, the NETPATH results, combined with independent data, support a single model, which encompassed each of the significant reactions that occurred in this system. The most plausible NETPATH model must contain precipitation of calcite (from dedolomitization), magnesium-for-sodium exchange (ion exchange adsorbed fraction data), evaporation, and a high partial pressure of carbon dioxide (closed system - dedolomitization). NETPATH model 2 (Figure 7.17) represents all of these reaction processes. Results for the other irrigation and ground water samples are presented in Figure 7.18. Each irrigation and ground water sample set yields results with some variation in the chemical reactions that were calculated, however in general most of the sample pairs corroborate the results from the representative samples from May 2005.

MODEL 2

CALCITE	-0.41
GYPSUM	0.30
DOLOMITE	0.71
CO2 GAS	2.8
Mg/Na EX	0.21

Evaporation factor: 1.5 656g H2O remain

Figure 7.17. Most plausiable NETPATH model result for the Lemitar site samples from May 2005. Final remaining model based on the criteria that both calcite and dolomite are present in the soil; dedolomitization must be represented by calcite formation and magnesium for sodium ion exchange.

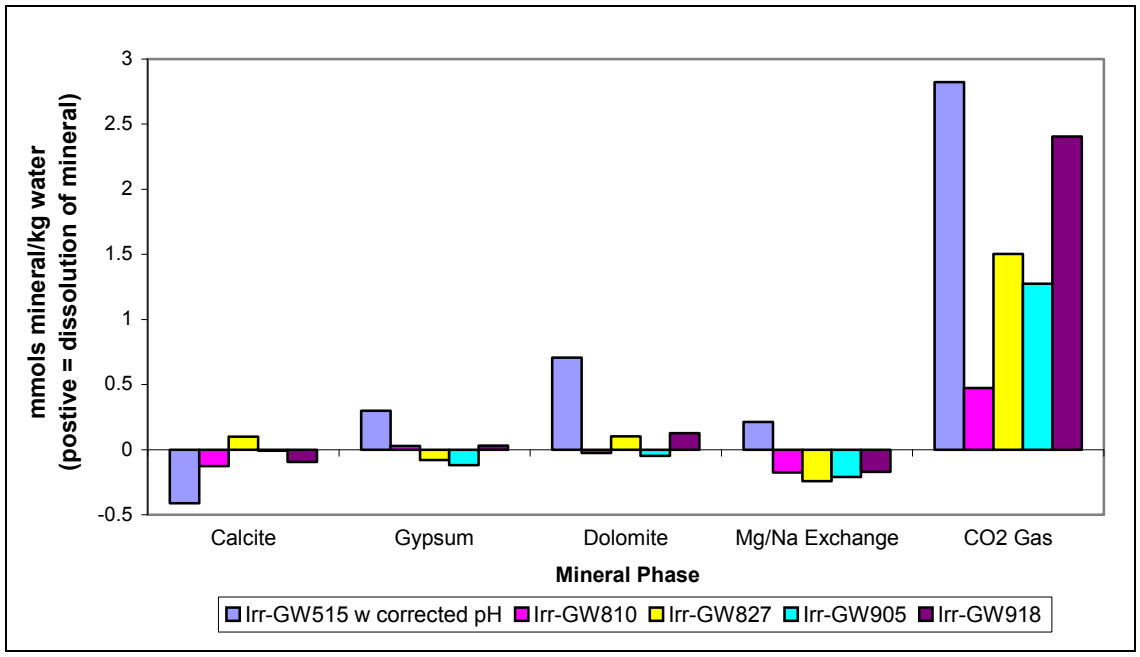

Figure 7.18. NETPATH results for all Irrigation to ground water sample pairs. Irr-GW515 refers to the model for irrigation and ground water sample collected on May 15th 2005. Note: for May sample pairs the number indicates the date the ground water sample was collected, all May models use one irrigation water sample collected on May 15th 2005.

7.8 Implications for Rio Grande (i.e. Solute Burdens)

Lemitar modeling thus far illustrates relevant subsurface reaction mechanisms, which affect the chemistry of the irrigation water as it percolates through soil. This section will provide evidence that the Lemitar site indeed replicates the same reactions that occur through the Rio Grande Basin. To this end, a water and solute budget were complied for both the Lemitar farm and the river reach in which it

resides; the San Acacia to San Marcial reach. The water and solute budgets from the Lemitar site are compared to that of the SA-SM reach.

7.8.1 Water Balance Comparison, Lemitar to Socorro County

The water budget is calculated to assess the amount of water that infiltrates into the soil capturing only the water that is capable of facilitating mineral phase reactions. An estimate of applied irrigation water quantity and the number of acres irrigated for the year 2005 has been compiled from the personal records of Robert Bowman (Lemitar site) and *Longworth et. al* [2008]. Data from Socorro County was divided in half (to better estimate irrigated acreage in the San Acacia-to-San Marcial river reach) and utilized in-lieu of direct acreage data from San Acacia to San Marcial. Applied irrigated acres from Socorro County are the number of acres irrigated with surface water found in State Engineer report 51 [*Wilson*, 2003]. All required data for the water balance are presented in Table 7.13 as applied irrigation amount normalized to area, such that the two datasets can be readily compared. The irrigated acres are the acres within Socorro County irrigated from surface water only in 1999. The data from 1999 was utilized as an estimate of the average acreages irrigated in the 1980's. The Office of the State Engineer reported data from 1985, but noted that the 1985 acreage was much lower than other years in the 1980's due to higher-than-normal rainfall and flooding in some areas [*Wilson*, *1986*]. The difference in irrigated acres was about 1,000 acres; 11,242 acres in 1985 compared to 11045 in 1999 and 12,427 acres in 2005. The application quantity and the evaporative quantity

were confirmed through personal communication with Michael Shivers, a USDA District Conservationist.

Table 7.13 Water balance comparison between Lemitar and Socorro County.

	Lemitar Site	½ Socorro County MRGCD only
Irrigated Area (m2)	3.2E+04	2.2E+07
Applied to farms (m3/yr)	3.4E+04	3.8E+07
Qapplied (m/yr)	1.07	1.51
Qevap (m/yr)	0.37	0.85
Qeff (m/yr)	0.70	0.85

From Table 7.13, *Qapplied* refers to the amount of water diverted from the canal and applied to the field. *Qevap* is the amount of water lost to evaporation and transpiration. Finally, *Qeff* is the quantity of irrigation water that infiltrates into the soil, which is calculated as *Qapplied* - *Qevap*. The evapotransporation rate was computed based on the difference in chloride concentration between irrigation and ground water samples from May 2005 at the Lemitar site. The ET based on chloride difference is 34% of the applied water (this includes water taken-up for beneficial use by the crop). An ET rate of 34% at the Lemitar site works out to a 0.37m/yr ET rate. ET for the rest of the region was estimated based on the ET from a medium-quality cool season blue grass. A rate of 0.85 m per year was calculated with a modified Penman-Monteith equation using climate data from the Lemitar Nature Center. A detailed description for the NMSU ET equation can be found at http://weather.nmsu.edu/pmcomp.htm [*NMSU website, 2008*]. Uncertainty bounds are estimated for the ET based on various crops ET calculated from the NMSU equation. ET varies by about 0.4 m; a grass field produces an ET of 0.85 m/yr to an alfalfa which produces an ET of 1.28 m/yr. The ET rate computed for the Lemitar site (34%

based on chloride differences) is much lower than the expected ET for the rest of the river reach (56% based on the NMSU website and personal communication with Michael Shivers, a USDA District Conservationist). From Table 7.13, the Lemitar site received less irrigation water than the average applied to farmland in Socorro County. According to the data, approximately 0.7 m of water infiltrate into the subsurface on the Lemitar site whereas 0.85 m on average infiltrate in Socorro County. The water fluxes from Lemitar and Socorro County were multiplied by their respective solute concentrations to calculate the solute burden that enters the river.

7.8.2 Solute Budget Comparison, Lemitar to Socorro County

The solute budget reveals the quantity of solute that reaches the river each year due to irrigation practices. Chemical load differences between the predicted ground water concentration (the concentration in Q_{eff}, see Figure 7.5) and the ground water at the Lemitar site were compared to the load difference between the calculated solute load at San Acacia (San Acacia+, for details on San Acacia+ calculation see Chapter 8) and the observed load at San Marcial. Figure 7.19 illustrates the amount of solutes per acre that enter the river each year from mineral interactions. The numerical solute amounts are presented in Table 7.14. As compared to the Lemitar site data, the San Acacia-to-San Marcial reach data show that slightly greater quantities of solutes are sent to the Rio Grande per acre. In-as-much as the Lemitar site applies less water, there is a higher percentage of evaporation and thus the Q_{eff} or pore water has a higher concentration of solutes than in the average from Socorro County. Pore water with a higher concentration of solutes dissolves fewer minerals. Also notice the Lemitar site accumulates bicarbonate while the SA-SM reach loses it

significantly. The bicarbonate phase variation is likely due to the degassing of the large partial pressure of CO_2 contained in the ground water. Other than the mentioned deviations, the Lemitar data and the San Acacia+ and San Marcial chemistry match well in the direction and quantity of solute mass from interactions with minerals. This suggests that the subsurface reaction mechanisms observed at the Lemitar site also occur throughout the basin from San Acacia to San Marcial.

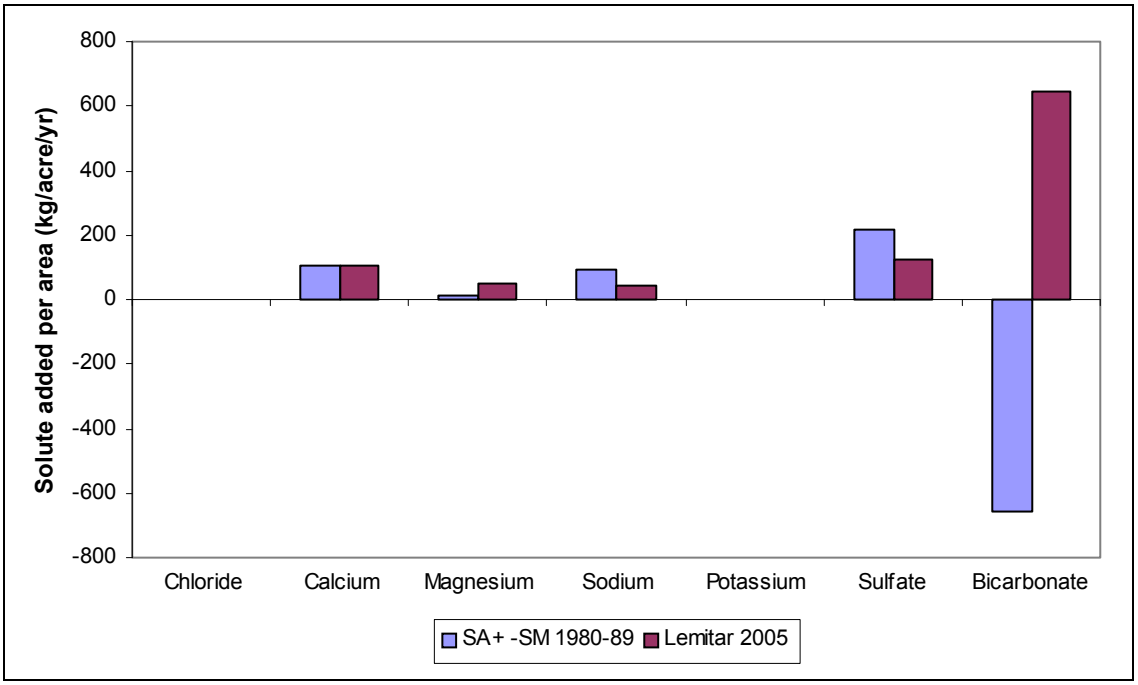

Figure 7.19. Solute added to Rio Grande from Lemitar (red bars) and SA+-SM irrigation.

Table 7.14. Solute added to Rio Grande from irrigation diversion in Lemitar and in the San Acacia to San Marcial.

	SA+ -SM 1980-1989	Lemitar 2005
Chloride	0	0
Calcium	103	103
Magnesium	13	52
Sodium	92	42
Potassium	0.6	1.5
Sulfate	219	123
Bicarbonate	-655	647

Note: Units = kilogram/acre/year.

7.8.3 NETPATH Modeling Comparision, Upscaling Lemitar to RG Reach

NETPATH was utilized further to model subsurface reactions for the reach from San Acacia to San Marcial. The 1980's chemical record is the most complete for all river reaches, such that only data from the 1980's was modeled. The chemistry data for San Acacia+ and San Marcial were input into NETPATH. Model constraints and chemistry are presented in Table 7.15. The phases included in the SA-SM model differ slightly from those phases presented in the Lemitar model. Calcite, dolomite, gypsum, and carbon dioxide remain consistent but the SA+ - SM model included a generic plagioclase mineral ($Ca_{0.38}$ $Na_{0.62}Al_{1.38}Si_{2.63}O_8$) and accounted for clay material with calcium montorillonite and kaolinite instead of ion exchange. The plagioclase and clay material phase additions were added to account for the variable reaction pathways in this much larger modeled area. In the Lemitar model, the soil was contained in a small area that had been used for farmland since the 1850's. The SA-SM reach consists of an area where entering water might flow through a number of pathways before exiting at San Marcial. Moreover, the modeling required a limited number of phases in order to achieve a manageable number of output results. NETPATH found four possible models (Figure 7.20) that satisfy the constraints with the given phases.

Table 7.15. NETPATH constraints for SA+ - SM, (mmols/kg water).

Constraints	Initial	Final
Carbon	2.5	2.3
Calcium	1.2	1.2
Magnesium	0.35	0.36
Sodium	2.0	2.1
Chloride	0.76	0.76
Sulfur	0.97	1.0
Silica	0.37	0.37

MODEL 1	
KAOLINIT	-0.18
CO2 GAS	-0.20
CALCITE	-0.059
GYPSUM	0.050
DOLOMITE	0.012
PLAGAN38 +	0.14
Evaporation factor:	1.0
1kg H2O remain	

MODEL 3	
KAOLINIT	-2.4
CALCITE	-0.26
Ca-MONT	1.2
GYPSUM	0.050
DOLOMITE	0.012
PLAGAN38 +	0.14
Dilution factor:	1.0
1kg H2O remain	

MODEL 2	
KAOLINIT	0.46
CO2 GAS	-0.26
Ca-MONT	-0.35
GYPSUM	0.050
DOLOMITE	0.012
PLAGAN38 +	0.14
Dilution factor:	1.0
1 kg H2O remain	

MODEL 4	
CO2 GAS	-0.22
CALCITE	-0.042
Ca-MONT	-0.10
GYPSUM	0.050
DOLOMITE	0.012
PLAGAN38 +	0.14
Dilution factor:	1.0
1 kg H2O remain	

Figure 7.20. NETPATH model results for San Acacia+ - San Marcial utilizing data from the 1980's. Constraints = C, Ca, Mg, S, Na, Cl, S, and Si. Phases = calcite, dolomite, gypsum, CO_2 gas, plagioclase mineral ($Ca_{0.38}Na_{0.62}Al_{1.38}Si_{2.63}O_8$) and calcium montorillonite.

Model results for the SA+-SM reach are narrowed by the same principles as discussed for the Lemitar models. Since the Lemitar site is contained within the SA-SM reach, it is reasonable to assume the same mineral phases should be present. Models are specified to contain calcite, dolomite, gypsum and carbon dioxide. Thus SA+-SM models 2 and 3 appear incomplete for lack of calcite and carbon dioxide reactions, respectively. The remaining models (models 1 and 4) contain the required phases with similar quantities of each mineral involved in the reactions. The difference between models 1 and 4 is the clay phase; model 1 has the formation of kaolinite while calcium montmorillonite is formed in model 4. Kaolinite is unlikely to be forming in the alkaline soil of New Mexico [Personal communication, George Austin, New Mexico Bureau of Geology, 2008]. For this reason model 4 is considered the best representation for reactions occurring between San Acacia and San Marcial. Model 4, uses calcite, dolomite, gypsum, carbon dioxide, plagioclase and calcium montmorillonite to account for the chemical differences between San Acacia+ and San Marcial. Comparing the NETPATH results from the Lemitar site

to those from the Rio Grande SA-SM reach reveals striking similarities (Figure 7.21). Both models utilize calcite, dolomite, gypsum, and CO_2. However, the San Acacia+ to San Marcial model includes plagioclase ($Ca_{0.38}$ $Na_{0.62}Al_{1.38}Si_{2.63}O_8$) and accounts for clay materials with calcium montorillonite rather than magnesium/sodium exchange. Although the inclusion of plagioclase is geologically plausible, it may not be kinetically realistic. The mineral plagioclase has a slower dissolution rate than the carbonate minerals (dolomite and calcite). Alternative models might substitute a more kinetically reasonable mineral that could account for the difference in sodium concentration. The SA+ - SM modeling yields results that correlate to the processes presented at the Lemitar site; dedolomitization, carbon dioxide gas exchange, and clay material interaction. Thus supporting the hypothesis that the subsurface interaction mechanisms observed in Lemitar also explain chemical changes throughout the Rio Grande basin.

San Acacia+ - San Marcial	
MODEL 4	
CALCITE	-0.042
GYPSUM	0.050
DOLOMITE	0.012
CO2 GAS	-0.22
PLAGAN38 +	0.14
Ca-MONT	-0.10
Dilution factor:	1.0

Lemitar: Irr - GW	
MODEL 2	
CALCITE	-0.41
GYPSUM	0.30
DOLOMITE	0.71
CO2 GAS	2.8
Mg/Na EX	0.21
Evaporation factor:	1.5
	656g H2O remain

Figure 7.21. Comparison of NETPATH most plausible model results for the Lemitar site (samples from May 2005) and SA+ - SM (decadal data from the 1980's). Mineral transfers are in mmols/kg water.

I used the NETPATH results from both the Lemitar and the SA+ - SM reach to calculate the total amount of mineral phase that has undergone alteration. The amount of mineral gained or lost per acre per year is presented in Table 7.16. The Lemitar model computed a greater amount of mineral phase reacted as compared to the San Acacia-to-San Marical river reach. Notice that Table 7.14 and Table 7.16 show an opposite trend, Table 7.14 shows larger solute residuals in the SA+-SM river reach, while Table 7.16

shows that the Lemitar site requires greater quantities of mineral phases. The explanation for the trend reversal between the Tables is attributed to two important assumptions. The solute load comparison in Figure 7.19 is based on the assumption that the mineral interactions, which create the solute load difference between San Acacia and San Marcial come solely from irrigated acreages. However, it is possible that reactions occur within riparian areas, the river or drainage canals, which would decrease the load that is sent to the river per acre. In addition, the Lemitar site investigation modeled mineral interactions between irrigation and ground water with the implied assumption that the solutes added from these interactions ultimately flushed into the river. However, it is likely that the ground water chemistry undergoes additional mineral interactions upon entry into the drainage system. The dissolved solutes may become unstable as the ground water discharges to the surface water system, particularly due to the degassing of carbon dioxide from the ground water into the atmosphere. This idea was investigated with a NETPATH model, which attempted to simulate the mineral interactions between ground water and drain water. Unfortunately, the results from the ground-water-to-drain model did not yield useful results due to inability to accurately estimate the chemistry of the drain. Local drain chemistry could not be obtained nor an accurate measure of any brine seepage into the drain. Further effort could be devoted to understanding the changes between ground water and drain water as it likely affects the quantities of solute that enter the Rio Grande. Based on these uncertainties and discrepancies, the mass of each mineral gained or lost due to irrigation probably somewhere between the quantities presented in Table 7.14, but is estimated to be closer to the San Acacia-to-San Marcial model.

Table 7.16. Quantity of mineral gained or lost from the soil at the Lemitar site and between San Acacia and San Marcial.

Phases	Lemitar (kg/acre/yr)	SA - SM (kg/acre/yr)
Calcite	-177.37	-29.01
Gypsum	221.61	59.05
Dolomite	562.52	14.58
CO2	536.54	-66.29
Plagioclase 38	N/A	262.58
Ca-Mont	N/A	-293.21
Mg/Na Mg loss	-22.39	N/A
Mg/Na Na release to GW	21.18	N/A

7.9 Conclusions

The Lemitar site was utilized to understand changes in Rio Grande chemistry due to subsurface reactions. The Rio Grande water that is diverted for irrigation is evaporated leaving about 65% to infiltrate into the soil and undergo dedolomitization and ion exchange; ground or drain water then discharges back into the river with increased solute concentrations and degasses excess CO2 into the atmosphere. I have attributed the chemical differences between irrigation and ground water to ion exchange between magnesium and sodium, in-gassing of carbon dioxide, and the process of dedolomitization. When the Lemitar reaction mechanisms are compared to the chemical variations between San Acacia-to-San Marcial, they show a qualitative resemblance. Since the subsurface mechanisms have been identified and supported, NETPATH modeling will be used throughout the Rio Grande Basin to investigate chemical transformations from Lobatos, CO to El Paso, TX.

CHAPTER 8
RIO GRANDE NETPATH MODELING

The differences between modeled upstream+ and downstream solute loads (solute budget chapter) are attributed to subsurface reactions. The investigation described in Chapter 7 was applied to all reaches of the Rio Grande during the 1980s. Mass-transfer modeling was performed using the geochemical computer program NETPATH. The models and results presented in this chapter are simple generalized attempts at understanding geochemical reactions in the Rio Grande Basin. The models do not capture any temporal variation, which could greatly affect the mineral mass transfers. For example, dilute spring runoff would likely dissolve additional minerals, whereas dry early winter conditions may lead to the oversaturation and precipitation of minerals that were found to dissolve in this analysis. However, the results presented remain useful as a basic effort to evaluate the geochemical processes that may affect the chemistry of the Rio Grande.

8.1 Methodology and Chemical Data

Rio Grande historic and modeled average decadal concentration data is presented in Table 8.1. Upstream+ modeled chemistry is listed with the corresponding downstream measured value. These concentrations have been entered into the USGS program NETPATH, which calculates possible combinations of mineral reactions, which

stoichiometrically account for chemical variations between two waters along a flow path from input phases and constraints. NETPATH reports all the possible combinations of phase interactions (dissolution, precipitation, ion exchange) that satisfy the chemical differences in the given constraints (e.g. calcium, sulfate, sodium) between the initial water and the final water. Within the model each constraint must be present in at least one phase and the number of constraints must be less than the number of phases. If a model is over constrained, NETPATH may not be able to compute any combination of mineral interactions that meet the given constraints. In contrast, when a NETPATH model is under constrained, the number of reaction combinations that satisfy the constraints may be numerous and unmanageable.

Solute concentrations for each river reach are presented in millimoles per kilogram of initial water in Tables 8.2 a-j. These tables illustrate the modeled and measured concentrations of constrained elements within each river section. General chemistry used for NETPATH was calculated as described in Chapter 5. NETPATH Rio Grande modeling required additional chemical information and some alterations were made to the mass balance. The storage component of the solute load from Elephant Butte Reservoir was considered to have a negligible affect on the concentration and has been omitted. Iron, aluminum, and silica have been included such that the saturation index for silicate and clay mineral phases was computed in the model. The pH, temperature, dissolved oxygen, iron, and silica were averaged monthly over the decade of the 1980's. However, iron data was not available at Elephant Butte or Caballo. Aluminum was also included though due to insufficient data during the 1980's, an average was calculated over the entire period of record using all the available data.

The chemical charge balance shown in Table 8.1, checked for chemically balanced data at each location. NETPATH attributed all chemical variation to mineral reactions, a calculation requiring the initial and final waters to be chemically balanced. The percent difference between cations and anions fell within an acceptable range of less than 5% for most of the river reaches. Charge balances fell outside the acceptable range (as high as 12%) at the three stations between Elephant Butte Dam and El Paso. The unbalanced chemical concentrations were attributed to the limited amount of data available for Elephant Butte and Caballo Reservoirs. The bicarbonate and potassium records at these locations were particularly limited, leaving the decade average to be derived mainly from regression. A high charge imbalance greatly increases the uncertainty of the data, particularly important in the NETPATH calculations. The NETPATH model assumes that all chemical variations between upstream+ and downstream stations were derived from mineral reactions. If the solute mass residuals between stations are generated from uncertainties in the chemical data, the quantities of mass attributed to mineral reactions may be questionable. However, the likely source of uncertainty is derived from regressed data in the bicarbonate record. Because the other solute records have sufficient data, I assumed the solute load residuals represent quantities derived from interactions with mineral phases. Although, there are considerable uncertainties in quantifying the mass transfers, the Rio Grande NETPATH analysis remains useful in describing chemical transfer mechanisms.

Table 8.1. General chemistry for Rio Grande locations: modeled upstream+ and measured downstream values. Units are mg/L unless otherwise noted.

Station Location Name	Temp	pH	Ca	Mg	Na	K	Cl	SO_4	HCO_3	Fe	Al	SiO_2	O_2	pCO2 (Atm)	Charge Balance %
Lobatos+	11.41	8.02	29.29	5.80	13.54	3.00	4.53	30.85	98.67	5.1E-05	2.3E-05	25.11	9.3	7.73E-04	4.5
Taos	11.41	8.02	25.99	5.12	15.11	2.84	4.51	34.39	84.83	5.1E-05	2.3E-05	24.22	9.5	6.66E-04	4.7
Taos+	14.14	8.25	33.68	6.39	15.69	2.49	4.49	47.22	96.97	3.4E-05	4.5E-05	24.22	9.5	4.56E-04	4.7
Otowi	14.14	8.25	32.95	6.14	15.27	2.42	4.36	46.72	106.18	3.4E-05	4.5E-05	19.70	9.7	5.00E-04	0.7
Otowi+	12.44	8.08	33.69	6.46	17.21	2.59	5.54	50.29	111.54	1.9E-05	2.5E-05	19.70	9.7	7.68E-04	-0.1
SF	12.44	8.08	34.35	6.32	16.78	2.61	5.40	50.39	124.34	1.9E-05	2.5E-05	18.54	9.7	8.56E-04	-3.5
SF+	14.37	8.09	36.95	6.79	23.05	2.98	11.26	58.11	133.74	2.1E-05	1.6E-05	18.54	9.7	9.16E-04	-3.5
ABQ	14.37	8.09	37.84	6.54	22.12	3.03	11.27	58.51	131.62	2.1E-05	1.6E-05	19.18	9.1	9.01E-04	-3.3
ABQ+	15.78	8.16	43.71	7.53	26.00	3.67	13.63	67.35	152.50	1.9E-05	5.8E-06	19.18	9.1	8.94E-04	-3.3
Bern	15.78	8.16	41.55	6.92	28.76	3.63	12.91	65.80	130.11	1.9E-05	5.8E-06	22.17	8.9	7.64E-04	1.6
Bern+	16.49	8.18	46.20	8.25	39.35	4.22	21.15	88.30	135.70	3.2E-05	7.6E-06	22.17	8.9	7.55E-04	1.6
SA	16.49	8.18	47.97	8.49	40.95	4.03	20.64	90.17	157.03	3.2E-05	7.6E-06	22.00	8.9	8.72E-04	-0.6
SA+	15.62	8.04	46.82	8.57	45.92	4.08	26.99	93.50	150.80	3E-05	4.5E-05	22.00	8.9	1.17E-03	-0.4
SM	15.62	8.04	49.09	8.85	47.95	4.09	26.99	98.30	136.44	3.0E-05	4.5E-05	22.32	8.5	1.06E-03	3.3
SM+	12.86	8.20	56.09	10.07	54.76	4.67	30.77	111.96	155.81	No Data	No Data	22.32	8.5	7.89E-04	3.4
EBD	12.86	8.20	53.24	11.42	62.24	4.97	38.70	141.96	66.16	No Data	No Data	16.38	6.8	3.34E-04	12
EBD+	15.09	8.10	57.64	12.69	72.81	5.31	55.13	157.05	72.75	1.2E-05	7.8E-06	16.38	6.8	4.75E-04	9.8
Caballo	15.09	8.10	54.24	12.29	72.10	5.61	53.10	142.39	74.36	1.2E-05	7.8E-06	16.21	7.8	4.87E-04	11.1
Caballo+	15.35	8.09	67.63	15.74	100.72	6.65	90.84	185.95	100.33	1.8E-05	2.1E-05	16.21	7.8	6.72E-04	7.1
El Paso	15.35	8.09	73.77	15.59	119.01	6.70	93.25	208.21	102.26	1.8E-05	2.1E-05	19.95	8.7	6.81E-04	9.5

Table 8.2a. Chemical concentrations in millimoles/kg water for Lobatos+ (Lobatos cross section + tributaries + ground water + brine) to Taos.

Constraints	Lobatos+ Initial (mmoles/kg water)	Taos Jct Final (mmoles/kg water)
C	1.64	1.41
Ca	0.73	0.65
Mg	0.24	0.21
Na	0.59	0.66
Cl	0.13	0.13
S	N/A	N/A
Si	0.42	0.40

Table 8.2b. Chemical concentrations in mmoles/kg water for Taos+ to Otowi.

Constraints	Taos+ Initial (mmoles/kg water)	Otowi Final (mmoles/kg water)
C	1.58	1.73
Ca	0.84	0.82
Mg	0.26	0.25
Na	0.68	0.66
Cl	0.13	0.12
S	N/A	N/A
Si	0.40	0.33

Table 8.2c. Chemical concentrations in mmoles/kg water for Otowi+ to San Felipe.

Constraints	Otowi+ Initial (mmoles/kg water)	SF Final (mmoles/kg water)
C	1.85	2.06
Ca	0.84	0.86
Mg	0.27	0.26
Na	0.75	0.73
Cl	0.16	0.15
S	N/A	N/A
Si	0.33	0.31

Table 8.2d. Chemical concentrations in mmoles/kg water for San Felipe+ to Albuquerque.

Constraints	SF+ Initial (mmoles/kg water)	ABQ Final (mmoles/kg water)
C	2.21	2.17
Ca	0.92	0.94
Mg	0.28	0.27
Na	1.00	0.96
Cl	0.32	0.32
S	N/A	N/A
Si	0.31	0.32

Table 8.2e. Chemical concentrations in mmoles/kg water for Albuquerque+ to Bernardo.

Constraints	ABQ+ Initial (mmoles/kg water)	Bernardo Final (mmoles/kg water)
C	2.50	2.13
Ca	1.09	1.04
Mg	0.31	0.28
Na	1.13	1.25
Cl	0.38	0.36
S	0.70	0.69
Si	0.32	0.37

Table 8.2f. Chemical concentrations in mmoles/kg water for Bernardo+ to San Acacia.

Constraints	Bernardo+ Initial (mmoles/kg water)	SA Final (mmoles/kg water)
C	2.22	2.57
Ca	1.15	1.20
Mg	0.34	0.35
Na	1.71	1.78
Cl	0.60	0.58
S	0.92	0.94
Si	0.37	0.37

Table 8.2g. Chemical concentrations in mmoles/kg water for San Acacia+ to San Marcial.

Constraints	SA+ Initial (mmoles/kg water)	SM Final (mmoles/kg water)
C	2.50	2.26
Ca	1.17	1.23
Mg	0.35	0.36
Na	2.00	2.09
Cl	0.76	0.76
S	0.97	1.02
Si	0.37	0.37

Table 8.2h. Chemical concentrations in mmoles/kg water for San Marcial+ to Elephant Butte Dam.

Constraints	SM+ Initial (mmoles/kg water)	EBD Final (mmoles/kg water)
C	2.55	1.08
Ca	1.40	1.33
Mg	0.41	0.47
Na	2.38	2.71
Cl	0.87	1.09
S	1.17	1.48
Si	0.37	0.27

Table 8.2i. Chemical concentrations in mmoles/kg water for Elephant Butte Dam to Caballo Dam.

Constraints	EBD+ Initial (mmoles/kg water)	Caballo Final (mmoles/kg water)
C	1.20	1.22
Ca	1.44	1.35
Mg	0.52	0.51
Na	3.17	3.14
Cl	1.56	1.50
S	1.64	1.48
Si	0.27	0.27

Table 8.2j. Chemical concentrations in mmoles/kg water for Caballo+ to El Paso.

Constraints	Caballo+ Initial (mmoles/kg water)	El Paso Final (mmoles/kg water)
C	1.65	1.68
Ca	1.69	1.84
Mg	N/A	N/A
Na	4.38	5.18
Cl	2.56	2.63
S	1.94	2.17
Si	0.27	0.33

8.2 Model Parameters: Phases and Constraints

Each modeled upstream+ location is used as the initial water and the downstream location is the final water input into NETPATH. Since the entire Rio Grande valley was formed through rifting, each river reach contains many of the same parameters. Similar mineral phases and constraining elements were incorporated into each reach model, yet slight variations were required. Phases were included based on the local geology and a previous modeling effort by *Plummer et al* [2004].

A simplified geologic map of New Mexico is given in Figure 8.1. Specified mineral phases are presented in Table 8.3 (all included phases) and divided based on river reach in Table 8.4. Plagioclase and orthoclase were identified as the most common silicate minerals [*Anderholm,* 1985] and were represented by plagioclase-38 as specified in *Plummer* [2*004*]. Biotite was only used in northern sections, above Bernardo, as a magnesium source. Olivine was only included between Taos to Otowi due to the presence of basalt. The most common clays found in the basin are calcium smectites and mixed layer illite-smectites specifically Ca-montorillonite [*Anderholm,* 1985], thus all reach models include Ca-montmorillonite. Mg-montmorillonite was added when necessary as a source or sink for magnesium. Calcite, dolomite and gypsum are known to exist in many of the sediments in the Albuquerque-Belen basin in calcite cement, gypsum beds, or

contained in the sediment [*Anderholm,* 1985]. Calcite was included in each reach but dolomite and gypsum were only included selectively. Gypsum was added below Albuquerque, where quaternary sediments containing gypsiferous eolian deposits (Figure 8.1, the yellow stars) and the Yeso and Seven rivers formations are exposed at the surface. Dolomite was included in the three reaches between Bernardo and Elephant Butte Dam, areas that surround the location (Lemitar) where dolomite was identified in soils as well as some of the areas containing carbonate minerals (Figure 8.1, blue areas). Additional mineral phases, beyond those listed in Table 8.4, were not included because the number of solutions reported by NETPATH became unmanageable. The solutions will reflect various reaction combinations, which stoichiometrically satisfy the constraints, when phases are added but not constraints, the number of possible solutions increases because the number of different combinations increases. In certain river reaches, NETPATH computed over 20 possible solutions many of these solutions differ only by the amount of mineral dissolution. For example, if there are 5 minerals that contain magnesium, the various solutions could use any combination from one to 5 of the phases to account for the magnesium variations. In order to add additional phases, more chemical information would be necessary. Cation exchange reactions were only included in reaches where a sodium source or sink was required.

Elements constrained within each reach are illustrated in Table 8.5. Carbon, calcium, magnesium, sodium, chloride, and silica are used in all models except at El Paso. The magnesium constraint was removed at El Paso due to an inability for NETPATH to calculate a set of reactions, which satisfied all given constraints. The Caballo+-El Paso model was over constrained and thus magnesium was removed from

the constraints. Because magnesium could not be used to constrain the model, phases that contain only magnesium, such as Mg-montmorillonite, had to be removed. In order to constrain reactions with gypsum, sulfur was added as a constraining element in the models below the Albuquerque+ to Bernardo reach. Potassium was not utilized to constrain any models due to a lack of available data, which resulted in model errors due to over constraining the NETPATH solutions.

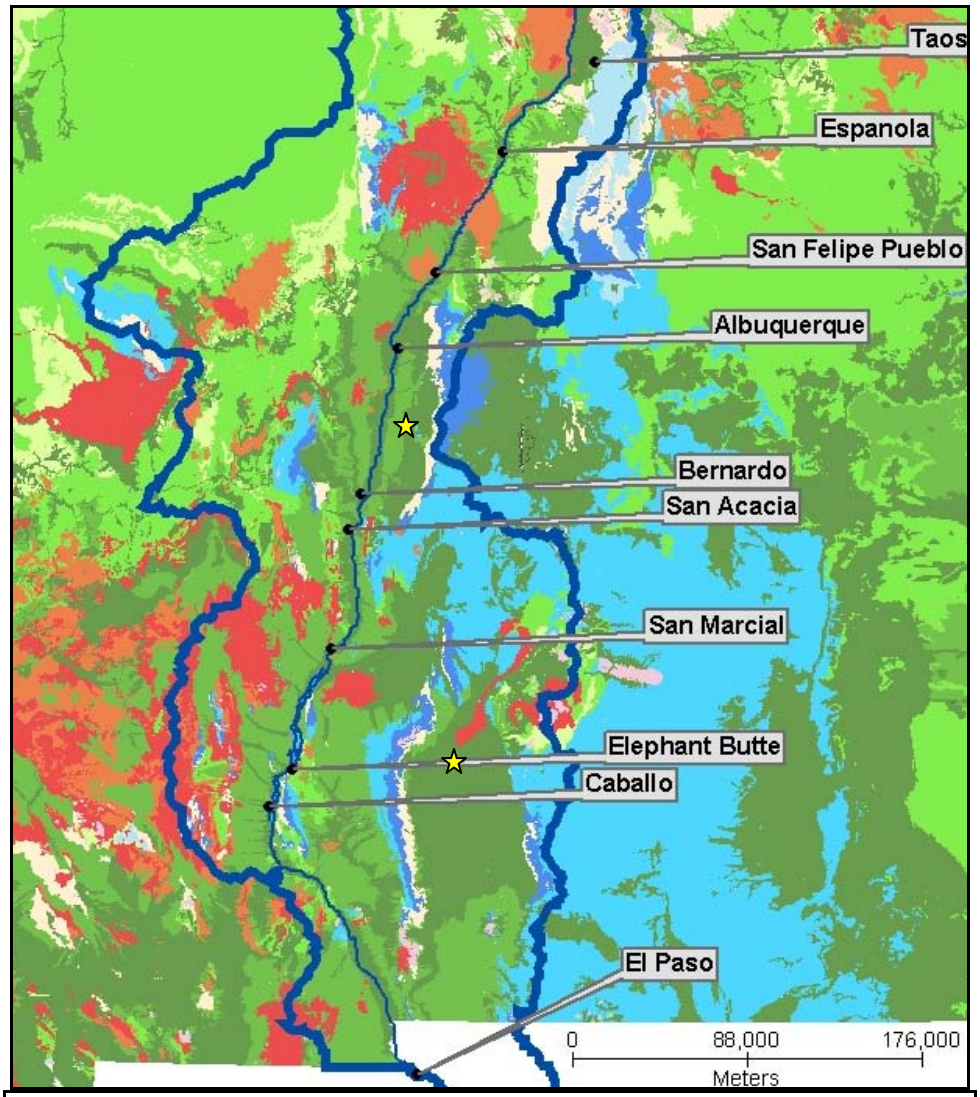

Figure 8.1. Simplified geologic map of New Mexico. Red and orange areas are volcanic rocks, blue and green areas are sedimentary rocks. The Rio Grande watershed and the Rio Grande are in dark blue. The two yellow stars above Bernardo and next to Caballo indicated areas containing gypsiferous eolian sediments. Note: The Otowi Bridge gaging station is represented by the nearby city of Española.

Table 8.3. Rio Grande NETPATH model possible phases.

Phases	Formulas	Notes
Gypsum	$CaSO_4$	Positive = dissolution of gypsum
Dolomite	$CaMg(CO_3)_2$	Positive = dissolution of dolomite
CO_2 gas	$CO_{2(gas)}$ -> $CO2_{(aq)}$	Positive = ingassing of CO_2
Calcite	$CaCO_3$	Positive = dissolution of calcite
Plagioclase-38	$Ca_{0.38}\ Na_{0.62}Al_{1.38}Si_{2.63}O_8$	Positive = dissolution of plagioclase-38
Olivine	Mg_2SiO_4	Positive = dissolution of olivine
Biotite	$KMg_{1.5}AlFe_{1.5}Si_3O_{10}$	Positive = dissolution of biotite
Kaolinite	$Al_2Si_2O_5(OH)_4$	Positive = dissolution of kaolinite
Ca-Montmorillonite	$Ca_{0.167}Al_{2.33}Si_{3.67}O_{10}(OH)_2$	Positive = dissolution of Ca-Mont
Mg-Montmorillonite	$Mg_{0.167}Al_{2.33}Si_{3.67}O_{10}(OH)_2$	Positive = dissolution of Mg-Mont
Ca/Na Exchange	$Na_2X + Ca^{2+}$ -> $CaX + 2Na^+$	Positive = releases Na to solution (ie GW)

Table 8.4. Phases for NETPATH separated by model (upstream+ - downstream).

River Reach	Plagioclase-38	Olivine	Biotite	Calcite	Dolomite	Gypsum	CO_2 gas	Kaolinite	Ca-Mont	Mg-Mont	Ca/Na Exchange
Lobatos+ - Taos	X		x	x			x	x	x	x	
Taos+ - Otowi	X	x	x	x			x	x	x	x	
Otowi+ - SF	X		x	x			x	x	x		
SF+-ABQ	X		x	x			x	x	x	x	x
ABQ+ - Bernardo	X		x	x		x	x	x	x	x	
Bernardo+ -SA	X			x	x	x	x	x	x		
SA+-SM	X			x	x	x	x	x	x		
SM+-EBD	X			x	x	x	x	x	x		x
EBD+-Caballo	X			x		x	x	x	x	x	
Caballo+ - El Paso	X			x		x	x	x	x		x

Table 8.5. Rio Grande NETPATH constraints.

River Reach	Carbon	Calcium	Magnesium	Sodium	Chloride	Silica	Sulfur
Lobatos+ - Taos	x	x	x	x	x	x	
Taos+ - Otowi	x	x	x	x	x	x	
Otowi+ - SF	x	x	x	x	x	x	
SF+-ABQ	x	x	x	x	x	x	
ABQ+ - Bernardo	x	x	x	x	x	x	x
Bernardo+-SA	x	x	x	x	x	x	x
SA+-SM	x	x	x	x	x	x	x
SM+-EBD	x	x	x	x	x	x	x
EBD+-Caballo	x	x	x	x	x	x	x
Caballo+ - El Paso	x	x		x	x	x	x

8.3 Saturation Indices

The saturation index (SI) for all minerals at all locations is shown Tables 8.6a and 8.6b. Recall from equation 7.3 that the SI is equal to the log of the ion activity product divided by the thermodynamic equilibrium constant. Calcite, aragonite and dolomite are under-saturated in some reaches and over-saturation in others. The remaining phases (gypsum, kaolinite, albite, anorthite, potassium feldspar and calcium montmorillonite) are consistently undersaturated. Recall from Chapter 7 that the pCO_2 is in atmospheres and its saturation is referenced to one atmosphere. Thus, the pCO_2 given is the log of the partial pressure divided by 1 atmosphere [personal communication with David Parkhurst, USGS], indicating that pCO_2 saturations of less than –3.5 are undersaturated and will accept CO_2 from the atmosphere.

Table 8.6a. Saturation indices, Lobatos+ through Bernardo.

Phases	Lobatos+	Taos Jct	Taos+	Otowi	Otowi+	SF	SF+	ABQ	ABQ+	Bernardo
Calcite	-0.13	-0.24	0.17	0.20	0.04	0.09	0.18	0.19	0.38	0.30
Aragonite	-0.28	-0.40	0.02	0.05	-0.12	-0.06	0.03	0.03	0.23	0.15
Dolomite	-0.81	-1.04	-0.18	-0.13	-0.48	-0.39	-0.17	-0.19	0.23	0.04
Gypsum	-2.32	-2.32	-2.11	-2.12	-2.08	-2.08	-2.01	-1.99	-1.90	-1.92
Kaolinite	-1.42	-1.42	-1.83	-1.83	-1.81	-1.82	-2.47	-2.47	-3.55	-3.54
Albite	-3.65	-3.60	-3.76	-3.77	-3.93	-3.94	-4.09	-4.11	-4.39	-4.35
Anorthite	-8.16	-8.21	-7.78	-7.79	-8.29	-8.28	-8.69	-8.68	-9.43	-9.45
K-Feldspar	-1.80	-1.82	-2.08	-2.09	-2.25	-2.25	-2.51	-2.50	-2.79	-2.79
Ca-Mont	-3.21	-3.22	-3.72	-3.72	-3.79	-3.79	-4.53	-4.53	-5.67	-5.67
Illite	-3.71	-3.74	-4.06	-4.07	-4.26	-4.27	-4.93	-4.93	-5.95	-5.96
pCO_2	-3.11	-3.18	-3.34	-3.30	-3.11	-3.07	-3.04	-3.05	-3.05	-3.12

Table 8.6b Saturation indices, Bernardo+ through El Paso.

Phases	Bernardo+	SA	SA+	SM	SM+	EBD	EBD+	Caballo	Caballo+	El Paso
Calcite	0.38	0.45	0.27	0.24	0.46	0.06	0.06	0.05	0.23	0.26
Aragonite	0.23	0.30	0.12	0.09	0.31	-0.09	-0.09	-0.10	0.08	0.11
Dolomite	0.24	0.38	0.01	-0.04	0.35	-0.37	-0.33	-0.34	0.04	0.06
Gypsum	-1.78	-1.76	-1.76	-1.72	-1.62	-1.55	-1.50	-1.55	-1.40	-1.33
Kaolinite	-3.46	-3.46	-1.50	-1.50	No Data	No Data	-3.38	-3.37	-2.32	-2.33
Albite	-4.16	-4.15	-3.24	-3.22	No Data	No Data	-4.20	-4.20	-3.37	-3.30
Anorthite	-9.22	-9.21	-7.64	-7.62	No Data	No Data	-9.38	-9.39	-8.28	-8.26
K-Feldspar	-2.68	-2.71	-1.84	-1.84	No Data	No Data	-2.87	-2.85	-2.09	-2.09
Ca-Mont	-5.57	-5.57	-3.32	-3.32	No Data	No Data	-5.66	-5.66	-4.31	-4.31
Illite	-5.79	-5.80	-3.70	-3.70	No Data	No Data	-5.85	-5.84	-4.48	-4.48
pCO_2	-3.12	-3.06	-2.93	-2.98	-3.10	-3.48	-3.32	-3.31	-3.17	-3.17

Note: Albite, Anorthite and Potassium Feldspar represent Plagioclase-38.

8.4 Mineral Mass Transfer Results

Phases, constraints and chemical data for each reach have been input into NETPATH yielding results of mass transfer reactions that account for the solute residuals (Chpater 6). As previously discussed (Chapter 7), NETPATH reports all possible reaction combinations from the initial chemistry and the given phases to produce the final chemistry. All of the potential solutions are presented in Appendix C. The solutions presented in this chapter are the best representations of the subsurface reactions occurring within each river reach (Figures 8.2-8.11 and Table 8.7). The representative models were chosen based on saturation indices and the quantity of mineral involved in the reaction. Mass-transfer results reveal silicate-weathering reactions dominate chemical transformations in northern river reaches, transitioning into carbonate dissolution and dedolomitization reactions in central/southern New Mexico. A previously developed NETPATH model for chemical variations along ground water flow paths [*Plummer et. al*., 2004] reported similar results, but did not convert these to river-scale mass balances.

Plummer et al [2004] developed a NETPATH model to investigate mineral transfers along ground water flow paths in the Middle Rio Grande from Cochiti Lake to San Acacia. The study included 288 ground water samples organized into 12 categories based on chemistry and location. Recharge waters were used as the initial chemistry with the ground-water samples as the final. In areas where geology and isotopic data suggested ground-water mixing, the proper calculations were added into NETPATH. *Plummer et al* [2004] included the following mineral phases: calcite, plagioclase, CO_2, kaolinite, silcate, calcium-sodium exchange, gypsum, and organic matter. The *Plummer et al* [2004] model results suggested that many locations required the dissolution of plagioclase feldspar, silica and gypsum as well as calcite precipitation, kaolinite formation and sodium released from Ca/Na ion exchange (Figure 8.12).

The *Plummer et. al.* [2004] model and the 1980's Rio Grande decadal model yield similar results, both required clay formation, cation exchange, and the dissolution of gypsum as well as silicate and carbonate minerals. On average, the decadal and *Plummer et al* [2004] models tend to correlate mechanistically. Both models similar quantities of mineral mass transfers that included the following phases: calcium, gypsum, plagioclase, clay formation and exchange.

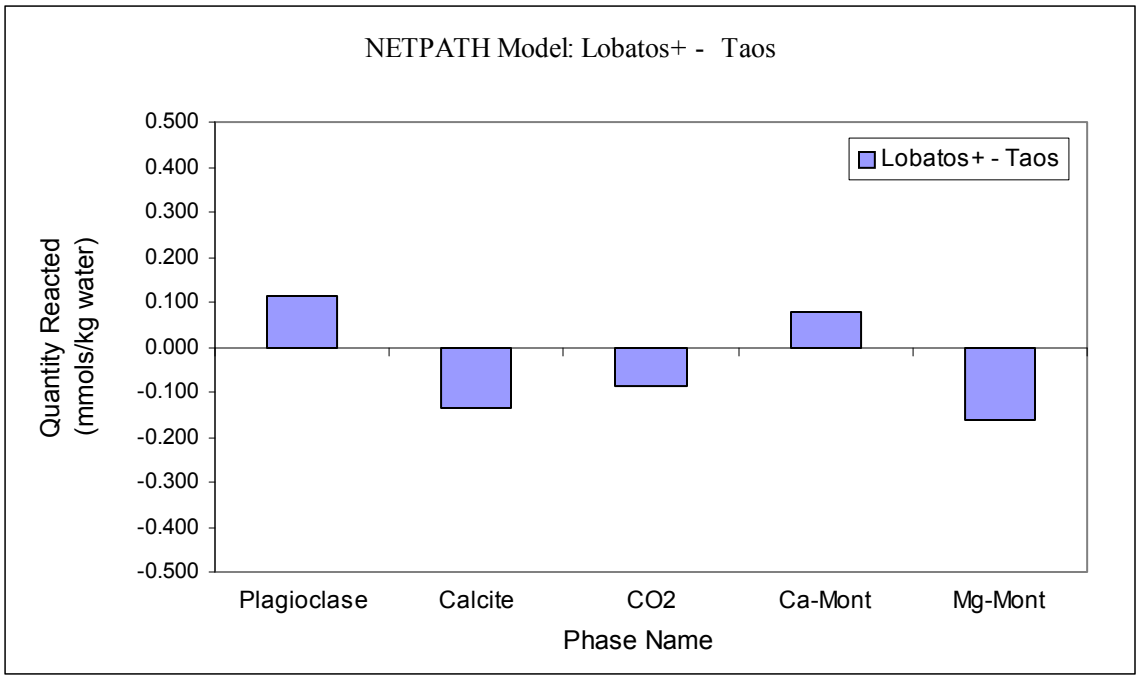

Figure 8.2. NETPATH model results: best representation for Lobatos+ to Taos Junction.

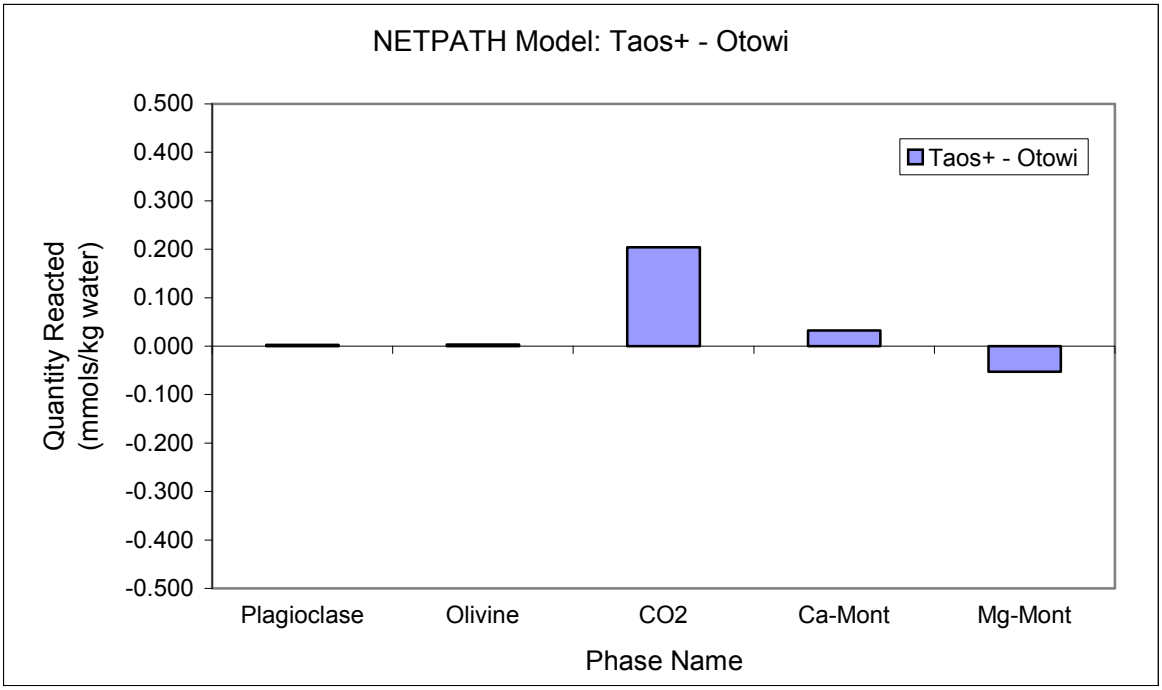

Figure 8.3. NETPATH model results: best representation for Taos+ to Otowi.

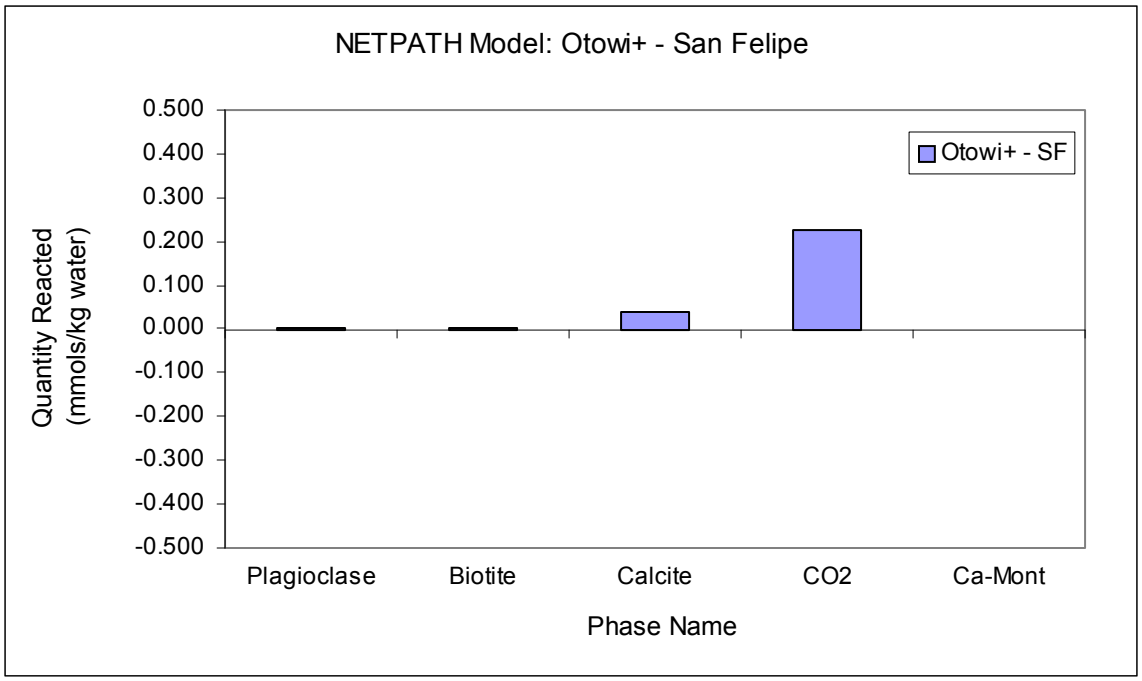

Figure 8.4. NETPATH model results: best representation for Otowi+ to San Felipe.

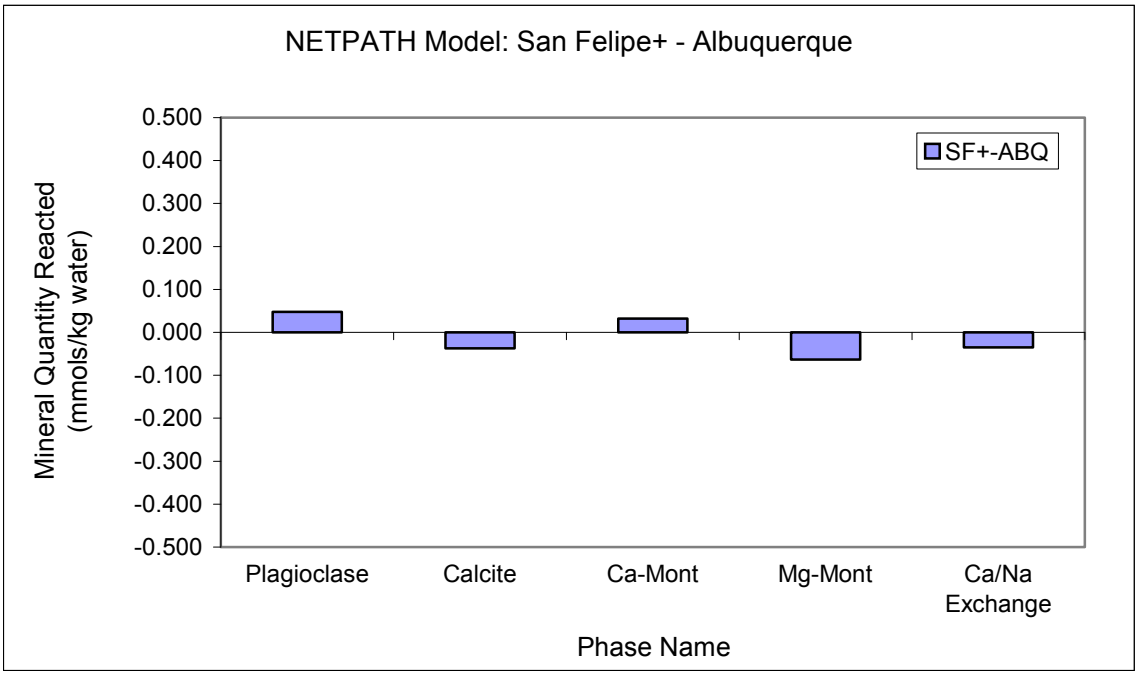

Figure 8.5. NETPATH model results: best representation for San Felipe+ to Albuquerque.

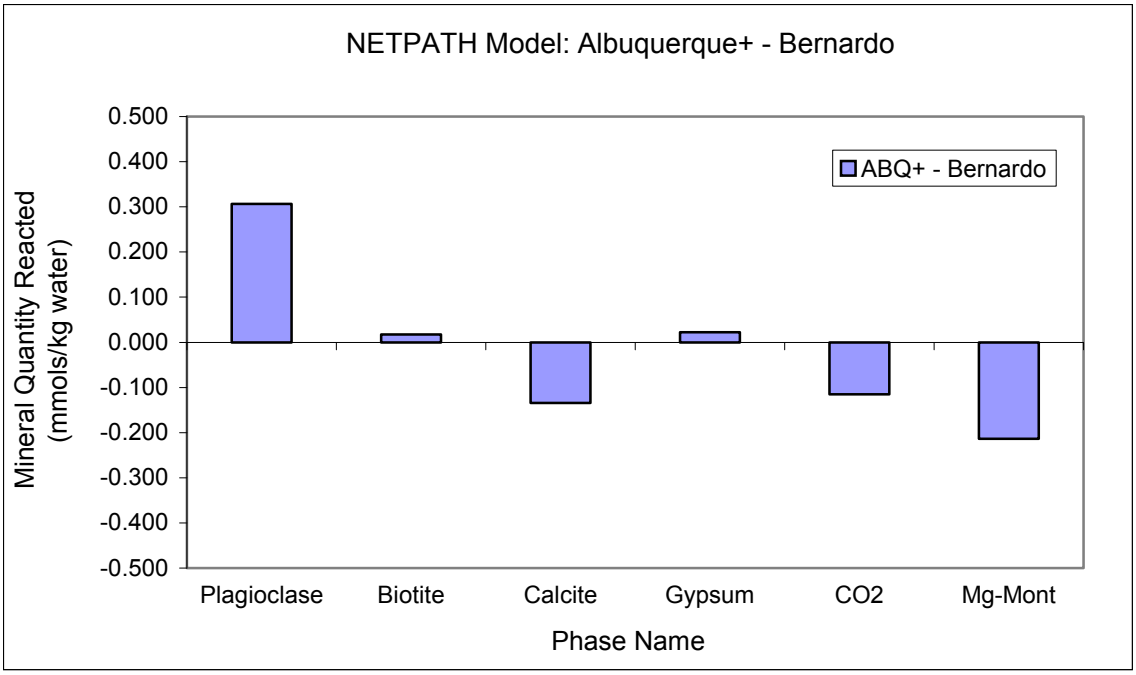

Figure 8.6. NETPATH model results: best representation for Albuquerque+ to Bernarado.

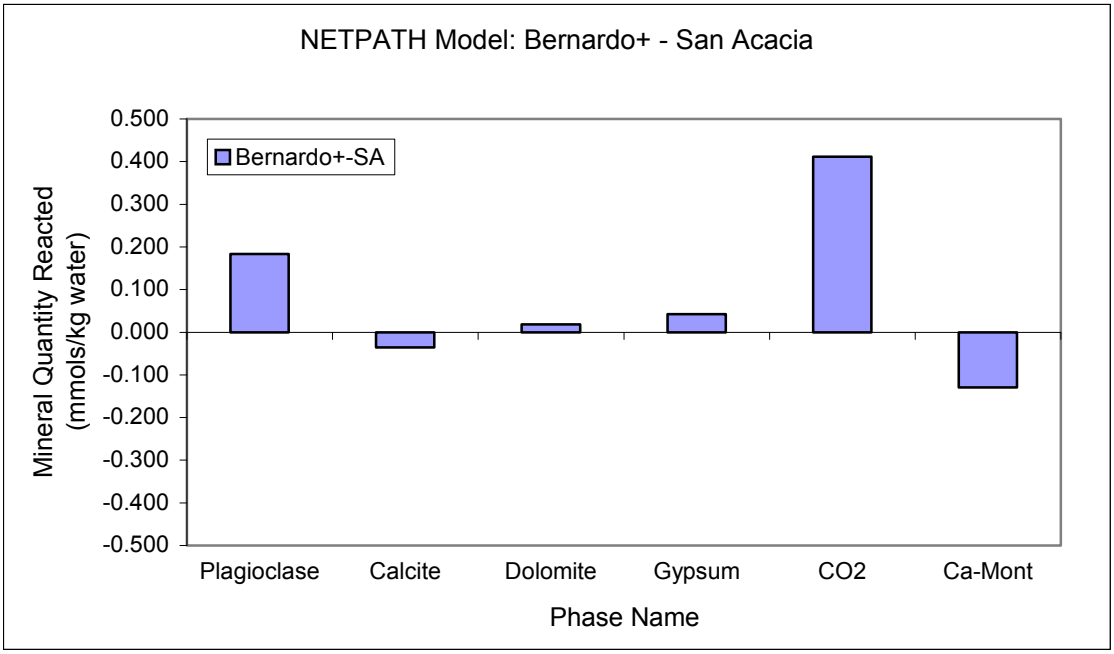

Figure 8.7. NETPATH model results: best representation for Bernardo+ to San Acacia.

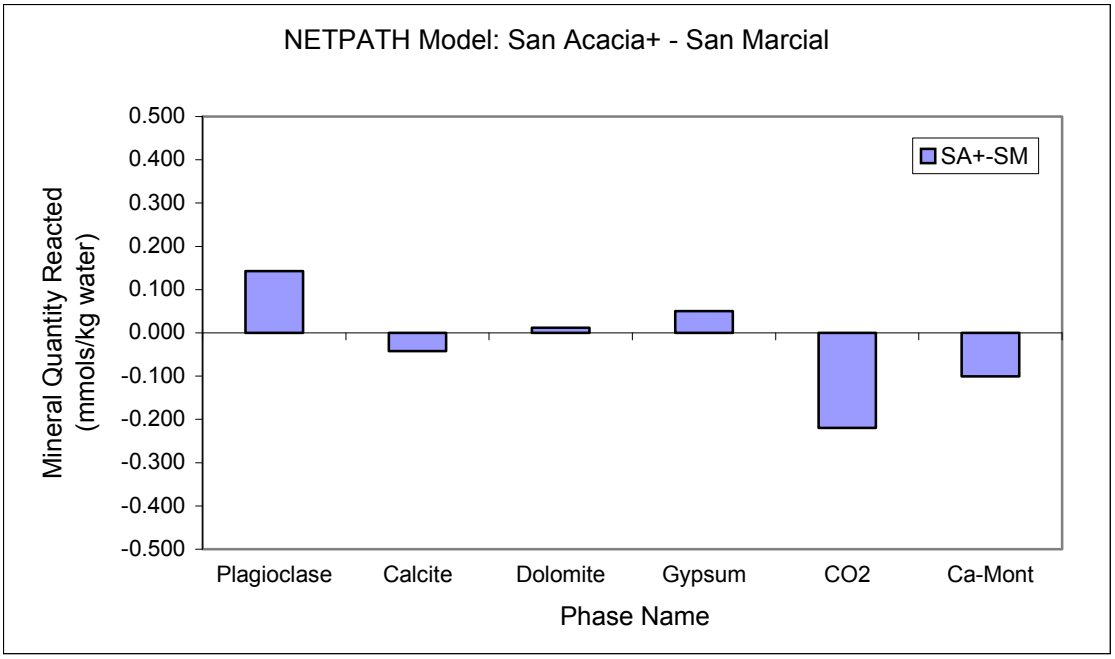

Figure 8.8. NETPATH model results: best representation for San Acacia+ to San Marcial.

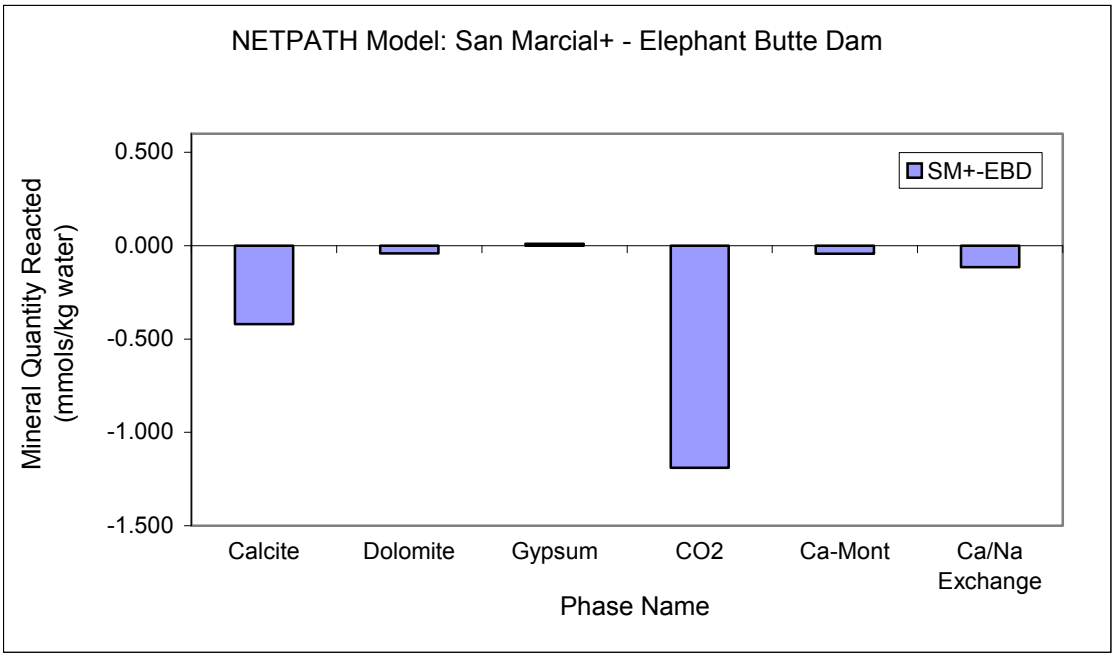

Figure 8.9. NETPATH model results: best representation for San Marcial+ to Elephant Butte Dam.

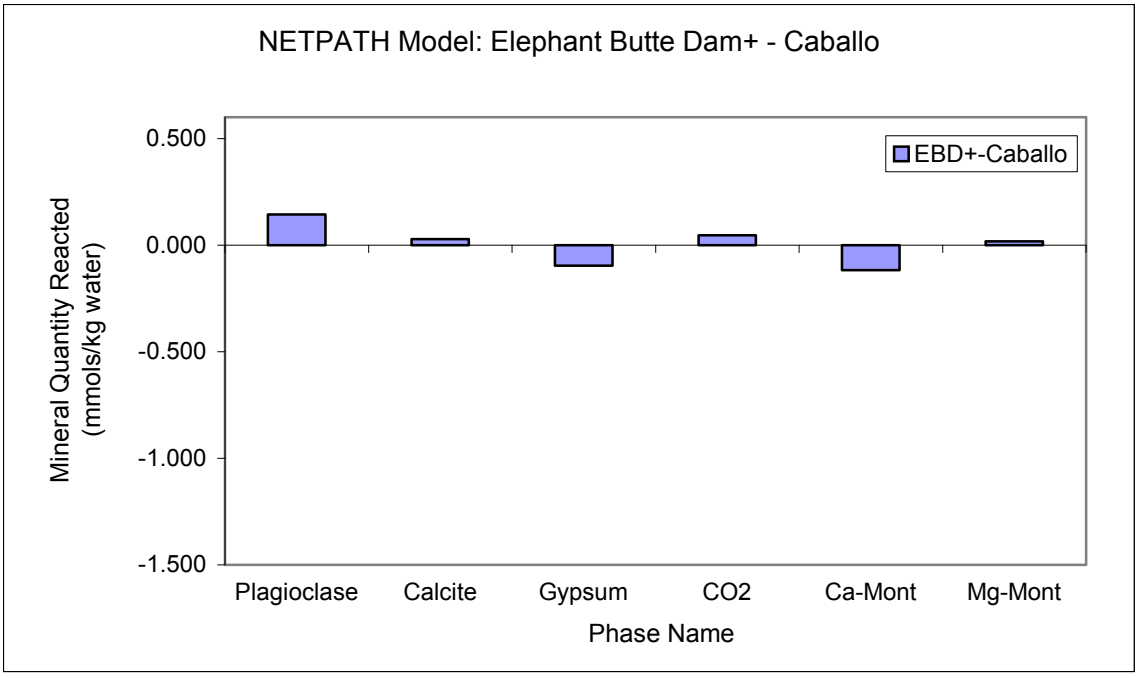

Figure 8.10. NETPATH model results: best representation for Elephant Butte Dam+ to Caballo.

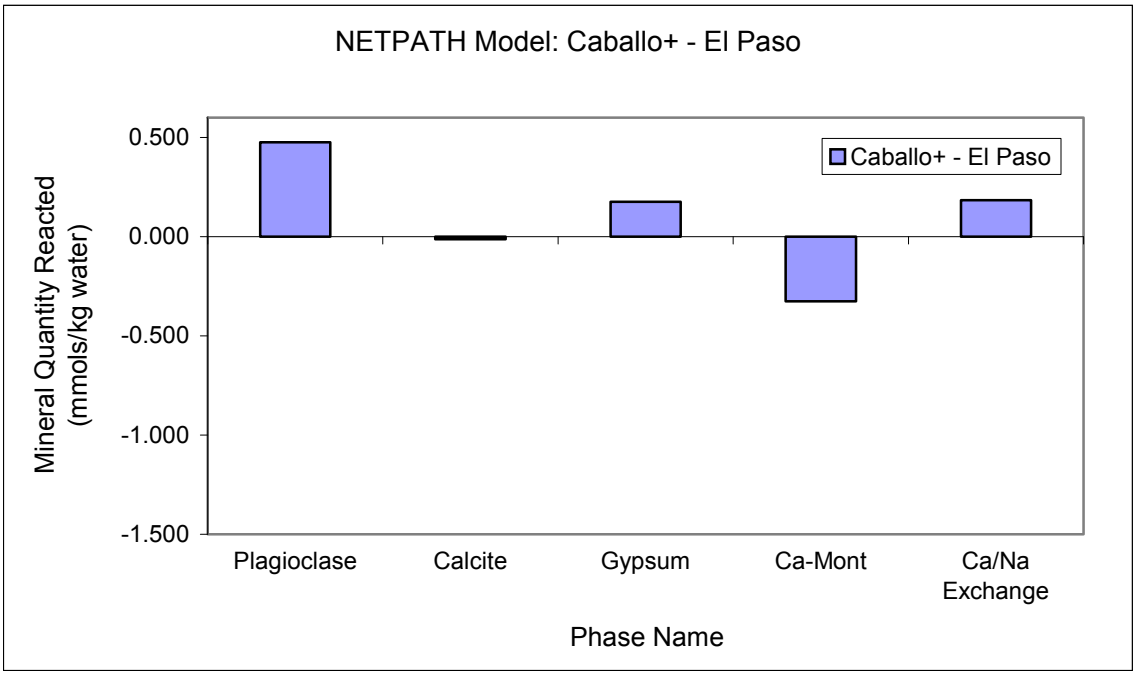

Figure 8.11. NETPATH model results: best representation for Caballo+ to El Paso.

Table 8.7. Summary of representative NETPATH models for upstream+-downstream locations. Units are mmoles mineral/kg initial water.

Phases	Plagioclase	Olivine	Biotite	Calcite	Dolomite	Gypsum	CO2	Ca-Mont	Mg-Mont	Ca/Na Exchange
Lobatos+ - Taos	0.11			-0.14			-0.09	0.08	-0.16	
Taos+ - Otowi	0.00	0.00					0.20	0.03	-0.05	
Otowi+ - SF	0.00		0.00	0.04			0.23	0.00		
SF+-ABQ	0.05			-0.04				0.03	-0.06	-0.04
ABQ+ - Bernardo	0.31		0.02	-0.13		0.02	-0.11		-0.21	
Bern.+-SA	0.18			-0.04	0.02	0.04	0.41	-0.13		
SA+-SM	0.14			-0.04	0.01	0.05	-0.22	-0.10		
SM+-EBD				-0.42	-0.04	0.01	-1.19	-0.04		-0.11
EBD+- Caballo	0.14			0.03		-0.10	0.05	-0.12	0.02	
Caballo+ - El Paso	0.48			-0.01		0.18		-0.33		0.18

Zone no.	Hydrochemical zone	Average mass transfer (mmols per kg water)								Evap-oration Factor
		Calcite	Plag-ioclase	CO_2	Kaol-inite	SiO_2	Ca-Na Ex-change	Gypsum	CH_2O	
1	Northern Mountain Front	0.1	0.3	1.1	- 0.2	- 0.2	- 0.2	0.1	nd	1.1
2	Northwestern	0.1	0.0	0.0	0.0	0.0	0.8	0.3	nd	1.1
3	West Central	0.4	0.1	0.3	- 0.1	- 0.4	1.8	0.9	nd	1.1
4	Western Boundary	- 4.0	0.1	- 0.2	- 0.1	0.3	2.9	7.3	nd	0.7
5	Rio Puerco	- 2.0	0.2	1.4	- 0.1	0.2	- 3.2	1.2	nd	1.2
6	Southwestern Mountain Front	- 1.0	0.1	- 1.2	- 0.1	- 0.5	0.0	0.0	nd	2.2
7	Abo Arroyo	- 0.7	0.1	- 0.6	- 0.1	- 0.1	0.0	- 0.4	nd	3.4
8	Eastern Mountain Front	- 0.3	0.3	0.4	- 0.2	- 0.2	0.1	0.2	nd	0.9
9	Tijeras Fault Zone	- 0.8	0.6	- 0.1	- 0.4	- 0.8	- 0.3	0.6	nd	2.1
10	Tijeras Arroyo	- 0.9	0.2	0.0	- 0.1	- 0.2	- 0.1	0.7	nd	1.1
11	Northeastern	- 1.2	0.6	- 0.2	- 0.4	- 0.7	0.4	1.6	nd	1.5
12	Central	0.0	0.2	0.1	- 0.1	0.2	0.1	- 0.1	0.3	1.3

Figure 8.12. Results of ground water modeling in NETPATH for regions in the Middle Rio Grande (Cochiti Lake to San Acacia). [*Plummer*, 2004]

8.5 Note on Mineral Interaction Locations

The location of these modeled mineral mass transfers has not been explicitly described. The results from Lemitar (Chapter 7) show that mineral interactions occur in

agricultural soil. However, interactions between minerals and Rio Grande water may also occur under riparian areas or within canal and drain channels. For example, the Bernardo to San Acacia reach has minimal acres devoted to agriculture yet a large solute addition was computed. The likely location for mineral interactions in the Bernardo to San Acacia reach is under riparian areas. This document notates the existence of important mineral interactions but was unable to focus on the location of these interactions. Further research is needed to identify the exact locations of any water/mineral interactions.

8.6 Conclusions

I attributed the residual solute quantities calculated from the Rio Grande mass balance (Chapter 6) to subsurface reactions. Northern Rio Grande chemical mass transfers are controlled by silicate weathering reactions, transforming olivine, plagioclase and biotite into clay minerals such as calcium or magnesium montmorillonite. In areas with heavy irrigation, carbonate interactions account for the majority of mass transfers and tend to support the dedolomitization process for the precipitation of calcite and the dissolution of dolomite and gypsum reactions as presented in detail in Chapter 7. The quantities and minerals that were presented illustrate likely mineral interactions that could account for the residual solute quantities. The quantities of mineral phases are average estimates of likely mineral interactions, but do not cover seasonal variations nor include all the possible phases that might contribute to the solute residuals. Although these modeling results represent a drastically simplified picture of the Rio Grande system, the results illustrate likely processes and general mineral classes that contribute to the residual solute mass.

CHAPTER 9
CONCLUSIONS

Many studies have investigated the downstream salinization of the Rio Grande, most concluded that anthropogenic features (reservoirs, diversion dams and the irrigation network) contributed to the salt increase with distance downstream. In particular, the enhanced evaporation rate due to irrigated agriculture is cited in early work as the major cause for salinization [*Lippincott*, 1939]. Although the irrigation network increases evaporation, it was through the historical flushing of accumulated salt that the canal system contributed most effectively to river salinization.

The solute load of the Rio Grande overall progressively decreased with time, yet experienced oscillating periods of increased load. Particularly high solute loads were observed during the 1900's, 1930's and 1940's, with high loads in the 1970's and 1980's (Figure 9.1). The solute increases during the early 1900's were attributed to higher river discharges and the lack of storage capacity (Reservoirs were not constructed until 1911). High solute loads during the 1930's and 1940's were ascribed to a flushing of shallow ground water enhanced by the installation of an extensive drainage network in 1928 [*NRC*, 1938; *Wilcox*, 1957; *Trock et al*., 1978]. Higher discharges flowed in the Rio Grande during the 1970's and 1980's causing the solute loads to increase. Additionally, small quantities of salt may have accumulated in agricultural soils during the 1950's and 1960's when the basin experienced excessively dry conditions.

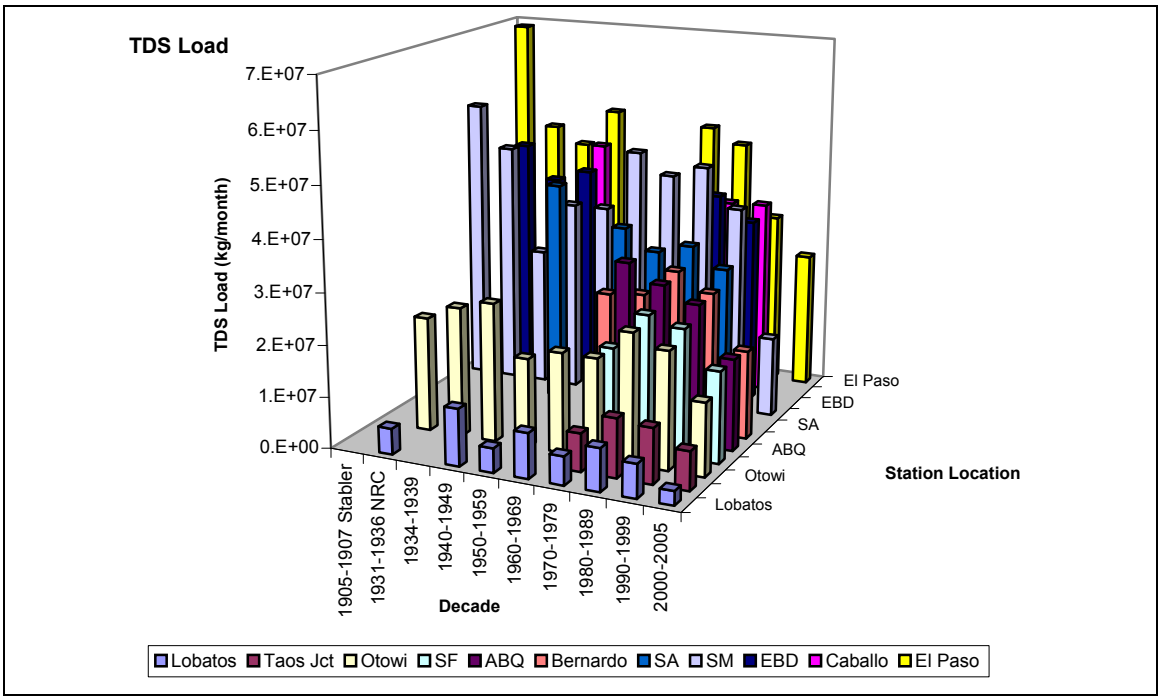

Figure 9.1. Total dissolved solids load at each Rio Grande cross-section.

Salt accumulation and evaporation are not the only factors affecting the chemistry of the Rio Grande. Recent studies identified seepage from geologically controlled brine as a significant contributor of solutes to the upper Rio Grande [*Moore and Anderholm*, 2002; *Mills*, 2003; *Phillips et al*, 2003; *Lacey*, 2006]. *Lacey* [2006] presented data to suggest that brine seepage was negatively correlated to Rio Grande discharge. In the dry months of September and October, when the river discharge is low, larger quantities of brine enter the river. If evaporation and brine seepage were the sole factors affecting the salinity of the Rio Grande, there would be a strong negative correlation between the TDS concentration and the discharge. Because brine is diluted by the amount of water in the Rio Grande, the more water in the river, the less influence brine has on the chemistry of the river. If the Rio Grande system were controlled solely by brine seepage, the relationship between concentration and discharge in the river would resemble Figure 9.2,

where the TDS concentration increases during periods of low flow and the decreases when the river discharge is high. However, the data presented in this thesis suggests that brine, evaporation, tributaries, wastewater treatment plants and interactions with mineral phases all significantly affect the chemistry of the river. Mineral interactions are controlled by the saturation of each element and the stability of each mineral in the system. A larger quantity of water can contain a larger amount of dissolved solids, i.e. a larger load, but the ratio of solutes per volume remains constant based on the solute/mineral equilibrium. In a system dominated by solute mass transfers the load would increase proportionally and the concentration would remain constant with fluctuations in discharge. If mineral reactions controlled the behavior of solutes in the Rio Grande, assuming the minerals interactions were not rate-limited, the concentration would remain constant because minerals would dissolve or precipitate based on the saturation of each mineral and the amount of river water. Figure 9.3 illustrates a theoretical river system controlled by solute mass transfers between the river and mineral phases.

TDS concentration and discharge in the Rio Grande matches neither of the theoretical models completely, yet exhibits both patterns through time. In Figure 9.4, the total dissolved solids concentration and discharge are plotted monthly from 1974-1983 at the San Marcial gaging station. In certain months the concentration follows the same trend as the discharge (either increasing or decreasing along with the discharge), while at other times there is the strong negative correlation indicative of brine domination. The Rio Grande follows neither source trend completely, indicating that the system is

controlled by a mixing of these dominant processes as well as the other point-source additions of salt (i.e. tributaries and wastewater effluent).

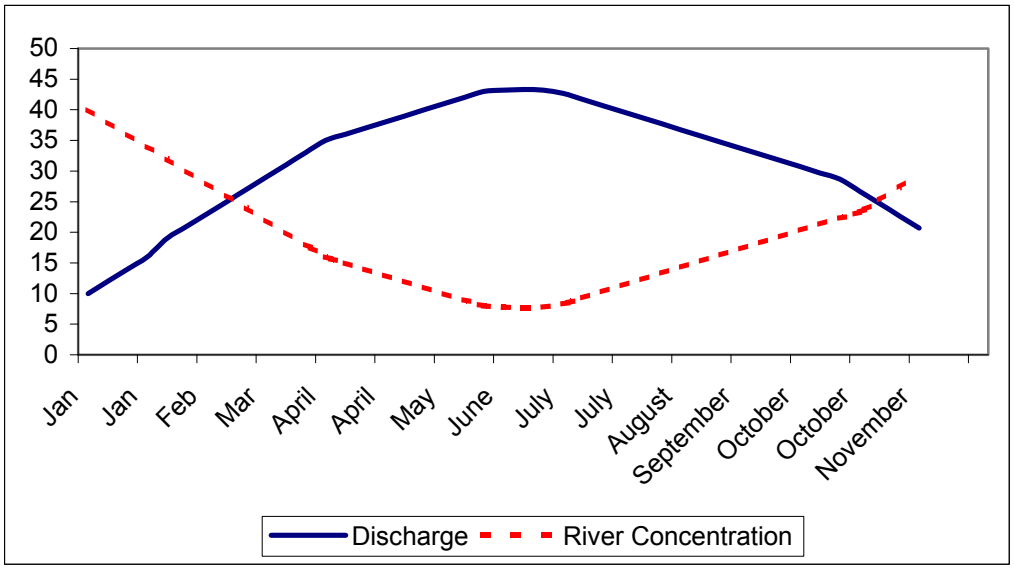

Figure 9.2. Concentration and discharge comparison for a theoretical river system dominated by brine seepage.

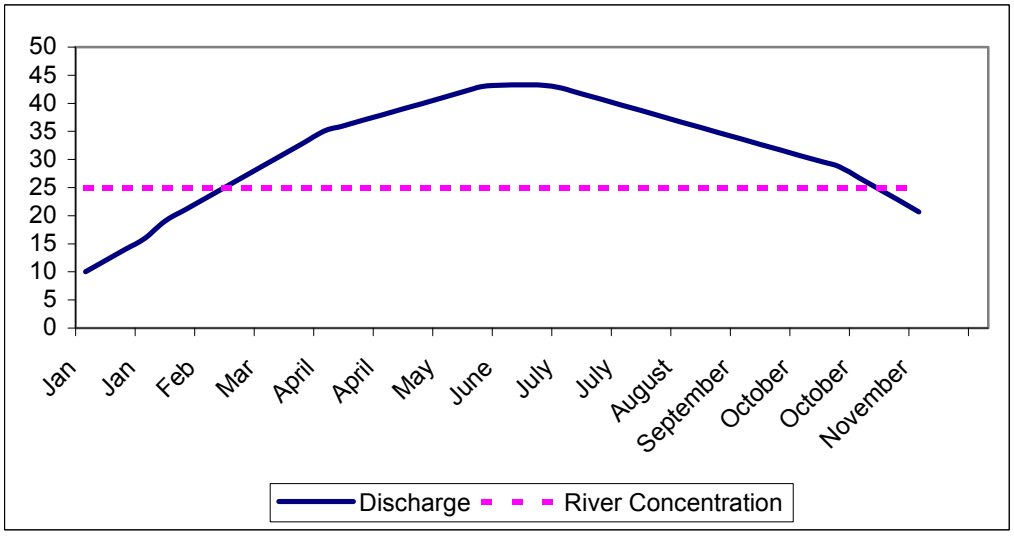

Figure 9.3. Concentration and discharge comparison for a theoretical river system dominated by mineral interactions.

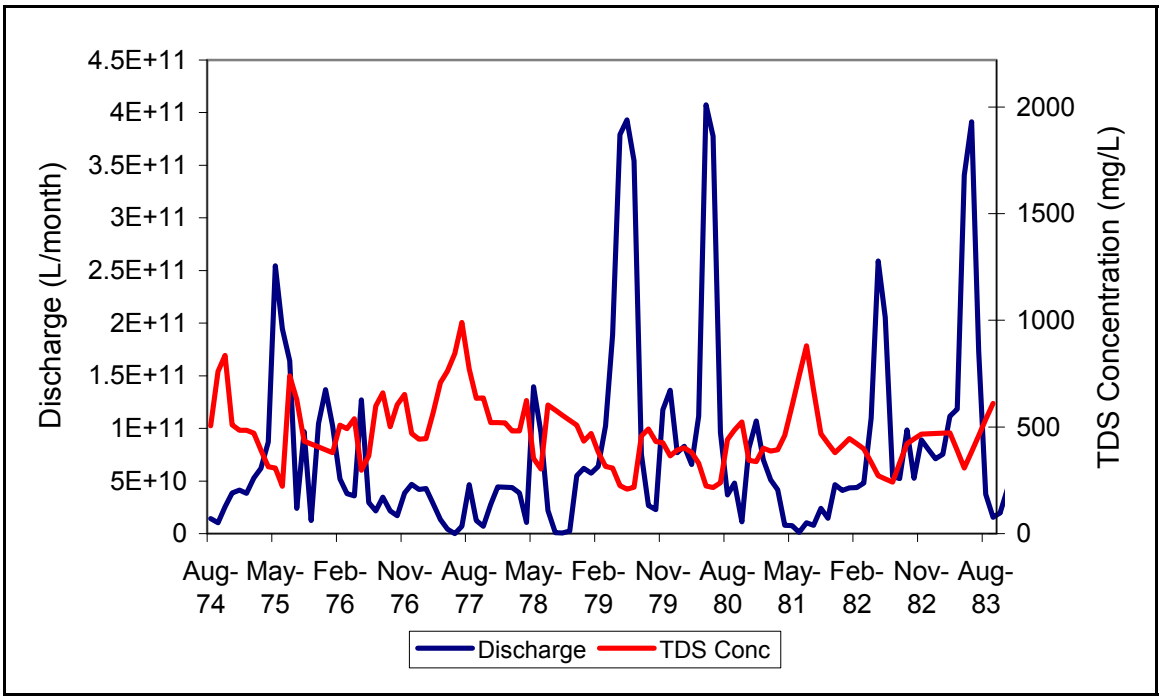

Figure 9.4. Total dissolved solids concentration compared to discharge for the Rio Grande at San Marcial, 1974-1983.

Compositional investigation also suggests that brine, tributaries and mineral interactions significantly affect Rio Grande chemistry. The Rio Grande transforms from a calcium bicarbonate water to a sodium-sulfate-chloride dominated water as it flows from Lobatos, Colorado into El Paso, Texas. Northern river reaches are compositionally similar to tributary chemistry, whereas southern river sections become increasing pulled toward the chemical composition of local brine seepage. The Rio Grande is compositionally divided at Elephant Butte Reservoir. Differences above and below Elephant Butte Reservoir are illustrated in Figure 5.2, where the anion composition shifts from a bicarbonate–chloride water to a sulfate-chloride water. This anion shift may be caused by carbonate mineral precipitation, likely calcite, within Elephant Butte Lake. In addition, 1905-1907 chemical data suggests that solutes are affected within Elephant Butte Reservoir.

9.1 Quantification of Major Salinity Sources

The various processes that affect the chemistry of the Rio Grande are presented in Figures 9.5-9.12, where the load from each source is quantified over all river reaches. In the northern river reaches, tributaries add the largest amount of solutes. In the middle Rio Grande valley the wastewater treatment plant and mineral interactions account for most of the solute increase in the TDS as well as most of the constituents. The loss of solutes through mineral interactions is largest between San Marcial and Elephant Butte Dam. Brine inflow, ground water seepage and mineral interactions yield the majority of solute additions (or losses) in the southern river reaches below Elephant Butte Dam. The amount of each solute added to the river through mineral mass transfers from irrigation practices is shown in Figure 9.13 based on irrigated acreage within each reach. The overall amount of mineral involved in mass transfers is presented in Table 9.1 based on the number of irrigated acreages with in each river reach. On average similar quantities of plagioclase, gypsum and calcite were dissolved or precipitated respectively. The reaches between Bernardo and Caballo add the largest amount of solutes per acre. Evaporation also contributes to the salinity increase. Table 9.2 reports the percentage of water lost due to evapotranspiration. The modeled evapotranspiration varied between 2 and 44% depending on the reach.

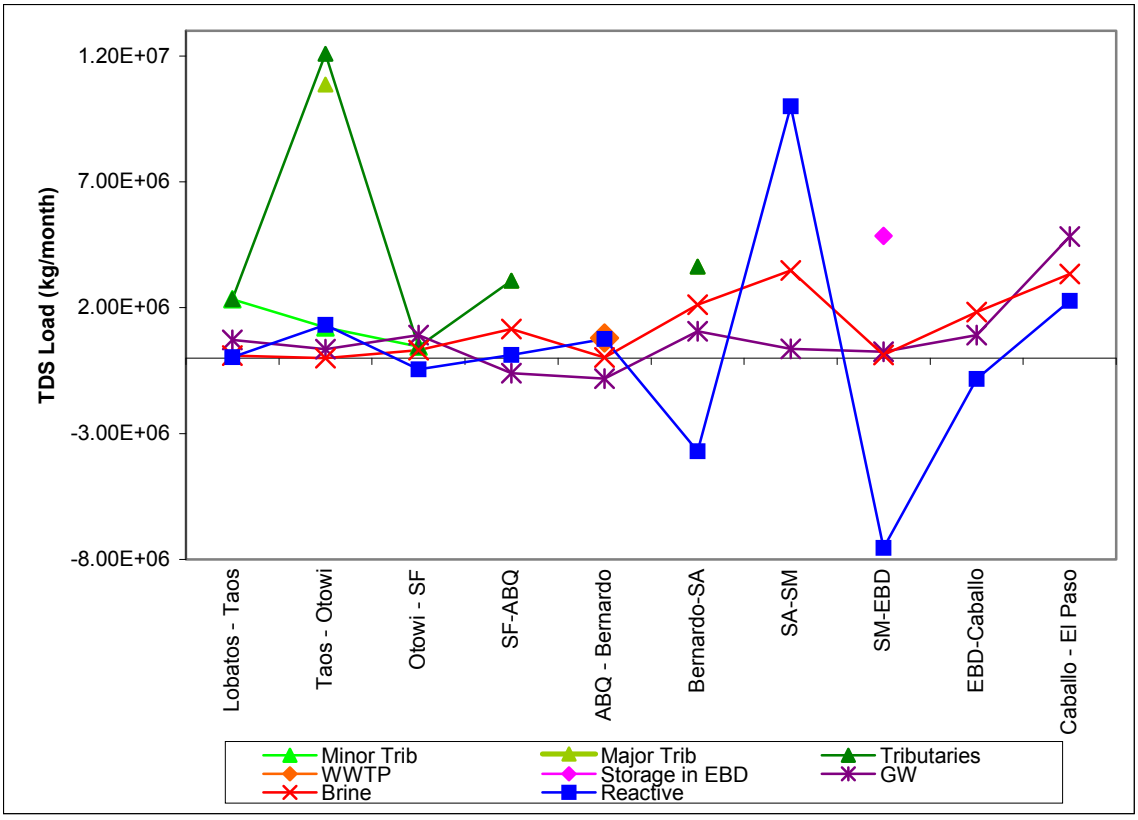

Figure 9.5 Source contributions of total dissolved solids for all river reaches, 1980-1989.

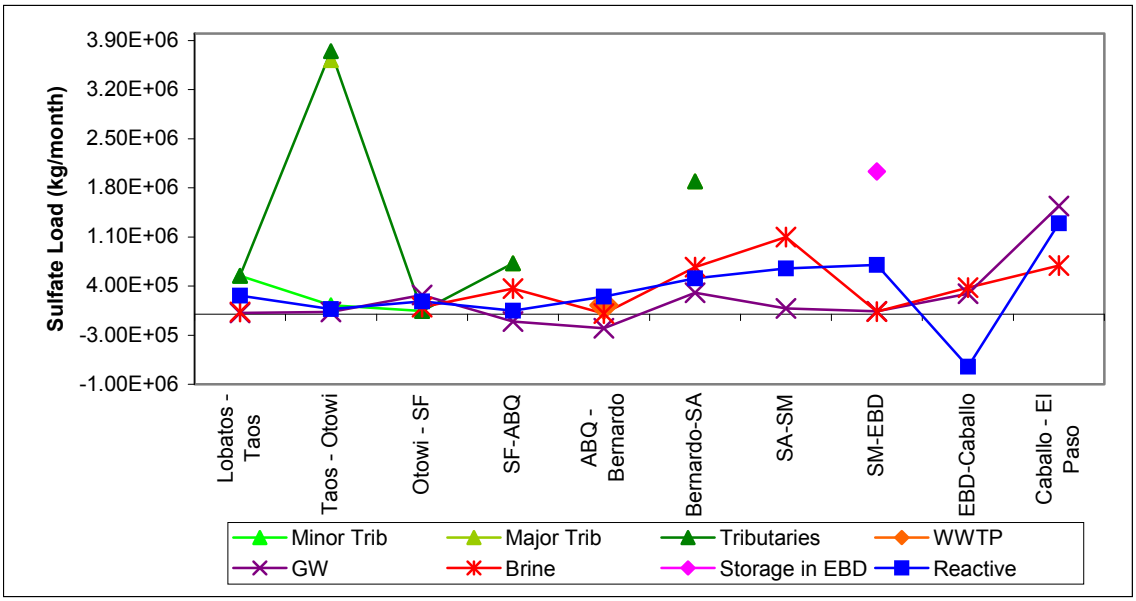

Figure 9.6 Source contributions of sulfate for all river reaches, 1980-1989.

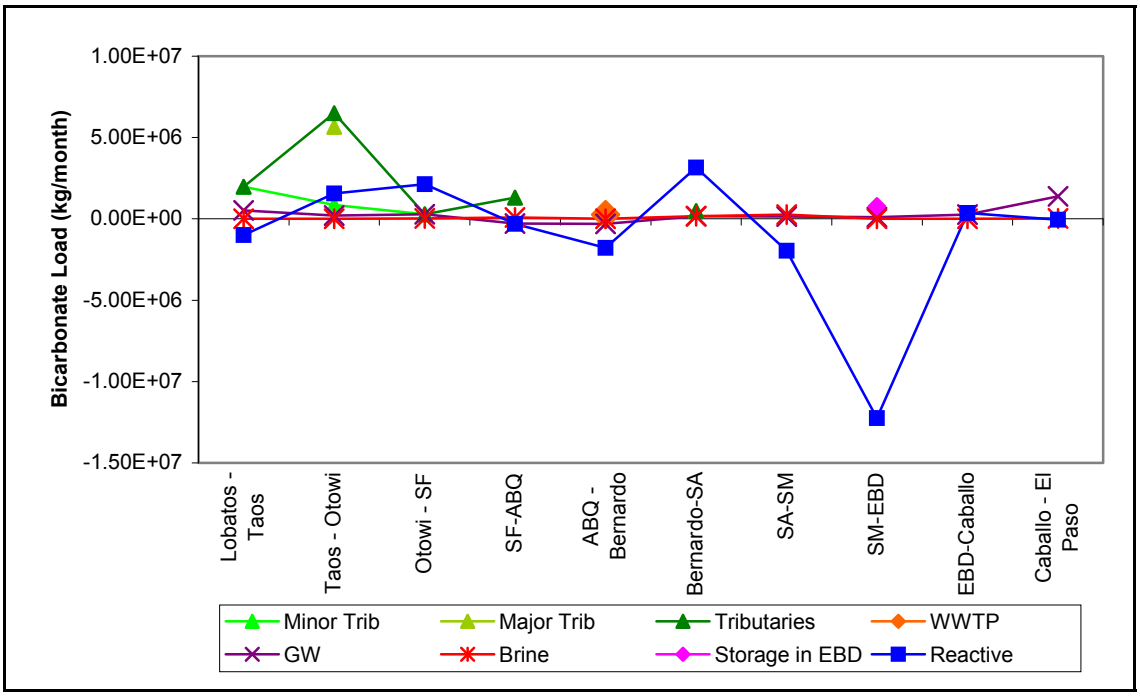

Figure 9.7 Source contributions of bicarbonate for all river reaches, 1980-1989.

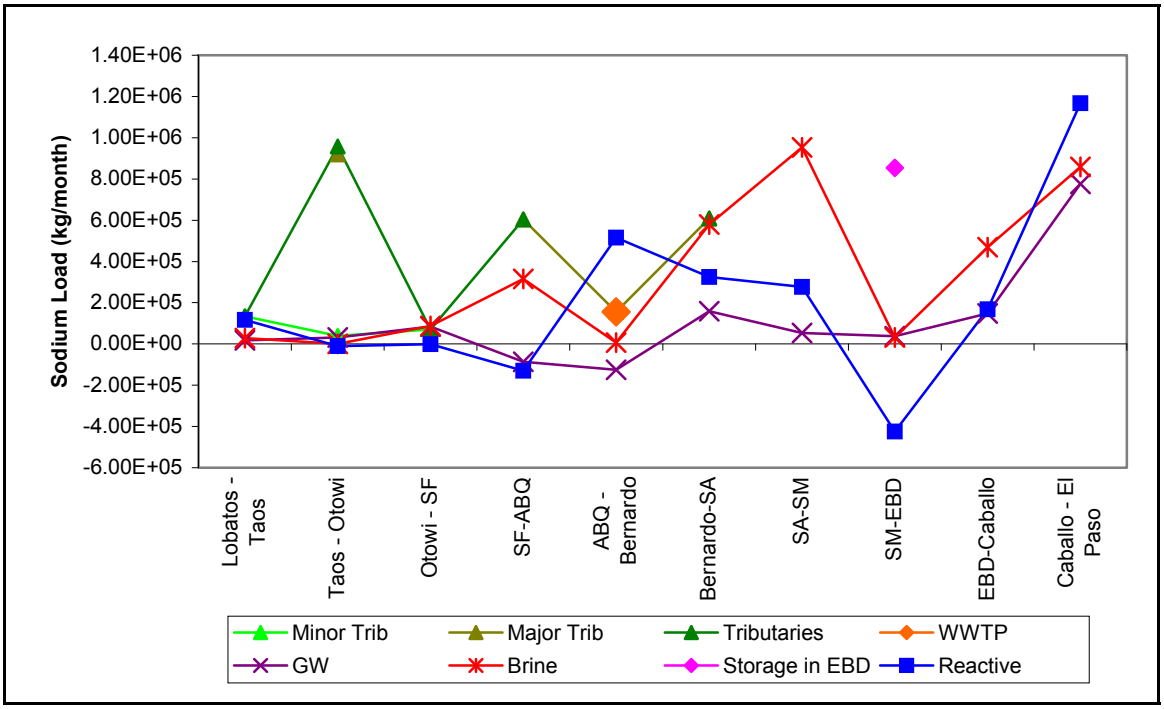

Figure 9.8 Source contributions of sodium for all river reaches, 1980-1989.

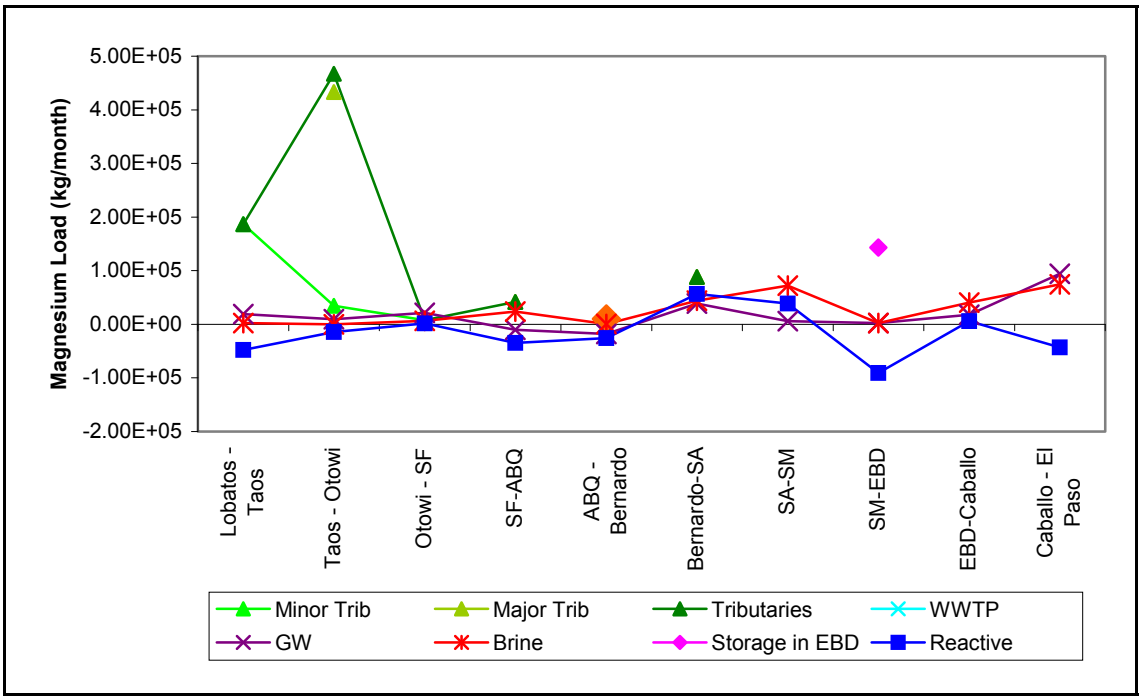

Figure 9.9 Source contributions of magnesium for all river reaches, 1980-1989.

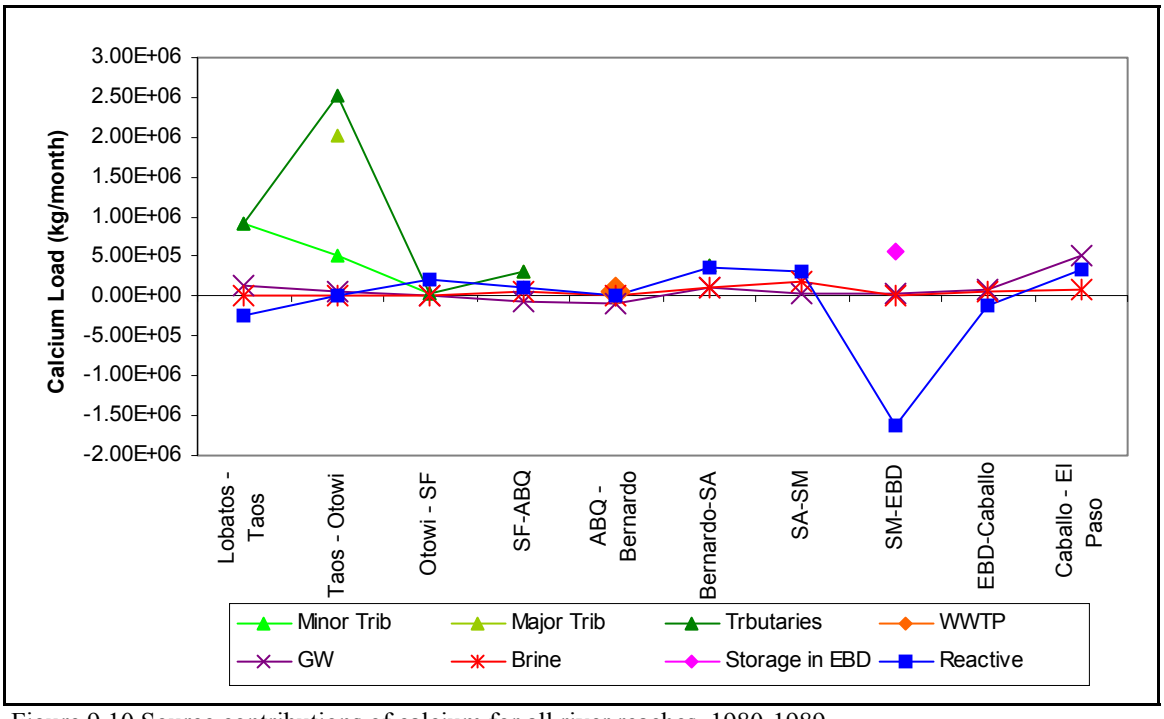

Figure 9.10 Source contributions of calcium for all river reaches, 1980-1989.

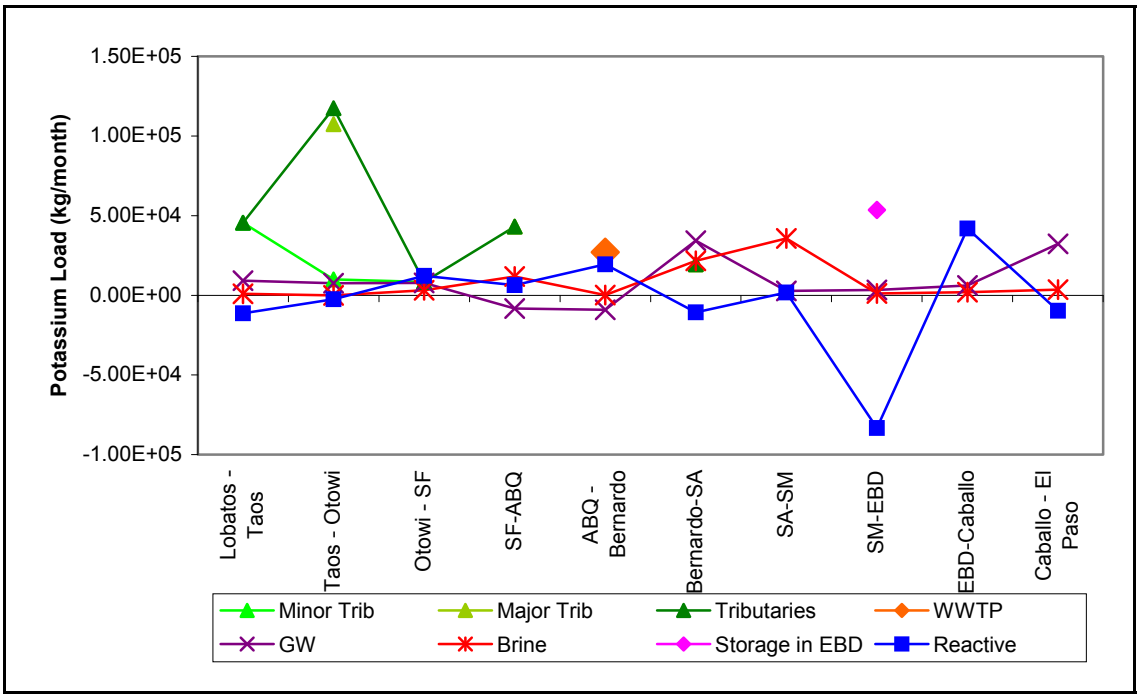

Figure 9.11 Source contributions of potassium for all river reaches, 1980-1989.

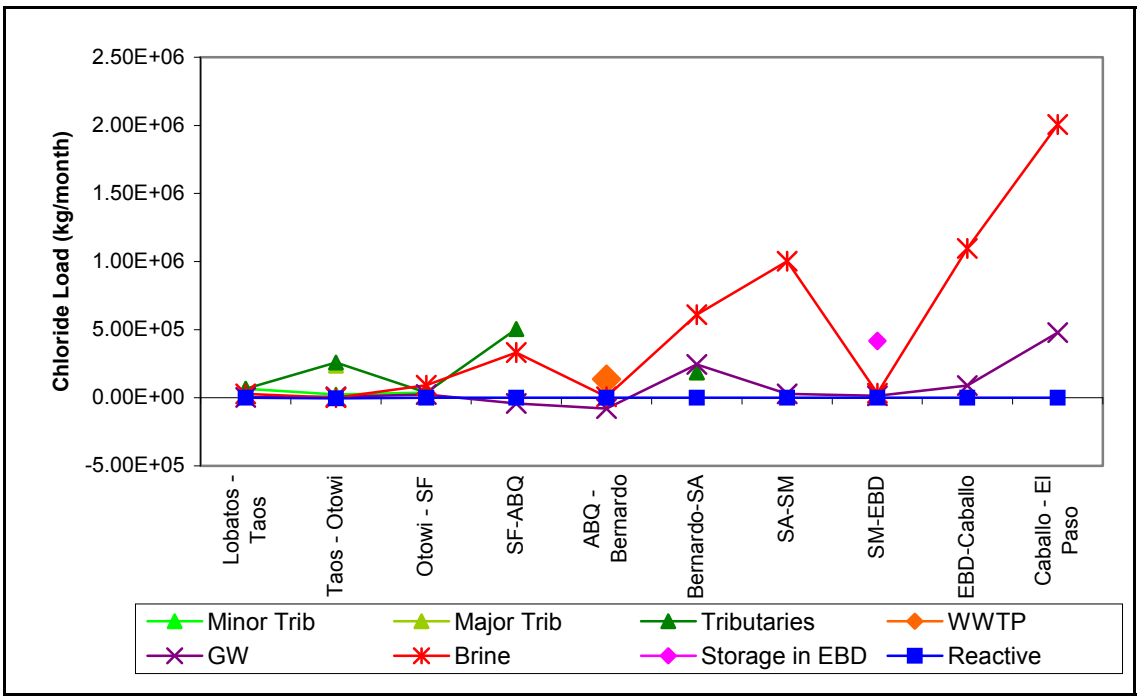

Figure 9.12 Source contributions of chloride for all river reaches, 1980-1989.

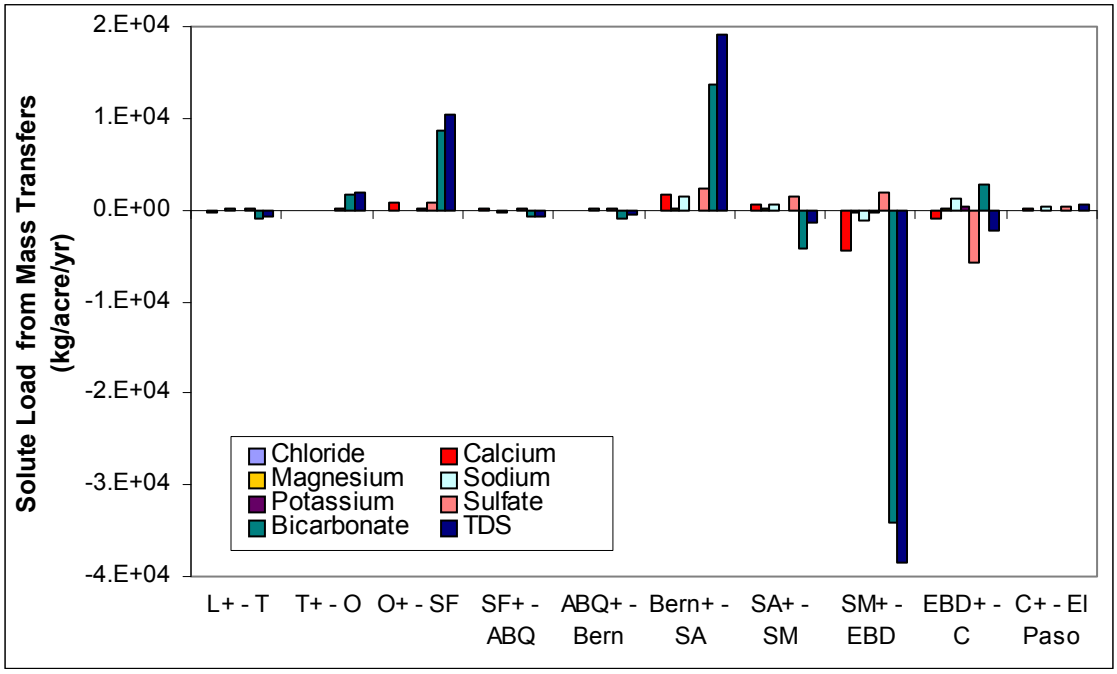

Figure 9.13. Solute load added from mass transfer interactions from each river reach, normalized by the irrigated acreage. Data is from 1980-1989.

Table 9.1. Mineral quantities dissolved or precipitated per acre within each reach. (kg of mineral/acre/yr)

kg Mineral/ acre/yr	Lobatos+ - Taos	Taos+ - Otowi	Otowi+ - SF	SF+- ABQ	ABQ+ - Bernardo	Bernardo +-SA	SA+- SM	SM+- EBD	EBD+- Caballo	Caballo + - El Paso
Plagioclase-38	0.0014	$3x10^{5}$	$5x10^{6}$	0.0009	0.0056	0.0047	0.0036		0.0023	0.0095
Olivine		0.0001								
Biotite			$8x10^{6}$		0.0002					
Calcite	-0.0045		0.0020	-0.0018	-0.0066	-0.0024	-0.0029	-0.0250	0.0012	-0.0007
Gypsum					0.0006	0.0017	0.0020	0.0003	-0.0024	0.0055
Dolomite						0.0007	0.0004	-0.0013		
Ca-Mont	0.0006	0.0002	$-5x10^{5}$	0.0004		-0.0021	-0.0016	-0.0006	-0.0012	-0.0041
Mg-Mont	-0.0013	-0.0003		-0.0007	-0.0025				0.0002	
CO2	-0.0066	0.0126	0.0263		-0.0128	0.0641	-0.0342	-0.1609	0.0045	
Ca/Na Ca loss				0.0043				0.0170		-0.0245
Ca/Na Na release to GW				-0.0075				-0.0297		0.0428

Table 9.2. Percentage of water lost due to evapotranspiration.

River Reach	% ET
Lobatos - Taos	3
Taos - Otowi	2
Otowi - SF	3
SF-ABQ	5
ABQ - Bernardo	19
Bernardo-SA	2
SA-SM	9
SM-EBD	18
EBD-Caballo	6
Caballo - El Paso	44

Figures 9.5-9.12 illustrate the significance of salt addition from brine seepage and mineral transfer interactions. The quantification of salt from these sources provides practical information useful in the management of salinity in the Rio Grande. The major anion and cation solute loads are particularly valuable to investigate the mechanisms by which mass transfer interactions add salt to the river. The mechanisms include aluminosilicate weathering reactions, dedolomitization, dissolution of minerals and ion exchange interactions. Northern Rio Grande subsurface reactions are controlled by silicate weathering reactions, transforming olivine, plagioclase and biotite into clay minerals such as calcium or magnesium montmorillonite. In contrast, carbonate interactions and cation exchange dominated solute mass transfers in southern regions.

Further investigation of agricultural processes illuminated mineral reactions that occurred in agricultural soils, riparian areas or in the conveyance channels. Chemical differences between irrigation and ground water have been attributed to ion exchange between magnesium and sodium, in-gassing of carbon dioxide, and the process of dedolomitization, which is precipitation of calcite and the dissolution of dolomite and gypsum. The Lemitar reaction mechanisms paralleled the chemical variations between

the San Acacia to San Marcial reach illustrating a qualitative corroboration between the models which suggests the mechanisms identified at a small farm in Lemitar are the same chemical mechanisms that likely affect marco-scale reactive solute behavior along the Rio Grande.

The increase in TDS with distance downstream produces potential water quality problems for southern basin users. State and Federal agencies are in the process of identifying practical methods to manage the salinity in the Rio Grande basin. Methods for decreasing evapotranspiration and intercepting brine seepage have been discussed as possible mitigation tools. Based on the work presented in this thesis, solute interactions with mineral phases contribute significant quantities of salt to the river and may pose obstacles for salinity management in the Rio Grande. Assuming that both mentioned salinity control proposals (ET reduction and brine interception) are able to reduce the salinity neither proposal considers possible affects from mineral interactions. For example, if all the brine from the locations of significant brine influx (San Acacia, above Elephant Butte Reservoir, Seldon Canyon – near Leasburg and El Paso) could be removed, a significant amount of salt would remain in the river due to mineral interactions. In addition, removal of brine could alter the stability between the river and minerals leading to larger mineral dissolution. Further research to identify the specific locations of mineral interactions (i.e. agricultural land, riparian areas, etc.) should assist in the search for a practical salinity mitigation technique.

BIBLIOGRAPHY

Anderholm, S.K., *Clay-Sized Fraction and Powdered Whole-Rock x-ray Analyses of Alluvial Basin Deposits in Central and Southern New Mexico*. U.S. Geological Survey: Albuquerque, NM, 11 pp., 1985.

Anderholm, S.K, Water-Quality Assessment of the Rio Grande Valley, Colorado, New Mexico, and Texas—Shallow Ground-Water Quality of a Landuse Area in the San Luis Valley, South-central Colorado, 1993, *Water Resources Investigations Report 96-4249, 94 pp.*, 1996.

Anderholm, S.K, Water-Quality Assessment of the Rio Grande Valley, Colorado, New Mexico, and Texas—Surface-Water Quality, Shallow Ground-Water Quality, and Factors Affecting Water Quality in the Rincon Valley, South-Central New Mexico, 1994-95, *Water Resources Investigations Report 96-4249, 117 pp.*, 2002.

Back, W., Hanshaw, B.B., Plummer, L.N., Rahn, P.H., Rightmire, C.T., Rubin Meyer, Process and rate of dedolomitization: Mass transfer and 14C dating in a regional carbonate aquifer, *Geologic Society of America Bulletin,* 94, 1415-1429, 1983.

Bexfield, L.M., and S. K. Anderholm, Water-Quality Assessment of the Rio Grande Valley, Colorado, New Mexico, and Texas—Ground-Water Quality in the Rio Grande Flood Plain, Cochiti Lake, New Mexico, to El Paso, Texas, 1995, *Water Resources Investigations Report 96-4249, 93 pp.*, 1997.

CDWR, *Rio Grande overview*, Colorado's Decision Support Systems, Colorado Division of Water Resources, ftp://dwrftp.state.co.us/cdss/ovw/in/RGDSS_overview.pdf, 2000.

Clark, J. D., Mauger, H., The Chemical Characteristics of the Waters of the Middle Rio Grande Conservancy District. *The University of New Mexico Bulletin*, 2, 1-40 pp., 1932.

Drever, J. I., *The Geochemistry of Natural Waters: Surface and Groundwater Environments*, 3rd Ed., 436 pp., Prentice Hall, New Jersey, 2002.

Ellis, S.R., Levings, G.W., Carter, L. F., Richey, S.F., and Radell, M.J., Rio Grande Valley, Colorado, New Mexico, and Texas, *Water Resources Bulletin*, 2, 617-646 pp., 1993.

Farnsworth, R.K., Thompson, E.S., and Peck, E.L., 1982, Evaporation atlas for the contiguous 48 United States: National Oceanic and Atmospheric Administration and National Weather Service, *NOAA Technical Report,* NWS 33, June 1982, map 3.

Hanshaw, B. B., Back, W. and Johnson, W. R., *Soil Survey of Socorro County Area, New Mexico*, United States Department of Agriculture, 1984.

Harmel, R. D., R. J. Cooper, R. M. Slade, R. L. Haney, J. G. Arnold, Cumulative Uncertainty in Measured Streamflow and Water Quality Data for Small Watersheds, *American Society of Agricultural and Biological Engineers*, v. 49, n. 3, 689-701 pp., 2006.

Hendrickx, J. M. H., *Water quality protection for El Paso County Water Improvement District No. 1*, Draft report to the El Paso County Water Improvement District No. 1, 32 pp. plus appendices., 1998.

Johnson, N., Managing Water for People and Nature, *Science* 292, 1071-1072, 2001.

Johnson, P. S., and J. W. Shomaker, *New Mexico's Water: Perceptions, Reality, and Imperatives, Background Report for the 28th New Mexico First Town Hall*, New Mexico First, 76 pp., Albuquerque, New Mexico, 2002.

Lacey, L. F., *Quantifying and Characterization Chloride Sources in the Rio Grande,* M. S. thesis, 167 pp., New Mexico Institute of Mining and Technology, Socorro, New Mexico, 2006.

Levings, G. W., D. F. Healy, S. F. Richey, and L. F. Carter, Water Quality in the Rio Grande Valley, Colorado, New Mexico and Texas, 1992-95, *U. S. Geological Survey Circular 1162,* 39 pp., 1998.

Lippincott, J. B., Southwest Border Water Problems, *Journal of the American Water Works Association*, 31, 1-28 pp., 1939.

Longworth, P.E., Valdez, J.M., Magnuson, P.E. Albury, E.S., Keller, J., New Mexico Water Use by Categories in 2005, New Mexico, *New Mexico State Engineer Technical Report 52*, 111 pp., Santa Fe, New Mexico, 2008.

Lucero, B., Margaret Sanchez, and Jim Puissant*, The History of Albuquerque's Wastewater Treatment.* www.webster.edu/~enviss/water.html, 2008.

Machette, M. *Field and Laboratory Procedures Used in a Soil Chronosequence Study.* Washington, United States Government, 1986.

Meybeck, M., Global Occurrence of Major Elements in Rivers: in *Treatise on Geochemistry*, edited by H. D. Holland and K. K. Turekian, Vol. 5, in *Surface and Ground Water, Weathering, and Soils* (J. I. Drever; ed.), Pergamon, Oxford, 207-223 pp., 2003.

Mills, S. K., *Quantifying Salinization of the Rio Grande Using Environmental Tracers,* M. S. thesis, 397 pp., New Mexico Institute of Mining and Technology, Socorro, New Mexico, 2003.

Moore, S. J., Bassett, R.L., Liu,B., Wolf, C.P. and Doremus, D., Geochemical Tracers to Evaluate Hydrogeologic Controls on River Salinization, *Ground Water*, 2008.

Moore, S. J., and S. K. Anderholm, Spatial and Temporal Variations in Streamflow, Dissolved Solids, Nutrients, and Suspended Sediment in the Rio Grande Valley Study Unit, Colorado, New Mexico, and Texas, 1993-95, *Water Resources Investigations Report 02-4224, 52 pp.*, 2002.

National Resources Committee (NRC), *Regional Planning Report part VI, Rio Grande Joint Investigation in the Upper Rio Grande Basin in Colorado, New Mexico, and Texas, 1936-1937*, U. S. Government Printing Office, 566 pp., Washington, D.C., 1938.

New Mexico State University (NMSU), evaporation calculator. http://weather.nmsu.edu/pmcomp.htm, *2008*.

Newton, B. T., *Geologic Controls on Shallow Groundwater in the Socorro Basin, New Mexico,* M. S. thesis, 163 pp., New Mexico Institute of Mining and Technology, Socorro, New Mexico, 2005.

S. S Papadopulos and Associates, *Middle Rio Grande Water Supply Study*, Unpublished report prepared for the U. S. Army Corps of Engineers Albuquerque District, 70 pp. plus figures and tables, 2000.

S. S Papadopulos and Associates, *Assessment of Flow Conditions and Seepage on the Rio Grande and Adjacent Channels, Isleta to San Marcial, Summer 2001*, Unpublished report prepared with Mussetter Engineering, Inc. for the New Mexico Interstate Stream Commission, 24 pp. plus appendices, 2002a.

S. S Papadopulos and Associates, *Middle Rio Grande Conservancy District Efficiency and Metering Program*, Report prepared for the New Mexico Interstate Stream Commission, 105 pp. plus Figures and appendices, 2002b.

Phillips, F. M., J. F. Hogan, S. K. Mills, and J. M. H. Hendrickx, Environmental Tracers Applied to Quantifying Causes of Salinity in Arid-Region Rivers: Preliminary Results from the Rio Grande, Southwestern USA, *Water Resources Perspectives: Evaluation, Management and Policy*, edited by A. S. Alsharhan and W.W. Wood, Elsevier Science, Amsterdam, 327-334 pp., 2003.

Plummer, L. N., An Interactive Code (NETPATH) for Modeling Net Geochemical Reactions along a Flow Path. Reston, Virginia, *Water-Resources Investigations Report*, 227, 1991.
NETPATH USGS website: http://wwwbrr.cr.usgs.gov/projects/GWC_coupled/netpath/.

Plummer, L. N., Bexfield, L. M., Anderholm, S. K., Sanford, W. E., Busenberg, E., Geochemical Characteristics of Ground-Water Flow in the Santa Fe Group Aquifer System, Middle Rio Grande Basin, New Mexico, *U. S. Geological Survey Water Resources Investigations Report 03-4131*, 245 pp. plus appendices, 2004.

Plummer, L. N., Busby, J.F, Roger, W.L., and Hanshaw, B.B., Geochemical Modeling of the Madison Aquifer in Parts of Montana, Wyoming, and South Dakota, *Water Resources Research*, 26, 9, 1981-2014 pp., 1990.

Plummer, L. N., Jones, B.F, and Truesdell, A.H., WATEQF—A FORTRAN IV version of WATEQ, a computer program for calculating chemical equilibria of natural waters, *U.S Geological Survey Water Resources Investigations Report 76-13*, 61 pp., 1976.

Postel, S., *Pillar of Sand: Can the Irrigation Miracle Last?*, W. W. Norton and Company, 313 pp., London, 1999.

Rio Grande Compact Commission, *Annual Report of the Rio Grande Compact Commission 1999,* reported to the governors of Colorado, New Mexico, and Texas, 2000.

Scurlock, D., *From the Rio to the Sierra: An Environmental History of the Middle Rio Grande Basin*, General Technical Report 5 (RMRS-GTR-5), U.S. Department of Agriculture, Forest Service, Rocky Mountain Research Station, 440 pp., 1998.

Stabler, H., Some stream waters of the western United States, *U. S. Geological Survey Water Supply Paper 274,* 188 pp., 1911.

Towne, L., Infrastructure and Management of the Middle Rio Grande, in *Water Resources of the Middle Rio Grande —San Acacia to Elephant Butte Decision-Makers Field Guide*, edited by P.S.J. L. Greer Price, and Douglas Bland, New Mexico Bureau of Geology. 37-42 pp., 2007

Trock, W. L., P. C. Huszar, G. E. Radosevich, G. V. Skogerboe, and E. C. Vlachos, *Socio-economic and Institutional Factors in Irrigation Return Flow Quality Control Volume III: Middle Rio Grande Valley Case Study*, report EPA-600/2-78-174c, Environmental Protection Agency, 1978.

USBR, *Dataweb, Dams and Reservoirs*, http://www.usbr.gov/dataweb/dams/, 2008.

USDA-SCS Staff. *Soil Survey Laboratory Methods and Procedures for Collecting Soil Samples,* U.S. Gov. Print. Office, Washington, DC, 1972.

USDA Staff. *Diagnosis and Improvement of Saline and Alkaline Soils*, USDA Agriculture, Handbook 60, L.A. Richards (ed.), U.S. Gov. Print. Office, Washington, DC, 1954.

U.S. Fish and Wildlife, Hydrologic and Biologic Data for the Water-Quality Assessment in Relation to Rio Grande Silvery Minnow Habitats, Middle Rio Grande, New Mexico, 2002-2003. U.S. Fish and Wildlife Service Draft Report, 25pp. plus appendices, 2004.

U.S. Fish and Wildlife Service History of the Bosque del Apache website, 2000. http://library.fws.gov/Refuges/bosque.pdf

USGS, *NWISWeb Data for the Nation*, United States Geological Survey, http://waterdata.usgs.gov/nwis, 2008.

USGS, *Historical Rio Grande Flow Conditions*, International Boundary and Water Commission, http://www.ibwc.state.gov/wad/histflo1.htm, 2008b.

Veenhuis, J. E., Summary of flow loss between selected cross sections on the Rio Grande in and near Albuquerque, New Mexico, *U. S. Geological Survey Water-Resources Investigations Report 02-4131, 30 pp.*, 2002.

Vengosh, A., Salinization and Saline Environments: in *Treatise on Geochemistry*, edited by H. D. Holland and K. K. Turekian, Vol. 9 Environmental Geochemistry, 1-35 pp., Pergamon, Oxford, 2007.

Wilcox, L. V., Analysis of salt balance and salt-burden data on the Rio Grande, in *Problems of the Upper Rio Grande: an Arid Zone River, Publication No.1*, edited by P. C. Duisberg, pp. 39-44, U. S. Commission for Arid Resource Improvement and Development, Socorro, New Mexico, 1957.

Wilkins, D. W., Summary of the southwest alluvial basins regional aquifer-system analysis in parts of Colorado, New Mexico, and Texas, *U. S. Geological Survey Professional Paper 1407A,* 49 pp., 1998.

Williams, J. H., *Salt Balance in the Rio Grande Project from San Marcial, New Mexico to Fort Quitman, Texas*, M.S Thesis, 80 pp., New Mexico State University, Las Cruces, New Mexico, 2001.

Wilson, B., *Water Use in New Mexico in 1985,* New Mexico, New Mexico State Engineer Technical Report 46, 84 pp., Santa Fe, New Mexico, 1986.

Wilson, C. A., R. R. White, B. R. Orr, and G. R. Roybal, *Water resources of the Rincon and Mesilla Valleys and Adjacent Areas, New Mexico*, New Mexico State Engineer Technical Report 43, 66 pp., Santa Fe, New Mexico, 1981.

Wilson, C. A., Lucero, L. A., Romero, J. T., Romero, P. J., *Water use by categories in New Mexico counties and river basins, and irrigated acreage in 2000,* New Mexico, New Mexico State Engineer Technical Report 51, 164 pp., Santa Fe, New Mexico, 2003.

Winograd, I. J., *Ground-water conditions and geology of Sunshine Valley and western Taos County, New Mexico*, New Mexico State Engineer Technical Report 12, 70 pp., Santa Fe, New Mexico, 1959.

Wozniak, F.E., *Irrigation in the Rio Grande Valley, New Mexico: a study of the development of irrigation systems before 1945*, Report on Contract BOR-87-1, U.S. Dept. Agric., 130 pp., Bureau of Reclamation, Southwest Office, Amarillo, TX, 1987.

APPENDIX A
DISCHARGE AND SOLUTE DATA

This appendix is contained in an excel file on the enclosed CD. The file contains discharge and solute concentration information. The 11 main channel Rio Grande stations, the four major tributaries (Rio Chama, Jemez, Rio Puerco and Rio Salado) and the two LFCC stations (San Acacia and San Marcial) are presented for each constituent: calcium, magnesium, sodium, potassium, chloride, sulfate, bicarbonate, EC and TDS. Each tab within the EXCEL file denotes one USGS gaging station and contains discharge, solute concentration and load information. See Chapter 4 for further explanation regarding the data sources, quantity and how the data was adjusted. Decade averages are listed on the far right at column BL and row 210 of each tab. All station decadal load and concentration are presented in a tab labeled “summary”. Average monthly information is also presented with a separate tab for each month.

APPENDIX B
REGRESSION EQUATIONS AND R^2 COEFFICIENTS

This appendix is contained in an excel file on the enclosed CD. The file contains the regression equations used to fill months with missing solute data. Solute data was regressed against electrical conductivity, total dissolved solids and discharge. The regression equations are included in separate tabs within excel based on regression type. Regression equations for the 11 main channel Rio Grande stations as well as the major tributaries are presented for each constituent: calcium, magnesium, sodium, potassium, chloride, sulfate, bicarbonate and TDS. Further explanation regarding the use of the regressed data can be found in Chapter 4. The excel file tabs are labeled as follows: RG Stations RegwEC for regression against electrical conductivity at the USGS stations on the Rio Grande, Tribs RegwEC for regression against electrical conductivity at the USGS stations on major tributaries, RG Stations RegwDis for regression against discharge at the USGS stations on the Rio Grande, Tribs RegwDis for regression against discharge at the USGS stations on major tributaries. In each tab the columns are labeled by solute with the regression equation in one column and the R^2coeffiecint in the right-adjacent column.

APPENDIX C
MASS BALANCE MODEL

This appendix is contained in an excel file on the enclosed CD. The file contains the mass balance model utilized to compute the total solute load passing at each Rio Grande cross section based on the summation of the known solute sources. A water mass balance model and a solute mass balance for each of the major ions were calculated and are each contained in a separate EXCEL tab. For each mass balance the various sources contributing or removing water and solutes are stacked vertically for the decades from 1930-2005. See Chapter 4 for further explanation regarding the data sources, quantity and how the data was adjusted and Appendix A for river, tributary and LFCC data. For information on how the model was constructed, see Chapter 6.

APPENDIX D
MASS BALANCE RESULTS SUMMARY

This appendix is contained in an excel file on the enclosed CD. The file contains a summary of the water and solute mass balance results. The model is contained in Appendix C and the surface water data in Appendix A. In addition, the modeled result for the upstream+ calculation is reported alongside the downstream Rio Grande station. Mass balance results are presented for the decades contained between 1930 and 2005 for the ten modeled river reaches (Lobatos-Taos Jct, Taos Jct -Otowi, Otowi-San Felipe, San Felipe-Albuquerque, Albuquerque-Bernardo, Bernardo-San Acacia, San Acacia-San Marcial, San Marcial-Elephant Butte, Elephant Butte-Caballo and Caballo-El Paso. For additional information on the modeled results or how the mass balance models were constructed, see Chapter 6.